The Use of Triaxial Accelerometry for Measuring Stride Parameters and Vertical Stiffness in Team-Sport Athletes

Horsley, Benjamin

Horsley, Benjamin (2024) The Use of Triaxial Accelerometry for Measuring Stride Parameters and Vertical Stiffness in Team-Sport Athletes [PhD Thesis]. Australian Catholic University. DOI: https://doi.org/10.26199/acu.904q2

The Use of Triaxial Accelerometry for Measuring Stride Parameters and Vertical Stiffness in Team-Sport Athletes

By

Benjamin Horsley

In Total Fulfilment of the Degree of

Doctor of Philosophy

School of Behavioural and Health Sciences

Australian Catholic University

Melbourne, Victoria

Australia

Statement of Authorship and Sources

This thesis contains no material that has been extracted in whole or in part from a thesis that I have submitted towards the award of any other degree or diploma in any other tertiary institution.

No other person's work has been used without due acknowledgment in the main text of the thesis.

All research procedures reported in the thesis received the approval of the relevant Ethics/Safety Committees.

Benjamin Horsley   Date   28/02/2024

Acknowledgements

There are so many words I could use to describe the feelings and emotions that the last four-and-a-half years have brought. Challenging. Frustrating. Stressful. Rewarding. I could go on. It is evident from these descriptions that this PhD has been a rollercoaster of a ride (guess it would not be a PhD otherwise!), and I certainly could not have made it to the end without the support and contributions of many people along the way.

The wide-ranging support I have received at Australian Catholic University has been one of the biggest positives about completing a PhD at this institution. This is reflected by the contributions from Professor Shona Halson, Professor Justin Kemp, Jessica Dickson, Dr. Nirav Maniar, Dr. Daniel Chalkley, Associate Professor Michael Cole and Dr. Rich Johnston, particularly. Your input and assistance cannot be underestimated. Irrespective of whether you were directly on my supervisory panel or not, you were so accommodating with your time and expertise in helping me complete my respective projects. I am so grateful, and I hope one day I may be able to return the favour. Thank you.

To David O'Donovan, Florin Stroiescu and Joel McWilliam from STATSports®. Thank you for your expertise and allowing us to use your devices in a specialised way. You were very helpful in answering any questions we had along the way, and it was great to have you, Joel, get to see the outcomes of my work at my Final Year Review presentation.

I understand it may be unorthodox to acknowledge participants here, but given the logistical challenges of collecting data off-site (including Melbourne's unreliable weather!), not to mention how difficult recruitment was, I want to make a special thank you to all those who undertook my PhD research. The outcomes of this thesis would not be possible without your participation.

To Mum, Dad, my brother, Nicholas, and his fiancé, Amelia. Thank you for your unwavering support. You have always been there for me, but it has been particularly paramount throughout this PhD. There has no doubt been some down times over this journey, and your listening ear and words of advice have been incredibly helpful. I know I can always count on you!

To my amazing partner, Samantha. No one has lived this journey with me more than you. You have ridden every bump along the way with me, and in moments where things had got the better of me, you always found a way to inspire and motivate me to stay the course. There is no doubt in my mind that this PhD would have been 10 times harder without your incredible support. I cannot wait to celebrate with you and hopefully we get to graduate together as that will be something very special.

Finally, I want to reserve this last paragraph for my two primary supervisors, Professor Stuart Cormack and Dr. Paul Tofari. Where do I even begin? It would be easy to dedicate an entire page just to you two! Both of you have been first-class to work with throughout this entire process. You have prioritised me since day one, pushed me and challenged my thinking (particularly during those final few weeks!), and empowered me to really take ownership of this PhD. I have learnt so much from you, and through your resolute support, I walk away from this PhD a better researcher and practitioner. Yes, I am responsible for much of this work, but this thesis simply does not happen without you two by my side. I honestly could not have asked for two better supervisors. Thank you for everything you have done for me.

Table of Contents

List of Publications Related to This Thesis

1. Horsley, B.J., et al., *Does site matter? Impact of Inertial Measurement Unit placement on the validity and reliability of stride variables during running: a systematic review and meta-analysis.* Sports Medicine, 2021. **51**: p. 1449-1489.

2. Horsley, B.J., et al., *Validity and reliability of thoracic-mounted Inertial Measurement Units to derive gait characteristics during running.* The Journal of Strength and Conditioning Research, 2023. **38**(2): p. 274-282.

3. Horsley, B.J., et al., *Thoracic-worn accelerometers detect fatigue-related changes in vertical stiffness during sprinting.* The Journal of Strength and Conditioning Research, 2023. **38**(2): p. 283-289.

List of Figures

List of Tables

Abbreviations and Units

BT:	Blue Trident
CI:	confidence interval
CMJ:	countermovement jump
COM_{dis}:	centre of mass displacement
CV:	coefficient of variation
$deg \cdot s^{-1}$:	degrees per second
DJ:	drop jump
DSL:	Dynamic Stress Load
ES:	effect size
FT:CT	flight time:contraction time
G:	gauss
g:	gravitational acceleration
GAS:	General Adaptation Syndrome
GNSS:	global navigation satellite system
GRF:	ground reaction force
Hz:	hertz
IC:	initial contact
ICC:	intraclass correlation coefficient
IMTP:	isometric mid-thigh pull

IMU:	inertial measurement unit
$km \cdot h^{-1}$:	kilometres per hour
kN:	kilonewtons
$kN \cdot m^{-1}$:	kilonewtons per metre
K_{leg}:	leg stiffness
K_{vert}:	vertical stiffness
LFF:	Low frequency fatigue
LoA:	limits of agreement
MD:	mean difference
$m \cdot min^{-1}$:	metres per minute
$m \cdot s^{-1}$:	metres per second
NMF:	neuromuscular fatigue
OTS:	Overtraining syndrome
RPE:	rating of perceived exertion
$SAFT^{90}$:	soccer-specific aerobic fitness test
SD:	standard deviation
SJ:	squat jump
$steps \cdot min^{-1}$:	steps per minute
SWC:	smallest worthwhile change
TE:	typical error

TO:	toe-off
$vGRF_{peak}$:	peak vertical ground reaction force
Yo-Yo IR1:	Yo-Yo Intermittent Recovery Level 1

Abstract

Inertial Measurement Units (IMUs) provide a means for analysing running gait in the field without the need for extensive lab-based equipment. These sensors have been validated for use on the lower limbs and lumbosacral region but have not been extensively validated at other body regions. In team-sport, athletes commonly wear global navigation satellite system (GNSS) units on the thoracic spine to quantify distance and speed. These GNSS units also contain IMUs which may allow the measurement of running gait characteristics, such as contact time, step length and vertical stiffness (K_{vert}), that GNSS is unable to capture. These data provide more granular information on running activity that can be used to provide insight into the mechanistic changes in movement strategy, such as those occurring in the presence of fatigue, that may precede, or occur independently of any modification in distance and speed. Given IMUs are already available in GNSS units, the thoracic spine site is potentially attractive for practitioners as it provides the possibility of measuring distance and speed from GNSS and running gait from inertial sensors to provide a comprehensive analysis of running activity all from the one device. However, the validity and reliability of thoracic-mounted IMUs to derive a range of gait characteristics across multiple running speeds has not been thoroughly explored. Therefore, the overarching aim of this thesis was to determine the validity and reliability of running gait characteristics obtained from IMUs worn on the thoracic spine and assess their effectiveness for the assessment of fatigue-induced changes.

A potential challenge for analysing running gait from the thoracic spine level is the mounting position is further away from the foot-ground interface than other common attachment sites. However, whether placement site itself is a limiting factor to validity and reliability is unclear. The first aim of this thesis (Study 1) was to conduct a systematic review and meta-analysis to investigate the impact of IMU placement site on the validity and reliability

of spatiotemporal variables, peak ground reaction force and K_{vert} in running. Thirty-nine studies were identified for the systematic review from which nine underwent meta-analysis to assess the absolute mean difference (MD) and 95% confidence interval (CI) between IMU-derived measures of running gait and those from accepted criterion sources (i.e., motion capture, high-speed camera, force plate and photocell systems). Meta-analysis revealed no significant differences for IMUs attached to the foot, tibia and lumbar spine compared to criterion sources for contact time (foot: -11.47 ms [-45.68, 22.74], p = 0.43; tibia: 22.34 ms [-18.59, 63.27], p = 0.18; lumbar spine: -48.74 ms [-120.33, 22.85], p = 0.12), flight time (foot: 11.93 ms [-8.88, 32.74], p = 0.13), step frequency (foot: 0.45 step·min^{-1} [-1.75, 2.66], p = 0.47; lumbar spine: -3.45 step·min^{-1} [-16.28, 9.39], p = 0.37) and step length (foot: 0.21 cm [-1.76, 2.18], p = 0.69). For reliability, the coefficient of variation (CV) was ≤12.1% in studies that assessed spatiotemporal gait characteristics, peak vertical ground reaction force ($vGRF_{peak}$) and K_{vert} from the foot, lumbar spine and thoracic spine sites. Therefore, measurement site does not appear to be a critical factor to validity and reliability, and this may allow measurement of running gait from the level of the thoracic spine.

A number of factors other than IMU location appear more critical to validity and reliability, including how initial contact (IC) and toe-off (TO) are determined from the type(s) of sensor used (e.g., accelerometer, gyroscope or combination of both), the axis (or axes) from which peaks are identified, or sampling and filtering approaches. These events underpin the analysis of running gait, but neither IC nor TO have been examined from the thoracic spine site relative to a criterion. This formed the foundation for Study 2, where the aim was to assess the validity and reliability of thoracic-mounted IMUs to derive a range of gait characteristics across different running speeds. Sixteen participants performed 40 m run-throughs at 3-4, 5-6 and 7-8 m·s^{-1} while wearing an IMU on each tibia, one on the lumbar spine and three on the thoracic spine. For the thoracic spine site, two GNSS devices were worn on top of each other, while one Blue Trident IMU was attached ~1 cm below. A gait event detection algorithm validated at the lumbar spine was modified and applied to data measured from the thoracic spine site where detection of IC was evaluated with the F1 score, while nonparametric limits of agreement (LoA) were used to assess the agreement (MD ± standard deviation [SD]) of the calculated gait characteristics with tibia and lumbar spine criterion sites. Test-retest error (CV [95% CI]) established reliability of gait characteristics derived from thoracic-worn IMUs. Thoracic-mounted IMUs detected a nearly perfect proportion (F1 ≥0.95) of IC events compared to criterion sites. Step length had the strongest agreement (0 ± 0.04 m) at 3-4 $m \cdot s^{-1}$, while contact time improved from 3-4 (-0.028 ± 0.018 s) to 7-8 $m \cdot s^{-1}$ (-0.004 ± 0.013 s). All values for K_{vert} fell within the LoA at 7-8 $m \cdot s^{-1}$. Test-retest error was ≤12.8% for all gait characteristics obtained from IMUs within GNSS units, where step length at 7-8 $m \cdot s^{-1}$ had the highest reliability (CV = 1.5% [1.8, 3.2]). Contact time (CV = 3.4-4.1%) and $vGRF_{peak}$ (CV = 2.3-3.0%) were consistent across all speeds, while K_{vert} was most reliable at 3-4 $m \cdot s^{-1}$ (6.8% [5.2, 9.6]). The thoracic spine site is suitable to derive a variety of selected gait characteristics, including K_{vert}, from IMUs within GNSS units which eliminates the need for additional sensors at other sites.

With the validity and reliability of thoracic-mounted IMUs confirmed, this work next focused on assessing their ability to detect changes in running gait characteristics. Study 3 assessed this from GNSS-embedded accelerometers using a repeated sprint protocol that has been shown to modify gait characteristics measured from force plates. In addition, this study examined whether any modifications in gait coincided with changes in a range of countermovement jump (CMJ) variables. Sixteen participants performed single and repeated CMJs on a force plate and the same series of 40 m run-throughs as Study 2 before and after a 12 x 40 m repeated sprint protocol. Changes in running gait and CMJ performance were assessed using a linear mixed-effects model (effect size [ES] [95% CI]) where significance was set at p < 0.05. A significant reduction in K_{vert} occurred at 7-8 m·s^{-1} (-8.51 kN·m^{-1} [-13.9, -3.11]; p = 0.007; ES [95% CI] = -0.39 [-0.62, -0.15]) which coincided with a decreased jump height (-0.03 m [-0.04, -0.01]; p=0.002; ES [95% CI] = -0.87 [-1.41, -0.30]). However, no other gait characteristics were significantly different pre versus post 12 x 40 m sprints, irrespective of speed. The reduction in K_{vert} during sprinting, a result consistent with lab-based studies, demonstrates the sensitivity of thoracic-worn accelerometers for detecting fatigue-related changes in running gait. This presents an opportunity to monitor K_{vert} in high-speed running throughout training or matches which could be used to provide additional insight into changes in athlete movement strategy during running. In turn, this could be useful data for monitoring running specific fatigue in sport. However, a repeated sprint protocol does not result in altered gait mechanics in subsequent running at lower speeds. This may be because it is possible to maintain components of gait (e.g., contact time, flight time etc.) at slow speeds whilst running at high-speed may place constraints on the ability to manipulate these variables. In addition, the substantially lower distances covered in 12 x 40 m sprints compared to that of competition may not provide a large enough stimulus to elicit changes in gait at low speed. It is possible a combination of repeated sprints and high volumes of submaximal running may induce a different fatigue response at slower speeds than that observed in Study 3.

Given the protocol of the previous study was not a realistic representation of intermittent and multidirectional team-sport activity profile, Study 4 utilised the soccer-specific aerobic fitness test (SAFT^{90}) as the fatigue intervention to assess the changes in running gait within and post-match. The SAFT^{90} elicits similar volumes of running (~10-11 km) to competitive matches but allows greater experimental control for measuring the fatigue response within and post-match in a timely manner. Additional aims of this study were to assess the responses in a range of jump variables and whether the fatigue-related changes in running gait were impacted by lower body strength and power or intermittent endurance capacity. Eight participants performed a battery of tests to profile their physical capacity which included CMJ, drop jump (DJ), squat jump (SJ), isometric mid-thigh pull and Yo-Yo Intermittent Recovery Level 1 test. Approximately five days later, participants completed the $SAFT^{90}$ match simulation over 2 x 45-minute halves (3 x 15-minute segments per half) where running gait was assessed via additional 40 m run-throughs, as per Studies 2 and 3, pre-match and immediately following each 15-minute segment. Jump performance (CMJ, DJ and SJ) was also assessed pre-match, during the 15-minute halftime interval and post-match. To assess the time-course of recovery of running gait and jump variables, participants completed the same 40 m run-throughs and CMJ, DJ and SJ tests on the ensuing three days post-match (24, 48 and 72 hours). However, the results of this study are incomplete due to delays caused by the COVID-19 pandemic. Although a comprehensive statistical analysis has not been performed, mean ± SD values of contact time, step length and K_{vert} in running and passive stiffness in jumping from the data collected to this point (*n* = 8) are provided. Contact time went from 0.225 ± 0.018 s pre-match to 0.232 ± 0.017 s post-match at 3-4 $m \cdot s^{-1}$, while at 7-8 $m \cdot s^{-1}$, contact time was 0.136 ± 0.011 s pre-match and 0.141 ± 0.011 s following the first 15-minute segment of the $SAFT^{90}$ in the second half. Step length at 5-6 $m \cdot s^{-1}$ was 1.68 ± 0.18 m pre-match but 1.59 ± 0.14 m at $post_{48}$, while K_{vert} at 7-8 $m \cdot s^{-1}$ was 92.01 ± 17.84 $kN \cdot m^{-1}$ and 88.64 ± 24.07 $kN \cdot m^{-1}$ at pre- and post-match time points, respectively. Passive stiffness from the DJ went from 9.36 ± 5.17 $kN \cdot m^{-1}$ pre-match to 8.47 ± 3.86 $kN \cdot m^{-1}$ and 7.78 ± 3.92 $kN \cdot m^{-1}$ at halftime and $post_{72}$, respectively.

In summary, Study 1 demonstrated that IMU placement site is not a limiting factor to the measurement of running gait, which can in fact be validly and reliably measured from multiple locations (foot, tibia and lumbar spine). The results from Study 2 confirm this as it was shown thoracic-worn IMUs, including those contained in GNSS units, are accurate for event detection (a previously unreported finding) and are valid and reliable for deriving a range of spatiotemporal gait characteristics, $vGRF_{peak}$ and K_{vert} at different running speeds. Practitioners do not need to use additional sensors at other sites to analyse running gait but can instead take advantage of commonly worn sensors contained in GNSS units. These are also sensitive to detecting fatigue, as demonstrated in Study 3 which showed reductions in K_{vert} during sprinting. This result is consistent with the fatigue-induced changes of K_{vert} seen in other lab-based studies, and it provides evidence of the changes that occur in running at a mechanistic level that have so far not been quantifiable from GNSS-embedded IMUs. This allows for potential practical applications such as monitoring changes in K_{vert} and other metrics within training and matches which may reduce the requirement of additional testing protocols (e.g., CMJ) to assess fatigue. In addition, running gait characteristics, such as $vGRF_{peak}$, may be useful for informing the delivery of lower-limb injury rehabilitation or to assess changes in movement (running) strategy following concussion. Overall, the findings presented in this work support the use of IMUs contained within GNSS units for the analysis of running gait in the field.

1 Chapter 1: Introduction and Overview

This introductory chapter provides a general overview of the underlying concepts and research addressed in this thesis and is a prelude to the systematic review and meta-analysis study.

Monitoring training and competition load is important for optimising adaptation and minimising the risk of unintended fatigue, injury or illness, and may be quantified by internal or external measures [1]. In running-based sports, it is common to quantify external load using global navigation satellite system (GNSS) units to determine the distances and speeds an athlete has run [2]. Although distance and speed are useful measures of external load, GNSS cannot account for non-locomotor activity, such as jumps, changes of direction, foot-ground impacts or collisions [3-6]. Without the quantification of these other forms of physical stress, it is possible external load may be underestimated. However, there are other wearable technology solutions that overcome some of the limitations of GNSS and are capable of quantifying different movement patterns other than distance and speed [7].

Inertial measurement units (IMUs) contain high sample rate (≥100 Hz) accelerometers, gyroscopes and magnetometers which measure the gravitational acceleration, angular velocity rate and orientation of the unit in three axes (anteroposterior, mediolateral and vertical). A variety of external load metrics can be derived from IMUs that enable a detailed analysis of player movement and are capable of detecting sport-specific tasks, such as fast bowling and throwing events, tackles and changes of direction to name a few [4, 5, 8, 9]. One accelerometer-derived metric that is often used in sport is PlayerLoad™ which is calculated from the summation of instantaneous rate of change in acceleration in each of the three axes that provides a gross representation of overall external load [10]. PlayerLoad™ has been shown to be sensitive to fatigue as measured by a reduction in the contribution of the vertical accelerometer vector to the total PlayerLoad™ value, and this suggests athletes adopt a different movement strategy when fatigued [11, 12]. However, PlayerLoad™ does not specifically tell you the precise mechanisms that have resulted in any change in the composite accelerometer vectors.

A proposed explanation for changes to the way PlayerLoad™ is produced is alterations in vertical stiffness (K_{vert}) [11]. Stiffness represents the body's ability to resist deformation in response to a given force [13]. In running, K_{vert} describes the motion of the centre of mass during ground contact in relation to the vertical ground reaction force, and may be calculated from a spring-mass model equation with a small number of input variables (i.e., contact time, flight time and body mass) [14]. Fatigue-induced modifications to the spring-mass system result in an impaired ability to resist collapse of the lower body during ground contact which is characterised by a "Groucho" running pattern (i.e., increased knee flexion and displacement of centre of mass) that may result in a higher oxygen cost at a given speed [15]. Given the implications K_{vert} has on running performance, it is worthwhile quantifying it along with its constituent parts (i.e., contact time and flight time) to understand how fatigue impacts an athlete's running gait mechanics.

The analysis of running gait has traditionally been performed in lab-based settings utilising motion capture or force plate measuring systems [16]. However, it is also possible to derive running gait characteristics from IMUs which allows analysis within an athlete's normal training or competition environment [17, 18]. Gait event detection algorithms have been developed to identify initial contact (IC) and toe-off (TO) from the peaks in IMU signals (i.e., accelerometer or gyroscope) that can subsequently be used for the calculation of running spatiotemporal variables, including those used for quantifying K_{vert} (i.e., contact time and flight time) [17-19]. However, the analysis of running gait requires attaching IMUs to the foot, tibia or lumbosacral region [17-19], whereas these devices are contained in GNSS units and worn at the level of the thoracic spine in many running-based sports [11]. Despite IMUs being readily available within GNSS units, practitioners are currently required to use additional IMUs for gait analysis. However, in cases where IMUs are attached to the lower limb in contact sports, there poses the potential for injury resulting from impact [20]. In addition, it may not be feasible to use additional devices given the cost associated with purchasing multiple IMUs to analyse a large group of athletes and likely limits the ability to record data during matches where foot- or tibia-mounted IMUs are not permitted.

Preliminary work has investigated the validity and reliability of IMUs attached to the thoracic spine to derive temporal characteristics of gait (i.e., contact time and flight time) and K_{vert}, but the findings have been inconsistent [21, 22]. For example, earlier work reported Pearson correlation coefficients as high as 0.98 for contact time and K_{vert}, respectively, compared to instrumented treadmill values [21]. Conversely, Pearson correlation values were only 0.66 for thoracic-derived K_{vert} compared to a force plate and the coefficient of variation (CV) for reliability was 9.5% in another study [22]. In addition, the methods used in such studies are difficult to replicate due to a lack of information on the steps used to determine discrete gait events (IC and TO) from the inertial data [21, 22]. As a result, it is unclear whether the thoracic spine site is, in fact, valid and reliable to analyse running gait from IMUs, so a thorough investigation is required. Should the level of the thoracic spine be a viable attachment site for IMUs, it has the potential to allow practitioners to measure running gait alongside distance and speed metrics from the one device, minimising the need for multiple sensors that is currently a requirement. Given IMUs are already contained in GNSS units, this could provide opportunities to monitor changes in running gait in team-sport training and matches where these data may be useful for a detailed analysis of modifications to athlete movement (running) strategy during fatigue.

This thesis comprehensively assesses the validity and reliability of IMUs attached to the thoracic spine to derive gait characteristics during running and determine whether fatigue-induced changes in an athlete's running pattern are quantifiable from this site. The specific aims of this research were:

- Conduct a systematic review and meta-analysis to examine the impact of IMU placement site on the validity and reliability of gait characteristics during running (See: Study 1 – Chapter 3).
- Determine the validity and reliability of IMUs attached on the thoracic spine to derive gait characteristics during running and compare the outcome measures to those calculated from IMUs worn on the tibia and lumbar spine (See: Study 2 – Chapter 4).
- Investigate the impact a repeated sprint protocol has on changes in gait characteristics derived from IMUs attached to the thoracic spine (See: Study 3 – Chapter 5).
- Assess the impact of a simulated team-sport match on the time-course of changes in gait characteristics derived from thoracic-mounted IMUs and determine whether physical capacity (lower body strength, power and intermittent endurance capacity) protects against fatigue-related changes in gait (See: Study 4 – Chapter 6).

Overall, following the current chapter this thesis comprises:

- Chapter 2 which is a narrative review introducing the theoretical concepts underpinning this thesis.

- Chapter 3 which contains a systematic review and meta-analysis about the impact of IMU placement on the validity and reliability of deriving running gait characteristics.
- Chapters 4-5 which contain published experimental studies addressing the aims outlined above.
- Chapter 6 which details the progress of a third experimental study that was ultimately impacted by delays in participant recruitment and data collection following the COVID-19 pandemic.
- Chapter 7 which comprises an overall discussion, conclusion and limitations of this body of work.
- Chapter 8 which provides an extended methodology.

2 Chapter 2: Narrative Review

This narrative review chapter is an extension to the introductory chapter and provides an extended theoretical background for the concepts covered in subsequent sections of this thesis.

2.1 Training Process

Athletes undertake training to maximise their technical, tactical, psychological and physical performance. The training process requires careful consideration and planning to achieve an optimal balance between training stress and recovery in order to maximise adaptation [1]. This adaptive process to training may be explained by the General Adaptation Syndrome (GAS) which describes the different stages of the physiological response to stress [23]. An athlete's performance decreases when exposed to an acute training stress (alarm stage), whereas in the days following, adaptation occurs and performance improves above initial levels (resistance stage) [23, 24]. However, when recovery is insufficient and an athlete is continually exposed to training stressors, adaptation is impeded and a decrement in performance will result (exhaustion stage) [23]. The fitness-fatigue model conceptualises performance as a function of fitness minus fatigue [25, 26]. Performance is increased when fitness exceeds fatigue, whereas performance is reduced when fatigue outweighs fitness [26]. The GAS and fitness-fatigue models provide a theoretical framework for the adaptation process and the different responses to training. Understanding fitness and fatigue influences physical performance allows optimal planning of training in order to elicit the required performance outcomes [25]. An important part of the planning process is the quantification of training and competition in order to ensure adaptation whilst minimising unplanned fatigue, injury or illness [1].

2.2 Quantifying Training Load

Training load can be quantified via internal or external measures, where internal load refers to the pyscho-physiological response of the athlete, whereas external load captures what the athlete did [1]. Examples of internal load measures include rating of perceived exertion [27], heart rate and blood lactate concentration [28]. Conversely, examples of external load include distance, speed and number of skill executions [29]. External load is often measured in sport using time-motion analysis via microtechnology sensors such as global navigation satellite system (GNSS) tracking that allows real-time data collection during training and competition [30]. This technology provides data on the position of an athlete over time and can be used to profile the distances covered in a range of speed and acceleration zones [31-34]. However, due to requiring satellite signal, GNSS is largely limited to use in outdoor sports [30]. Other technologies, such as computer vision and local positioning systems (LPS), exist that make tracking the position of an athlete possible in indoor sports [35, 36]. A variety of external load metrics can be derived from GNSS, but representations of high speed running and sprinting, particularly over short distances or during non-linear movements, are more susceptible to error [2]. In addition, GNSS cannot quantify non-locomotor actions such as jumps, impacts or collisions that are common in many team-sports [3, 4]. Despite some limitations of GNSS, an area of focus for practitioners using this technology has been the potential to quantify fatigue development in matches, and some work has shown the possibility of this as measured by reductions in high-intensity running [31, 37]. However, GNSS-derived metrics, such as high-intensity running, can be maintained even in the presence of fatigue [38]. Additionally, such metrics may also be influenced by other contextual factors, such as team or opposition tactics, playing position and scoreline [34]. As a result, this makes classifying an athlete as fatigued based on GNSS data alone difficult, so other assessments and/or technology should therefore be considered.

2.3 Assessment of Fatigue

Fatigue itself is a disabling symptom in which physical and cognitive function is limited by interactions between fatiguability and perceived fatiguability [39]. The duration and intensity of exercise impacts the extent of acute fatigue experienced by the athlete which results in reduced force production capability and short-term decrements in performance [40]. However, fatigue is a necessary stage in the adaptation process [1]. Periods of planned high-load training aim to induce what is referred as “functional overreaching” which, when followed by a period of recovery, results in improved capacity [41]. When high training loads are continued for extended periods, athletes can enter a state of “non-functional overreaching” which is characterised by performance decrements that may last for weeks [41]. The continuation of excessively high loads has the potential to lead to “Overtraining Syndrome” (OTS) which is characterised by performance decrements and psychological disturbance in the absence of any underlying disease/medical condition which can persist for weeks or months despite reductions in load [42]. However, diagnosis is difficult and evidence relating to understanding OTS in athletes is limited [43]. Therefore, it is important to minimise unplanned fatigue and reduce the potential for subsequent injury or illness.

2.3.1 Direct Measures of Fatigue

During exercise performance, the fatigue-induced changes in force production capability can originate at the central nervous system (central fatigue) or in the musculature and supporting cellular structures (peripheral fatigue) [40]. The origin of neuromuscular fatigue (NMF) can be differentiated post-exercise using electrical or magnetic stimulation [44, 45]. Central fatigue is representative of a reduction in neural drive to the muscle (i.e., proximal of the neuromuscular junction), and this occurs when stimulation results in a force response during a maximal voluntary contraction which indicates that activation of the muscle is less than maximal [44, 45]. Conversely, peripheral fatigue is a loss of force-generating capacity of the muscle's contractile mechanism [46]. Peripheral fatigue is determined to be the limiting factor to force production when no increase in force is observed following a superimposed twitch using electrical or magnetic stimulation [45]. Team-sport matches (both simulated and real) have been shown to result in reductions in voluntary muscle activation (representing central fatigue) post-match [47, 48], while other work has shown similar reductions in voluntary muscle activation and potentiated twitch (suggesting peripheral fatigue) as soon as halftime [49, 50]. Although electrical or magnetic stimulation provides a gold standard assessment of NMF and allows the location at which fatigue occurs to be identified, it is an impractical measure to use in field settings [51]. Stimulation techniques require extensive equipment and are limited to laboratory settings. In addition, such assessments usually involve isometric-only exercises which do not reflect the stretch-shortening cycle (SSC) activity seen in team-sport, such as running and jumping [52].

2.3.2 Performance Tests to Assess Fatigue

Many sports require repetitive SSC activity which can result in low-frequency fatigue (LFF) [51]. Low Frequency Fatigue may manifest as reduced rate of force development during maximal exertions or a decline in power output in sustained dynamic exercise [51, 53]. As a result, SSC tasks may be useful for the assessment of NMF [51]. A commonly used SSC activity prevalent in team-sport for the assessment of NMF is the countermovement jump (CMJ). [54, 55]. Whilst some research has used outcome measures from a CMJ (e.g., jump height) [56-58], metrics such as flight time:contraction time (FT:CT) representing movement strategy may be more sensitive than outcome measures in the assessment of fatigue [11, 12]. However, despite its validity, reliability and sensitivity to fatigue, the CMJ can only be performed post training or matches, and as such, it does not give an indication of fatigue during the activity (i.e., sport) itself and requires completion of an additional task to training and/or competition. Furthermore, although a CMJ and running both involve the SSC, the assessment of fatigue during running would be the most ecologically valid solution. As the SSC and stiffness of the lower-limb (particularly leg stiffness [K_{leg}] and vertical stiffness [$K_{vert)}$]) are two important neuromuscular components that regulate elastic energy utilisation during running [59], it is potentially an attractive proposition for practitioners to be able to monitor these characteristics in the field. Fortunately, commonly available sensors in the form of inertial measurement units (IMUs) may allow this.

2.4 Inertial Sensors

The quantification of more non-linear movements, such as distance and speed from GNSS, is becoming increasingly popular in applied sports science and research [7]. This is possible via IMUs which contain high sample rate (e.g., 100 Hz) triaxial accelerometers, gyroscopes and magnetometers which provide data on gravitational acceleration, change in rotational angle and heading location of the device, respectively. Historically, accelerometers have been used in tracking physical activity and sleep patterns in clinical and general populations [60, 61]. However, IMUs may also be used for more advanced movement pattern detection in sport, such as, but not limited to, identifying tackles and collisions in contact sports [4, 62], the automatic detection of pitching and throwing events in baseball [8] and fast bowling deliveries in cricket [9, 63]. Although a variety of manufacturers (e.g., IMeasureU Ltd., Xsens, Stryd, PlayerMaker™ etc.) provide commercially available stand-alone IMUs that can be used in sport, these sensors are also contained with GNSS units commonly worn by team-sport athletes. As such, the external load of athletes can be quantified during regular training and matches using a variety of metrics derived from the inertial data (e.g., accelerometer).

2.4.1 Proprietary Accelerometer Metrics

In team-sport, it is common to quantify accelerometer-derived load using proprietary metrics [10, 64]. One of the most commonly used metrics within sports science practice and research is Catapult Sports' PlayerLoad™ which is based on the summation of instantaneous rate of change in acceleration in each of the vertical, mediolateral and anteroposterior axes and provides a gross representation of overall external load [65]. Dynamic Stress Load (DSL) is the STATSports® (another major GNSS technology provider) equivalent to PlayerLoad™ where its calculation is similarly based on linear accelerations in the three movement planes [64, 66]. PlayerLoad™, particularly, has been shown to be sensitive to detecting fatigue during simulated and real team-sport matches [11, 12]. From this work, athletes deemed fatigued due to decrements in FT:CT from a CMJ had a reduction in the contribution of the vertical accelerometer vector to the total PlayerLoad™ value during team-sport activity, and this suggests there is a fatigue-driven modification to movement strategy [11, 12]. However, a limitation of proprietary metrics like PlayerLoad™ is that they do not explain the precise mechanisms responsible for the modification to the individual accelerometer vectors' contribution to total the PlayerLoad™ value. Given fatigue can manifest in altered running gait mechanics [67, 68], it may be plausible to suggest that reductions to the vertical vector may be a result in changes to K_{vert} and its underlying components (e.g., contact time and flight time) [11].

2.5 Lower-limb Stiffness

Stiffness itself describes the body's ability to withstand deformation in response to a given force [13], where during the contact or stance phase of running, the leg's behaviour is like that of a spring as it compresses and decompresses in a cyclical manner [59, 69]. Greater lower-limb stiffness is suggested to be favourable in activities where transferring a given impulse more rapidly would be advantageous, such as during running at near maximum velocities [70]. There are different ways in which to assess lower-limb stiffness during running, and these include the calculation of K_{leg} and K_{vert}.

2.5.1 Leg Stiffness

One type of lower-limb stiffness is K_{leg} which is defined as the ratio of peak vertical ground reaction force to peak leg compression during the contact phase of running.[71], and essentially describes how the tissues of the leg (i.e., muscles, tendons and ligaments) behave under compression. Peak vertical ground reaction force increases with running velocity, but leg stiffness tends to be maintained due to the length of the leg spring also increasing with speed [14, 72]. The change in total leg length with velocity is explained by increases in the arc through which the legs travel, and the ensuing increases in leg spring length offset those for peak vertical ground reaction force [13]. Subsequently, other measures of stiffness, such as K_{vert}, have been proposed to be more sensitive than K_{leg} when investigating the relationships with running performance [73].

2.5.2 Vertical Stiffness

Unlike K_{leg} which describes the amount of leg compression during running, K_{vert} represents the vertical motion of the centre of mass during ground contact after application of vertical ground reaction force [13]. Several models exist to calculate K_{vert}, but it is most commonly obtained from the quotient of maximum ground reaction force and centre of mass displacement [74]. Given peak vertical ground reaction force is an input variable for the calculation of K_{vert}, it would appear reasonable to suggest that increases in force would mirror those in K_{vert}. However, this is not the case as displacement of the centre of mass is reduced at higher velocities compared to slower speeds, so increases in K_{vert} during high velocity running tends to be mediated by increases in step frequency and decreases in contact time [75]. Conversely, in a fatigued state, K_{vert} has been shown to be reduced, and this can result in the adoption of a "Groucho" running pattern [15].

2.5.3 Groucho Running

The reduction in K_{vert} with fatigue has been identified because of increases in centre of mass displacement and ground contact time (i.e., stance phase of the running gait cycle). As a result of the mechanical changes in COM and contact time, runners take on a Groucho running pattern that is characterised by increased knee flexion, or simply running with the knees bent more than usual where the flight phase is essentially absent [15]. This running pattern has implications for sprinting performance and the ability to accelerate and decelerate which are important qualities for team-sport [15, 67]. In addition, due to the longer contact times during the stance phase, athletes who adopt a Groucho-style running pattern have a higher oxygen cost at a given speed [15]. This ultimately reduces running economy and further compromises an already inefficient movement pattern [15]. Couple the potential deleterious effects of fatigue on running mechanics and efficiency with the fact many team-sports are running-based, it would appear useful to monitor within field settings. The ability to quantify running gait metrics, such as K_{vert}, would also allow the analysis of individual athlete running patterns at a more discrete level than global external load metrics (e.g., distance, speed, PlayerLoad™ etc.) and provide insight into changes in movement strategy as a result of fatigue or during the rehabilitation process from lower limb injury.

2.6 Gait Analysis

Assessment of the biomechanical features of running gait, including spatiotemporal variables (e.g., contact time, step frequency and step length), K_{vert} and its constituent parts (e.g., peak vertical ground reaction force), has traditionally been conducted in laboratory settings [16, 67]. The analysis of running gait from technologies such as video analysis, three-dimensional motion capture, force plates and instrumented treadmills has allowed a more extensive understanding of the characteristics of gait and how these are affected under a variety of conditions, such as fatigue [67, 76]. However, such tightly controlled lab-based environments are not readily accessible by athletes [77]. As such, field based alternatives for the analysis of running gait may be useful. Due to their portability and small size, IMUs offer an attractive solution for practitioners to gain insight into discrete metrics related to running gait within an applied setting [78].

2.6.1 IMUs for Gait Analysis

Numerous studies have demonstrated the validity and reliability of IMUs for deriving a variety of spatiotemporal variables compared to accepted criterions for gait analysis (e.g., motion capture and fore plate systems) [17, 21, 79-82]. These studies have largely involved attaching IMUs to the foot, distal end of the tibia and on the lumbosacral region and used varying levels of computation to identify patterns within the inertial data that are representative of key gait events, such as initial contact (IC) and toe-off (TO). This has typically been analysed from accelerometer data alone [17, 19, 79], while other studies have leveraged the gyroscope sensor to detect IC and TO [18, 83]. By analysing the accelerometer or gyroscope waveforms from data collected from IMUs attached to the lower-limb or lumbosacral region, it is possible to calculate a variety of spatiotemporal variables, including contact time, flight time, step frequency and step length, and use some of these (e.g., contact time and flight time) as inputs to estimate of K_{vert} [17, 79, 83-85]. However, validation and reliability studies have largely been conducted using IMU attachment locations that are not reflective of where these sensors are worn in team-sport (i.e., the thoracic spine).

2.6.2 Thoracic Spine Placement

In team-sport athletes, GNNS devices are worn at the level of the thoracic spine, and as they also house IMUs, using data from these sensors at this location is an attractive option for practitioners. However, few studies have assessed the validity or reliability of IMUs contained within GNSS units worn on the thoracic spine for quantifying running gait metrics [21, 22, 86]. As a result, for practitioners to analyse running gait in the field, they are currently limited to wearing additional IMUs at other sites (e.g., foot or distal tibia). This is likely not practical due to the cost of purchasing additional IMUs and in sports where contact may pose a potential risk of injury when IMUs are attached to sites other than the thoracic spine [20]. Although the level of the thoracic spine may be considered too far from the foot-ground interface to analyse accurately and reliably running gait compared to more traditional attachments (e.g., foot), it is currently unclear whether placement site itself is a limiting factor to validity and reliability. Consequently, there is a need for further investigation into whether the thoracic spine is a viable site for attaching IMUs to analyse running gait in the field.

3 Chapter 3: Study One – Does Site Matter? Impact of Inertial Measurement Unit Placement on Validity and Reliability of Stride Variables During Running: A Systematic Review and Meta-analysis

Publication statement:

This chapter is in the publication form of the following paper in *Sports Medicine*.

Horsley, B.J., et al., *Does site matter? Impact of Inertial Measurement Unit placement on the validity and reliability of stride variables during running: a systematic review and meta-analysis.* Sports Medicine, 2021. **51**: p. 1449-1489.

Please note that “stride variables” is used throughout this chapter as an overarching term to describe spatiotemporal, force and stiffness measures of running gait. All other chapters of this thesis use “running gait characteristics” instead following feedback during the review process of subsequent papers.

3.1 Abstract

Background: Inertial measurement units (IMUs) are used for running gait analysis in a variety of sports. These sensors have been attached at various locations to capture stride data. However, it is unclear if different placement sites affect the derived outcome measures.

Objective: The aim of this systematic review and meta-analysis was to investigate the impact of placement on the validity and reliability of IMU-derived measures of running gait.

Methods: Online databases SPORTDiscus with Full Text, CINAHL Complete, MEDLINE (Ebscohost), EMBASE (Ovid) and Scopus were searched from the earliest record to 6 August 2020. Articles were included if they 1) used an IMU during running 2) reported spatiotemporal variables, peak ground reaction force (GRF) or vertical stiffness and 3) assessed validity or reliability. Meta-analyses were performed for a pooled validity estimate when 1) studies reported means and standard deviation for variables derived from the IMU and criterion 2) used the same IMU placement and 3) determined validity at a comparable running velocity ($\leq$1 m·s^{-1} difference).

Results: Thirty-nine articles were included, where placement varied between the foot, tibia, hip, sacrum, lumbar spine (LS), torso and thoracic spine (TS). Initial contact, toe-off, contact time (CT), flight time (FT), step time, stride time, swing time, step frequency (SF), step length (SL), stride length, peak vertical and resultant GRF and vertical stiffness were analysed. Four variables (CT, FT, SF and SL) were meta-analysed, where CT was compared between foot, tibia and LS placements and SF was compared between foot and LS. Foot placement data was meta-analysed for FT and SL. All data are mean difference (MD [95%CI]). No significant difference was observed for any site compared to the criterion for CT (foot: -11.47 ms [-45.68, 22.74], p = 0.43; tibia: 22.34 ms [-18.59, 63.27], p = 0.18; LS: -48.74 ms [-120.33, 22.85], p = 0.12), FT (foot: 11.93 ms [-8.88, 32.74], p = 0.13), SF (foot: 0.45 step·min^{-1} [-1.75, 2.66], p =

0.47; LS: -3.45 step·min^{-1} [-16.28, 9.39], p = 0.37) and SL (foot: 0.21 cm [-1.76, 2.18], p = 0.69). Reliable derivations of CT (coefficient of variation [CV] <9.9%), FT (CV <11.6%) and SF (CV <4.4%) were shown using foot- and LS-worn IMUs, while the CV was <7.8% for foot-determined stride time, SL and stride length. Vertical GRF was reliable from the LS (CV = 4.2%) and TS (CV = 3.3%) using a spring-mass model, while vertical stiffness was moderately (r = 0.66) and nearly perfectly (r = 0.98) correlated with criterion measures from the TS.

Conclusion: Placement of IMUs on the foot, tibia and LS are suitable to derive valid and reliable stride data, suggesting measurement site may not be a critical factor. However, evidence regarding the ability to accurately detect stride events from the TS is unclear and this warrants further investigation.

3.2 Introduction

It is common practice to quantify the activities performed by athletes, or external load, to plan and monitor training and competition load [87]. Tracking technology, such as video-based systems, global positioning systems (GPS) and local positioning systems (LPS), measure athlete displacement and calculate velocity and acceleration [33, 88-90]. However, due to its low sampling frequency (e.g. 10 Hz), GPS is limited in its ability to accurately capture changes in velocity or high-speed movements over short distances and when movements are nonlinear, such as changes of direction [91-93]. Although LPS (1000 Hz) sample at a higher rate than GPS, neither technology can account for non-locomotor activity, such as impacts or collisions [10, 62, 94, 95]. To overcome some of the limitations of GPS and LPS, inertial measurement units (IMUs), comprising accelerometers, gyroscopes and magnetometers, can provide additional information on athlete activity profiles [20, 96].

Triaxial accelerometers measure acceleration in the anteroposterior, mediolateral and vertical axes and typically capture data between 100 and 1000 Hz [20, 65, 97]. Gyroscopes and magnetometers measure device orientation and direction, respectively [98]. Accelerometers have been used for quantifying daily physical activity and estimating energy expenditure [99-103] and their use is now common in athletes [3, 8, 62, 63, 95]. Accelerometer-derived metrics, such as PlayerLoad™, provide an indication of global external load from the summation of instantaneous rate of change of acceleration in the anteroposterior, mediolateral and vertical axes [65, 104]. However, PlayerLoad™ is a relatively gross measure that does not offer insight into discrete movements, such as stride variables. Instead, patterns in the signals of IMUs can be explored to identify foot contacts to calculate different stride variables, which may help in understanding the way in which athletes produce a given load [11, 38].

The detection of gait events, such as initial contact (IC) and toe-off (TO), is possible using accelerometer and gyroscope data [17, 19, 105]. Identifying these key events allows for the calculation of spatiotemporal parameters, including contact time, flight time, step and stride times, step frequency and step and stride lengths [17, 79, 83-85]. The acceleration signal from IMUs may also be used to estimate ground reaction forces (GRFs) and vertical stiffness to describe the impact forces experienced by athletes and their ability to absorb force during running [21, 22, 106-108]. Deriving stride variables is important for evaluating an athlete's gait pattern and may help to inform injury mitigation and performance enhancement strategies [16]. However, device placement may influence the derived outcome measures and should be considered when using IMUs to capture stride data [109, 110].

Placement of IMUs for analysis of running gait can vary between the foot [6, 17, 83], distal and mid tibia [19, 20, 108], lumbosacral region [17, 79, 84] or thoracic spine [21, 107, 110]. Given accelerometers measure acceleration of the segment to which it is attached, there are some potential issues associated with placement on the upper body to measure accelerations occurring at the lower limb and derive valid and reliable stride data [109]. Attachment location is an important consideration due to signal attenuation, whereby acceleration magnitudes dissipate from the foot to the torso during ground contact in running [111-113]. Although securing IMUs to the foot may provide the most accurate derivations of stride variables [83, 85, 97], this site may not be practical in some sports (such as those that involve kicking), while other work has noted the potential for injury in contact sports using IMUs attached to the tibia [6]. Given IMUs have been utilised at various sites for the analysis of running gait in the literature, it is important to understand if IMU placement affects the derived outcome measures. This may help inform practitioners which attachment location is most appropriate for deriving valid and reliable stride data based on the constraints of the sport they work in. Therefore, the aim of this systematic review and meta-analysis is to report on the validity and reliability of inertial sensors to calculate spatiotemporal variables, GRF and vertical stiffness during running with respect to sensor placement.

3.3 Methods

3.3.1 Systematic Review Protocol

The protocol for this systematic review was registered on PROSPERO and can be accessed at https://www.crd.york.ac.uk/prospero/display_record.php?ID=CRD42020160325. All procedures were performed in accordance with the PRISMA guidelines [114].

3.3.2 Eligibility Criteria

Articles were eligible for inclusion in this systematic review if they 1) were published in English 2) used an accelerometer, gyroscope or a combination of both technologies 3) had participants jog, run or sprint during data collection 4) reported at least one of the following outcome variables: IC, TO, contact time, flight time, step time, stride time, swing time, step frequency, step length, stride length, peak vertical or resultant GRF or vertical stiffness and 5) assessed validity or reliability.

3.3.3 Search Strategy

Keywords in the title and abstract of records, combined with relevant subject heading terms, such as Medical Subject Headings (MeSH), were systematically searched in SPORTDiscus with Full Text, CINAHL Complete, MEDLINE (Ebscohost), EMBASE (Ovid) and Scopus from the earliest record up until 6 August 2020. The following keyword search string was used in each electronic database (which is also detailed in Table 3-1):

(jog* OR run* OR sprint*) AND (acceleromet* OR "global positioning system" OR GPS OR gyroscope* OR IMU OR inertial* OR microtechnolog* OR “wearable sensor”) AND (acceleration* OR event* OR fatigue* OR force* OR GRF OR kinematic* OR kinetic* OR parameter* OR reliab* OR stance OR step* OR stiff* OR stride* OR strike* OR temporal OR valid*)

3.3.4 Study Selection

Search results were exported to reference management software EndNote X9.3.3 (Clarivate Analytics, Philadelphia, USA) where duplicates were removed. Two authors (BJH and PJT) then independently screened the title and abstract of each record in the Rayyan web-based systematic review tool (available at www.rayyan.qcri.org). The full text of potentially eligible articles was retrieved and one author (BJH) performed a final eligibility assessment, which was later checked by a second author (PJT). Discrepancies in article selection were resolved by a third author (SJC). The reference lists of all retrieved articles were also examined to determine any other articles that may be relevant to the review.

3.3.5 Data Extraction

Data relating to participant characteristics (age, body mass, height and activity level), sensor specifications (brand, model, range and sampling frequency), sensor location (foot, distal/mid tibia, hip, sacrum, lumbar and thoracic spine), criterion used for validity (brand, model and sampling frequency), running activity performed (number, duration or distance of runs, velocity), outcome variables analysed (temporal, spatial, GRF and vertical stiffness) and measures of validity and reliability were extracted from each included study. Definitions for the variables analysed in this review are presented in Table 3-2. Running velocity, temporal and spatial variables and GRF are reported in metres per second ($m \cdot s^{-1}$), milliseconds (ms), centimetres (cm) and Newtons (N), respectively. Where included studies did not report results in the aforementioned units, values were converted to enable better comparison between studies.

3.3.6 Assessment of Methodological Quality

The methodological quality of each included study was assessed using a modified assessment scale of Downs and Black [115]. Of the 27 criteria, the most relevant to the study designs included in this review were applied, which is consistent with other reviews [30, 116]. Each study was therefore assessed for quality of reporting (1-4, 6, 7 and 10), external validity (11 and 12) and internal validity bias (16, 18 and 20) based on 12 criteria. The criteria were evaluated as yes, no or unclear, with the score out of 12 determined from the number of items that were answered yes.

Table 3-1. Keywords used in electronic database search.

	Concept 1 Activity	Concept 2 Sensor	Concept 3 Measure
Keywords	Jog* Run* Sprint*	Acceleromet* "Global Positioning System" GPS Gyrocope* IMU Inertial* Microtechnolog* "Wearable sensor"	Acceleration* Event* Fatigue* Force* GRF Kinematic* Kinetic* Parameter* Reliab* Stance Step* Stiff* Stride* Strike* Temporal Valid*
MeSH Terms (SPORTDiscus)	JOGGING RUNNING SPRINTING	ACCELEROMETERS GLOBAL Positioning System GPS Receivers	ACCELERATION (Mechanics) FATIGUE KINEMATICS KINEMATICS in sports
MeSH Terms (MEDLINE)	Jogging Running	Accelerometry Microtechnology Wearable Electronic Devices	Acceleration Fatigue Spatio-Temporal Analysis
MeSH Terms (CINAHL)	Jogging Running Sprinting	Accelerometers Global Positioning System Microtechnology Wearable Sensors	Acceleration (Mechanics) Fatigue Ground Reaction Force Kinematics Kinetics Reliability Validity

Table 3-2. Definitions of stride variables.

Variable	Definition
Initial contact	The time instant when the foot initiates contact with the ground [83].
Toe-off	The time instant when the foot ends contact with the ground [83].
Contact time	Time between initial contact to toe-off of each foot [21, 79]
Flight time	Time between toe-off and initial contact of the contralateral foot [21].
Step time	Time between initial contacts of the contralateral foot [79].
Stride time	Time between initial contacts of the same foot [79, 86].
Swing time	Time between toe-off to initial contact of the same foot [105].
Step frequency	Number of ground contact events per minute [85].
Step length	Length or distance between initial contacts of the contralateral foot [85].
Stride length	Length or distance between initial contacts of the same foot [117].
Ground reaction force	The force the ground exerts on the body during foot-ground contact [118].
Vertical stiffness	The quotient of maximum ground reaction force and centre of mass displacement [14].

3.3.7 Data Analysis

The values of validity and reliability for each stride variable are presented in the tables below and included throughout the results sections.

3.3.7.1 Meta-analysis

Meta-analyses were performed when there were at least two studies that 1) reported means and standard deviation (SD) for stride variables calculated from IMUs and reference systems 2) used the same IMU attachment site and 3) assessed validity at a comparable running velocity (≤ 1 $m \cdot s^{-1}$ difference). Authors that did not include absolute mean ± SD values for the computed stride variables were contacted to gain the additional data. Raw outcome data was not obtained for 22 studies and were thereby ineligible for inclusion in any meta-analysis [19, 21, 22, 79, 80, 83, 86, 108, 110, 117, 119-130]. Where there were multiple effects reported for different running velocities from a single study, data was aggregated so only a single effect was included in the meta-analysis [131]. However, when validity was assessed using IMUs from two different manufacturers [85] or criterion measures [105, 132] in a single study, effects were treated independently and both were included in the meta-analysis. Data pertaining to criterion validity was pooled from studies that used different reference measurement systems. Specifically, effects were pooled from studies that used motion capture [105], force plates [17, 133, 134], high-speed camera [85, 97, 132] and photocell systems [81, 132, 135]. This approach was used due to the limited number of studies with comparable methodologies and previous work demonstrating that optical timing and motion capture systems and force plate systems are all considered as criterion methods for gait analysis [136-138].

Where there was sufficient data to group effects based on eligibility criteria, meta-analyses were performed using random-effects models with the Meta statistical package in R software (version 3.6.3, R Foundation for Statistical Computing) to produce a pooled estimate of the mean difference (MD) in absolute units [139]. When studies could be pooled based on different IMU attachment sites for the same variable, subgroup analysis was performed to test whether placement differs in terms of their effects, with the significance level set at $p < 0.05$ [140].

The level of statistical heterogeneity was quantified by calculating the I^2 statistic [141]. Statistical heterogeneity was considered low ($I^2 < 25\%$), moderate ($I^2 = 25\text{-}49\%$) and high ($I^2 > 50\%$) [141]. When 1^2 was high ($I^2 > 50\%$), leave-one-out analysis was performed to determine the studies that contributed most to heterogeneity and had a high influence on the overall effect [142]. Moderator analysis was also conducted to determine how much the criterion measure contributed to the observed variability of effect sizes between studies [143]. Where the criterion does not have a significant moderating effect, heterogeneity may be attributable to an unidentified source [143]. A meta-regression model was applied to the moderator analysis using the metareg function in R software [144]. Statistical significance was set at $p < 0.05$.

Effect sizes and their respective confidence intervals (CI), along with the overall MD for pooled effects, were visualised as forest plots [145]. In forest plots, studies are represented by a point estimate, bounded by a 95% CI for the effect [145]. The summary effect (MD) is symbolised by the polygon at the bottom of the plot [145]. The width of the polygon indicates the 95% CI. Studies that exhibit larger squares contribute more to the summary effect (MD) compared to studies with smaller squares [145].

3.4 Results

3.4.1 Study Identification and Selection

A total of 4,654 records were identified through the database searches. An additional three articles were included through reference list searches. Following deduplication, title and abstract screening and a thorough full text screen of each record, 39 studies met the eligibility criteria and were included in the review [17, 19, 21, 22, 79-81, 83-86, 97, 105-108, 110, 117, 119-130, 132-135, 146-150]. An outline of this process using the PRISMA flow diagram is presented in Figure 3.1.

3.4.2 Study Characteristics

A summary of the characteristics of each study is presented in Table 3-3. A total of 657 participants were included across 39 studies (mean ± SD 16.8 ± 10.2), where the populations sampled included healthy active adults (*n* = 15 studies), recreational/amateur (*n* = 12) and high-level runners (*n* = 5), team-sport athletes (*n* = 6), elite track and field athletes (*n* = 1) and triathletes (*n* = 1). Sensor placement varied between foot [17, 81, 83, 85, 97, 117, 119, 122, 125, 126, 133, 148], distal and mid tibia [19, 80, 105, 108, 124, 126, 133, 134, 147], hip [130], sacrum [79, 123], lumbar spine [17, 22, 84, 129, 132, 133, 135, 146], torso [120] and thoracic spine [21, 22, 86, 106, 107, 110, 127, 149]. Two studies used multiple sensors and a combination of placements to derive stride variables [121, 150]. Validity was assessed using force plate systems (*n* = 17) [19, 22, 80, 84, 86, 106-108, 110, 121, 123-125, 127, 130, 133, 134], optical motion capture (*n* = 7) [79, 105, 117, 119, 121, 129, 148], instrumented treadmill (*n* = 7) [17, 21, 83, 120, 122, 126, 150], high-speed camera (*n* = 4) [84, 85, 97, 132], photocell systems (*n* = 3) [81, 132, 135], foot-mounted accelerometer (*n* = 1) [146], in-shoe piezo-electric force sensitive resistors (FSR) (*n* = 1) [128] and different stride time calculation methods (*n* = 1) [147] as criterions. Reliability was assessed in nine studies [22, 81, 97, 108, 110, 125, 132, 146, 149]. Contact time was the most commonly reported variable (*n* = 16) [17, 21, 79-81, 83-85, 97, 105, 119, 120, 132-134, 146], while six studies derived spatial data (step length and stride length) from accelerometers and gyroscopes [81, 85, 117, 119, 135, 148]. Eleven studies estimated peak vertical and resultant GRF [22, 106-108, 110, 121-123, 127, 130, 150], whereas three studies used accelerometers to derive vertical stiffness [21, 22, 149].

3.4.3 Methodological Quality

Based on the number of criteria that were answered yes, the methodological quality of included studies ranged from 7 to 10 out of 12, with a mean score of 9 out of 12 (see Table 3-4). Out of the 39 studies, 24 did not include p-values alongside validity or reliability outcomes [17, 19, 21, 22, 79, 83, 84, 105, 107, 108, 117, 120-122, 124, 125, 127-130, 135, 146, 147, 149], two studies did not clearly report subject characteristics [84, 128], while another study did not provide a description of the running protocol used for assessing validity [126]. Five studies scored a yes for detailing the source population from which subjects were recruited [19, 126, 146, 149, 150], whereas this was unclear in the remaining studies.

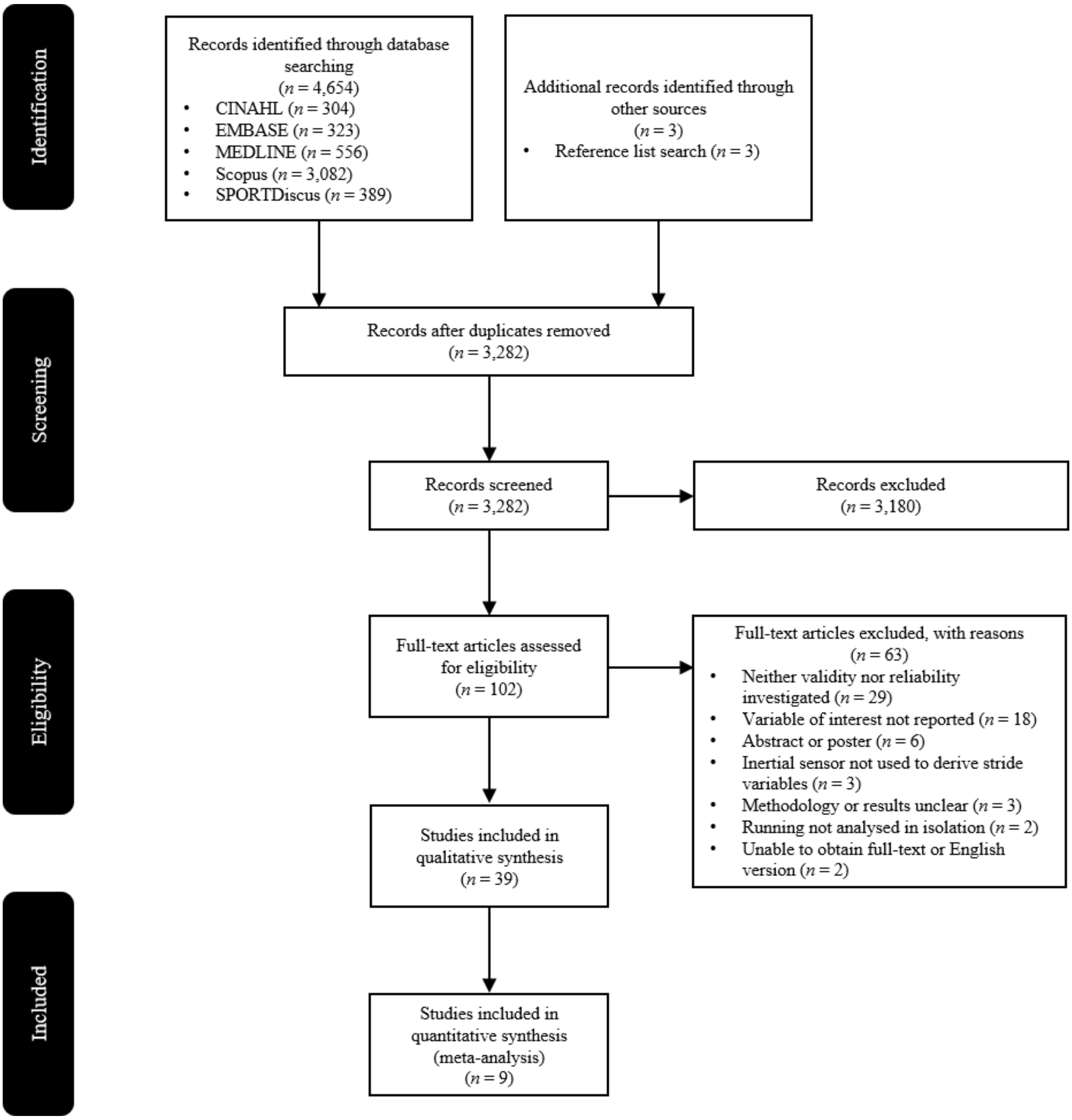

Figure 3.1. Flow chart of study selection process.

Table 3-3. Study characteristics for the 39 studies included in the review.

Study	Sample (age, mass, height)	Sensor	Hardware	Sensor placement	Criterion	Activity	Variable(s)	Methodological quality
Ammann et al. (2016) [97]	7 male and 5 female high-level running athletes (31 ± 6 y, 68.6 ± 11.6 kg, 1.70 ± 0.08 m)	IMU (PARTwear, HuCE-microLab, University of Applied Sciences, Biel, Switzerland)	Triaxial accelerometer (± 16 g), triaxial gyroscope and triaxial magnetometer sampled at 1000 Hz	Foot (fixed to the lace of the shoe)	High-speed camera (Camera Marathon Ultra CL600, Videal AG, Niederönz, Switzerland) sampled at 1000 Hz	3 x 40 m runs at 4.3 ± 0.7, 6.2 ± 0.7 and 8.0 ± 0.5 $m \cdot s^{-1}$	Contact time	10/12
Aubol & Milner (2020) [19]	9 male and 10 female recreational runners (26.2 ± 3.8 y, 71.5 ± 7.1 kg, 1.78 ± 0.06 m)	Accelerometer (Model 356A45, PCB Piezotronics, Depew, NY)	Triaxial accelerometer (± 16 g) sampled at 201.03 Hz)	Distal tibia	Force plate (AMTI, Inc., Watertown, MA) sampled at 1000 Hz	10 x 17 m runs at 3.0 ± 0.2 $m \cdot s^{-1}$	Initial contact	10/12
Benson et al. (2019) [17]	8 male and 4 female recreational runners (26.2 ± 3.8 y, 71.5 ± 7.1 kg, 1.78 ± 0.06 m)	Accelerometer (Shimmer3®, Shimmer Inc., Dublin, Ireland)	Triaxial accelerometer (± 16 g) sampled at 201.03 Hz)	Dorsal foot and lumbar spine	Instrumented split-belt treadmill (Bertec Inc., Columbus, OH) sampled at 1000 Hz	90 s runs at 2.7, 3.3 and 3.6 $m \cdot s^{-1}$	Initial contact, toe-off and contact time	9/12
Bergamini et al. (2012) [84]	5 elite track and field athletes	IMU (FreeSense, Sensorize, Italy)	Triaxial accelerometer (± 6 g) and triaxial gyroscope (± 500°s^{-1}) sampled at 200 Hz	Lumbar spine (L1 level)	Six adjacent force platforms (Z20740AA, Kistler, Switzerland) sampled at 200 Hz and high-speed camera (Casio Exilim EX-F1, Japan) sampled at 300 Hz	3 x 60 m maximal sprints	Contact time and stride time	8/12
Brahms et al. (2018) [148]	7 male and 4 female healthy adults (22.3 ± 1.5 y, 76.04 ± 3.19 kg, 175.2 ± 23.1 cm)	IMU (Xsens, Enschede, the Netherlands)	Triaxial accelerometer, triaxial gyroscope and triaxial magnetometer sampled at 100 Hz	Mid-foot	6-camera 3D motion capture system sampled at 100 Hz	20 x 10 m runs at 2.7 to 4.4 $m \cdot s^{-1}$	Stride length	10/12
Buchheit et al. (2015) [21]	1 team-sport athlete (36 y, 80 kg, 182 cm)	Accelerometer (SPI HPU, GPSports, Canberra, Australia)	Triaxial accelerometer (± 16 g) sampled at 100 Hz	Thoracic spine (T2 level)	Instrumented treadmill (ADAL3D-WR, MD, HEF Tecmachine, Andrézieux-Boutheon, France) sampled at 1000 Hz	2 x 3 runs at 2.8 $m \cdot s^{-1}$; 6 runs at 4.7 $m \cdot s^{-1}$; 6 runs at 6.7 $m \cdot s^{-1}$	Contact time, flight time and vertical stiffness	9/12
Buchheit et al. (2018) [149]	18 elite academy soccer athletes (17 ± 2 y)	Accelerometer (SPI HPU, GPSports, Canberra, Australia)	Triaxial accelerometer (± 16 g) sampled at 100 Hz	Thoracic spine	N/A	4 x ~60 m runs at 6.1-6.7 $m \cdot s^{-1}$)	Vertical stiffness	10/12

Table 2.3. Study characteristics for the 39 studies included in the review (continued).

Study	Sample (age, mass, height)	Sensor	Hardware	Sensor placement	Criterion	Activity	Variable(s)	Methodological quality
Chew et al. (2018) [119]	10 healthy males (25.5 ± 3.8 y, 65.5 ± 15.2 kg, 174.4 ± 19.5 cm)	IMU (Opal, APDM Inc.)	Triaxial accelerometer (± 6 g) and triaxial gyroscope (± 2000°s^{-1}) sampled at 128 Hz	Foot (fixed to the shoe)	Optical motion capture system (Qualisys, Qualisys AB) sampled at 128 Hz	3 min runs at 2.2, 2.5, 2.8 and 3.1 m·s^{-1}	Initial contact, toe-off, contact time, flight time, stride time and stride length	10/12
Dorschky et al. (2019) [121]	10 healthy male subjects (27.1 ± 2.6 y, 76.9 ± 8.6 kg, 1.82 ± 0.05 m)	IMU (Portabiles GmbH, Erlangen, DE)	Triaxial accelerometer (± 16 g) and triaxial gyroscope (± 200°s^{-1}) sampled at 1000 Hz	Midfoot, lateral tibia, left and right lateral thigh and lumbar spine	Optical motion capture system (Vicon MX, Oxford, UK) sampled at 200 Hz and one force plate (Kistler Instruments Corp, Winterhur, CH) sampled at 1000 Hz	Runs over a force platform at 3.0-3.3 m·s^{-1}, 3.9-4.1 m·s^{-1} and 4.7-4.9 m·s^{-1}	Vertical ground reaction force	9/12
Edwards et al. (2019) [110]	10 male rugby union athletes (21 ± 2 y, 81.8 ± 11.1 kg, 1.81 ± 0.50 m)	Accelerometer (SPI HPU, GPSports, Canberra, Australia)	Triaxial accelerometer (± 16 g) sampled at 100 Hz	Thoracic spine (T1-T6 vertebrae)	Two floor-embedded force platforms (Type 9281CA and 9821EA, Kistler, Winterhur, Switzerland) sampled at 1200 Hz	Ten runs over a force platform at 3.3, 5.0 and 6.7 m·s^{-1}	Vertical ground reaction force	10/12
Eggers et al. (2018) [22]	10 male and 7 female healthy adults (18-40 y, 70.4 ± 9.7 kg, 1.73 ± 0.06 m)	Accelerometer (wGT3X-BT, ActiGraph, Pensacola, FL, USA)	Triaxial accelerometer (± 8 g) sampled at 100 Hz	Lumbar spine (L2) and thoracic spine	Four 600 x 400 mm force plates (model BP400600-1000, Advanced Mechanical Technology, Inc., Watertown, MA, USA) sampled at 2000 Hz	2 min continuous shuttle runs over 20 m at 3.3 m·s^{-1}	Vertical ground reaction force and vertical stiffness	9/12
Fadillioglu et al. (2020) [134]	13 male healthy adults (26.1 ± 2.9 y, 78.4 ± 5.9 kg, 178.7 ± 5.5 cm)	Gyroscope (ADXRS652, Analog Devices Inc., Norwood, MA, USA)	Uniaxial gyrosope (± 250°s^{-1}) sampled at 1500 Hz	Tibia	Two floor-embedded force plates (BP600900, Advanced Mechanical Technology, Inc., Watertown, MA, USA)	3 trials of moderate and fast running (velocity not reported)	Initial contact, toe off and contact time	10/12
Falbriard et al. (2018) [83]	28 male and 13 female healthy adults (29 ± 6 y, 70 ± 10 kg, 174 ± 8 cm)	IMU (Physilog 4, Gait Up, Switzerland)	Triaxial accelerometer (± 16 g) and triaxial gyroscope (± 2000°s^{-1}) sampled at 500 Hz	Dorsal foot	Instrumented treadmill (T-170-FMT, Arsalis, Belgium) sampled at 1000 Hz	30 s runs ranging between 2.8 m·s^{-1} and 5.6 m·s^{-1}	Initial contact, toe-off, contact time, flight time, swing time and step time	9/12
Garcia-Pinillos et al. (2018) [81]	18 male recreational endurance runners (34 ± 7 y, 70.5 ± 6.2 kg, 1.76 ± 0.05 m)	IMU (Stryd™, Stryd Powermeter, Stryd Inc., Boulder, CO, USA)	Triaxial accelerometer and triaxial gyroscope	Foot	OptoGait system (Optogait; Microgate, Bolzano, Italy)	3 min runs ranging between 2.2 m·s^{-1} and 5.6 m·s^{-1} (0.3 m·s^{-1} increments)	Contact time, flight time, step frequency and step length	10/12

Table 2.3. Study characteristics for the 39 studies included in the review (continued).

Study	Sample (age, mass, height)	Sensor	Hardware	Sensor placement	Criterion	Activity	Variable(s)	Methodological quality
Garcia-Pinillos et al. (2019) [85]	44 male and 5 female amateur endurance runners (26 ± 8 y, 71 ± 10 kg, 1.74 ± 0.07 m)	IMU (Stryd™ [Stryd Powermeter, Stryd Inc. Boulder CO, USA]; RunScribe™ [Scribe Lab. Inc. San Francisco CA, USA])	Triaxial accelerometer and triaxial gyroscope Triaxial accelerometer, triaxial gyroscope and triaxial magnetometer sampled at 500 Hz	Foot	High-speed camera (Imaging Source DFK 33UX174, The Imaging Source Europe GmbH; Germany) sampled at 1000 Hz	3 min self-selected comfortable running velocity (3.25 ± 0.36 $m \cdot s^{-1}$)	Contact time, flight time, step frequency and step length	10/12
Gindre et al. (2016) [132]	20 male runners (31.6 ± 9.2 y, 72.5 ± 9.8 kg, 178 ± 5.4 cm)	Accelerometer (Myotest®, Myotest SA, Sion, Switzerland)	Triaxial accelerometer sampled at 500 Hz	Lumbar spine (level with naval)	Optojump Next® (Microgate, Bolzano, Italy) sampled at 1000 Hz and high-speed video camera (Casio High Speed EXILIM EX-FH25®, CASIO Europe GmbH, Norderstedt, Germany) sampled at 300 Hz	2 x 60 m runs at 3.3, 4.2, 5 and 5.8 $m \cdot s^{-1}$	Contact time, flight time and step frequency	10/12
Gouttebarge et al. (2015) [146]	11 male and 3 female recreational runners (45 ± 14 y, 77 ± 11 kg, 181 ± 7 cm)	Accelerometer (Myotest®, Myotest SA, Sion, Switzerland)	Triaxial accelerometer sampled at 200-500 Hz	Lumbar spine	Foot-mounted accelerometer (± 6 g, MMA7361L, Freescale Semiconductor, Austin, Texas, USA) sampled at 1000 Hz	3 x 400 m runs at 2.8, 3.3 and 3.9 $m \cdot s^{-1}$	Contact time and step frequency	10/12
Gurchiek et al. (2017) [123]	12 male and 3 female subjects (23.2 ± 2.1 y, 75.5 ± 12.6 kg, 1.8 ± 0.1 m)	IMU (Yost Data Logger 3-Space Sensor, YEI Technology, Portsmouth, OH)	Triaxial accelerometer (± 24 g) and triaxial gyroscope (± 2000°s^{-1}) sampled at 450 Hz	Sacrum	Force plate (AMTI, Watertown, MA, USA) sampled at 1000 Hz	Six linear standing sprint starts	Vertical and resultant ground reaction force	10/12
Kenneally-Dabrowski et al. (2018) [86]	13 male professional rugby union athletes (23.8 ± 2.4 y, 102.5 ± 12.2 kg, 186.6 ± 8.4 cm)	Accelerometer (GPSports, Canberra, Australia)	Triaxial accelerometer (± 16 g) sampled at 100 Hz	Thoracic spine	Eight 600 x 900 mm force plates (Kistler, Amherst, MA, USA) sampled at 1000 Hz	3 x 40 m maximal sprints (8.64 ± 0.5)	Stride time	10/12
Lee et al. (2010) [79]	6 male and 4 female national standard runners (30.3 ± 7.9 y, 67.7 ± 9.5 kg, 174.3 ± 5.7 cm)	Accelerometer (KXM52 – 1050 Kionix, NY, USA)	Triaxial accelerometer sampled at 100 Hz	Sacrum (S1)	Optical motion capture system (Proreflex MCU, Qualisys Medical AB, Gothenburg, Sweden) sampled at 500 Hz	3 x 5 min runs at 2.8-3.3 $m \cdot s^{-1}$, 3.6-4.2 $m \cdot s^{-1}$ and 4.4-5.3 $m \cdot s^{-1}$	Contact time, step time and stride time	9/12

Table 2.3. Study characteristics for the 39 studies included in the review (continued).

Study	Sample (age, mass, height)	Sensor	Hardware	Sensor placement	Criterion	Activity	Variable(s)	Methodological quality
Machulik et al. (2020) [135]	18 male and 10 female runners (28.2 ± 3.8 y, 70.6 ± 10.7 kg, 175.5 ± 9.5 cm)	IMU (Humotion SmarTracks Integrated)	Triaxial accelerometer (± 16 g, 400 Hz), triaxial gyroscope (± 2000°s^{-1}, 400 Hz) and triaxial magnetometer (100 Hz)	Lumbar spine	Optojump Next® (Microgate, Bolzano, Italy) sampled at 1000 Hz	3 x 60 m runs jogging (3.8 ± 0.7 m·s^{-1}) and sprinting 6.8 ± 1.0 m·s^{-1})	Step frequency and step length	9/12
McGrath et al. (2012) [105]	4 male and 1 female healthy adults (26-32 y)	IMU (Shimmer, Shimmer Inc., Dublin, Ireland)	Triaxial gyroscope sampled at 102.4 Hz	Tibia	Cartesian Optoelectronic Dynamic Anthropometer (CODA) motion analysis system (Charnwood Dynamics Ltd, Leicestershire, UK) sampled at 200 Hz	2 x 20 s runs at 2.2 m·s^{-1} and 3.3 m·s^{-1}	Initial contact, toe-off, contact time, swing time and stride time	9/12
Mitschke et al. (2017) [125]	21 male subjects (28.9 ± 10.8 y, 74.4 ± 7.1 kg, 177.0 ± 5.2 cm)	Accelerometer (ADXL278, Analog Devices Inc., Norwood, MA, USA)	Biaxial accelerometer (± 687 m·s^{-2}) sampled at 1000 Hz	Heel	One 60 x 90 cm force platform (Kistler, 9287 BA) sampled at 1000 Hz	30 x 15 m runs at 3.5 ± 0.1 m·s^{-1}	Initial contact	9/12
Mitschke et al. (2017) [124]	12 recreational rearfoot strike runners (24.8 ± 4.5 y, 72.3 ± 7.8 kg, 176.0 ± 5.4 cm) and 11 recreational forefoot strike runners (26.3 ± 3.2 y, 74.5 ± 7.5 kg, 177.0 ± 3.6 cm)	IMU (ICM-20601, InvenSense, San Jose, CA, USA)	Triaxial accelerometer (± 353 m·s^{-2}), triaxial gyroscope (± 4000°s^{-1}) sampled at 3570 Hz	Tibia (medial aspect)	One 0.6 x 0.9 m force plate (9287 BA, Kistler, Winterthur, Switzerland) sampled at 3570 Hz	5 x 15 m runs at a self-selected velocity (3.26 ± 0.4 m·s^{-1})	Initial contact	9/12
Mo & Chow (2018) [133]	7 male and 4 female healthy adults (25.5 ± 4.2 y, 58.8 ± 5.3 kg, 168.3 ± 9.1 cm)	IMU (MyoMOTION MR3, Noraxon, USA)	Triaxial accelerometer (± 16 g) sampled at 200 Hz	Dorsal foot, tibia and lumbar spine (L5-S1)	Three force platforms (Bertec, FP4060-07, USA) sampled at 2000 Hz	10 x 10 m runs at 3.1 ± 0.1 m·s^{-1} and 4.1 ± 1.2 m·s^{-1}	Initial contact, toe-off and contact time	10/12
Nedergaard et al. (2018) [107]	20 healthy male athletes (22 ± 4 y, 76 ± 11 kg, 178 ± 8 cm)	Accelerometer (MinimaxX S4, Catapult Innovations, Scoresby, Australia)	Triaxial accelerometer (± 13 g) sampled at 100 Hz	Thoracic spine	One 0.9 x 0.6 m^2 Kistler force platform (9287C, Kistler Instruments Ltd., Winterthur, Switzerland) sampled at 3000 Hz	Four runs over a force platform at 2, 3, 4 and 5 m·s^{-1}	Resultant ground reaction force	9/12

Table 2.3. Study characteristics for the 39 studies included in the review (continued).

Study	Sample (age, mass, height)	Sensor	Hardware	Sensor placement	Criterion	Activity	Variable(s)	Methodological quality
Neugebauer et al. (2014) [130]	19 male and 20 female subjects (21.2 ± 1.3 y, 67.6 ± 11.5 kg, 1.73 ± 0.12 m)	Accelerometer (GT3X+ AM, ActiGraph, Pensacola, FL, USA)	Triaxial accelerometer (± 6 g) sampled at 100 Hz	Hip	Force plate (Kistler Corporation, Model 9281B, Amherst, NY, USA) sampled at 1000 Hz	8-10 x 15 m runs ranging between 2.2 $m \cdot s^{-1}$ and 4.1 $m \cdot s^{-1}$ (0.3 $m \cdot s^{-1}$ increments)	Vertical ground reaction force	9/12
Ngoh et al. (2018) [122]	7 healthy male subjects (21.3 ± 0.5 y, 63 ± 6.1 kg, 174.9 ± 6.6 cm)	IMU (Opal, APDM Inc.)	Triaxial accelerometer (± 6 g), triaxial gyroscope (± 200°s^{-1}) and triaxial magnetometer (± 6 Gauss)	Dorsal foot	Instrumented treadmill (Mercury, H/P Cosmos Sports and Medical GmbH)	1 min runs at 2.2, 2.5 and 2.8 $m \cdot s^{-1}$	Vertical ground reaction force	9/12
Norris et al. (2016) [147]	1 male and 5 female recreational runners (33.5 ± 5.8 y, 71.1 ± 12.2 kg, 1.66 ± 0.08 m)	Accelerometer (Shimmer 2r, Shimmer Inc., Dublin, Ireland)	Triaxial accelerometer (± 16 g) sampled at 204.8 Hz	Distal tibia	Four varying accelerometer-derived stride time calculation methods	Running at a self-selected velocity during a half-marathon training programme	Stride time	9/12
Pairot de Fontenay et al. (2020) [126]	19 male and 13 female healthy adults (27.0 ± 5.5 y, 69.1 ± 11.4 kg, 174.4 ± 8.5 cm)	IMU (MilestonePod [Milestone Sports, Long Beach, CA, USA]; Zoi [Runteq, Tampere, Finland]; RunScribe™ [Montara, CA, USA]; Moov Now™ [Moov, San Mateo, CA, USA]; TgForce, Kelsec Systems Inc., Montreal, Canada])	Not reported	Dorsal foot and distal tibia	Instrumented treadmill (Bertec, Columbus, OH, USA) sampled at 1000 Hz	Not reported	Step frequency	10/12
Pogson et al. (2020) [127]	10 male and 5 female team-sport athletes (23 ± 1 y, 74 ± 9 kg, 1.74 ± 0.08 m)	Accelerometer (MinimaxX S5, Catapult Innovations, Scoresby, Australia)	Triaxial accelerometer (± 16 g) sampled at 100 Hz	Thoracic spine	In-ground force platform (9287B, Kistler Holding AG, Winterthur, Switzerland) sampled at 3000 Hz	Straight overground accelerated, decelerated and constant speed running between 2 $m \cdot s^{-1}$ and 8 $m \cdot s^{-1}$ (1 $m \cdot s^{-1}$ increments)	Resultant ground reaction force	9/12

Table 2.3. Study characteristics for the 39 studies included in the review (continued).

Study	Sample (age, mass, height)	Sensor	Hardware	Sensor placement	Criterion	Activity	Variable(s)	Methodological quality
Raper et al. (2018) [108]	4 male (27.00 ± 5.48 y, 66.00 ± 5.29 kg, 177.50 ± 4.65 cm) and 6 female (26.83 ± 3.06 y, 54.83 ± 3.19 kg, 164.50 ± 2.88 cm) professional triathletes	Accelerometer (ViPerform v5, DorsaVi, Melbourne, Australia)	Triaxial accelerometer	Tibia (medial border)	Eight piezoelectric force plates (Kistler Instrument Group, Amherst, New York, United States of America) sampled at 1000 Hz	10 x 50 m runs at 5.2 ± 0.6 $m \cdot s^{-1}$	Vertical ground reaction force	9/12
Sinclair et al. (2013) [80]	11 male and 5 female healthy adults (29.4 ± 5.7 y, 67.8 ± 10.7 kg, 1.73 ± 4.87 m)	Accelerometer (Biometrics ACL 300, UK)	Triaxial accelerometer sampled at 1000 Hz	Distal tibia	Force platform (Kistler Ltd; Model 9281CA, Kistler Instruments Ltd., Alton, Hampshire) sampled at 1000 Hz	10 runs at 4 $m \cdot s^{-1}$	Initial contact, toe-off and contact time	10/12
Tan et al. (2019) [128]	20 healthy subjects	Accelerometer (Shimmer3®, Shimmer Inc., Dublin, Ireland)	Triaxial accelerometer (± 8 g) sampled at 128 Hz	Distal tibia	In-shoe piezo-electric force sensitive resistors	Treadmill running overground running and outdoor running	Initial contact and toe-off	7/12
Watari et al. (2016) [120]	14 male and 8 female semi-elite runners (28.2 ± 10.1 y, 65.4 ± 8.1 kg, 1.73 ± 0.75 m)	Accelerometer (Forerunner 620, Garmin International Inc., Olathe, KS)	Not reported	Torso (near xiphoid process of the sternum)	Instrumented treadmill (Bertec, Columbus, OH) sampled at 1000 Hz	60 s runs at 2.7, 3.0, 3.3, 3.6 and 3.9 $m \cdot s^{-1}$	Contact time	9/12
Winter et al. (2016) [129]	6 male and 4 female recreational runners (27.5 ± 9.5 y, 69.5 ± 11.8 kg, 175.8 ± 8.1 cm)	Accelerometer (ADXL202, Analog Devices Inc., Norwood, MA, USA)	Triaxial accelerometer (± 8 g) sampled at 100 Hz	Lumbar spine	12-camera motion analysis system (NEXUS v1.8, Vicon Motion Systems Ltd. UK) sampled at 100 Hz	5 x 50 m runs overground	Initial contact and toe-off	9/12
Wouda et al. (2018) [150]	8 experienced male runners (25.1 ± 5.2 y, 77.7 ± 9.4 kg, 183.7 ± 4.5 cm)	IMU (Xsens, Enschede, the Netherlands)	Triaxial accelerometer, triaxial gyroscope and triaxial magnetometer sampled at 240 Hz	Lower legs and pelvis	S-Mill instrumented treadmill (ForceLink, Culemborg, the Netherlands) sampled at 1000 Hz	3 min runs at 2.8, 3.3 and 3.9 $m \cdot s^{-1}$	Vertical ground reaction force	11/12
Wundersitz et al. (2013) [106]	12 male and 5 female team-sport athletes (21 ± 2 y, 78.2 ± 11.6 kg, 1.82 ± 0.08 m)	Accelerometer (SPI Pro, ASP00725, GPSports, Canberra, Australia)	Triaxial accelerometer (± 8 g) sampled at 100 Hz	Thoracic spine (T2)	In-ground force plate (BP600900, Advanced Mechanical Technology Inc., Watertown, MA, USA) sampled at 100 Hz	5 x 10 m runs in a straight-line (5.4 ± 0.4 $m \cdot s^{-1}$) and 5 x 10 m angled runs at 45º (4.8 ± 0.4 $m \cdot s^{-1}$), 90º (4.1 ± 0.3 $m \cdot s^{-1}$) and 180º (3.5 ± 0.3 $m \cdot s^{-1}$)	Vertical and resultant ground reaction force	10/12

Table 2.3. Study characteristics for the 39 studies included in the review (continued).

Study	Sample (age, mass, height)	Sensor	Hardware	Sensor placement	Criterion	Activity	Variable(s)	Methodological quality
Zrenner et al. (2018) [117]	21 male and 6 female amateur runners (24.9 ± 2.4 y, 178. 6 ± 8.0 cm)	IMU (miPod sensor)	Triaxial accelerometer (± 16 g) and triaxial gyroscope (± 2000°s^{-1}) sampled at 200 Hz	Foot (midsole)	Motion capture system (Vicon Motion Systems Inc., Oxford, UK) sampled at 200 Hz	10 runs at 2-3 $m{\cdot}s^{-1}$, 10 runs at 3-4 $m{\cdot}s^{-1}$, 15 runs at 4-5 $m{\cdot}s^{-1}$, 15 runs at 5-6 $m{\cdot}s^{-1}$	Stride length	9/12

Abbreviations: °s^{-1}, degrees per second; cm, centimetres; g, gravitational acceleration; Hz, hertz; IMU, inertial measurement unit; kg, kilograms; m, metres; m^2, metres squared; $m{\cdot}s^{-1}$, metres per second; mm, millimetres; s, seconds; y, years.

Table 3-4. Methodological quality of included studies.

Author(s)	Hypothesis/ aim/objective described	Main outcomes described	Subject characteristics described	Intervention described	Main findings described	Random variability established	Probability values reported	Potential subjects representative of source population	Subjects representative of source population	Data dredging	Appropriate statistical tests	Outcome measures valid and reliable	Score (/12)
Ammann et al., (2016)	Y	Y	Y	Y	Y	Y	Y	U	U	Y	Y	Y	10
Aubol & Milner (2020)	Y	Y	Y	Y	Y	Y	N	U	Y	Y	Y	Y	10
Benson et al., (2019)	Y	Y	Y	Y	Y	Y	N	U	U	Y	Y	Y	9
Bergamini et al., (2012)	Y	Y	N	Y	Y	Y	N	U	U	Y	Y	Y	8
Brahms et al., (2018)	Y	Y	Y	Y	Y	Y	Y	U	U	Y	Y	Y	10
Buchheit et al., (2015)	Y	Y	Y	Y	Y	Y	N	U	U	Y	Y	Y	9
Buchheit et al., (2018)	Y	Y	Y	Y	Y	Y	N	U	Y	Y	Y	Y	10
Chew et al., (2018)	Y	Y	Y	Y	Y	Y	Y	U	U	Y	Y	Y	10
Dorschky et al., (2019)	Y	Y	Y	Y	Y	Y	N	U	U	Y	Y	Y	9
Edwards et al., (2019)	Y	Y	Y	Y	Y	Y	Y	U	U	Y	Y	Y	10

Table 2.4. Methodological quality of included studies (continued).

Author(s)	Hypothesis/ aim/objective described	Main outcomes described	Subject characteristics described	Intervention described	Main findings described	Random variability established	Probability values reported	Potential subjects representative of source population	Subjects representative of source population	Data dredging	Appropriate statistical tests	Outcome measures valid and reliable	Score (/12)
Eggers et al., (2018)	Y	Y	Y	Y	Y	Y	N	U	U	Y	Y	Y	9
Fadillioglu et al., (2020)	Y	Y	Y	Y	Y	Y	Y	U	U	Y	Y	Y	10
Falbriard et al., (2018)	Y	Y	Y	Y	Y	Y	N	U	U	Y	Y	Y	9
Garcia-Pinillos et al., (2018)	Y	Y	Y	Y	Y	Y	Y	U	U	Y	Y	Y	10
Garcia-Pinillos et al., (2019)	Y	Y	Y	Y	Y	Y	Y	U	U	Y	Y	Y	10
Gindre et al., (2016)	Y	Y	Y	Y	Y	Y	Y	U	U	Y	Y	Y	10
Gouttebarge et al., (2015)	Y	Y	Y	Y	Y	Y	N	U	Y	Y	Y	Y	10
Gurchiek et al., (2017)	Y	Y	Y	Y	Y	Y	Y	U	U	Y	Y	Y	10
Kenneally-Dabrowski et al., (2018)	Y	Y	Y	Y	Y	Y	Y	U	U	Y	Y	Y	10
Lee et al., (2010)	Y	Y	Y	Y	Y	Y	N	U	U	Y	Y	Y	9

Table 2.4. Methodological quality of included studies (continued).

Author(s)	Hypothesis/ aim/objective described	Main outcomes described	Subject characteristics described	Intervention described	Main findings described	Random variability established	Probability values reported	Potential subjects representative of source population	Subjects representative of source population	Data dredging	Appropriate statistical tests	Outcome measures valid and reliable	Score (/12)
Machulik et al., (2020)	Y	Y	Y	Y	Y	Y	N	U	U	Y	Y	Y	9
McGrath et al., (2012)	Y	Y	Y	Y	Y	Y	N	U	U	Y	Y	Y	9
Mitschke et al., (2017a)	Y	Y	Y	Y	Y	Y	N	U	U	Y	Y	Y	9
Mitschke et al., (2017b)	Y	Y	Y	Y	Y	Y	N	U	U	Y	Y	Y	9
Mo & Chow (2018)	Y	Y	Y	Y	Y	Y	Y	U	U	Y	Y	Y	10
Nedergaard et al., (2018)	Y	Y	Y	Y	Y	Y	N	U	U	Y	Y	Y	9
Neugebauer et al., (2014)	Y	Y	Y	Y	Y	Y	N	U	U	Y	Y	Y	9
Ngoh et al., (2018)	Y	Y	Y	Y	Y	Y	N	U	U	Y	Y	Y	9
Norris et al., (2016)	Y	Y	Y	Y	Y	Y	N	U	U	Y	Y	Y	9
Pairot de Fontenay et al., (2020)	Y	Y	Y	N	Y	Y	Y	U	Y	Y	Y	Y	10

Table 2.4. Methodological quality of included studies (continued).

Author(s)	Hypothesis/ aim/objective described	Main outcomes described	Subject characteristics described	Intervention described	Main findings described	Random variability established	Probability values reported	Potential subjects representative of source population	Subjects representative of source population	Data dredging	Appropriate statistical tests	Outcome measures valid and reliable	Score (/12)
Pogson et al., (2020)	Y	Y	Y	Y	Y	Y	N	U	U	Y	Y	Y	9
Raper et al., 2018)	Y	Y	Y	Y	Y	Y	N	U	U	Y	Y	Y	9
Sinclair et al., (2013)	Y	Y	Y	Y	Y	Y	Y	U	U	Y	Y	Y	10
Tan et al., (2019)	Y	Y	N	Y	Y	N	N	U	U	Y	Y	Y	7
Watari et al., (2016)	Y	Y	Y	Y	Y	Y	N	U	U	Y	Y	Y	9
Winter et al., (2016)	Y	Y	Y	Y	Y	Y	N	U	U	Y	Y	Y	9
Wouda et al., (2018)	Y	Y	Y	Y	Y	Y	Y	U	Y	Y	Y	Y	11
Wundersitz et al., (2013)	Y	Y	Y	Y	Y	Y	Y	U	U	Y	Y	Y	10

Table 2.4. Methodological quality of included studies (continued).

Author(s)	Hypothesis/ aim/objective described	Main outcomes described	Subject characteristics described	Intervention described	Main findings described	Random variability established	Probability values reported	Potential subjects representative of source population	Subjects representative of source population	Data dredging	Appropriate statistical tests	Outcome measures valid and reliable	Score (/12)
Zrenner et al., (2018)	Y	Y	Y	Y	Y	Y	N	U	U	Y	Y	Y	9
Total Y (/39)	39	39	37	38	39	38	24	0	5	39	39	39	
Total N (/39)	0	0	2	1	0	1	15	0	0	0	0	0	
Total U (/39)	0	0	0	0	0	0	0	39	34	0	0	0	

Abbreviations: Y, yes; N, no; U, unclear.
Score out of 12 is representative of the number of items answered yes.

3.4.4 Stride Variables

The results for each stride variable examined in this review are described in the following sections.

3.4.4.1 Initial Contact

Validity outcomes for the detection of IC using IMUs secured to the foot, distal and mid tibia and lumbar spine are presented in Table 3-5. Mean relative differences (-16.0 to 3.3 ms) and estimation errors (-6.0 to 4.3 ms) were generally low for foot placement [17, 119, 133], while another study reported IC could be detected with a precision (median ± inter-quartile range [IQR]) of 2.0 ± 1.0 ms from a foot-mounted IMU [83]. Contrasting results were evident for placement on the tibia. Using only the angular velocity signal from a gyroscope, errors were as high as 64.2 ms compared to motion capture in one study [105], while another study detected IC from gyroscope data with an absolute mean error of 13.0 ± 6.0 ms to that of a force plate [134]. The mean relative difference (-38.0 ± 10.7 ms) was greater than that observed for the foot using tibial acceleration data [133], while other studies showed improved validity for determining IC from tibia-mounted IMUs compared to force plate measures (MD = -0.5 ± 0.3 ms, mean bias = -2.3 ± 4.7 ms, mean error = 1.68 ms) (see Table 3-5) [19, 80, 124]. In another study using tibia-mounted accelerometers, IC was detected with an accuracy of F_1 = 0.92-0.96 compared to those events determined from in-shoe piezo-electric FSRs [128]. The F_1 score is a measure of a test's accuracy, where an F_1 score of 1 reflects perfect precision and recall [151]. Detection of IC was slightly earlier (4.7 ms) at 3.3 $m \cdot s^{-1}$ from a lumbar spine-mounted IMU compared to the foot, but 2.4 ms slower at 4.1 $m \cdot s^{-1}$ [133]. The largest difference from force plate-identified IC was 53.0 ms for the lumbar spine [17].

3.4.4.2 Toe-off

Table 3-6 documents the validity statistics from studies that determined the accuracy of IMUs to detect TO. Between 2.2 and 4.1 $m \cdot s^{-1}$, the mean relative difference and estimation errors for the detection of TO from foot-mounted IMUs ranged from -53.8 to 32.0 ms and -4.3 to 16.3 ms, respectively [17, 119, 133]. Errors up to -32.4 ms were shown using a gyroscope attached to the tibia [105], while another study using angular velocity data from the tibia showed TO was determined after force plate detection (absolute mean error > 23.0 ms) [134]. Smaller mean absolute and relative differences were observed for determining TO from tibial acceleration data (< 8.8 ms and < 1.0 ms, respectively) [133], while TO was detected with an accuracy of F_1 = 0.77-0.86 from accelerometers secured to the distal tibia when in-shoe piezo-electric FSRs were the criterion [128]. A time lag of 7.6 to 24.0 ms was present for the detection of TO from an IMU secured to the lumbar spine compared to values obtained from a force plate [17, 133].

Table 3-5. Validity summary statistics for initial contact.

Study	Sensor	Criterion	Site	Running velocity m·s^{-1} ± SD	Statistic 1	Statistic 2
Chew et al. (2018) [119]	IMU (Opal, APDM Inc.)	Motion capture system	Foot		ME ± SD (ms)	RMSE (ms)
				2.2 2.5 2.8 3.1	-2.6 ± 12.8 -6.0 ± 14.1 4.3 ± 17.9 3.0 ± 14.1	4.7 5.3 8.3 4.7
Falbriard et al. (2018) [83]	IMU (Physilog 4, Gait Up, Switzerland)	Instrumented treadmill	Foot		Median bias ± IQR (ms)	Median precision ± IQR (ms)
				2.8-5.6	11.0 ± 10.0	2.0 ± 1.0
Mo & Chow (2018) [133]	IMU (MyoMOTION MR3, Noraxon, USA)	Force plate	Foot		MRD ± SD (ms)	MAD ± SD (ms)
				3.1 ± 0.1 4.1 ± 1.2	-7.3 ± 3.3 3.3 ± 4.7	5.2 ± 3.4 4.2 ± 4.7
Benson et al. (2019) [17]	Accelerometer (Shimmer3®, Shimmer Inc., Dublin, Ireland)	Force plate	Foot		MD (ms)	95% LoA (ms)
				3.3	-16.0	-58.0, 27.0
Mitschke et al. (2017) [125]	Accelerometer (ADXL278, Analog Devices Inc., Norwood, MA, USA)	Force plate	Heel		MD (ms)	
				3.5 ± 0.1	0.7 ± 2.6	
Sinclair et al. (2013) [80]	Accelerometer (Biometrics ACL 300, UK)	Force plate	Tibia		ME (95% CI) (ms)	AE (95% CI) (ms)
				4.0	1.7 (-2.9, 6.3)	5.5 (1.9, 9.0)
Tan et al. (2019) [128]	Accelerometer (Shimmer3®, Shimmer Inc., Dublin, Ireland)	In-shoe piezo-electric force sensitive resistors	Tibia		F_1 score	
				Not reported	0.92-0.96	
McGrath et al. (2012) [105]	IMU (Shimmer, Shimmer Inc., Dublin, Ireland)	Motion capture system Hreljac and Marshal (2000)	Tibia		True error (ms)	% error
				2.2 3.3	33.4 24.1	0.8 0.5
	IMU (Shimmer, Shimmer Inc., Dublin, Ireland)	Motion capture system Zeni et al., (2008)	Tibia		True error (ms)	% error
				2.2 3.3	64.2 61.7	1.5 1.4
Mitschke et al. (2017) [124]	IMU (ICM-20601, InvenSense, San Jose, CA, UDA) Sinclair et al., (2013)	Force plate	Tibia		MD (ms)	
				3.26 ± 0.4	11.5 ± 4.2	
	IMU (ICM-20601, InvenSense, San Jose, CA, UDA) Mercer et al., (2003)	Force plate	Tibia		MD (ms)	
				3.26 ± 0.4	-1.1 ± 10.7	
	IMU (ICM-20601, InvenSense, San Jose, CA, UDA) Maiwald et al., (2015)	Force plate	Tibia		MD (ms)	
				3.26 ± 0.4	-0.5 ± 0.3	
	IMU (ICM-20601, InvenSense, San Jose, CA, UDA) Sabatini et al., (2005)	Force plate	Tibia		MD (ms)	
				3.26 ± 0.4	-5.1 ± 3.0	
Mo & Chow (2018) [133]	IMU (MyoMOTION MR3, Noraxon, USA)	Force plate	Tibia		MRD ± SD (ms)	MAD ± SD (ms)
				3.1 ± 0.1 4.1 ± 1.2	-38.0 ± 10.7 -16.7 ± 11.9	19.5 ± 6.5 17.4 ± 11.0
Aubol & Milner (2020) [19]	Accelerometer (Model 356A45, PCB Piezotronics, Depew, NY)	Force plate	Tibia		Mean bias (ms)	95% LoA (ms)
				3.0 ± 0.2	-2.3 ± 4.7	-6.8, 11.5
Fadillioglu et al. (2020) [134]	Gyroscope (ADXRS652, Analog Devices Inc., Norwood, MA, USA)	Force plate	Tibia		AME ± SD (ms)	RAME ± SD (%)
				Moderate Fast	10.0 ± 4.0 13.0 ± 6.0	3.4 ± 1.4 5.5 ± 2.7

Table 2.5. Validity summary statistics for initial contact (continued).

Study	Sensor	Criterion	Site	Running velocity m·s^{-1} ± SD	Statistic 1	Statistic 2
Winter et al. (2016) [129]	Accelerometer (ADXL202, Analog Devices Inc., Norwood, MA, USA)	Motion capture system	Lumbar spine		TEE (ms)	Pearson's *r*
				Self-paced	0.8	0.99
Mo & Chow (2018) [133]	IMU (MyoMOTION MR3, Noraxon, USA)	Force plate	Lumbar spine		MRD ± SD (ms)	MAD ± SD (ms)
				3.1 ± 0.1	-2.6 ± 4.9	9.0 ± 2.0
				4.1 ± 1.2	5.7 ± 5.0	6.2 ± 4.6
Benson et al. (2019) [17]	Accelerometer (Shimmer3®, Shimmer Inc., Dublin, Ireland)	Force plate	Lumbar spine		MD (ms)	95% LoA (ms)
				3.3	53.0	24.0, 82.0

Abbreviations: AE, absolute error; AME, absolute mean error; CI, confidence interval; F_1 score, weighted average of precision and recall; IMU, inertial measurement unit; IQR, inter-quartile range; LoA, limits of agreement; MAD, mean absolute difference; MD, mean difference; ME, mean error; MRD, mean relative difference; ms, milliseconds; m·s^{-1}, metres per second; RAME, relative absolute mean error; RMSE, root mean square error; SD, standard deviation; TEE, typical error of the estimate.
Negative values represent a time lead in the detection of initial contact by the IMU compared to the criterion.
Velocity reported with or without ± SD, depending on the method used in each study. A velocity range is presented for Falbriard et al. (2018) as validity outcomes were reported from pooled speeds.
Values converted to milliseconds where required.

Table 3-6. Validity summary statistics for toe-off.

Study	Sensor	Criterion	Site	Running velocity $m \cdot s^{-1}$ ± SD	Statistic 1	Statistic 2
Chew et al. (2018) [119]	IMU (Opal, APDM Inc.)	Motion capture system	Foot		ME ± SD (ms)	RMSE (ms)
				2.2	3.3 ± 20.9	9.0
				2.5	16.3 ± 16.7	11.1
				2.8	-4.3 ± 15.0	7.6
				3.1	2.6 ± 19.5	11.0
Falbriard et al. (2018) [83]	IMU (Physilog 4, Gait Up, Switzerland)	Instrumented treadmill	Foot		Median bias ± IQR (ms)	Median precision ± IQR (ms)
				2.8-5.6	-4.0 ± 7.0	4.0 ± 2.0
Mo & Chow (2018) [133]	IMU (MyoMOTION MR3, Noraxon, USA)	Force plate	Foot		MRD ± SD (ms)	MAD ± SD (ms)
				3.1 ± 0.1	-32.0 ± 14.1	25.0 ± 7.5
				4.1 ± 1.2	-53.8 ± 8.1	27.6 ± 7.6
Benson et al. (2019) [17]	Accelerometer (Shimmer3®, Shimmer Inc., Dublin, Ireland)	Force plate	Foot		MD (ms)	95% LoA (ms)
				3.3	32.0	-84.0, 148.0
Sinclair et al. (2013) [80]	Accelerometer (Biometrics ACL 300, UK)	Force plate	Tibia		ME (95% CI) (ms)	AE (95% CI) (ms)
				4.0	-3.6 (-5.4, 1.8)	5.0 (3.5, 8.5)
Tan et al. (2019) [128]	Accelerometer (Shimmer3®, Shimmer Inc., Dublin, Ireland)	In-shoe piezo-electric force sensitive resistors	Tibia		F_1 score	
				Not reported	0.77-0.81	
McGrath et al. (2012) [105]	IMU (Shimmer, Shimmer Inc., Dublin, Ireland)	Motion capture system Hreljac and Marshal (2000)	Tibia		True error (ms)	% error
				2.2	-32.4	0.7
				3.3	-28.8	0.8
	IMU (Shimmer, Shimmer Inc., Dublin, Ireland)	Motion capture system Zeni et al., (2008)	Tibia		True error (ms)	% error
				2.2	-15.1	0.7
				3.3	-24.2	0.7
Mo & Chow (2018) [133]	IMU (MyoMOTION MR3, Noraxon, USA)	Force plate	Tibia		MRD ± SD (ms)	MAD ± SD (ms)
				3.1 ± 0.1	0.0 ± 4.1	5.1 ± 2.1
				4.1 ± 1.2	1.0 ± 7.8	8.8 ± 3.7
Fadillioglu et al. (2020) [134]	Gyroscope (ADXRS652, Analog Devices Inc., Norwood, MA, USA)	Force plate	Tibia		AME ± SD (ms)	RAME ± SD (%)
				Moderate	26.0 ± 20.0	8.0 ± 4.8
				Fast	23.0 ± 23.0	9.4 ± 8.8
Winter et al. (2016) [129]	Accelerometer (ADXL202, Analog Devices Inc., Norwood, MA, USA)	Motion capture system	Lumbar spine		TEE (ms)	Pearson's *r*
				Self-paced	0.8	0.99
Mo & Chow (2018) [133]	IMU (MyoMOTION MR3, Noraxon, USA)	Force plate	Lumbar spine		MRD ± SD (ms)	MAD ± SD (ms)
				3.1 ± 0.1	7.6 ± 9.9	15.2 ± 5.0
				4.1 ± 1.2	9.4 ± 12.7	20.3 ± 8.2
Benson et al. (2019) [17]	Accelerometer (Shimmer3®, Shimmer Inc., Dublin, Ireland)	Force plate	Lumbar spine		MD (ms)	95% LoA (ms)
				3.3	24.0	-15.0, 63.0

Abbreviations: AE, absolute error; AME, absolute mean error; CI, confidence interval; F_1 score, weighted average of precision and recall; IMU, inertial measurement unit; IQR, inter-quartile range; LoA, limits of agreement; MAD, mean absolute difference; MD, mean difference; ME, mean error; MRD, mean relative difference; ms, milliseconds; $m \cdot s^{-1}$, metres per second; RAME, relative absolute mean error; RMSE, root mean square error; SD, standard deviation; TEE, typical error of the estimate. Negative values represent a time lead in the detection of toe-off by the IMU compared to the criterion.
Velocity reported with or without ± SD, depending on the method used in each study. A velocity range is presented for Falbriard et al. (2018) as validity outcomes were reported from pooled speeds.
Values converted to milliseconds where required.

3.4.4.3 Contact Time

Validity outcomes reported from studies using placement on the foot, tibia, lumbar spine, torso and thoracic spine to derive contact time is presented in Table 3-7. The concurrent validity of an IMU fixed to the foot showed a deviation to high-speed camera measures between -3.3 and -0.1%, a mean bias between -5.6 and 0.4 ms and intraclass correlation coefficient (ICC) values as high as 0.97 for contact time across velocities of 4.3 ± 0.7 $m \cdot s^{-1}$, 6.2 ± 0.7 $m \cdot s^{-1}$ and 8.0 ± 1.6 $m \cdot s^{-1}$ [97]. When a photocell system was the criterion, ICC values were as low as 0.1 at 5.6 $m \cdot s^{-1}$ using a foot placement [81]. Pearson correlation analysis showed a large agreement (r = 0.96) between a tibial accelerometer estimate of contact time and force plate [80], whereas contrasting results were evident for contact time calculated from gyroscope data (see Table 3-7) [105, 134]. True error and ICC outcomes were > 63.4 ms and < 0.32, respectively, compared to motion capture [105], whereas differences to force plate were smaller (> -12.0 ms) in another study using angular velocity data to determine contact time [134]. Compared to motion capture and force plate, small biases (0.8-1.1 ms) and estimation errors (5.0 ms) were shown for contact time when an IMU was placed on the sacrum and lumbar spine, respectively [79, 84]. However, significant differences ($p < 0.05$) were reported in another study using the lumbar spine when photocell (> -35.0%) and high-speed camera (> -31.0%) measures of contact time were used as the reference [132]. In a study comparing contact times derived from different accelerometer attachment sites, the lumbar spine showed a smaller difference from force plate-determined contact time (< 8.7%) to the values obtained from the tibia (< 17.3%) and foot (< 26.6%), with each site significantly correlated ($r > 0.74$, $p < 0.05$) with force plate (see Table 3-7) [133]. Similar results reported in a more recent study showing the mean lumbar spine-force plate difference (-29.0 ms) was less than that observed between foot-force plate (47.0 ms). In that study, accelerometers placed on the lumbar spine underestimated mean contact time compared to force plate, whereas foot acceleration overestimated by 18.0 ms [17]. Contact time derived from an accelerometer secured to the thoracic spine showed a mean bias of -10.4% and a nearly perfect correlation (r = 0.98) with an instrumented treadmill [21]. However, data from only one participant was analysed [21].

Three studies assessed the reliability of IMUs on the foot and lumbar spine to calculate contact time (see Table 3-8). The coefficient of variation (CV) was < 2.3% across velocities ranging between 2.2 and 5.6 $m \cdot s^{-1}$, while the standard error of measurement (SEM) was highest at 2.2 $m \cdot s^{-1}$ (5.0 ms) [81]. Good absolute and relative between-trial reliability was established using an accelerometer mounted on the lumbar spine (CV < 9.9%, ICC > 0.88) [132], while lower ICC values ranging from -0.24 to 0.67 were reported for inter-day reliability in another study using a lumbar spine-mounted accelerometer [146]. Greater SEM values were observed for lumbar spine-determined contact time (> 10.1 ms) compared to foot placement (< 5.0 ms) [81, 146].

Data collected between 3.3 and 4.3 $m \cdot s^{-1}$ was pooled to determine the effect of IMU placement on the accuracy of contact time compared to criterion measures (see Figure 3.2). There was a significant difference in the overall effect of different IMU attachment sites (p = 0.02). Contact time derived from the foot (MD [95% CI] -11.47 ms [-45.68, 22.74], p = 0.43), tibia (MD [95% CI] 22.34 ms [-18.59, 63.27], p = 0.18) and lumbar spine (MD [95% CI] -48.74 ms [-120.33, 22.85], p = 0.12) was not significantly different to the criterion. All subgroups were associated with high heterogeneity (I^2 > 54.1%). Leave-one-out analysis for foot and lumbar spine sites revealed that there was no single study influential enough to substantially change the overall heterogeneity (I^2 > 83.4%) or pooled MD. In contrast, heterogeneity could be explained for the tibia site by omitting one study [134] (I^2 = 0%), with the same study also having an influential effect on the overall result for tibia-determined contact time (MD [95% CI] 34.68 ms [11.16, 58.19], p = 0.02). Moderator analysis showed the type of criterion measure was not significantly associated with the observed variance in effect sizes ($p = 0.15$).

Table 3-7. Validity summary statistics for contact time.

Study	Sensor	Criterion	Site	Running velocity $m \cdot s^{-1} \pm SD$	Sensor mean ± SD ms	Criterion mean ± SD ms	Statistic 1	Statistic 2	Statistic 3	Statistic 4	Statistic 5
Ammann et al. (2016) [97]	IMU (PARTwear, HuCE-microLab, University of Applied Sciences, Biel, Switzerland)	High-speed camera	Foot				ICC (95% CI)	Systematic bias (ms)	%D		
				4.3 ± 0.7	185.5 ± 21.7	194.6 ± 34.3	0.97 (0.92, 0.99)	-5.6*	-3.3 ± 5.0		
				6.2 ± 0.7	145.5 ± 20.9	147.4 ± 20.3	0.96 (0.92, 0.98)	-0.7	-0.8 ± 6.2		
				8.0 ± 1.6	118.3 ± 11.6	117.5 ± 9.0	0.81 (0.65, 0.89)	0.4	-0.1 ± 6.7		
Chew et al. (2018) [119]	IMU (Opal, APDM Inc.)	Motion capture system	Foot				ME ± SD (ms)	RMSE (ms)			
				2.2	Not reported	Not reported	-6.1 ± 6.2	7.8			
				2.5			-8.2 ± 5.3	9.2			
				2.8			-8.1 ± 3.1	9.1			
				3.1			-8.1 ± 2.5	10.0			
Falbriard et al. (2018) [83]	IMU (Physilog 4, Gait Up, Switzerland)	Instrumented treadmill	Foot				Median bias ± IQR (ms)	Median precision ± IQR (ms)			
				2.8-5.6	Not reported	Not reported	-15.0 ± 12.0	5.0 ± 3.0			
Garcia-Pinillos et al. (2018) [81]	IMU (Stryd™, Stryd Powermeter, Stryd Inc., Boulder, CO, USA)	Photocell system	Foot				ICC	Pearson's *r*			
				2.2-5.6	311.5 ± 11.5 to 175.5 ± 3.3	340.0 ± 28.0 to 175.0 ± 6.0	0.06-0.46	0.08-0.66**			
Mo & Chow (2018) [133]	IMU (MyoMOTION MR3, Noraxon, USA)	Force plate	Foot				MRD ± SD (ms)	Pearson's *r*	%D	MAD ± SD (ms)	
				3.1 ± 0.1	228.0 ± 23.0	253.0 ± 10.0	-24.7 ± 14.8	0.88*	11.9 ± 4.8	29.3 ± 11.5	
				4.1 ± 1.2	159.0 ± 13.0	215.0 ± 7.0	-56.0 ± 9.6	0.74*	26.6 ± 4.3	34.2 ± 10.4	
Benson et al. (2019) [17]	Accelerometer (Shimmer3®, Shimmer Inc., Dublin, Ireland)	Force plate	Foot				MD (ms)	95% LoA (ms)			
				3.3	320.1 ± 41.5	270.6 ± 25.4	47.0	-59.0, 154.0			
Garcia-Pinillos et al. (2019) [85]	IMU (RunScribe™, Scribe Lab. Inc. San Francisco CA, USA)	High-speed camera	Foot				ICC (95% CI)	Pearson's *r*	MD (%)	MD (ms)	Systematic bias ± RE (ms)
				3.3 ± 0.4	261.0 ± 28.0	267.0 ± 28.0	0.90 (0.80, 0.94)	0.83	2.3**	-6.0	-6.0 ± 16.0
	IMU (Stryd™, Stryd Powermeter, Stryd Inc. Boulder CO, USA)	High-speed camera	Foot				ICC (95% CI)	Pearson's *r*	MD (%)	MD (ms)	Systematic bias ± RE (ms)
				3.3 ± 0.4	253.0 ± 22.0	267.0 ± 28.0	0.81 (0.29, 0.93)	0.82	5.2***	-14.0	-15.0 ± 16.0
Sinclair et al. (2013) [80]	Accelerometer (Biometrics ACL 300, UK)	Force plate	Tibia				ME (95% CI) (ms)	Pearson's *r*	AE (95% CI) (ms)		
				4.0	185.30	190.46	-5.2 (0.9, 10.2)	0.96	11.5 (8.1, 14.9)		
McGrath et al. (2012) [105]	IMU (Shimmer, Shimmer Inc., Dublin, Ireland)	Motion capture system [Hreljac and Marshal (2000)]	Tibia				ICC	True error (ms)	% error		
				2.2	390.0 ± 30.0	440.0 ± 20.0	0.32	-66.4	15.2		
				3.3	450.0 ± 51.0	390.0 ± 60.0	0.30	-63.4	16.7		

Table 2.7. Validity summary statistics for contact time (continued).

Study	Sensor	Criterion	Site	Running velocity m·s^{-1} ± SD	Sensor mean ± SD ms	Criterion mean ± SD ms	Statistic 1	Statistic 2	Statistic 3	Statistic 4	Statistic 5
McGrath et al. (2012) [105]	IMU (Shimmer, Shimmer Inc., Dublin, Ireland)	Motion capture system [Zeni et al., (2008)]	Tibia				ICC	True error (ms)	% error		
				2.2	390.0 ± 30.0	460.0 ± 10.0	0.26	-79.1	19.8		
				3.3	450.0 ± 51.0	420.0 ± 10.0	0.29	-90.2	22.4		
Mo & Chow (2018) [133]	IMU (MyoMOTION MR3, Noraxon, USA)	Force plate	Tibia				MRD ± SD (ms)	Pearson's *r*	%D	MAD ± SD (ms)	
				3.1 ± 0.1	291.0 ± 15.0	253.0 ± 10.0	38.0 ± 9.4	0.78*	15.6 ± 3.0	39.4 ± 8.0	
				4.1 ± 1.2	248.0 ± 39.0	215.0 ± 7.0	32.9 ± 34.1	0.74*	17.3 ± 14.1	30.9 ± 18.9	
Fadillioglu et al. (2020) [134]	Gyroscope (ADXRS652, Analog Devices Inc., Norwood, MA, USA)	Force plate	Tibia				MD (ms)	95% LoA (ms)			
				2.6 ± 0.4	297.0 ± 43.0	309.0 ± 45.0	-12.0	-83.0, 59.0			
				3.9 ± 0.6	225.0 ± 42.0	232.0 ± 26.0	-7.0	-85.0, 71.0			
Lee et al. (2010) [79]	Accelerometer (KXM52 – 1050 Kionix, NY, USA)	Motion capture system	Sacrum				Mean bias (ms)	Pearson's *r*	SE (ms)	95% LoA (ms)	
				2.8-3.3	Not reported	Not reported	1.1	0.91	0.9	-25.0, 22.0	
				3.6-4.2			2.2	0.94	0.7	-20.0, 16.0	
				4.4-5.2			0.8	0.90	0.9	-24.0, 23.0	
Bergamini et al. (2012) [84]	IMU (FreeSense, Sensorize, Italy)	Force plate	Lumbar spine				ME (ms)	LoA (ms)			
				Maximal sprint	122.9 ± 10.9	123.3 ± 13.1	5.0	25.0			
	IMU (FreeSense, Sensorize, Italy)	High-speed camera	Lumbar spine				ME (ms)	LoA (ms)			
				Maximal sprint	105.2 ± 4.5	103.6 ± 7.7	5.0	25.0			
Gouttebarge et al. (2015) [146]	Accelerometer (Myotest®, Myotest SA, Sion, Switzerland)	Foot-mounted accelerometer	Lumbar spine				ICC (95% CI)				
				2.8	172.0 ± 15.0	297.1 ± 20.0	0.49 (-0.03, 0.80)				
				3.3	159.1 ± 17.0	278.4 ± 25.0	0.50 (-0.02, 081)				
				3.9	144.2 ± 16.0	251.3 ± 24.0	0.48 (-0.07, 0.81)				
Gindre et al. (2016) [132]	Accelerometer (Myotest®, Myotest SA, Sion, Switzerland)	Photocell system	Lumbar spine				ICC	CV%	MD (%)		
				3.3	166.0 ± 15.0	268.0 ± 17.0	0.63	17.7	-38.0*		
				4.2	154.0 ± 15.0	237.0 ± 15.0	0.67	16.2	-35.0*		
				5.0	135.0 ± 16.0	208.0 ± 13.0	0.75	16.4	-35.0*		
				5.8	116.0 ± 16.0	182.0 ± 16.0	0.82	17.9	-36.0*		
	Accelerometer (Myotest®, Myotest SA, Sion, Switzerland)	High-speed camera	Lumbar spine				ICC	CV%	MD (%)		
				3.3	166.0 ± 15.0	252.0 ± 17.0	0.72	15.9	-34.0*		
				4.2	154.0 ± 15.0	223.0 ± 13.0	0.47	14.1	-31.0*		
				5.0	135.0 ± 16.0	198.0 ± 12.0	0.63	14.7	-32.0*		
				5.8	116.0 ± 16.0	173.0 ± 12.0	0.74	16.0	-33.0*		

Table 2.7. Validity summary statistics for contact time (continued).

Study	Sensor	Criterion	Site	Running velocity m·s^{-1} ± SD	Sensor mean ± SD ms	Criterion mean ± SD ms	Statistic 1	Statistic 2	Statistic 3	Statistic 4	Statistic 5
Mo & Chow (2018) [133]	IMU (MyoMOTION MR3, Noraxon, USA)	Force plate	Lumbar spine				MRD ± SD (ms)	Pearson's *r*	%D	MAD ± SD (ms)	
				3.1 ± 0.1	263.0 ± 15.0	253.0 ± 10.0	10.3 ± 8.9	0.83*	6.3 ± 1.8	15.9 ± 4.7	
				4.1 ± 1.2	220.0 ± 18.0	215.0 ± 7.0	4.6 ± 12.1	0.89*	8.7 ± 3.7	18.7 ± 7.5	
Benson et al. (2019) [17]	Accelerometer (Shimmer3®, Shimmer Inc., Dublin, Ireland)	Force plate	Lumbar spine				MD (ms)	95% LoA (ms)			
				3.3	241.8 ± 30.2	270.6 ± 25.4	-29.0	-69.0, 10.0			
Watari et al. (2016) [120]	Accelerometer (Forerunner 620, Garmin International Inc., Olathe, KS)	Instrumented treadmill	Torso				Mean bias (ms)	CCC			
				2.7	Not reported	Not reported	-17.0	0.69			
				3.0			-10.1	0.77			
				3.3			-5.8	0.87			
				3.6			-2.6	0.83			
				3.9			-1.4	0.84			
Buchheit et al. (2015) [21]	Accelerometer (SPI HPU, GPSports, Canberra, Australia)	Instrumented treadmill	Scapula				Mean bias (90% CI) (%)	Pearson's *r* (90% CI)	CV% (90% CI)		
				2.8-7.5	Not reported	Not reported	-10.4 (-12.3, -9.8)	0.98 (0.97, 0.99)	3.9 (3.4, 4.6)		

Abbreviations: %D, percentage difference; AE, absolute error; CCC, concordance correlation coefficient; CI, confidence interval; CV, coefficient of variation; ICC, intraclass correlation coefficient; IMU, inertial measurement unit; IQR, inter-quartile range; LoA, limits of agreement; MAD, mean absolute difference; MD, mean difference; ME, mean error; MRD, mean relative difference; ms, milliseconds; m·s^{-1}, metres per second; RE, random error; RMSE, root mean square error; SD, standard deviation; SE, standard error.
Negative values represent an underestimation of contact time calculated by the IMU compared to the criterion.
Velocity reported with or without ± SD, depending on the method used in each study. A velocity range is presented for Falbriard et al. (2018) and Buchheit et al. (2015) as validity outcomes were reported from pooled speeds.
Values converted to milliseconds where required.
*$p < 0.05$.
**$p < 0.01$.
***$p < 0.001$.

Study or Subgroup	IMU Mean	IMU SD	IMU Total	Criterion Mean	Criterion SD	Criterion Total	Mean Difference IV, Random, 95% CI
Foot							
Ammann et al. (2016) [16]	185.50	21.70	12	194.60	34.30	12	-9.10 [-32.06; 13.86]
Benson et al. (2019) [30]	320.10	41.50	12	270.60	25.40	12	49.50 [21.97; 77.03]
Garcia-Pinillos et al. (2018) [71]	226.18	6.45	18	245.02	14.00	18	-18.85 [-25.97; -11.73]
Garcia-Pinillos et al. (2019a) [35]	261.00	28.00	49	267.00	28.00	49	-6.00 [-17.09; 5.09]
Garcia-Pinillos et al. (2019b) [35]	253.00	22.00	49	267.00	28.00	49	-14.00 [-23.97; -4.03]
Mo & Chow (2018) [69]	159.00	13.00	11	215.00	7.00	11	-56.00 [-64.73; -47.27]
Total (95% CI)			**151**			**151**	**-11.47 [-45.68; 22.74]**
Heterogeneity: $Tau^2 = 584.48$; $Chi^2 = 96.47$, df = 5 ($P < 0.01$); $I^2 = 95\%$							
Test for overall effect: $t_5 = -0.86$ ($P = 0.43$)							
Tibia							
Fadillioglu et al. (2020) [70]	225.00	42.00	13	232.00	26.00	13	-7.00 [-33.85; 19.85]
McGrath et al. (2012a) [29]	450.00	51.00	5	390.00	60.00	5	60.00 [-9.02; 129.02]
McGrath et al. (2012b) [29]	450.00	51.00	5	420.00	10.00	5	30.00 [-15.55; 75.55]
Mo & Chow (2018) [69]	248.00	39.00	11	215.00	7.00	11	33.00 [9.58; 56.42]
Total (95% CI)			**34**			**34**	**22.34 [-18.59; 63.27]**
Heterogeneity: $Tau^2 = 370.93$; $Chi^2 = 6.54$, df = 3 ($P = 0.09$); $I^2 = 54\%$							
Test for overall effect: $t_5 = 1.74$ ($P = 0.18$)							
Lumbar spine							
Benson et al. (2019) [30]	241.80	30.20	12	270.60	25.40	12	-28.80 [-51.13; -6.47]
Gindre et al. (2016a) [68]	160.00	15.00	20	252.50	16.00	20	-92.50 [-102.11; -82.89]
Gindre et al. (2016b) [68]	160.00	15.00	20	237.50	15.00	20	-77.50 [-86.80; -68.20]
Mo & Chow (2018) [69]	220.00	18.00	11	215.00	7.00	11	5.00 [-6.41; 16.41]
Total (95% CI)			**63**			**63**	**-48.74 [-120.33; 22.85]**
Heterogeneity: $Tau^2 = 2179.67$; $Chi^2 = 189.62$, df = 3 ($P < 0.01$); $I^2 = 98\%$							
Test for overall effect: $t_5 = -2.17$ ($P = 0.12$)							

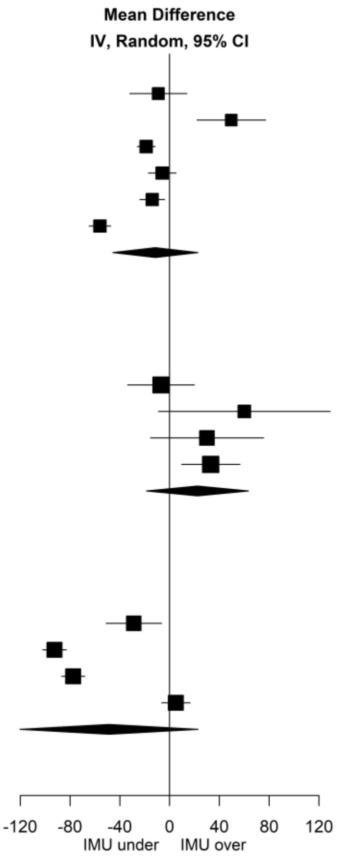

Figure 3.2. Forest plot displaying the effect of contact time (ms) calculated from IMUs worn on the foot, tibia and lumbar spine between 3.3 and 4.3 $m \cdot s^{-1}$. Data are presented as means and SD of IMU- and criterion-derived contact time. Data from the RunScribe™ sensor is shown in Garcia-Pinillos et al. (2019a), while data from the Stryd™ device is shown in Garcia-Pinillos et al. (2019b). Two different motion capture algorithms were used as criterions for McGrath et al. (2012a and b). Gindre et al. (2016a and b) is represented by high-speed camera and photocell system criterions, respectively. CI, confidence interval; df, degrees of freedom; IMU, inertial measurement unit; IV, instrumental variable; over, overestimation; SD, standard deviation; under, underestimation.

Table 3-8. Reliability summary statistics for each analysed stride variable.

Study	Variable	Site	Running velocity $m \cdot s^{-1}$ ± SD	Statistic 1	Statistic 2	Statistic 3	Statistic 4	Statistic 5
Ammann et al. (2016) [97]	Contact time	Foot		CV%	ICC			
			4.3-8.0	2.9-3.8	0.91-0.96			
Garcia-Pinillos et al. (2018) [81]	Contact time	Foot		CV%	SEM (ms)			
			2.2-5.6	1.2-2.3	1.0-5.0			
Gouttebarge et al. (2015) [146]	Contact time	Lumbar spine		SEM (ms)	ICC (95% CI)			
			2.8		-0.24 (-0.69, 0.32)			
			3.3	14.8	0.35 (-0.23, 0.74)			
			3.9	10.1	0.67 (0.22, 0.88)			
Gindre et al. (2016) [132]	Contact time	Lumbar spine		CV%	ICC			
			3.3	6.5	0.99			
			4.2	6.7	0.88			
			5.0	8.3	0.95			
			5.8	9.9	0.97			
Garcia-Pinillos et al. (2018) [81]	Flight time	Foot		CV%	SEM (ms)			
			2.2-5.6	3.7-11.6	3.0-8.0			
Gindre et al. (2016) [132]	Flight time	Lumbar spine		CV%	ICC			
			3.3	4.6	0.94			
			4.2	4.8	0.95			
			5.0	5.2	0.98			
			5.8	5.2	0.98			
Mitschke et al. (2017) [125]	Stride time	Heel		CV%				
			3.5 ± 0.1	2.6-3.5				
Garcia-Pinillos et al. (2018) [81]	Step frequency	Foot		CV%	SEM ($step \cdot min^{-1}$)			
			2.2-5.6	1.1-2.0	1.7-2.8			
Gouttebarge et al. (2015) [146]	Step frequency	Lumbar spine		SEM ($step \cdot min^{-1}$)	ICC (95% CI)			
			2.8	3.5	0.82 (0.52, 0.94)			
			3.3	4.1	0.78 (0.44, 0.92)			
			3.9	3.0	0.92 (0.77, 0.97)			
Gindre et al. (2016) [132]	Step frequency	Lumbar spine		CV%	ICC			
			3.3	4.4	0.94			
			4.2	3.9	0.82			
			5.0	4.1	0.84			
			5.8	4.1	0.94			
Garcia-Pinillos et al. (2018) [81]	Step length	Foot		CV%	SEM (cm)			
			2.2-5.6	1.1-2.1	107.1-241.2			
Mitschke et al. (2017) [125]	Stride length	Heel		CV%				
			3.5 ± 0.1	4.9-7.8				
Raper et al. (2018) [108]	vGRF	Tibia		SEM (95% CI) (N)	ICC (95% CI)	SEM (95% CI) (%)	MDC (95% CI) (N)	MDC (95% CI) (%)
			5.2 ± 0.6	99.8 (82.1, 119.1)	0.88 (0.83, 0.92)	7.0 (5.7, 8.3)	276.7 (227.3, 330.1)	19.3 (15.9, 23.0)
Eggers et al. (2018) [22]	vGRF	Lumbar spine		CV% (90% CI)	ICC (90% CI)	TEE (90% CI) (N)		
			3.3	4.2 (3.3, 6.1)	0.93 (0.84, 0.97)	0.3 (0.2, 0.4)		
Buchheit et al. (2018) [149]	vGRF	Thoracic spine		CV% (90% CI)	ICC (90% CI)	TE (90% CI) (N)	SWC (%)	
			6.1-6.7	17.1 (13.6, 25.1)	0.47 (0.12, 0.72)	0.8 (0.6, 1.1)	5.0	
Eggers et al. (2018) [22]	vGRF	Thoracic spine		CV% (90% CI)	ICC (90% CI)	TEE (90% CI) (N)		
			3.3	3.3 (2.5, 4.7)	0.95 (0.89, 0.98)	0.3 (0.2, 0.4)		
Edwards et al. (2019) [110]	vGRF	Thoracic spine		CV%	ICC	TE (N)		
			3.3	17.8	0.47	2.6		
			5.0	18.6	0.50	2.9		
			6.7	21.8	0.31	2.9		
Eggers et al. (2018) [22]	Vertical stiffness	Lumbar spine		CV% (90% CI)	ICC (90% CI)	TEE (90% CI) ($kN \cdot m^{-1}$)		
			3.3	12.1 (9.3, 17.6)	0.70 (0.41, 0.86)	0.7 (0.5, 1.0)		

Table 2.8. Reliability summary statistics for each analysed stride variable (continued).

Study	Variable	Site	Running velocity $m \cdot s^{-1} \pm SD$	Statistic 1	Statistic 2	Statistic 3	Statistic 4	Statistic 5
Buchheit et al. (2018) [149]	Vertical stiffness	Thoracic spine		CV% (90% CI)	ICC (90% CI)	TE (90% CI) ($kN \cdot m^{-1}$)	SWC (%)	
			6.1-6.7	11.0 (8.6, 15.6)	0.75 (0.52, 0.88)	0.5 (0.7, 1.2)	4.0	
Eggers et al. (2018) [22]	Vertical stiffness	Thoracic spine		CV% (90% CI)	ICC (90% CI)	TEE (90% CI) ($kN \cdot m^{-1}$)		
			3.3	9.5 (7.3, 13.7)	0.71 (0.44, 0.87)	0.7 (0.5, 1.0)		

Abbreviations: CI, confidence interval; cm, centimetres; CV, coefficient of variation; ICC, intraclass correlation coefficient; $kN \cdot m^{-1}$; kilo Newtons per metre; MDC, minimal detectable change; ms, milliseconds; $m \cdot s^{-1}$, metres per second; N, Newtons; SD, standard deviation; SEM, standard error of measurement; $step \cdot min^{-1}$; steps per minute; SWC, smallest worthwhile change; TE, typical error; TEE, typical error of the estimate.
Running velocity reported with or without ± SD, depending on the method used in each study. Values presented for Ammann et al. (2016) and Garcia-Pinillos et al. (2018) represents reliability assessed at a range of speeds.
Values converted to milliseconds, centimetres or Newtons where required.

3.4.4.4 Flight Time

Results from studies reporting the criterion validity of IMU-derived flight time are documented in Table 3-9. For placement at the foot, ICC values were as high as 0.81 at 5.6 m·s^{-1} and 0.86 at 3.3 m·s^{-1} compared to photocell and high-speed camera measures of flight time [81, 85]. Low estimation errors (< 8.2 ms) and median ± IQR bias (15.0 ± 12.0 ms) and precision (5.0 ± 3.0 ms) were reported for foot-determined flight time versus motion capture and instrumented treadmill values, respectively [83, 119]. There was a significant difference (p < 0.05) from high-speed camera and photocell system criterions when a lumbar spine placement was used to calculate flight time across a range of velocities (3.3-5.8 m·s^{-1}; 41.0 to 103%) (see Table 3-9) [132], while the bias was -25.8% for thoracic spine-determined flight time in another study using an instrumented treadmill as the reference [21]. The observed difference for lumbar and thoracic spine sites was greater than that of a foot placement (< 15.1%) [85].

For reliability (see Table 3-8), the CV was as high as 11.6% at 2.2 m·s^{-1} for flight time derived from an IMU on the foot [81], while CV values were < 5.2% between trials using a lumbar spine-mounted accelerometer [132].

Outcome data between 3.3 and 4.2 m·s^{-1} was pooled from two studies [81, 85] to perform a meta-analysis assessing the effect of foot-determined flight time (I^2 = 59%; see Figure 3.3). Meta-analysis demonstrated that foot-determined flight time is not significantly different to reference measures (MD [95% CI] 11.93 ms [-8.88, 32.74], p = 0.13). Leave-one-out and moderator analyses were not performed due to only two studies in the meta-analysis.

Table 3-9. Validity summary statistics for flight time.

Study	Sensor	Criterion	Site	Running velocity m·s^{-1} ± SD	Sensor mean ± SD ms	Criterion mean ± SD ms	Statistic 1	Statistic 2	Statistic 3	Statistic 4	Statistic 5
Chew et al. (2018) [119]	IMU (Opal, APDM Inc.)	Motion capture system	Foot				ME ± SD (ms)	RMSE (ms)			
				2.2	Not reported	Not reported	6.1 ± 6.2	7.8			
				2.5			8.2 ± 5.3	9.2			
				2.8			8.1 ± 3.1	10.1			
				3.1			8.1 ± 2.5	10.0			
Falbriard et al. (2018) [83]	IMU (Physilog 4, Gait Up, Switzerland)	Instrumented treadmill	Foot				Median bias ± IQR (ms)	Median precision ± IQR (ms)			
				2.8-5.6	Not reported	Not reported	15.0 ± 12.0	5.0 ± 3.0			
Garcia-Pinillos et al. (2018) [81]	IMU (Stryd^{TM}, Stryd Powermeter, Stryd Inc., Boulder, CO, USA)	Photocell system	Foot				ICC	Pearson's *r*			
				2.2-5.6	62.0 ± 16.9 to 137.6 ± 6.5	36.5 ± 25.4 to 133.7 ± 8.4	0.56-0.81	0.60**-0.83*			
Garcia-Pinillos et al. (2019) [85]	IMU (RunScribe^{TM}, Scribe Lab. Inc. San Francisco CA, USA)	High-speed camera	Foot				ICC (95% CI)	MD (%)	Pearson's *r*	MD (ms)	Systematic bias ± RE (ms)
				3.3 ± 0.4	96.0 ± 26.0	93.0 ± 25.0	0.86 (0.75, 0.92)	3.2	0.75***	3.0	3.0 ± 17.0
	IMU (Stryd^{TM}, Stryd Powermeter, Stryd Inc. Boulder CO, USA)	High-speed camera	Foot				ICC (95% CI)	MD (%)	Pearson's *r*	MD (ms)	Systematic bias ± RE (ms)
				3.3 ± 0.4	107.0 ± 23.0	93.0 ± 25.0	0.81 (0.18, 0.93)	15.1***	0.81***	14.0	15.0 ± 15.0
Gindre et al. (2016) [132]	Accelerometer (Myotest®, Myotest SA, Sion, Switzerland)	Photocell system	Lumbar spine				ICC	MD (%)	CV%		
				3.3	205.0 ± 13.0	101.0 ± 20.0	0.67	103*	24.7		
				4.2	204.0 ± 14.0	119.0 ± 20.0	0.72	71.0*	19.8		
				5.0	205.0 ± 15.0	131.0 ± 18.0	0.78	57.0*	17.1		
				5.8	202.0 ± 15.0	135.0 ± 17.0	0.82	50.0*	15.3		
	Accelerometer (Myotest®, Myotest SA, Sion, Switzerland)	High-speed camera	Lumbar spine				ICC	MD (%)	CV%		
				3.3	205.0 ± 13.0	117.0 ± 17.0	0.69	75.0*	20.5		
				4.2	204.0 ± 14.0	133.0 ± 18.0	0.66	52.0*	16.3		
				5.0	205.0 ± 15.0	143.0 ± 20.0	0.66	43.0*	14.8		
				5.8	202.0 ± 15.0	144.0 ± 18.0	0.77	41.0*	13.7		
Buchheit et al. (2015) [21]	Accelerometer (SPI HPU, GPSports, Canberra, Australia)	Instrumented treadmill	Scapula				Mean bias (90% CI) (%)	CV% (90% CI)	Pearson's *r* (90% CI)		
				2.8-7.5	Not reported	Not reported	-25.8 (-18.8, -27.7)	15.7 (13.5, 18.9)	0.68 (0.55, 0.78)		

Abbreviations: CI, confidence interval; CV, coefficient of variation; ICC, intraclass correlation coefficient; IMU, inertial measurement unit; IQR, inter-quartile range; MD, mean difference; ME, mean error; ms, milliseconds; m·s^{-1}, metres per second; RE, random error; RMSE, root mean square error; SD, standard deviation.
Negative values represent an underestimation of flight time calculated by the IMU compared to the criterion.
Velocity reported with or without ± SD, depending on the method used in each study. A velocity range is presented for Falbriard et al. (2018) and Buchheit et al. (2015) as validity outcomes were reported from pooled speeds.
Values converted to milliseconds where required.
*$p < 0.05$.
**$p < 0.01$.
***$p < 0.001$.

Study	IMU Mean	IMU SD	IMU Total	Criterion Mean	Criterion SD	Criterion Total	Weight	Mean Difference IV, Random, 95% CI
Garcia-Pinillos et al. (2018) [71]	120.32	16.15	18	100.65	19.77	18	29.9%	19.67 [7.88; 31.47]
Garcia-Pinillos et al. (2019a) [35]	96.00	26.00	49	93.00	25.00	49	34.2%	3.00 [-7.10; 13.10]
Garcia-Pinillos et al. (2019b) [35]	107.00	23.00	49	93.00	25.00	49	35.9%	14.00 [4.49; 23.51]
Total (95% CI)			**116**			**116**	**100.0%**	**11.93 [-8.88; 32.74]**

Heterogeneity: $Tau^2 = 40.00$; $Chi^2 = 4.83$, df = 2 (P = 0.09); $I^2 = 59\%$
Test for overall effect: $t_2 = 2.47$ (P = 0.13)

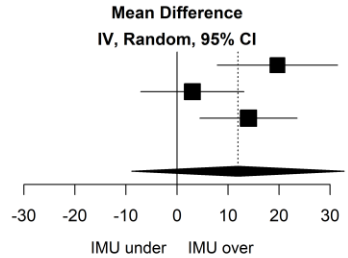

Figure 3.3. Forest plot displaying the effect of flight time (ms) calculated from IMUs worn on the foot between 3.3 and 4.2 m·s^{-1}. Data are presented as means and SD of IMU- and criterion-derived flight time. Data from the RunScribe™ sensor is shown in Garcia-Pinillos et al. (2019a), while data from the Stryd™ device is shown in Garcia-Pinillos et al. (2019b). CI, confidence interval; df, degrees of freedom; IMU, inertial measurement unit; IV, instrumental variable; over, overestimation; SD, standard deviation; under, underestimation.

3.4.4.5 Step Time

Validity outcomes from two studies that calculated step time are presented in Table 8. Compared to values obtained from an instrumented treadmill, step time determined from a foot-worn IMU was shown to have perfect agreement and a median ± IQR precision of 3.0 ± 2.0 ms across velocities ranging from 2.8 to 5.6 $m \cdot s^{-1}$ [83]. The mean bias for step time calculated from a sacrum-worn accelerometer ranged from -1.3 to -0.4 ms across velocities ranging between 2.8 and 5.2 $m \cdot s^{-1}$, showing a marginal underestimation of step time compared to measures derived from a motion capture system [79]. Sacrum-determined step time was most strongly correlated with motion capture at 2.8-3.3 $m \cdot s^{-1}$ ($r = 0.93$) [79].

3.4.4.6 Stride Time

Validity outcomes for IMU-determined stride time are outlined in Table 3-8. Stride time was calculated from IMUs worn on the foot [119], tibia [105, 147], sacrum [79], lumbar spine [84] and thoracic spine [86]. There was no significant difference ($p = 0.92$) between foot-worn IMU and motion capture calculations of stride time, where the mean error ranged from -4.0 ± 24.0 ms at 2.2 $m \cdot s^{-1}$ to 0.3 ± 22.1 ms at 3.1 $m \cdot s^{-1}$ [119]. Comparison between different stride time calculation methods using tibial accelerometry showed ICC values were > 0.95 [147], while in another study using tibia-mounted IMUs, ICC values ranged between 0.55 and 0.83 using two motion capture methods (see Table 3-8) [105]. Stride time derived from the sacrum and lumbar spine showed low errors (standard error < 0.8 ms, mean estimation error < 5.0 ms) compared to motion capture, force plate and high-speed camera measures, respectively [79, 84]. However, when an accelerometer was attached to the thoracic spine, there was a significant bias of -26.0 ms ($p = 0.00$) compared to force plate stride time [86], which is greater than the bias reported for the sacrum (-1.0-1.2 ms) [79].

One study (see Table 3-8) established the reliability of accelerometer-derived stride time across different sampling frequencies [125]. The CV of stride time was < 3.5% for accelerometer signals between 100 and 1000 Hz [125].

Table 3-10. Validity summary statistics for step time and stride time.

Study	Variable	Sensor	Criterion	Site	Running velocity m·s^{-1} ± SD	Sensor mean ± SD ms	Criterion mean ± SD ms	Statistic 1	Statistic 2	Statistic 3	Statistic 4
Falbriard et al. [83] (2018)	Step time	IMU (Physilog 4, Gait Up, Switzerland)	Instrumented treadmill	Foot				Median bias ± IQR (ms)	Median precision ± IQR (ms)		
					2.8-5.6	Not reported	Not reported	0 ± 0	3.0 ± 2.0		
Lee et al. (2010) [79]	Step time	Accelerometer (KXM52 – 1050 Kionix, NY, USA)	Motion capture system	Sacrum				Mean bias (ms)	95% LoA (ms)	SE (ms)	Pearson's *r*
					2.8-3.3	Not reported	Not reported	-0.7	-20.0, 18.0	0.7	0.93
					3.6-4.2			-1.3	-21.0, 18.0	0.8	0.78
					4.4-5.2			-0.4	-19.0, 19.0	0.8	0.76
Chew et al. (2018) [119]	Stride time	IMU (Opal, APDM Inc.)	Motion capture system	Foot				ME ± SD (ms)	RMSE (ms)		
					2.2	Not reported	Not reported	-4.0 ± 24.0	17.6		
					2.5			-3.2 ± 22.7	17.3		
					2.8			-1.0 ± 25.6	24.8		
					3.1			0.3 ± 22.1	21.4		
Norris et al. (2016) [147]	Stride time	Accelerometer (Shimmer 2r, Shimmer Inc., Dublin, Ireland)	Stride time calculation method [Mercer et al., (2003)]	Tibia				SE (ms)	CV%	ICC	
					Self-paced	740.0 ± 90.0	740.0 ± 100.0	8.0	1.1	0.99	
		Accelerometer (Shimmer 2r, Shimmer Inc., Dublin, Ireland)	Stride time calculation method [Mizrahi et al., (2000)]	Tibia				SE (ms)	CV%	ICC	
					Self-paced	740.0 ± 90.0	740.0 ± 100.0	7.0	0.9	0.99	
		Accelerometer (Shimmer 2r, Shimmer Inc., Dublin, Ireland)	Stride time calculation method [Purcell et al., (2006)]	Tibia				SE (ms)	CV%	ICC	
					Self-paced	740.0 ± 90.0	740.0 ± 100.0	10.0	1.3	0.99	
McGrath et al. (2012) [105]	Stride time	IMU (Shimmer, Shimmer Inc., Dublin, Ireland)	Motion capture system [Hreljac and Marshal (2000)]	Tibia				True error (ms)	% error	ICC	
					2.2	810.0 ± 10.0	810.0 ± 10.0	0.1	1.5	0.55	
					3.3	770.0 ± 20.0	780.0 ± 10.0	0.2	1.2	0.83	
		IMU (Shimmer, Shimmer Inc., Dublin, Ireland)	Motion capture system [Zeni et al., (2008)]	Tibia				True error (ms)	% error	ICC	
					2.2	810.0 ± 10.0	810.0 ± 10.0	0.29	1.27	0.57	
					3.3	770.0 ± 20.0	780.0 ± 10.0	0.29	1.26	0.69	
Lee et al. (2010) [79]	Stride time	Accelerometer (KXM52 – 1050 Kionix, NY, USA)	Motion capture system	Sacrum				Mean bias (ms)	95% LoA (ms)	SE (ms)	Pearson's *r*
					2.8-3.3	Not reported	Not reported	-0.5	-16.0, 15.0	0.6	0.98
					3.6-4.2			1.2	-17.0, 20.0	0.7	0.95
					4.4-5.2			-1.0	-21.0, 19.0	0.8	0.92

Table 2.10. Validity summary statistics for step time and stride time (continued).

Study	Variable	Sensor	Criterion	Site	Running velocity $m \cdot s^{-1} \pm SD$	Sensor mean ± SD ms	Criterion mean ± SD ms	Statistic 1	Statistic 2	Statistic 3	Statistic 4
Bergamini et al. (2012) [84]	Stride time	IMU (FreeSense, Sensorize, Italy)	Force plate	Lumbar spine				ME (ms)	LoA (ms)		
					Maximal sprint	485.0 ± 42.2	483.8 ± 41.4	5.0	25.0		
		IMU (FreeSense, Sensorize, Italy)	High-speed camera	Lumbar spine				ME (ms)	LoA (ms)		
					Maximal sprint	453.8 ± 14.2	453.7 ± 16.2	5.0	25.0		
Kenneally-Dabrowski et al. (2018) [86]	Stride time	Accelerometer (GPSports, Canberra, Australia)	Force plate	Thoracic spine				Mean bias (ms)	95% LoA (ms)	Spearman's *r*	
					8.64 ± 0.5	Not reported	Not reported	-26.0*	-91.0, 39.0	-0.18	

Abbreviations: CV, coefficient of variation; ICC, intraclass correlation coefficient; IMU, inertial measurement unit; IQR, inter-quartile range; LoA, limits of agreement; ME, mean error; ms, milliseconds; $m \cdot s^{-1}$, metres per second; RMSE, root mean square error; SD, standard deviation; SE, standard error.
Negative values represent an underestimation of step time and stride time calculated by the IMU compared to the criterion.
Velocity reported with or without ± SD, depending on the method used in each study. A velocity range is presented for Falbriard et al. (2018) as validity outcomes were reported from pooled speeds.
Values converted to milliseconds where required.
*$p < 0.05$.

3.4.4.7 *Swing Time*

Only two studies, each using different attachment sites, reported the validity of IMUs to derive swing time (see Table 3-11). Swing time calculated from a foot-worn IMU was shown to have a median ± IQR bias of 15.0 ± 12.0 ms and a median ± IQR precision of 5.0 ± 2.0 ms compared to values obtained from an instrumented treadmill [83]. Swing time, derived from the angular velocity signal about the *y*-axis from a tibia-mounted gyroscope, showed poor to moderate agreement (ICC < 0.38) when two established motion capture methods were used as criterion measures [105, 152, 153].

3.4.4.8 *Step Frequency*

Six studies quantified step frequency from foot-, tibia- and lumbar spine-worn IMUs, with reliability and validity values from each study presented in Table 3-8 and Table 3-12, respectively. Foot-determined step frequency was nearly perfectly correlated (ICC > 0.95) with photocell and high-speed camera measures across a range of velocities (2.2 to 5.6 $m \cdot s^{-1}$) [81, 85]. Biases were small (< 4.5 $step \cdot min^{-1}$) and correlations exhibited close to perfect agreement (r > 0.96, $p < 0.001$) with an instrumented treadmill in one study that used IMUs from five different manufacturers on the foot, heel and distal tibia (see Table 3-12) [126]. However, the authors did not report running velocity during the trials [126]. The difference between step frequency derived from foot- and lumbar spine-worn IMUs and high-speed camera and photocell systems ranged between -0.9 and 0.8% [85, 132], while another study that directly compared values obtained from a lumbar spine-worn accelerometer to a foot-mounted accelerometer during the same run protocol deemed validity as "good” (ICC = 0.78-0.90) between 2.8 and 3.9 $m \cdot s^{-1}$ [146]. Maximal sprinting (6.8 ± 1.0 $m \cdot s^{-1}$) resulted in a bias ranging between -25.9 and -6.5 $step \cdot min^{-1}$ for step frequency derived from an IMU on the lumbar spine [135].

Reliability (see Table 3-8) was established for foot-determined step frequency, where the CV and SEM ranged between 1.1 to 2.0% and 1.7 to 2.8 step·min^{-1}, respectively, across velocities (2.2 to 5.6 m·s^{-1}) [81]. The ICC values representing the reliability of lumbar spine-determined step frequency were > 0.78 [132, 146].

Data collected between 3.3 and 4.2 m·s^{-1} was grouped to produce a pooled validity estimate for foot- and lumbar spine-determined step frequency (see Figure 3.4). There was no significant difference between foot and lumbar spine estimates of step frequency (p = 0.20). Derivations of step frequency from the foot (MD [95% CI] 0.45 step·min^{-1} [-1.75, 2.66], p = 0.47) and lumbar spine (MD [95% CI] -3.45 step·min^{-1} [-16.28, 9.39], p = 0.37) was shown to not be significantly different to the criterion. As there were only two studies in each subgroup, leave-one-out and moderator analyses were not performed.

Table 3-11. Validity summary statistics for swing time.

Study	Sensor	Criterion	Site	Running velocity m·s^{-1} ± SD	Sensor mean ± SD ms	Criterion mean ± SD ms	Statistic 1	Statistic 2	Statistic 3
Falbriard et al. (2018) [83]	IMU (Physilog 4, Gait Up, Switzerland)	Instrumented treadmill	Foot				Median bias ± IQR (ms)	Median precision ± IQR (ms)	
				2.8-5.6	Not reported	Not reported	15.0 ± 12.0	5.0 ± 3.0	
McGrath et al. (2012) [105]	IMU (Shimmer, Shimmer Inc., Dublin, Ireland)	Motion capture system Hreljac and Marshal (2000)	Tibia				True error (ms)	% error	ICC
				2.2	460.0 ± 330.0	360.0 ± 10.0	65.9	18.7	0.38
				3.3	450.0 ± 20.0	390 ± 10.0	54.8	16.6	0.32
	IMU (Shimmer, Shimmer Inc., Dublin, Ireland)	Motion capture system Zeni et al., (2008)	Tibia				True error (ms)	% error	ICC
				2.2	460.0 ± 330.0	340.0 ± 10.0	78.8	26.8	0.32
				3.3	450.0 ± 20.0	360 ± 10.0	90.0	26.4	0.28

Abbreviations: ICC, intraclass correlation coefficient; IMU, inertial measurement unit; IQR, inter-quartile range; ms, milliseconds; m·s^{-1}, metres per second; SD, standard deviation.
A velocity range is presented for Falbriard et al. (2018) as validity outcomes were reported from pooled speeds.
Values converted to milliseconds where required.

Table 3-12. Validity summary statistics for step frequency.

Study	Sensor	Criterion	Site	Running velocity $m{\cdot}s^{-1}$ ± SD	Sensor mean ± SD $step{\cdot}min^{-1}$	Criterion mean ± SD $step{\cdot}min^{-1}$	Statistic 1	Statistic 2	Statistic 3	Statistic 4	Statistic 5
Garcia-Pinillos et al. (2018) [81]	IMU (Stryd^{TM}, Stryd Powermeter, Stryd Inc., Boulder, CO, USA)	Photocell system	Foot				ICC	Pearson's *r*			
				2.2-5.6	160.9 ± 6.8 to 191.8 ± 5.4	159.6 ± 6.3 to 193.2 ± 5.9	0.96-0.99	0.96-0.99***			
Garcia-Pinillos et al. (2019) [85]	IMU (RunScribe^{TM}, Scribe Lab. Inc. San Francisco, CA, USA)	High-speed camera	Foot				ICC (95% CI)	Pearson's *r*	MD ($step{\cdot}min^{-1}$)	MD (%)	Systematic bias ± RE ($step{\cdot}min^{-1}$)
				3.3 ± 0.4	168.1 ± 7.4	166.8 ± 7.7	0.96 (0.92, 0.98)	0.95***	1.3	0.8	1.3 ± 2.5
	IMU (Stryd^{TM}, Stryd Powermeter, Stryd Inc. Boulder, CO, USA)	High-speed camera	Foot				ICC (95% CI)	Pearson's *r*	MD ($step{\cdot}min^{-1}$)	MD (%)	Systematic bias ± RE ($step{\cdot}min^{-1}$)
				3.3 ± 0.4	166.7 ± 7.3	166.8 ± 7.7	0.97 (0.94, 0.98)	0.93***	-0.1	0.1	-0.1 ± 2.8
Pairot de Fontenay et al. (2020) [126]	IMU (MilestonePod, Milestone Sports, Long Beach, CA, USA)	Instrumented treadmill	Foot				Mean bias ($step{\cdot}min^{-1}$)	Pearson's *r*	95% LoA ($step{\cdot}min^{-1}$)		
				Not reported	Not reported	Not reported	1.6	0.99***	± 1.4		
	IMU (Zoi, Runteq, Tampere, Finland)	Instrumented treadmill	Foot				Mean bias ($step{\cdot}min^{-1}$)	Pearson's *r*	95% LoA ($step{\cdot}min^{-1}$)		
				Not reported	Not reported	Not reported	0.9	0.99***	± 1.3		
	IMU (RunScribe^{TM}, Montara, CA, USA)	Instrumented treadmill	Heel				Mean bias ($step{\cdot}min^{-1}$)	Pearson's *r*	95% LoA ($step{\cdot}min^{-1}$)		
				Not reported	Not reported	Not reported	1.1	0.99***	± 0.9		
Pairot de Fontenay et al. (2020) [126]	IMU (Moov Now^{TM}, Moov, San Mateo, CA, USA)	Instrumented treadmill	Tibia				Mean bias ($step{\cdot}min^{-1}$)	Pearson's *r*	95% LoA ($step{\cdot}min^{-1}$)		
				Not reported	Not reported	Not reported	2.3	0.98***	± 2.0		
	IMU (TgForce, Kelsec Systems Inc., Montreal, Canada)	Instrumented treadmill	Tibia				Mean bias ($step{\cdot}min^{-1}$)	Pearson's *r*	95% LoA ($step{\cdot}min^{-1}$)		
				Not reported	Not reported	Not reported	4.5	0.96***	± 6.1		
Gouttebarge et al. (2015) [146]	Accelerometer (Myotest®, Myotest SA, Sion, Switzerland)	Foot-mounted accelerometer	Lumbar spine				ICC (95% CI)				
				2.8	164.3 ± 7.0	165.6 ± 8.0	0.89 (0.69, 0.96)				
				3.3	168.9 ± 8.0	169.4 ± 8.0	0.78 (0.45, 0.96)				
				3.9	175.9 ± 10.0	175.7 ± 13.0	0.90 (0.72, 0.97)				

Table 2.12. Validity summary statistics for step frequency (continued).

Study	Sensor	Criterion	Site	Running velocity m·s^{-1} ± SD	Sensor mean ± SD step·min^{-1}	Criterion mean ± SD step·min^{-1}	Statistic 1	Statistic 2	Statistic 3	Statistic 4	Statistic 5
Gindre et al. (2016) [132]	Accelerometer (Myotest®, Myotest SA, Sion, Switzerland)	Photocell system	Lumbar spine				ICC	MD (%)	CV%		
				3.3	163.0 ± 10.0	163.0 ± 9.0	0.86	0.1	4.1		
				4.2	168.0 ± 9.0	169.0 ± 9.0	0.94	-0.5	3.9		
				5.0	177.0 ± 10.0	178.0 ± 10.0	0.93	-0.3	3.8		
				5.8	188.0 ± 11.0	190.0 ± 12.0	0.87	-0.8	4.6		
	Accelerometer (Myotest®, Myotest SA, Sion, Switzerland)	High-speed camera	Lumbar spine				ICC	MD (%)	CV%		
				3.3	163.0 ± 10.0	163.0 ± 9.0	0.89	0.2	3.9		
				4.2	168.0 ± 9.0	168.0 ± 9.0	0.95	-0.2	3.7		
				5.0	177.0 ± 10.0	176.0 ± 11.0	0.84	0.3	3.8		
				5.8	188.0 ± 11.0	190.0 ± 12.0	0.86	-0.9	4.6		
Machulik et al. (2020) [135]	IMU (Humotion SmarTracks Integrated System)	Photocell system	Lumbar spine				ICC (95% CI)	Systematic bias (step·min^{-1})	95% LoA (step·min^{-1})		
				3.8 ± 0.7	159.6 ± 7.8	168.6 ± 7.8	0.75-0.89 (0.48, 0.95)	-11.9 to -5.2	-20.8, 1.7		
				6.8 ± 1.0	206.4 ± 15.9	228.0 ± 19.2	0.90-0.94 (0.79, 0.97)	-25.9 to -6.5	-47.76, 6.1		

Abbreviations: CI, confidence interval; CV, coefficient of variation; ICC, intraclass correlation coefficient; IMU, inertial measurement unit; LoA, limits of agreement; MD, mean difference; m·s^{-1}, metres per second; RE, random error; SD, standard deviation; step·min^{-1}, steps per minute.
Negative values represent an underestimation of step frequency calculated by the IMU compared to the criterion.
Velocity reported with or without ± SD, depending on the method used in each study.
***$p < 0.001$.

Study or Subgroup	IMU Mean	IMU SD	IMU Total	Criterion Mean	Criterion SD	Criterion Total	Mean Difference IV, Random, 95% CI
Foot							
Garcia-Pinillos et al. (2018) [71]	173.48	7.47	18	173.80	7.50	18	-0.32 [-5.22; 4.57]
Garcia-Pinillos et al. (2019a) [35]	168.10	7.40	49	166.80	7.70	49	1.30 [-1.69; 4.29]
Garcia-Pinillos et al. (2019b) [35]	166.70	7.30	49	166.80	7.70	49	-0.10 [-3.07; 2.87]
Total (95% CI)			**116**			**116**	**0.45 [-1.75; 2.66]**
Heterogeneity: $Tau^2 = 0$; $Chi^2 = 0.54$, df = 2 (P = 0.76); $I^2 = 0\%$							
Test for overall effect: $t_2 = 0.88$ (P = 0.47)							
Lumbar spine							
Gindre et al. (2016a) [68]	165.50	9.50	20	166.00	9.00	20	-0.50 [-6.24; 5.24]
Gindre et al. (2016b) [68]	165.50	9.50	20	165.50	9.00	20	0.00 [-5.74; 5.74]
Machulik et al. (2020) [72]	159.60	7.80	28	168.60	7.80	28	-9.00 [-13.09; -4.91]
Total (95% CI)			**68**			**68**	**-3.45 [-16.28; 9.39]**
Heterogeneity: $Tau^2 = 23.70$; $Chi^2 = 8.89$, df = 2 (P = 0.01); $I^2 = 78\%$							
Test for overall effect: $t_2 = -1.16$ (P = 0.37)							

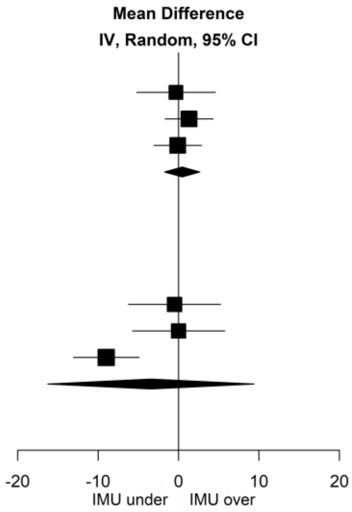

Figure 3.4. Forest plot displaying the effect of step frequency (step·min^{-1}) calculated from IMUs worn on the foot and lumbar spine between 3.3 and 4.2 m·s^{-1}. Data are presented as means and SD of IMU- and criterion-derived step frequency. Data from the RunScribe™ sensor is shown in Garcia-Pinillos et al. (2019a), while data from the Stryd™ device is shown in Garcia-Pinillos et al. (2019b). Gindre et al. (2016a and b) is represented by high-speed camera and photocell system criterions, respectively, where the authors reported the same values for each. CI, confidence interval; df, degrees of freedom; IMU, inertial measurement unit; IV, instrumental variable; over, overestimation; SD, standard deviation; under, underestimation.

3.4.4.9 Step Length

The validity of foot-mounted IMUs to quantify step length during running at different velocities (2.2 to 5.6 m·s^{-1}) was investigated in three studies (see Table 3-13). Pearson's correlation and ICCs showed step length, calculated from Stryd™ and RunScribe™ devices, was nearly perfectly correlated (r > 0.93, p < 0.001) with photocell and high-speed camera measures across all velocities [81, 85]. One study used placement on the lumbar spine and showed that biases increased and ICC values decreased from jogging (bias = 8.1-12.2 cm; ICC = 0.90-0.94) to sprinting (bias = 11.5-28.4 cm; ICC = 0.79-0.85) compared to a photocell system [135].

One study assessed the reliability of step length derived from a foot-mounted IMU (see Table 3-8), which showed the CV ranged from 1.1 to 2.1% across all velocities (2.2 to 5.6 m·s^{-1}), while the SEM was highest at 5 m·s^{-1} (241.2 cm) [81].

Data collected between 3.3 and 4.2 m·s^{-1} was grouped to produce a pooled validity estimate for foot-determined step length. Results from the meta-analysis are presented in Figure 3.5 and show that IMUs worn on the foot produce step length values that are not significantly different to reference measures (MD [95% CI] 0.21 cm [-1.76, 2.18], p = 0.69). No moderator analysis was performed due to I^2 = 0%.

3.4.4.10 Stride Length

Three studies determined the validity of foot-mounted IMUs to calculate stride length, where summary statistics from each study are documented in Table 3-13. Compared to motion capture, the mean error of IMU-derived stride length ranged from -0.5 to 46.0 cm [117, 119, 148]. The agreement between stride length determined from an IMU and motion capture system was improved during overground runs over 10 m (3.6 ± 0.3 m·s^{-1}; root mean square error [RMSE] = 8.3 cm) compared to running on a treadmill for 3 min at different velocities (2.2-3.1 m·s^{-1};

RMSE = 59.2-70.2 cm, r = 0.96, p < 0.001) [119, 148]. In a study comparing four different algorithms for computing stride length from IMU signals to a motion capture system, results showed that an algorithm based on foot trajectory performed best (mean error = 2.0 ± 14.1 cm, mean percentage error = 2.8%) than those based on stride time (mean error = 17.7 ± 57.3 cm, mean percentage error = 17.1%), foot acceleration (mean error = -0.5 ± 25.6 cm, mean percentage error = 7.9%) and deep learning (mean error = 2.5 ± 20.1 cm, mean percentage error = 5.9%) across a range of velocities up to 5.0 $m \cdot s^{-1}$ (see Table 3-13) [117].

The CV for within-subject variation of stride length across different sampling frequencies ranged from 4.9% at 1000 Hz to 7.8% at 100 Hz (see Table 3-8) [125].

Table 3-13. Validity summary statistics for step length and stride length.

Study	Variable	Sensor	Criterion	Site	Running velocity $m \cdot s^{-1} \pm SD$	Sensor mean ± SD cm	Criterion mean ± SD cm	Statistic 1	Statistic 2	Statistic 3	Statistic 4	Statistic 5	Statistic 6	Statistic 7
Garcia-Pinillos et al. (2018) [81]	Step length	IMU (Stryd™, Stryd Powermeter, Stryd Inc., Boulder, CO, USA)	Photocell system	Foot				ICC	Pearson's *r*					
					2.2-5.6	83.0 ± 3.6 to 173.9 ± 84.4	83.8 ± 3.6 to 172.9 ± 5.1	0.93-0.99	0.93-0.99***					
Garcia-Pinillos et al. (2019) [85]	Step length	IMU (RunScribe™, Scribe Lab. Inc. San Francisco CA, USA)	High-speed camera	Foot				ICC (95% CI)	Pearson's *r*	MD (cm)	MD (%)	Systematic bias ± RE (cm)		
					3.3 ± 0.4	116.3 ± 12.1	116.9 ± 12.5	0.97 (0.95, 0.98)	0.96***	-0.6	0.5	-0.6 ± 4.3		
		IMU (Stryd™, Stryd Powermeter, Stryd Inc. Boulder CO, USA)	High-speed camera	Foot				ICC (95% CI)	Pearson's *r*	MD (cm)	MD (%)	Systematic bias ± RE (cm)		
					3.3 ± 0.4	118.05 ± 13.47	116.89 ± 12.50	0.98 (0.96, 0.99)	0.94***	1.2	1.0	1.2 ± 3.9		
Machulik et al. (2020) [135]	Step length	IMU (Humotion SmarTracks Integrated)	Photocell system	Lumbar spine				ICC (95% CI)	Systematic bias (cm)	95% LoA (cm)				
					3.8 ± 0.7 6.8 ± 1.0	141.0 ± 26.0 196.0 ± 36.0	131.0 ± 20.0 173.0 ± 21.0	0.90-0.94 (0.79, 0.98) 0.79-0.85 (0.58, 0.93)	8.1-12.2 11.5-28.4	-14.2, 30.4 -7.1, 62.3				
Brahms et al. (2018) [148]	Stride length	IMU (Xsens, MTw)	Motion capture system	Foot				ICC (95% CI)	Pearson's *r*	MD (cm)	ME (cm)	% error	95% LoA (cm)	RMSE (cm)
					3.6 ± 0.3	259.2 ± 27.6	262.3 ± 27.2	0.96 (0.93, 0.97)	0.96***	-3.2	5.0	2.0	-18.3, 11.8	8.3
Chew et al. (2018) [119]	Stride length	IMU (Opal, APDM Inc.)	Motion capture system	Foot				ME ± SD (cm)	RMSE (cm)					
					2.2 2.5 2.8 3.1	Not reported	Not reported	32.3 ± 48.2 14.1 ± 46.0 44.0 ± 56.7 46.0 ± 62.6	62.4 70.2 63.8 59.2					
Zrenner et al. (2018) [117]	Stride length	IMU (miPod sensor): stride time-based algorithm	Motion capture system	Foot				ME ± SD (cm)	MAE (cm)	% error				
					2.0-6.0	Not reported	Not reported	17.7 ± 57.3	45.2	17.1				
		IMU (miPod sensor): acceleration-based algorithm	Motion capture system	Foot				ME ± SD (cm)	MAE (cm)	% error				
					2.0-6.0	Not reported	Not reported	-0.5 ± 25.6	19.9	7.9				
		IMU (miPod sensor): foot trajectory-based algorithm	Motion capture system	Foot				ME ± SD (cm)	MAE (cm)	% error				
					2.0-6.0	Not reported	Not reported	2.0 ± 14.1	7.6	2.8				
		IMU (miPod sensor): deep learning-based algorithm	Motion capture system	Foot				ME ± SD (cm)	MAE (cm)	% error				
					2.0-6.0	Not reported	Not reported	2.5 ± 20.1	15.3	5.9				

Abbreviations: CI, confidence interval; cm, centimetres; ICC, intraclass correlation coefficient; IMU, inertial measurement unit; LoA, limits of agreement; MAE, mean absolute error; MD, mean difference; ME, mean error; $m \cdot s^{-1}$, metres per second; RE, random error; RMSE, root mean square error; SD, standard deviation.
Negative values represent an underestimation of step length and stride length calculated by the IMU compared to the criterion.
Velocity reported with or without ± SD, depending on the method used in each study. A velocity range is presented for Zrenner et al. (2018) as validity outcomes were reported from pooled speeds.
Values converted to centimetres where required.
***$p < 0.001$.

Study	IMU Mean	IMU SD	IMU Total	Criterion Mean	Criterion SD	Criterion Total	Weight	Mean Difference IV, Random, 95% CI
Garcia-Pinillos et al. (2018) [71]	129.78	5.60	18	129.61	5.62	18	48.2%	0.16 [-3.50; 3.83]
Garcia-Pinillos et al. (2019a) [35]	116.30	12.10	49	116.90	12.50	49	27.3%	-0.60 [-5.47; 4.27]
Garcia-Pinillos et al. (2019b) [35]	118.10	13.50	49	116.90	12.50	49	24.4%	1.20 [-3.95; 6.35]
Total (95% CI)			**116**			**116**	**100.0%**	**0.21 [-1.76; 2.18]**

Heterogeneity: $Tau^2 = 0$; $Chi^2 = 0.25$, df = 2 (P = 0.88); $I^2 = 0\%$
Test for overall effect: $t_2 = 0.45$ (P = 0.69)

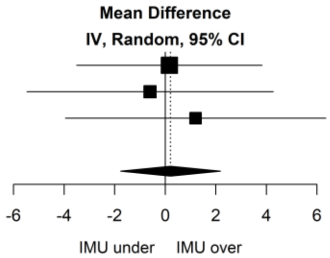

Figure 3.5. Forest plot displaying the effect of step length (cm) calculated from IMUs worn on the foot between 3.3 and 4.2 $m \cdot s^{-1}$. Data are presented as means and SD of IMU- and criterion-derived step length. Data from the RunScribe™ sensor is shown in Garcia-Pinillos et al. (2019a), while data from the Stryd™ device is shown in Garcia-Pinillos et al. (2019b). CI, confidence interval; df, degrees of freedom; IMU, inertial measurement unit; IV, instrumental variable; over, overestimation; SD, standard deviation; under, underestimation.

3.4.4.11 Ground Reaction Force

The outcomes for the 11 studies that investigated the validity of IMUs to estimate GRF are presented in Table 3-14. Two studies applied a neural network model to accelerometer data from the foot and thoracic spine to predict vertical and resultant GRF, respectively [122, 127]. The RMSE for vertical GRF determined from foot acceleration data was < 10.5 N compared to values obtained from an instrumented treadmill, while the mean signal cross-correlation was 0.99 when the entire vertical GRF waveform was evaluated [122]. A neural network method predicted resultant GRF from accelerometers worn on the thoracic spine with a mean coefficient of determination (r^2) value of 0.9 [127]. Attaching an accelerometer to the tibia [108] and hip [130] resulted in mean differences to force plate of 400.0 N and 106.4 N (~ 8.3%), respectively, for vertical GRF, whereas biases were smaller for the vertical (-34.1 N) and resultant (-29.7 N) components of peak force when an IMU was attached to the sacrum (see Table 3-14) [123]. One study that used a spring-mass model to calculate peak vertical force showed strong correlations between force plate-lumbar spine (r = 0.81) and force plate-thoracic spine (r = 0.79), while the CV was 9.2% and 9.6%, respectively [22]. When acceleration values were converted to Newtons by multiplying by body mass, larger measurement errors and weaker correlations were reported for both vertical (CV = 16.2%, r = 0.44, p < 0.01) and resultant GRF (CV = 16.4%) using a thoracic spine accelerometer [106, 110]. During slow (2 $m \cdot s^{-1}$) to moderate (5 $m \cdot s^{-1}$) speed running in another study, a single thoracic spine-mounted accelerometer was shown to be inadequate (RMSE > 509.2 N) for use with a mass-spring damper model to predict resultant GRF waveforms [107]. When multiple IMUs were used to estimate vertical GRF, the RMSE was 220.8 ± 45.7 N, while the root mean square deviation was 241.4 ± 59.6 N [121, 150].

The reliability of accelerometers to estimate vertical GRF was examined in four studies (see Table 3-8). For placement on the tibia, the SEM was 99.8 N (7.0%), whereas the minimal detectable change (MDC) was 276.7 N (19.3%) [108]. As with placement on the tibia (ICC = 0.88), lumbar spine (CV = 4.2%) and thoracic spine (CV = 3.3%) sites also showed reliable outcomes for vertical GRF derived from a spring-mass model during a continuous 2 min shuttle run [22]. However, when the same model was applied in another study using thoracic spine accelerometers, the authors classed the between-day typical error (TE; 0.8 N) and ICC (0.47) values as moderate [149]. Poor reliability was exhibited in a further study utilising accelerometers placed on the thoracic spine, whereby CV values were > 17.8% across velocities ranging between 3.3 and 6.7 $m \cdot s^{-1}$ [110].

Two studies reported mean ± SD values for thoracic spine-derived peak resultant GRF [106, 107]. However, as one study had an SD that was nearly as large as the mean [107], which suggests the data was not normally distributed and therefore not meeting the assumptions for a random-effects meta-analysis [154], these studies were not pooled.

3.4.4.12 Vertical Stiffness

Three studies examined the reliability and validity of accelerometers placed at the lumbar and thoracic spine to calculate vertical stiffness (see Table 3-8 and Table 3-15, respectively). A nearly perfect correlation (r = 0.98) between thoracic spine-determined vertical stiffness and that obtained from an instrumented treadmill was reported from a single participant in one study [21]. When a larger sample of participants were analysed in another study, correlations with force plate were not as strong between lumbar spine (r = 0.65) and thoracic spine (r = 0.66) estimates of vertical stiffness [22].

Inter-day reliability results were comparable between accelerometer placements, with a CV between 9.5 and 12.1% and ICC values 0.70-0.75 for both the lumbar and thoracic spine (see Table 3-8) [22, 149].

Table 3-14. Validity summary statistics for ground reaction force.

Study	Variable	Sensor	Criterion	Site	Running velocity $m \cdot s^{-1} \pm$ SD	Sensor mean ± SD N	Criterion mean ± SD N	Statistic 1	Statistic 2	Statistic 3	Statistic 4
Ngoh et al. (2018) [122]	vGRF	IMU (Opal, APDM Inc.)	Instrumented treadmill	Foot	2.2 2.5 2.8	Not reported	Not reported	RMSE ± SD (N) 10.5 ± 6.2 9.3 ± 4.4 10.5 ± 5.6	Signal cross-correlation 0.99 0.99 0.99		
Raper et al. (2018) [108]	vGRF	Accelerometer (ViPerform v5, DorsaVi, Melbourne, Australia)	Force plate	Tibia	5.2 ± 0.6	Not reported	Not reported	MD (N) 400.0			
Neugebauer et al. (2014) [130]	vGRF	Accelerometer (GT3X+ AM, ActiGraph, Pensacola, FL, USA)	Force plate	Hip	2.2-4.1	Not reported	Not reported	MD (N) 106.4	% MD ± SD 8.3 ± 3.7	Mean bias ± SD (N) -50.5 ± 130.4	95% LoA (N) -311.3, 210.3
Gurchiek et al. (2017) [123]	vGRF	IMU (Yost Data Logger 3-Space Sensor, YEI Technology, Portsmouth, OH)	Force plate	Sacrum	Not reported	Not reported	Not reported	RMSE (N) 77.1	Pearson's *r* 0.88^{**}	Systematic bias (N) -34.1	95% LoA (N) -171.8, 103.7
Eggers et al. (2018) [22]	vGRF	Accelerometer (wGT3X-BT, ActiGraph, Pensacola, FL, USA)	Force plate	Lumbar spine	3.3	Not reported	Not reported	CV% (90% CI) 9.2 (7.6, 11.7)	Pearson's *r* (90% CI) 0.81 (0.69, 0.89)	TEE (90% CI) (N) 0.71 (0.51, 1.05)	
Wundersitz et al. (2013) [106]	vGRF	Accelerometer (SPI Pro, ASP00725, GPSports Pty. Ltd., Canberra, Australia)	Force plate	Scapula	5.4 ± 0.5	1582.0 ± 408.0	1731.0 ± 245.0	CV% 16.2	Spearman's *r* 0.12		
Eggers et al. (2018) [22]	vGRF	Accelerometer (wGT3X-BT, ActiGraph, Pensacola, FL, USA)	Force plate	Scapula	3.3	Not reported	Not reported	CV% (90% CI) 9.6 (8.0, 12.3)	Pearson's *r* (90% CI) 0.79 (0.54, 1.0)	TEE (90% CI) (N) 0.76 (0.54, 1.14)	
Edwards et al. (2019) [110]	vGRF	Accelerometer (SPI HPU, GPSports Pty. Ltd., Canberra, Australia)	Force plate	Scapula	3.3-6.7	Not reported	Not reported	Pearson's *r* 0.44^{**}			
Wouda et al. (2018) [150]	vGRF	IMU (Xsens, Enschede, the Netherlands)	Instrumented treadmill	Lower legs and pelvis	3.3	2338.8 ± 256.4	2261.1 ± 101.0	RMSE ± SD (N) 220.8 ± 45.7	Pearson's *r* 0.96		
Dorschky et al. (2019) [121]	vGRF	IMU (Portabiles GmbH, Erlangen, DE)	Force plate	Foot, tibia, thighs and lumbar spine	3.0-4.9	Not reported	Not reported	RMSD ± SD (N) 241.4 ± 59.6	Pearson's *r* 0.94	rRMSD ± SD (%) 12.8 ± 3.6	

Table 2.14. Validity summary statistics for ground reaction force (continued).

Study	Variable	Sensor	Criterion	Site	Running velocity m·s^{-1} ± SD	Sensor mean ± SD N	Criterion mean ± SD N	Statistic 1	Statistic 2	Statistic 3	Statistic 4
Gurchiek et al. (2017) [123]	rGRF	IMU (Yost Data Logger 3-Space Sensor, YEI Technology, Portsmouth, OH)	Force plate	Sacrum				RMSE (N)	Pearson's *r*	Systematic bias (N)	95% LoA (N)
					Not reported	Not reported	Not reported	73.6	0.90**	-29.7	-163.9, 104.4
Wundersitz et al. (2013) [106]	rGRF	Accelerometer (SPI Pro, ASP00725, GPSports Pty. Ltd., Canberra, Australia)	Force plate	Thoracic spine				CV%	Spearman's *r*		
					5.4 ± 0.5	2194.0 ± 317.0	1755.0 ± 253.0	16.4	0.31		
Nedergaard et al. (2018) [107]	rGRF	Accelerometer (MinimaxX S4, Catapult Innovations, Scoresby, Australia)	Force plate	Thoracic spine				RMSE (N)			
					2.0	3124.4 ± 1422.7	1714.6 ± 162.6	509.2			
					3.0	4769.0 ± 3979.4	1896.2 ± 149.7	509.2			
					4.0	17562.8 ± 30118.0	2068.0 ± 118.6	706.8			
					5.0	6818.0 ± 5999.4	2084.7 ± 186.2	972.8			
Pogson et al. (2020) [127]	rGRF	Accelerometer (MinimaxX S5, Catapult Innovations, Scoresby, Australia)	Force plate	Thoracic spine				r^2			
					2.0-8.0	Not reported	Not reported	0.9			

Abbreviations: CI, confidence interval; CV, coefficient of variation; IMU, inertial measurement unit; LoA, limits of agreement; MD, mean difference; m·s^{-1}, metres per second; N, Newtons; r^2, coefficient of determination; rGRF, resultant ground reaction force; RMSD, root mean square deviation; RMSE, root mean square error; rRMSD, relative root mean square deviation; SD, standard deviation; TEE, typical error of the estimate; vGRF, vertical ground reaction force.
Negative values represent an underestimation of ground reaction force calculated by the IMU compared to the criterion.
Velocity reported with or without ± SD, depending on the method used in each study. A velocity range is presented for Neugebauer et al. (2014), Edwards et al. (2019), Dorschky et al. (2019) and Pogson et al. (2020) as validity outcomes were reported from pooled speeds.
Values converted to Newtons where required.
**$p < 0.01$.

Table 3-15. Validity summary statistics for vertical stiffness.

Study	Sensor	Criterion	Site	Running velocity m·s^{-1}	Sensor mean ± SD kN·m^{-1}	Criterion mean ± SD kN·m^{-1}	Statistic 1 (90% CI)	Statistic 2 (90% CI)	Statistic 3 (90% CI)
Eggers et al. (2018) [22]	Accelerometer (wGT3X-BT, ActiGraph, Pensacola, FL, USA)	Force plate	Lumbar spine	3.3	26.0 ± 5.0	24.9 ± 3.7	CV% 12.9 (10.7, 16.5)	Pearson's *r* 0.65 (0.44, 0.79)	TEE (kN·m^{-1}) 1.2 (0.8, 2.0)
Buchheit et al. (2015) [21]	Accelerometer (SPI HPU, GPSports, Canberra, Australia)	Instrumented treadmill	Thoracic spine	2.8-7.5	Not reported	Not reported	CV% 6.3 (5.5, 7.5)	Pearson's *r* 0.98 (0.97, 0.99)	Mean bias (%) -13.3 (-14.6, -11.9)
Eggers et al. (2018) [22]	Accelerometer (wGT3X-BT, ActiGraph, Pensacola, FL, USA)	Force plate	Thoracic spine	3.3	24.4 ± 3.8	24.9 ± 3.7	CV% 12.8 (10.6, 16.3)	Pearson's *r* 0.66 (0.46, 0.79)	TEE (kN·m^{-1}) 1.2 (0.8, 2.0)

Abbreviations: CI, confidence interval; CV, coefficient of variation; kN·m^{-1}, kilo Newtons per metre; m·s^{-1}, metres per second; SD, standard deviation; TEE, typical error of the estimate.
Negative values represent an underestimation of vertical stiffness calculated by the IMU compared to the criterion.
A velocity range is presented for Buchheit et al. (2015) as validity outcomes were reported from pooled speeds.

3.5 Discussion

This systematic review and meta-analysis summarises the validity and reliability of IMUs to derive spatiotemporal features of running gait and estimate peak GRF and vertical stiffness based on different attachment sites. Twelve variables were analysed across 39 studies, where the placement of IMUs varied between the foot, distal and mid tibia, hip, sacrum, lumbar spine, torso and thoracic spine. The results from reviewed studies and meta-analysis suggest it is possible to obtain valid and reliable stride data using IMUs attached at different sites. It appears that accuracy may depend more on the computational method used for identifying stride events (IC and TO) from inertial data rather than the attachment site itself.

Meta-analysis revealed that contact time and step frequency derived from IMUs placed at the foot, tibia and lumbar spine does not significantly differ to the criterion. However, some of these pooled analyses demonstrated high between-study heterogeneity ($I^2 > 54.1\%$), which could not be explained by differing criterion methods, nor by omitting one study for the foot and lumbar spine subgroups. Subsequently, the source of heterogeneity remains unclear for these sites, but could be due to other methodological factors such as the type of sensor, sampling rate, or computational method for identifying stride events. These potential moderating variables could not be investigated further due to insufficient reporting of data within those studies. Although there were no influential studies for the foot and lumbar spine subgroups, the pooled MD for contact time determined from the tibia was distorted when one study [134] was omitted. Removal of this study from the meta-analysis resulted in an overall effect that was significantly different ($p = 0.02$) to the criterion, which would have suggested the tibia is not a suitable site to determine contact time had the study not been included. Other work reviewed here demonstrated valid results for contact time using IMUs secured to the distal tibia [80]. Although this study was not eligible for inclusion in the meta-analysis due to insufficient reporting of data, it is possible it may have supported our findings in the final meta-analysis, where no significant difference (p = 0.18) was observed between the tibia and criterion. Furthermore, IC and TO have been detected with good accuracy from tibial acceleration data [19, 80, 128], which suggests this site is a viable option for calculating temporal variables, such as contact time.

Subgroup analysis was not possible for flight time and step length due to a limited number of studies meeting eligibility criteria for inclusion. However, studies that used foot-worn IMUs to determine these metrics were meta-analysed and demonstrated that estimates of flight time and step length was not significantly different from criterion measures, which is similar to the results reported for contact time and step frequency. Collectively, the results from the four meta-analyses highlight the utility of using IMUs for gait analysis, where the findings reported here may open opportunities for practitioners to use placement on the foot, tibia or lumbar spine to capture spatiotemporal features of an athlete's stride in the field. However, there has been little work done (two reviewed studies) applying gait event detection methods to inertial data from the thoracic spine to investigate the validity of this site to derive temporal variables, with one study only reporting a single observation (n = 1) [21, 86]. It is therefore unclear whether placement on the thoracic spine is also suitable to derive temporal stride data.

Peak vertical or resultant GRFs during running have traditionally been measured from force platforms [118, 155, 156]. However, IMUs are more accessible to an athlete's normal training and competition environment than force platforms and may provide a useful tool for quantifying surrogate measures of force during running-based sports [157]. A variety of different approaches were used to estimate peak GRFs in the studies reviewed here. Although meta-analysis was not possible, predictions of vertical GRF were shown to be most accurate when studies applied machine learning techniques or used multiple IMUs at different body segments [121, 122, 127, 150]. Given IMUs are commonly worn on the thoracic spine in sport, other studies investigated the validity of this site to predict GRFs from accelerometer data, with contrasting results. Acceleration data from the thoracic spine was inadequate to predict peak vertical and resultant GRF based on Newton's second law of motion (i.e. multiplying by body mass) [106, 110] and as input into a mass-spring-damper model [107]. Conversely, improved results were shown when peak vertical GRF was estimated from known contact time, flight time and body mass using a spring-mass model [22], while another study suggested accurate predictions of resultant GRFs from IMUs worn on the thoracic spine are possible by applying machine learning [127]. Based on the conflicting results from the studies reviewed here, it is unclear whether the accurate determination of peak vertical and resultant GRFs from accelerometer data at the thoracic spine is possible and warrants further investigation.

Two studies used estimations of peak vertical GRF to calculate vertical stiffness from IMUs worn the thoracic spine [21, 22]. Although the small biases and large to nearly perfect correlations in both studies appear promising for determining vertical stiffness using accelerometer data from this site, it is unclear whether placement on the thoracic spine is feasible for determining vertical stiffness when one study collected data from only one participant. Furthermore, calculating vertical stiffness using a spring-mass model approach, as per the method used in the two studies, is dependent on known contact time and flight time [14]. However, neither study provided a description of how IC and TO were determined mathematically from accelerometer data, nor how these events translated to accurate derivations of temporal variables [21, 22]. The ability of IMUs attached on the thoracic spine to correctly identify IC and TO events compared to a criterion should be explored more fully before practitioners can confidently use this site to 1) accurately calculate contact time and flight time and 2) use these metrics as inputs for estimating peak vertical GRF and vertical stiffness [63, 158].

Results from reviewed studies demonstrates that it is possible to obtain reliable derivations of contact time, flight time and step frequency from a foot or lumbar spine placement [81, 97, 132], while foot-worn IMUs can provide reproducible calculations of stride time, step length and stride length [81, 125]. Furthermore, placement on the tibia and lumbar and thoracic spine possessed excellent reliability for determining vertical GRF from accelerometer data [22, 108]. Collectively, these results indicate that IMUs possess good precision for calculating different stride variables [159]. Determining the sensitivity of IMU-derived stride variables by calculating the MDC or smallest worthwhile change (SWC) is also important so practitioners can determine whether changes in an athlete's gait pattern are real or due to error [54, 160, 161]. However, only two studies reported here determined the value (i.e. signal) that may constitute meaningful change for stride variables determined from IMUs [108, 149]. One study using tibia accelerometers calculated an MDC for peak vertical GRF that was higher than the SEM, suggesting that this metric may be sensitive to detect change when IMUs are secured to the tibia [108]. Conversely, the TE associated with thoracic spine-derived peak vertical GRF and vertical stiffness was greater than the SWC [149], which suggests this site is limited for detecting subtle changes in an athlete's gait pattern. No study determined the MDC or SWC for spatiotemporal variables, therefore future work may look to further our understanding of the signal-to-noise ratio of other stride metrics, such as from IMUs worn at various sites.

The use of IMUs in sport is increasingly being applied to gain additional insights (i.e. other than speed and distance) into the activity profiles of athletes. Practitioners can quantify proprietary designed metrics, such as PlayerLoad™ [10-12], estimate energy expenditure [162] and record the peak segmental acceleration values that occur during a variety of different team-sport movements [109, 163] using IMUs. There is an increasing body of evidence supporting the use of IMUs to capture characteristics of an athlete's stride, including spatiotemporal data [86], GRFs [106-108] and vertical stiffness [21, 149]. Capturing accurate stride variables appears possible across different sites using automated gait event detection techniques and may have practical application in profiling an athlete's stride in a variety of running-based sports. The use of IMUs may allow practitioners to perform gait analyses in the field to enhance their understanding of athlete movement strategy and monitor changes in stride variables that may occur with fatigue [11].

It is important to note that the meta-analyses in this review were impacted by a limited pool of eligible studies. It is likely that the results suffer from sparse data bias in instances where only two studies were meta-analysed due to relatively small sample sizes [164, 165]. Further research should include raw outcome data (mean ± SD values) alongside validity statistics in order to provide a complete summary of outcomes. Furthermore, the method adopted here treated three studies that used different IMUs or criterions as independent data sources [85, 105, 132]. It is possible that we may have observed a different finding had different IMUs or criterions not been treated independently within those studies. However, due to a limited number of studies, accounting for this dependency was not possible with the data available. Finally, data was only pooled within a velocity range of 3.3 to 4.3 $m \cdot s^{-1}$ due to eligibility criteria. As a result, meta-analyses here do not explain the effect of running velocity on validity, which may be an important distinction to make as previous work has shown that increased speed may lead to greater error in estimations of stride variables derived from IMUs [83, 110].

3.6 Conclusion

This review and meta-analysis demonstrated that valid and reliable derivations of stride metrics are possible from IMUs mounted on the foot, tibia and lumbar spine. This suggests that location may not be the most critical factor and that validity and reliability may be more dependent on the mathematic approach for detection of gait events. However, further work is warranted to explore the application of automated gait event detection algorithms on inertial data from the thoracic spine before practitioners can confidently use this site in the field to derive stride variables.

4 Chapter 4: Study Two – Validity and Reliability of Thoracic-Mounted Inertial Measurement Units to Derive Gait Characteristics During Running

Publication statement:

This chapter is in the publication form of the following paper accepted by *The Journal of Strength and Conditioning Research*.

Horsley, B.J., et al., *Validity and reliability of thoracic-mounted Inertial Measurement Units to derive gait characteristics during running.* The Journal of Strength and Conditioning Research, 2023. **38**(2): p. 274-282.

4.1 Linking Paragraph

The results from Study 1 demonstrate IMUs attached to the foot, tibia or lumbar spine can be used to analyse running gait in the field, suggesting placement site may not be the limiting factor to validity and reliability. This is potentially encouraging for deriving running gait characteristics from the level of the thoracic spine where IMUs are inbuilt into GNSS units commonly worn by athletes. However, it is unclear from the systematic review whether an IMU worn in this position can accurately detect events at the foot-ground interface and if it is, in fact, valid and reliable for deriving running gait characteristics. Therefore, the purpose of Chapter 4 was to determine the validity and reliability of thoracic-mounted IMUs for the quantification of gait characteristics at a variety of running speeds.

4.2 Abstract

Inertial Measurement Units (IMUs) attached to the tibia or lumbar spine can be used to analyse running gait, but with team-sports are often contained in global navigation satellite system (GNSS) units worn on the thoracic spine. We assessed the validity and reliability of thoracic-mounted IMUs to derive gait characteristics, including vertical ground reaction force ($vGRF_{peak}$) and vertical stiffness (K_{vert}). Sixteen recreationally active subjects performed 40 m run-throughs at 3-4, 5-6 and 7-8 $m{\cdot}s^{-1}$. IMUs were attached to the tibia, lumbar and thoracic spine, while two GNSS units were also worn on the thoracic spine. Initial contact (IC) from a validated algorithm was evaluated with F1 score and agreement (mean difference ± SD) of gait data with the tibia and lumbar spine using nonparametric limits of agreement (LoA). Test-retest error (CV [95% CI]) established reliability. Thoracic IMUs detected a nearly perfect proportion (F1 ≥0.95) of IC events compared to tibia and lumbar sites. Step length had the strongest agreement (0 ± 0.04 m) at 3-4 $m{\cdot}s^{-1}$, while contact time improved from 3-4 (-0.028 ± 0.018 s) to 7-8 $m{\cdot}s^{-1}$ (-0.004 ± 0.013 s). All values for K_{vert} fell within the LoA at 7-8 $m{\cdot}s^{-1}$. Test-retest error was ≤12.8% for all gait characteristics obtained from GNSS units, where K_{vert} was most reliable at 3-4 $m{\cdot}s^{-1}$ (6.8% [5.2, 9.6]) and $vGRF_{peak}$ at 7-8 $m{\cdot}s^{-1}$ (3.7% [2.5, 5.2]). The thoracic-spine site is suitable to derive gait characteristics, including K_{vert}, from IMUs within GNSS units, eliminating the need for additional sensors to analyse running gait.

4.3 Introduction

Athlete external load can be quantified using wearable sensors to assist with planning and monitoring training and competition [2]. Distance and speed are often measured using global navigation satellite system (GNSS) units, but they are susceptible to error when measuring high-speed and non-linear movements [2] and cannot account for non-locomotor activity, such as jumps, impacts or collisions [3, 4]. These data, in conjunction with distance and speed, are important to provide a complete understanding of athlete external load, but other sensors are required to quantify these discrete movements [7].

Inertial measurement units (IMUs), comprising triaxial accelerometers, gyroscopes and magnetometers, provide additional insights into athlete movement [7]. These devices sample at a higher rate (≥100 Hz) than GNSS (≤20 Hz) and measure gravitational acceleration, change in rotational angle and direction with respect to the Earth's magnetic field [5]. Inertial data has been used in sport to derive proprietary-designed load metrics, such as PlayerLoad™ [11], quantify jumps [3], collisions and tackles [4] and detect changes of direction [5]. In addition, IMUs may be used for running gait analysis in the field, where automatic event detection algorithms make it possible to identify initial contact (IC) and toe-off (TO) to calculate a variety of gait characteristics [17-19].

Contact time, flight time, step frequency and step length are metrics used to profile the spatiotemporal characteristics of running gait [67, 81]. In addition, contact time and flight time can be used in equations to estimate vertical stiffness (K_{vert}) which represents the deformation of the centre of mass during ground contact in running [14]. These variables have implications for running economy [69], injury [166] and fatigue management [67], and would be useful to quantify in running-based team-sports.

It has been demonstrated that IC and TO can be accurately detected from tibia-mounted IMUs compared to accepted criterions for gait analysis, such as force plates and high-speed cameras [18, 19]. In addition, meta-analysis has showed that the lumbar spine is also suitable to derive valid and reliable gait data [167]. However, IMUs are typically worn on the thoracic spine (within GNSS devices) in sport. This may present some potential challenges for accurately determining gait events due to signal attenuation as data capture points are higher up the kinetic chain [110]. In addition, GNSS devices are typically worn in manufacturer designed vests or in pouches sewn into the back of playing jerseys (as occurs in some sports), therefore any poorly fitted clothing is likely to lead to extraneous movement of the device which may also impact event detection [168]. However, having a method to detect discrete gait characteristics from IMUs contained within already worn GNSS devices would remove the need for additional sensors at other sites and increase the ability of practitioners to utilise these measures when monitoring athletes.

The validity of calculating spatiotemporal variables, such as contact time and flight time, vertical ground reaction force ($vGRF_{peak}$) and K_{vert} from thoracic spine IMUs has been assessed, but the findings are inconsistent [21, 22, 110]. Furthermore, unlike investigations using tibia or lumbar spine IMUs [17, 19], no study has quantified the ability of the thoracic spine to detect IC or TO compared to a criterion. Meta-analysis has suggested the mathematical approach taken to determining gait events impacts validity rather than the placement site itself [167]. Therefore, further work is warranted to investigate whether thoracic-worn IMUs can accurately detect IC and TO which would in turn provide practitioners with a readily accessible tool to analyse running gait in the field.

Determining the variability, or noise, is also important to inform whether meaningful changes can be detected in the characteristics of an athlete’s gait pattern from trunk-mounted sensors [161]. One study has assessed this for $vGRF_{peak}$ and K_{vert} from lumbar and thoracic sites at 3.3 m·s^{-1} [22], but reliability across a range of running speeds is unclear. There is also limited data on the reliability of spatiotemporal variables from the thoracic spine and this should be assessed to determine the ability to reliably detect gait pattern changes [167].

Therefore, the first aim of this study was to assess the validity of thoracic spine IMUs to detect gait events and derive spatiotemporal variables, $vGRF_{peak}$ and K_{vert} compared to those worn on the tibia and lumbar spine using two validated gait event detection algorithms [17]. Secondly, this study determined the reliability of gait characteristics measured at the thoracic spine site.

4.4 Methods

4.4.1 Experimental Approach to the Problem

The validity of spatiotemporal variables, $vGRF_{peak}$ and K_{vert} derived from the thoracic spine were assessed against tibia and lumbar spine criterion sites. Intra-day and inter-day reliability were established using a repeated trials approach. Subjects attended one familiarisation and two experimental sessions.

4.4.2 Subjects

Sample size was determined based on the 80% probability of observing a between trial intraclass correlation coefficient value of 0.90 with a 95% confidence interval (95% CI) width of 0.2 [169]. Therefore, 16 recreationally active and injury-free men and women were recruited for this study (age: 27.6 ± 3.7 years; height: 175.4 ± 9.9 cm; mass: 74.8 ± 10.7 kg). Eleven subjects were recreational runners who performed at least one training run per week, while 5 subjects were amateur team-sport athletes and were therefore training and competing 2-4 days per week. Subjects provided written informed consent prior to commencing in the study which was approved by the Australian Catholic University Human Research Ethics Committee (2020-11H).

4.4.3 Procedures

4.4.3.1 Familiarisation

Subjects were familiarised with 40 m run-throughs at 3-4, 5-6 and 7-8 $m \cdot s^{-1}$ that required them to accelerate for 20 m and maintain the target velocity between 20 and 40 m (see Figure 4.1). Dual-beam electronic timing gates (Swift DUO™, Swift Performance, Brisbane, Australia) were used to monitor velocity, and these have been shown to be reliable for measuring 40 m sprint time (coefficient of variation [CV] ≤1.3%) [170]. For each run-through, subjects were instructed to accelerate to the target velocity prior to reaching the 20 m gate, maintain the required velocity for 20 m, and avoid slowing down until they had passed the 40 m gate. This protocol was chosen due to the application of analysing gait characteristics during standardised running tests and the ability to identify matched periods of straight-line running in team-sport matches [161, 171].

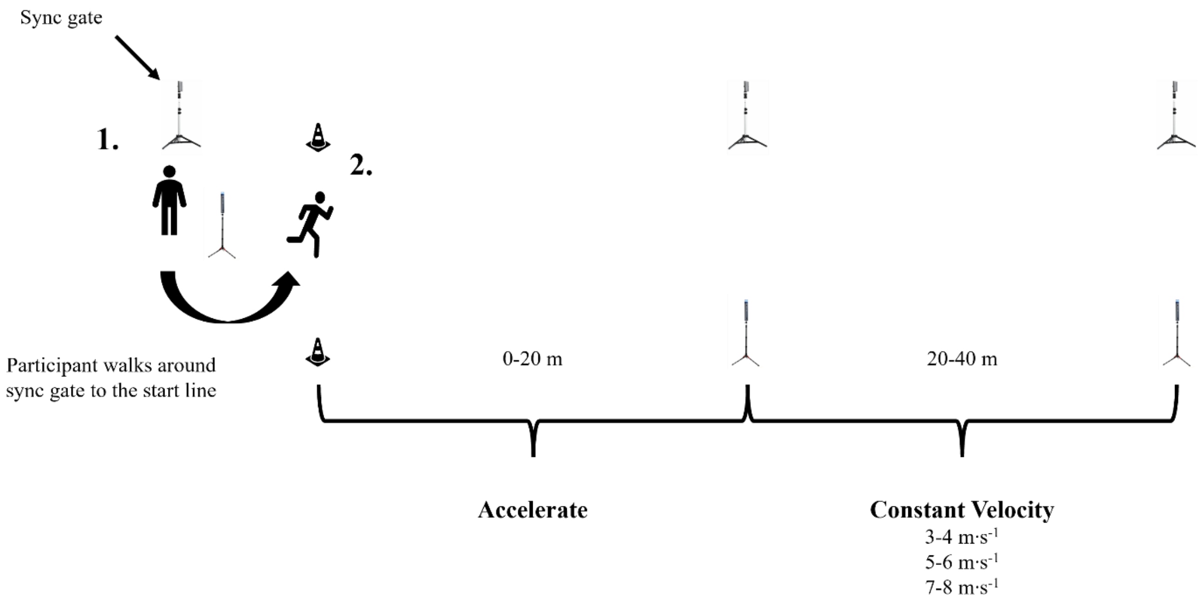

Figure 4.1. Schematic representation of the 40 m run-throughs.

4.4.3.2 Experimental Session

Subjects wore two GNSS devices (Apex, STATSports®, Newry, Northern Ireland; 84 x 43 x 20 mm; 72 g) and four IMUs (Blue Trident, IMeasureU, Auckland, New Zealand; 42 x 27 x 11 mm; 9.5 g) during the experimental trials (see Figure 4.2). Apex devices, which have an inbuilt triaxial accelerometer (ADXL375; 100 Hz; ±200 g), gyroscope (100 Hz; ±2000 deg·s^{-1}) and magnetometer (10 Hz; ±16 G), were worn on the upper back between the scapulae of each subject. One was housed in a tightly fitted vest and the other secured to the skin using Hypafix retention tape (Hypafix®, BSN medical, Hamburg, Germany). Two GNSS units were used to determine whether placing an IMU in a manufacturer-designed vest (which is typically the method during team-sport), impacts validity and reliability [168]. A Blue Trident IMU was attached to each tibia just above the medial malleolus using purpose-designed straps, while Hypafix retention tape attached two IMUs to the skin of the upper body, one at approximately the second lumbar vertebrae [17] and another 1 cm below the Apex devices on the thoracic spine (see Figure 4.2). Blue Trident high-g accelerometer data were collected at 1600 Hz and ±200 g in Nexus software (version 2.12.0, VICON, Oxford, UK).

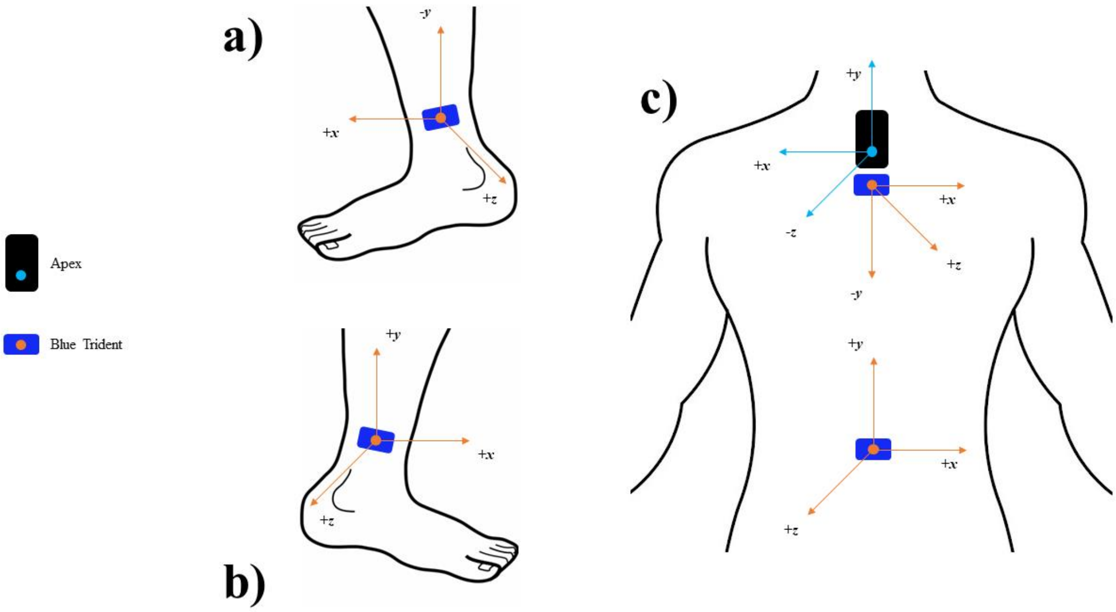

Figure 4.2. Orientation of accelerometer vectors for right tibia **(a),** left tibia **(b)** and lumbar and thoracic spine **(c)**. One Apex unit was secured direct to the skin, while another was worn over the top in a tightly fitted vest. The positive and negative directions of the *y* axis were different for each tibia **(a and b)** due to the way the Blue Trident sensors were attached on the medial aspect of the lower leg. The *x* axes of the Apex accelerometers were realigned during data processing so positive pointed right **(c)**. For the Blue Trident sensors, *y* and *z* axes of the right tibia **(a)** were flipped so positive was to the superior and right, respectively, and the *z* axes of the lumbar and thoracic spine were rotated so positive pointed anteriorly **(c)**. This was done to match the vector systems recognised by the algorithm described by the original authors [17].

Prior to testing, all subjects completed a 10-minute warm-up over 20 m which consisted of various running patterns, dynamic stretches (e.g., high knees, heel flicks, hurdle walk etc.) and one build-up run at ~70, 80 and 90% of maximal running speed. Accelerometer data from each IMU were synchronised with the timing gates by using an additional gate positioned 5 m behind the start line (0 m; see Figure 4.1). Subjects stood behind the sync gate and stomped their right leg while simultaneously swinging their arm through the gate and having a researcher firmly tap their thoracic-mounted GNSS units. This elicited an identifiable spike in the accelerometer data of the right tibia IMU and Apex devices that represented the start of the recording of the timing system. Subjects then performed the run-throughs as described earlier. Two successful trials at each speed (3-4, 5-6 and 7-8 $m \cdot s^{-1}$) were completed in a counterbalanced order. Trials were repeated if they fell outside of the desired velocity range by more than 0.1 $m \cdot s^{-1}$. The total number of trials performed at a given speed ranged from 2 to 4. The protocol was repeated 6.5 ± 2.7 days later.

4.4.3.3 Data Processing

Accelerometer data were downloaded as a CSV file from STATSports® Apex Unified Raw Data Parser software (version 4.6.0.184) and Nexus, respectively, and post-processing was completed in MATLAB (version 9.12.0.1956245, R2022a, MathWorks, Inc., Natick, MA, USA). Accelerometer axes were realigned from that outlined in Figure 4.2 to match the vectors recognised by the gait event detection algorithm [17]. Sync events (spikes) and 20 and 40 m split times were used as reference values to trim the accelerometer files so only the constant velocity data remained for analysis. Once trimmed, left and right tibia data were combined by maintaining the highest values between individual left and right data points in each accelerometer axis (x, y and z). This approach allowed the magnitude of peaks representing gait events to be maintained in the accelerometer waveform, particularly in the vertical (y) axis, while treating the tibia as a single site, like those on the trunk. Blue Trident data were downsampled to 100 Hz to match the sample rate of the Apex units using a moving average function, and a fourth order zero-lag Butterworth filter with a cutoff of 20 Hz was then applied [110]. Manufacturer pre-processing of Apex accelerometer files occurred prior to export from the Unified Raw Data Parser software, and this included filtering data using an Attitude and Heading Reference System (AHRS) algorithm with a cut-off frequency of ~50 Hz [172].

4.4.3.4 Algorithm

Two validated gait event detection algorithms were used to determine IC and TO from tibia and lumbar spine sites [17]. The lumbar spine algorithm was also applied to the thoracic spine to assess validity and reliability. Figure 4.3 and Figure 4.4 outline the steps for detecting IC and TO from each site, while further information can be found in the original work on the algorithms [17]. In contrast to the original study [17], the minimum time interval between IC events of ipsilateral limbs was adjusted from 0.50 to 0.20 s to detect left and right sides during trials completed at 3-4 and 5-6 $m \cdot s^{-1}$. For trials at 7-8 $m \cdot s^{-1}$, the minimum time interval was set to 0.18 s, which was informed by pilot testing and previously reported thresholds [167]. The window for TO occurred no later than 80% of the time between the prior IC and the next IC for trials analysed at 3-4 and 5-6 $m \cdot s^{-1}$ [173]. For trials at 7-8 $m \cdot s^{-1}$, the window for TO occurred no earlier than 0.10 s after the previous IC and no later than 55% of the time between the prior IC and the next IC [173].

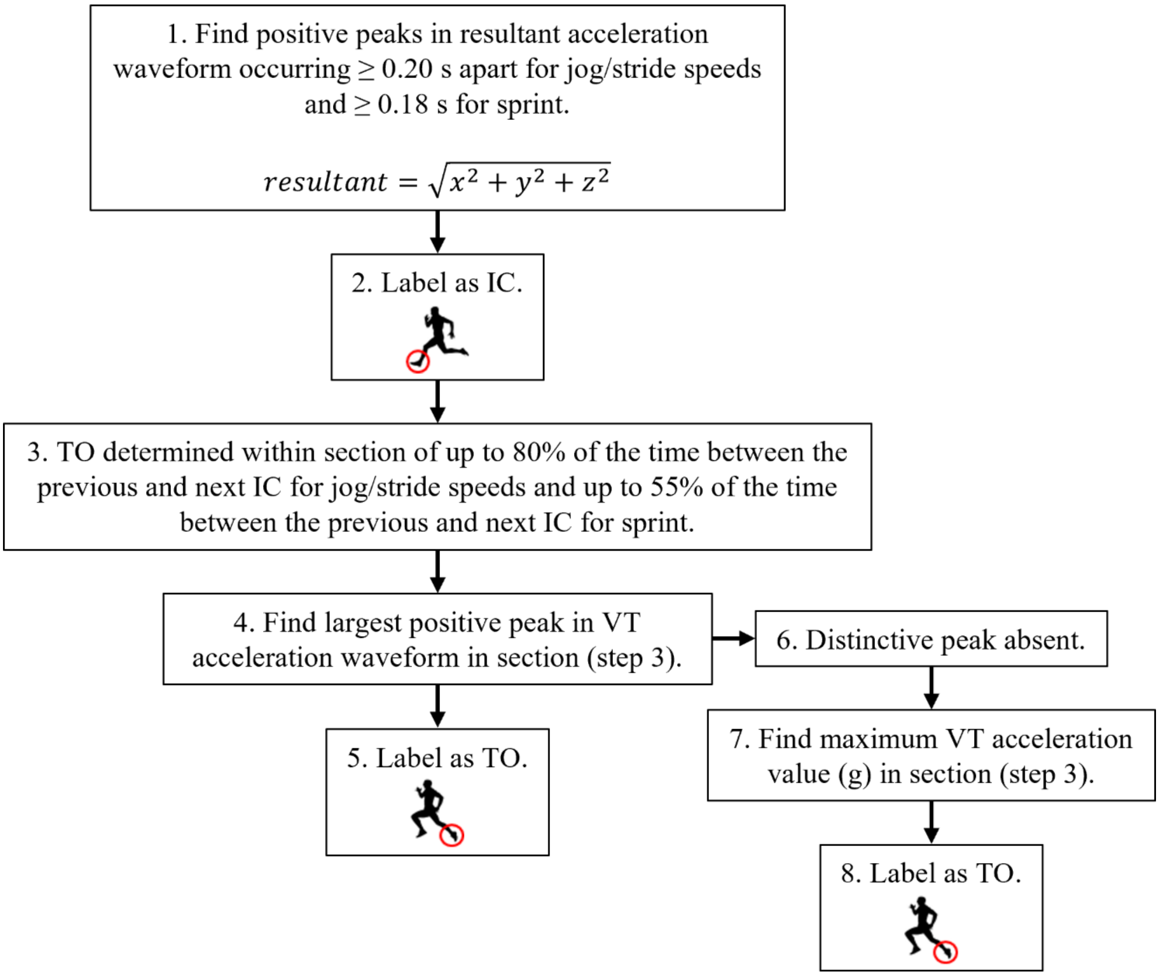

Figure 4.3. Flowchart illustrating how gait events (IC and TO) are determined from tibial accelerometer data [17]. Jog, stride and sprint speeds defined as 3-4, 5-6 and 7-8 m·s^{-1}, respectively. IC, initial contact; TO, toe-off; VT, vertical; g, gravitational acceleration; m·s^{-1}, metres per second.

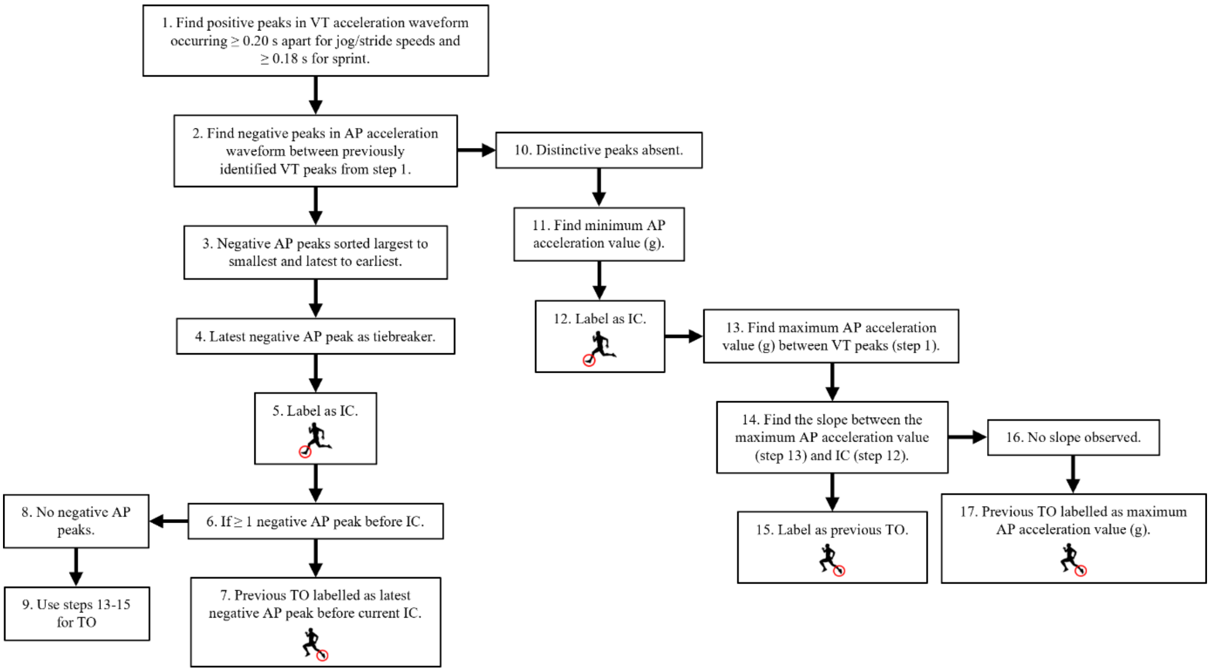

Figure 4.4. Flowchart illustrating how gait events (IC and TO) are determined from accelerometer data obtained from the lumbar and thoracic spine [17]. Jog, stride and sprint speeds defined as 3-4, 5-6 and 7-8 $m{\cdot}s^{-1}$, respectively. VT, vertical; AP, anteroposterior; IC, initial contact; TO, toe-off; $m{\cdot}s^{-1}$, metres per second.

4.4.3.5 Gait Characteristics

Contact time, step time, flight time, step frequency and step length were determined from IC and TO events using previously described calculation methods [81]. Contact time and flight time were then input into a spring-mass model equation to estimate K_{vert}, defined as the ratio of $vGRF_{peak}$ and centre of mass displacement (COM_{dis}) [14].

4.4.3.6 Statistical Analyses

Precision, recall and F1 score were calculated to evaluate the ability of IMUs located on the thoracic spine to correctly identify IC compared to tibia and lumbar spine criterion sites following an approach that has been used previously in gait analysis [128]. The method for calculating precision, recall and F1 score is outlined elsewhere [151]. These three measures range from 0 to 1 where the F1 score represents the harmonic mean between precision and recall [151]. An F1 score of 1 reflects perfect precision and recall [151].

Visual inspection of the data revealed a non-normal distribution of the between-site differences, and this was confirmed by the Shapiro-Wilk normality test. Therefore, nonparametric limits of agreement (LoA) were used to assess the level of agreement between sites [174]. Differences between sites were plotted against the average of the two sites (e.g., thoracic spine and tibia) on a scatter diagram to visualise the proportion of observations that fell within the LoA [174].

The typical error (TE; 95% CI) and CV (95% CI) were calculated to describe the intra-day and inter-day reliability of gait characteristics determined from the thoracic spine site. The median of the between-trial difference scores was used instead of the standard deviation (SD) to determine the typical error from skewed data [175].

4.5 Results

Group median ± interquartile range values for gait characteristics from each site and running speed are presented in Table 4-1.

Table 4-2 outlines the precision, recall and F1 scores between all thoracic spine sites and tibia and lumbar locations for detection of IC. Irrespective of running velocity, F1 scores for detecting IC from the thoracic spine were nearly perfect (F1 ≥0.95) across all between-site comparisons, while those determined at 3-4 $m \cdot s^{-1}$ were the largest (F1 = 0.96-0.99). On average, precision was 2% lower than recall at 7-8 $m \cdot s^{-1}$ which suggests that thoracic sites incorrectly detected a greater proportion of IC events at the fastest velocity compared to 3-4 and 5-6 $m \cdot s^{-1}$.

Table 4-1. Summary statistics (median ± IQR) for gait characteristics determined from each site and running speed.

	3-4 m·s^{-1}					5-6 m·s^{-1}					7-8 m·s^{-1}				
Variable	BT Tibia	BT Lumbar	BT Thoracic	Apex Thoracic (Skin)	Apex Thoracic (Vest)	BT Tibia	BT Lumbar	BT Thoracic	Apex Thoracic (Skin)	Apex Thoracic (Vest)	BT Tibia	BT Lumbar	BT Thoracic	Apex Thoracic (Skin)	Apex Thoracic (Vest)
Contact time (s)	0.250 ± 0.036	0.260 ± 0.036	0.230 ± 0.037	0.218 ± 0.036	0.220 ± 0.030	0.220 ± 0.032	0.220 ± 0.030	0.220 ± 0.030	0.180 ± 0.010	0.180 ± 0.010	0.120 ± 0.010	0.140 ± 0.015	0.130 ± 0.010	0.130 ± 0.020	0.130 ± 0.010
Step time (s)	0.370 ± 0.020	0.360 ± 0.040	0.350 ± 0.046	0.370 ± 0.030	0.370 ± 0.030	0.330 ± 0.030	0.325 ± 0.035	0.318 ± 0.040	0.320 ± 0.030	0.320 ± 0.040	0.260 ± 0.029	0.268 ± 0.035	0.260 ± 0.039	0.268 ± 0.030	0.260 ± 0.019
Flight time (s)	0.110 ± 0.036	0.090 ± 0.030	0.100 ± 0.030	0.150 ± 0.036	0.145 ± 0.03	0.100 ± 0.015	0.090 ± 0.040	0.080 ± 0.026	0.130 ± 0.021	0.140 ± 0.010	0.140 ± 0.019	0.130 ± 0.025	0.130 ± 0.010	0.130 ± 0.020	0.130 ± 0.020
Step freq. (steps·min^{-1})	162.16 ± 8.77	166.67 ± 17.59	171.43 ± 22.21	162.16 ± 13.53	162.16 ± 13.53	181.82 ± 17.08	185.71 ± 20.3	191.08 ± 23.53	187.5 ± 18.18	187.5 ± 23.53	230.77 ± 24.56	226.33 ± 33.06	230.77 ± 31.87	224.36 ± 25.65	230.77 ± 16.62
Step length (m)	1.32 ± 0.11	1.30 ± 0.15	1.26 ± 0.21	1.30 ± 0.10	1.30 ± 0.09	1.81 ± 0.24	1.78 ± 0.23	1.79 ± 0.20	1.76 ± 0.21	1.76 ± 0.23	1.99 ± 0.18	2.01 ± 0.31	1.95 ± 0.43	1.96 ± 0.19	1.97 ± 0.13
$vGRF_{peak}$ (kN)	1.67 ± 0.48	1.62 ± 0.38	1.66 ± 0.31	1.84 ± 0.32	1.85 ± 0.37	1.64 ± 0.38	1.59 ± 0.38	1.65 ± 0.46	1.87 ± 0.48	1.84 ± 0.42	2.52 ± 0.57	2.25 ± 0.47	2.36 ± 0.29	2.39 ± 0.33	2.40 0.40
K_{vert} (kN·m^{-1})	22.78 ± 7.67	19.65 ± 6.13	24.58 ± 7.29	29.01 ± 10.06	28.75 ± 9.05	26.68 ± 8.26	25.70 ± 8.35	25.48 ± 13.48	44.36 ± 13.89	40.14 ± 12.55	131.64 ± 19.09	99.01 ± 25.12	104.83 ± 17.14	104.92 ± 28.63	107.12 ± 15.8

IQR, inter-quartile range; m·s^{-1}, metres per second; BT, Blue Trident; freq., frequency; steps·min^{-1}, steps per minute; vGRF, peak vertical ground reaction force; kN, kilonewtons; K_{vert}, vertical stiffness; kN·m^{-1}, kilonewtons per metre.

Table 4-2. Precision, recall and F1 for initial contact detection.

	3-4 m·s^{-1}			5-6 m·s^{-1}			7-8 m·s^{-1}		
Comparison	P	R	F1	P	R	F1	P	R	F1
BT Thoracic vs. BT Tibia	0.99	0.93	0.96	0.99	0.92	0.96	0.96	0.98	0.97
Apex Thoracic (Skin) vs. BT Tibia	0.99	0.99	0.99	0.99	0.93	0.96	0.92	0.97	0.95
Apex Thoracic (Vest) vs. BT Tibia	0.99	0.98	0.99	0.99	0.92	0.96	0.93	0.97	0.95
BT Thoracic vs. BT Lumbar	0.99	0.93	0.96	0.98	0.96	0.97	0.98	0.98	0.98
Apex Thoracic (Skin) vs. BT Lumbar	0.98	0.98	0.98	0.98	0.96	0.97	0.93	0.96	0.95
Apex Thoracic (Vest) vs. BT Lumbar	0.98	0.98	0.98	0.98	0.95	0.97	0.94	0.95	0.95

m·s^{-1}, metres per second; P, precision; R, recall; BT, Blue Trident; TP, true positive; FP, false positive; FN, false negative.

Precision calculated as TP / (TP + FP). Recall calculated as TP / (TP + FN). F1 calculated as 2(P * R) / (P + R), where an F1 score of 1 represents perfect precision and recall.

Between-site nonparametric LoA statistics for gait characteristics are presented in Table 4-3, while Figure 4.5 and Figure 4.6 show the agreement between the Apex thoracic (vest) and Blue Trident tibia and lumbar sites. All differences (100%) for between-site comparisons were within the LoA for contact time, flight time and step time at 7-8 $m \cdot s^{-1}$ (see Table 4-3, Figure 4.5 and Figure 4.6). All differences for K_{vert} at 7-8 $m \cdot s^{-1}$ between Apex thoracic sites (skin and vest) and Blue Trident tibia were also within the LoA (see Table 4-3 and Figure 4.5). The strongest agreement was observed for both Apex thoracic sites (skin and vest) compared to Blue Trident lumbar for step length at 3-4 $m \cdot s^{-1}$, where the mean difference (MD) ± SD was 0 ± 0.04 m (see Table 4-3 and Figure 4.6). For K_{vert}, agreement was strongest at 5-6 $m \cdot s^{-1}$ between Blue Trident thoracic and lumbar sites (-0.50 ± 5.97 kN·m) but differed >20 kN·m at 7-8 $m \cdot s^{-1}$ for all thoracic sites compared to Blue Trident tibia (see Table 4-3 and Figure 4.5). The Apex thoracic (vest) predominantly underestimated contact time (LoA: -0.056 to -0.004 s) and overestimated K_{vert} (LoA: 1.27 to 29.97 kN·m) at 5-6 $m \cdot s^{-1}$ compared to Blue Trident tibia (see Figure 4.5). With the Blue Trident lumbar as the criterion, most differences were in the positive direction for K_{vert} from Apex thoracic (vest) at both 3-4 (LoA: 0.17 to 0.18.38 kN·m) and 5-6 $m \cdot s^{-1}$ (LoA: 2.57 to 27.09 kN·m) (see Figure 4.6).

Table 4-3. Nonparametric limits of agreement statistics for gait characteristics determined from the thoracic spine at each running velocity.

	Comparison	3-4 m·s^{-1}			5-6 m·s^{-1}			7-8 m·s^{-1}		
		MD ± SD	LoA	%	MD ± SD	LoA	%	MD ± SD	LoA	%
Contact time (s)										
	BT Thoracic vs. BT Tibia	-0.008 ± 0.024	-0.064, 0.036	90.6	0.003 ± 0.021	-0.052, 0.041	90.0	0.007 ± 0.009	-0.016, 0.021	100.0
	Apex Thoracic (Skin) vs. BT Tibia	-0.016 ± 0.021	-0.050, 0.028	90.6	-0.035 ± 0.014	-0.062, -0.010	90.0	0.008 ± 0.012	-0.027, 0.030	100.0
	Apex Thoracic (Vest) vs. BT Tibia	-0.017 ± 0.019	-0.048, 0.021	90.6	-0.033 ± 0.014	-0.056, -0.004	90.0	0.007 ± 0.011	-0.022, 0.023	100.0
	BT Thoracic vs. BT Lumbar	-0.020 ± 0.025	-0.075, 0.021	90.6	0.001 ± 0.021	-0.035, 0.035	90.0	-0.005 ± 0.010	-0.024, 0.021	100.0
	Apex Thoracic (Skin) vs. BT Lumbar	-0.028 ± 0.018	-0.069, 0.003	90.6	-0.037 ± 0.014	-0.061, -0.007	90.0	-0.004 ± 0.013	-0.035, 0.031	100.0
	Apex Thoracic (Vest) vs. BT Lumbar	-0.029 ± 0.016	-0.064, -0.002	90.6	-0.035 ± 0.013	-0.054, -0.005	90.0	-0.005 ± 0.012	-0.03, 0.022	100.0
Step time (s)										
	BT Thoracic vs. BT Tibia	-0.021 ± 0.025	-0.079, 0.012	90.6	-0.009 ± 0.020	-0.065, 0.038	90.0	-0.007 ± 0.02	-0.063, 0.031	100.0
	Apex Thoracic (Skin) vs. BT Tibia	-0.003 ± 0.003	-0.007, 0.005	90.6	-0.008 ± 0.013	-0.073, 0.004	90.0	-0.004 ± 0.025	-0.075, 0.063	100.0
	Apex Thoracic (Vest) vs. BT Tibia	-0.003 ± 0.003	-0.007, 0.005	90.6	-0.007 ± 0.013	-0.073, 0.006	90.0	-0.005 ± 0.024	-0.072, 0.053	100.0
	BT Thoracic vs. BT Lumbar	-0.016 ± 0.026	-0.079, 0.030	90.6	-0.006 ± 0.018	-0.052, 0.035	90.0	-0.006 ± 0.020	-0.058, 0.026	100.0
	Apex Thoracic (Skin) vs. BT Lumbar	0.001 ± 0.011	-0.008, 0.029	90.6	-0.008 ± 0.011	-0.043, 0.004	90.0	-0.003 ± 0.027	-0.071, 0.057	100.0
	Apex Thoracic (Vest) vs. BT Lumbar	0.001 ± 0.011	-0.012, 0.029	92.2	-0.007 ± 0.011	-0.043, 0.005	91.7	-0.004 ± 0.026	-0.067, 0.046	100.0
Flight time (s)										
	BT Thoracic vs. BT Tibia	-0.014 ± 0.025	-0.061, 0.031	90.6	-0.014 ± 0.013	-0.048, 0.008	90.0	-0.014 ± 0.013	-0.047, 0.009	100.0
	Apex Thoracic (Skin) vs. BT Tibia	0.016 ± 0.022	-0.028, 0.046	90.6	0.026 ± 0.017	-0.020, 0.053	91.7	-0.010 ± 0.016	-0.044, 0.029	100.0
	Apex Thoracic (Vest) vs. BT Tibia	0.017 ± 0.019	-0.025, 0.047	90.6	0.025 ± 0.017	-0.021, 0.052	90.0	-0.011 ± 0.014	-0.047, 0.020	100.0
	BT Thoracic vs. BT Lumbar	0.002 ± 0.019	-0.042, 0.035	90.6	-0.010 ± 0.016	-0.038, 0.021	90.0	-0.001 ± 0.014	-0.038, 0.021	100.0
	Apex Thoracic (Skin) vs. BT Lumbar	0.032 ± 0.021	-0.010, 0.069	90.6	0.031 ± 0.013	0.004, 0.059	90.0	0.003 ± 0.018	-0.038, 0.037	100.0
	Apex Thoracic (Vest) vs. BT Lumbar	0.033 ± 0.019	-0.003, 0.066	90.6	0.029 ± 0.013	0.001, 0.052	90.0	0.002 ± 0.017	-0.038, 0.037	100.0

Table 3-3. (continued).

	Comparison	3-4 $m \cdot s^{-1}$			5-6 $m \cdot s^{-1}$			7-8 $m \cdot s^{-1}$		
		MD ± SD	LoA	%	MD ± SD	LoA	%	MD ± SD	LoA	%
Step frequency ($steps \cdot min^{-1}$)										
	BT Thoracic vs. BT Tibia	19.02 ± 17.60	-1.14, 55.42	87.5	11.12 ± 13.57	-12.04, 43.53	88.3	9.68 ± 16.51	-23.65, 53.78	97.4
	Apex Thoracic (Skin) vs. BT Tibia	1.15 ± 2.00	-4.80, 4.05	87.5	4.09 ± 6.66	-4.52, 35.87	88.3	1.96 ± 18.43	-43.81, 57.53	97.4
	Apex Thoracic (Vest) vs. BT Tibia	1.17 ± 1.91	-4.69, 3.39	89.1	3.58 ± 6.61	-4.66, 34.76	88.3	3.23 ± 17.03	-33.87, 52.59	97.4
	BT Thoracic vs. BT Lumbar	12.54 ± 18.37	-19.34, 55.67	90.6	6.33 ± 13.48	-14.73, 39.95	88.3	6.39 ± 17.66	-15.65, 51.93	100.0
	Apex Thoracic (Skin) vs. BT Lumbar	-4.74 ± 9.25	-34.71, 1.75	90.6	0.95 ± 6.01	-10.80, 20.85	88.3	-1.33 ± 22.37	-51.77, 57.86	97.4
	Apex Thoracic (Vest) vs. BT Lumbar	-4.84 ± 9.31	-35.06, 1.84	87.5	0.41 ± 5.58	-9.47, 19.47	88.3	-0.06 ± 20.99	-41.84, 52.91	97.4
Step length (m)										
	BT Thoracic vs. BT Tibia	-0.08 ± 0.09	-0.27, 0.04	89.1	-0.05 ± 0.11	-0.35, 0.22	88.3	-0.06 ± 0.15	-0.46, 0.22	97.4
	Apex Thoracic (Skin) vs. BT Tibia	-0.01 ± 0.01	-0.03, 0.02	92.2	-0.05 ± 0.07	-0.40, 0.02	88.3	-0.04 ± 0.19	-0.54, 0.47	100.0
	Apex Thoracic (Vest) vs. BT Tibia	-0.01 ± 0.01	-0.03, 0.01	84.4	-0.04 ± 0.07	-0.40, 0.02	85.0	-0.05 ± 0.18	-0.52, 0.39	100.0
	BT Thoracic vs. BT Lumbar	-0.06 ± 0.10	-0.28, 0.12	92.2	-0.03 ± 0.10	-0.26, 0.19	86.7	-0.04 ± 0.15	-0.42, 0.20	97.4
	Apex Thoracic (Skin) vs. BT Lumbar	0.00 ± 0.04	-0.03, 0.11	82.8	-0.05 ± 0.06	-0.24, 0.02	88.3	-0.03 ± 0.20	-0.51, 0.42	100.0
	Apex Thoracic (Vest) vs. BT Lumbar	0.00 ± 0.04	-0.05, 0.11	92.2	-0.04 ± 0.06	-0.25, 0.02	90.0	-0.03 ± 0.19	-0.48, 0.34	97.4
$vGRF_{peak}$ (kN)										
	BT Thoracic vs. BT Tibia	-0.06 ± 0.16	-0.42, 0.18	90.6	-0.07 ± 0.09	-0.32, 0.13	88.3	-0.20 ± 0.12	-0.52, -0.02	100.0
	Apex Thoracic (Skin) vs. BT Tibia	0.11 ± 0.17	-0.23, 0.36	90.6	0.25 ± 0.14	0.02, 0.51	88.3	-0.17 ± 0.13	-0.43, 0.00	97.4
	Apex Thoracic (Vest) vs. BT Tibia	0.12 ± 0.14	-0.24, 0.34	89.1	0.24 ± 0.13	-0.01, 0.47	88.3	-0.18 ± 0.11	-0.39, -0.01	100.0
	BT Thoracic vs. BT Lumbar	0.05 ± 0.11	-0.20, 0.24	90.6	-0.05 ± 0.11	-0.24, 0.16	88.3	0.03 ± 0.14	-0.26, 0.24	100.0
	Apex Thoracic (Skin) vs. BT Lumbar	0.22 ± 0.14	-0.06, 0.47	90.6	0.28 ± 0.11	0.09, 0.56	86.7	0.05 ± 0.15	-0.17, 0.31	100.0
	Apex Thoracic (Vest) vs. BT Lumbar	0.22 ± 0.12	-0.01, 0.44	87.5	0.27 ± 0.11	0.04, 0.47	88.3	0.05 ± 0.14	-0.17, 0.32	97.4

Table 3-3. (continued).

	Comparison	3-4 $m{\cdot}s^{-1}$			5-6 $m{\cdot}s^{-1}$			7-8 $m{\cdot}s^{-1}$		
		MD ± SD	LoA	%	MD ± SD	LoA	%	MD ± SD	LoA	%
K_{vert} ($kN{\cdot}m^{-1}$)										
	BT Thoracic vs. BT Tibia	0.62 ± 6.81	-16.13, 14.38	90.6	-1.39 ± 6.55	-13.70, 14.07	88.3	-22.37 ± 17.63	-61.59, 14.70	97.4
	Apex Thoracic (Skin) vs. BT Tibia	4.96 ± 7.27	-9.17, 15.91	90.6	17.00 ± 7.26	3.33, 28.33	90.0	-20.72 ± 24.27	-61.40, 44.02	100.0
	Apex Thoracic (Vest) vs. BT Tibia	5.11 ± 6.36	-9.16, 15.53	89.1	15.30 ± 6.95	1.27, 29.97	86.7	-20.62 ± 20.6	-47.60, 29.21	100.0
	BT Thoracic vs. BT Lumbar	4.28 ± 5.63	-5.94, 17.44	89.1	-0.50 ± 5.97	-11.20, 10.78	88.3	7.48 ± 19.10	-39.42, 31.38	100.0
	Apex Thoracic (Skin) vs. BT Lumbar	8.71 ± 5.52	-1.24, 21.39	89.1	17.68 ± 6.72	3.46, 29.70	88.3	9.13 ± 24.55	-57.70, 60.70	94.7
	Apex Thoracic (Vest) vs. BT Lumbar	9.14 ± 4.96	0.17, 18.38	87.5	16.33 ± 6.12	2.57, 27.09	90.0	9.24 ± 22.26	-45.65, 44.62	97.4

Upper and lower LoA determined from the range of values that remain following removal of 10% of the ordered sample [174].

$m{\cdot}s^{-1}$, metres per second; MD, mean difference; SD, standard deviation; LoA, limits of agreement; %, percentage of values within LoA; BT, Blue Trident; $steps{\cdot}min^{-1}$, steps per minute; $vGRF_{peak}$, peak vertical ground reaction force; kN, kilonewtons; K_{vert}, vertical stiffness; $kN{\cdot}m^{-1}$, kilonewtons per metre.

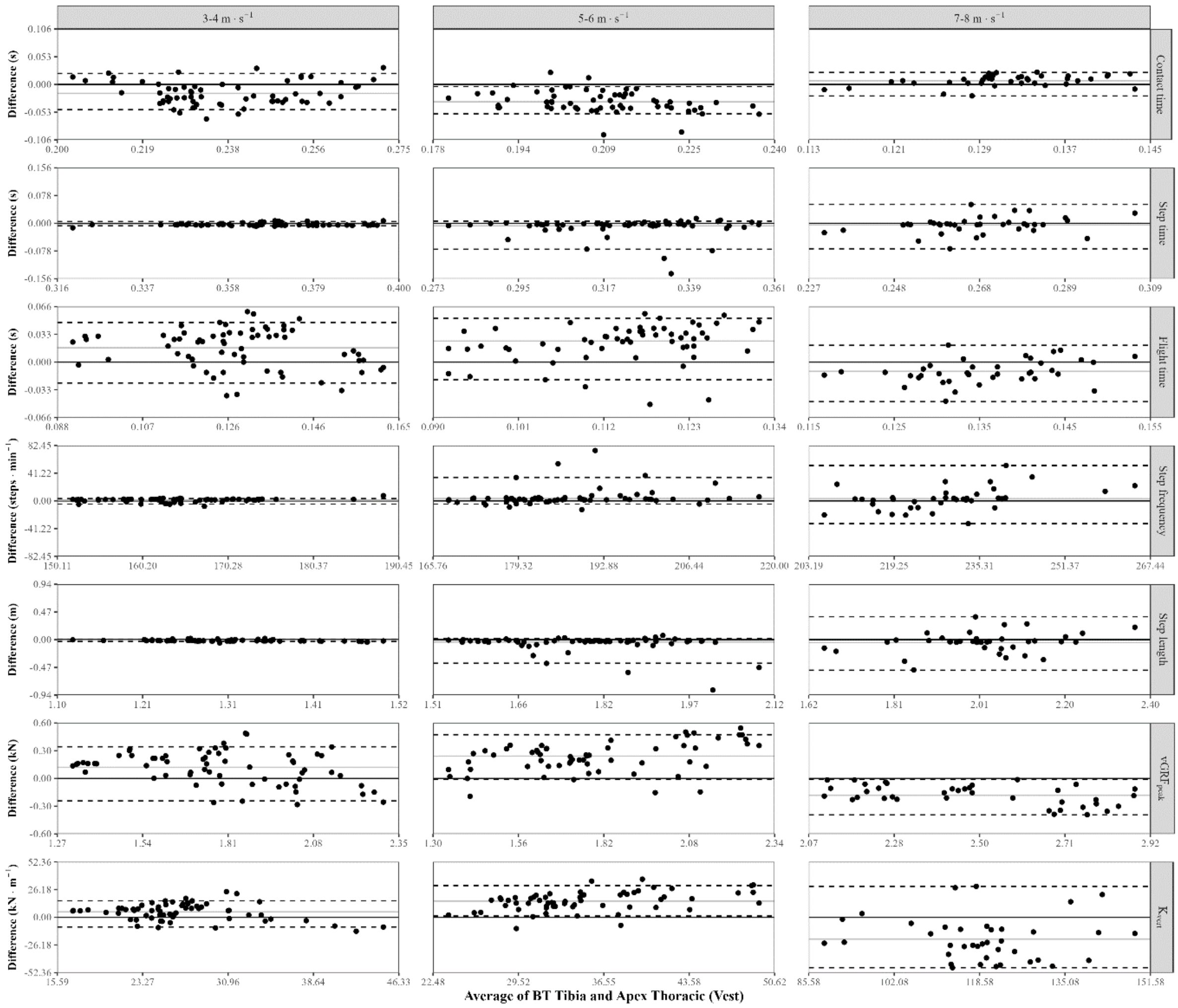

Figure 4.5. Scatter plot of the nonparametric limits of agreement between Apex thoracic (vest) and Blue Trident tibia for each gait characteristic and running velocity. Mean difference is represented by the grey horizontal line, while dashed lines are the nonparametric limits of agreement. Solid black line is zero mean difference. $m{\cdot}s^{-1}$, metres per second; $steps{\cdot}min^{-1}$, steps per minute; kN, kilonewtons, $vGRF_{peak}$, peak vertical ground reaction force; $kN{\cdot}m^{-1}$, kilonewtons per metre; K_{vert}, vertical stiffness; BT, Blue Trident.

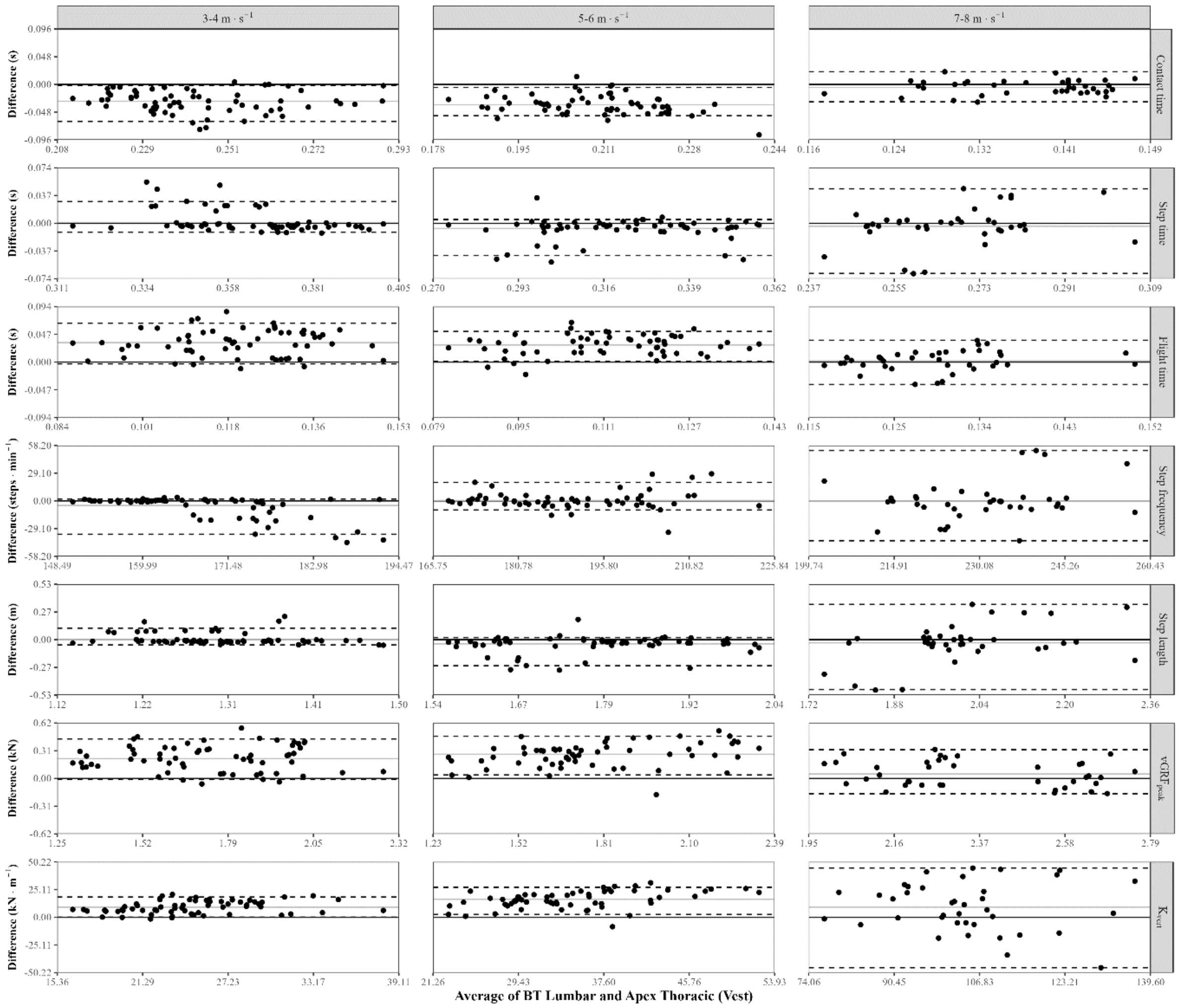

Figure 4.6. Scatter plot of the nonparametric limits of agreement between Apex thoracic (vest) and Blue Trident lumbar for each gait characteristic and running velocity. Mean difference is represented by the grey horizontal line, while dashed lines are the nonparametric limits of agreement. Solid black line is zero mean difference. $m{\cdot}s^{-1}$, metres per second; $steps{\cdot}min^{-1}$, steps per minute; kN, kilonewtons, $vGRF_{peak}$, peak vertical ground reaction force; $kN{\cdot}m^{-1}$, kilonewtons per metre; K_{vert}, vertical stiffness; BT, Blue Trident.

Inter-day reliability statistics are shown in Table 4-4 and Table 4-5 contains intra-day reliability outcomes. Step time and step frequency recorded from both Apex thoracic sites (skin and vest) at 3-4 $m{\cdot}s^{-1}$ showed the lowest between-day variation (CV ≤1.6%), while K_{vert} determined from Blue Trident thoracic at the same speed showed the highest (CV [95% CI] = 18.9% [14.4, 27.5]). Irrespective of running velocity, all but one gait characteristic from the Apex thoracic sites (skin and vest) showed a CV ≤7.7% (see Table 4-4), with K_{vert} at 7-8 $m{\cdot}s^{-1}$ being the highest for the vest (CV [95% CI] = 12.4% [9.5, 17.8]). The reproducibility of contact time (CV = 3.4-4.1%) and $vGRF_{peak}$ (CV = 2.3-3.2%) was consistent across speeds for Apex thoracic (vest), while flight time showed less variation at 7-8 $m \cdot s^{-1}$ (CV [95% CI] = 3.8% [2.9, 5.3]) than 3-4 $m \cdot s^{-1}$ (CV [95% CI] = 6.2% [4.8, 8.9]).

Table 4-4. Inter-day reliability statistics for gait characteristics determined from the thoracic spine at each running velocity.

		3-4 m·s^{-1}		5-6 m·s^{-1}		7-8 m·s^{-1}	
	Site	TE (95% CI)	CV% (95% CI)	TE (95% CI)	CV% (95% CI)	TE (95% CI)	CV% (95% CI)
Contact time (s)							
	BT Thoracic	0.020 (0.016, 0.028)	8.6 (6.6, 12.3)	0.016 (0.012, 0.022)	7.6 (5.8, 10.8)	0.007 (0.005, 0.010)	5.7 (4.4, 8.1)
	Apex Thoracic (Skin)	0.007 (0.005, 0.010)	3.4 (2.6, 4.7)	0.004 (0.003, 0.005)	1.9 (1.5, 2.7)	0.005 (0.004, 0.007)	4.1 (3.2, 5.8)
	Apex Thoracic (Vest)	0.007 (0.005, 0.010)	3.4 (2.7, 4.8)	0.007 (0.005, 0.010)	3.7 (2.9, 5.3)	0.006 (0.004, 0.008)	4.1 (3.2, 5.8)
Step time (s)							
	BT Thoracic	0.024 (0.019, 0.034)	6.6 (5.1, 9.4)	0.019 (0.015, 0.026)	5.8 (4.4, 8.2)	0.019 (0.015, 0.027)	7.4 (5.7, 10.5)
	Apex Thoracic (Skin)	0.005 (0.004, 0.007)	1.4 (1.1, 2.0)	0.007 (0.005, 0.010)	2.4 (1.8, 3.3)	0.006 (0.004, 0.008)	2.1 (1.7, 3.0)
	Apex Thoracic (Vest)	0.006 (0.005, 0.009)	1.6 (1.3, 2.3)	0.008 (0.006, 0.011)	2.5 (1.9, 3.5)	0.006 (0.004, 0.008)	2.1 (1.6, 2.9)
Flight time (s)							
	BT Thoracic	0.008 (0.006, 0.011)	7.7 (5.9, 11)	0.008 (0.006, 0.011)	11.6 (8.9, 16.6)	0.007 (0.005, 0.010)	6.1 (4.7, 8.6)
	Apex Thoracic (Skin)	0.007 (0.005, 0.010)	5.7 (4.4, 8.0)	0.006 (0.004, 0.008)	4.2 (3.3, 6.0)	0.006 (0.004, 0.008)	4.2 (3.2, 5.9)
	Apex Thoracic (Vest)	0.009 (0.007, 0.013)	6.2 (4.8, 8.9)	0.006 (0.004, 0.008)	4.1 (3.1, 5.8)	0.005 (0.004, 0.007)	3.8 (2.9, 5.3)
Step frequency (steps·min^{-1})							
	BT Thoracic	11.33 (8.81, 15.90)	6.5 (5.1, 9.3)	9.90 (7.69, 13.88)	5.6 (4.4, 8.0)	15.63 (12.15, 21.92)	7.2 (5.6, 10.3)
	Apex Thoracic (Skin)	2.30 (1.79, 3.23)	1.4 (1.1, 2.0)	4.67 (3.63, 6.55)	2.4 (1.8, 3.3)	4.84 (3.76, 6.80)	2.1 (1.6, 3.0)
	Apex Thoracic (Vest)	2.56 (1.99, 3.59)	1.6 (1.3, 2.3)	4.49 (3.49, 6.30)	2.5 (1.9, 3.5)	4.51 (3.50, 6.32)	2.1 (1.6, 2.9)
Step length (m)							
	BT Thoracic	0.09 (0.07, 0.12)	7.5 (5.8, 10.6)	0.13 (0.10, 0.19)	7.6 (5.9, 10.8)	0.17 (0.13, 0.24)	8.9 (6.8, 12.7)
	Apex Thoracic (Skin)	0.03 (0.03, 0.05)	2.8 (2.1, 3.9)	0.04 (0.03, 0.05)	1.9 (1.5, 2.7)	0.04 (0.03, 0.06)	2.2 (1.7, 3.2)
	Apex Thoracic (Vest)	0.04 (0.03, 0.05)	2.8 (2.2, 4.0)	0.03 (0.02, 0.04)	1.7 (1.3, 2.4)	0.03 (0.02, 0.04)	1.5 (1.1, 2.1)

Table 3-4. (continued).

	Site	3-4 m·s^{-1}		5-6 m·s^{-1}		7-8 m·s^{-1}	
		TE (95% CI)	CV% (95% CI)	TE (95% CI)	CV% (95% CI)	TE (95% CI)	CV% (95% CI)
$vGRF_{peak}$ (kN)							
	BT Thoracic	0.06 (0.04, 0.08)	3.3 (2.6, 4.7)	0.05 (0.04, 0.07)	3.0 (2.3, 4.2)	0.08 (0.06, 0.11)	3.7 (2.8, 5.2)
	Apex Thoracic (Skin)	0.04 (0.03, 0.05)	1.7 (1.4, 2.5)	0.04 (0.03, 0.05)	1.9 (1.4, 2.6)	0.07 (0.06, 0.1)	2.9 (2.2, 4.0)
	Apex Thoracic (Vest)	0.05 (0.04, 0.08)	3.0 (2.3, 4.2)	0.05 (0.04, 0.07)	3.2 (2.5, 4.5)	0.05 (0.04, 0.07)	2.3 (1.8, 3.2)
K_{vert} (kN·m^{-1})							
	BT Thoracic	3.37 (2.62, 4.73)	18.9 (14.4, 27.5)	3.52 (2.73, 4.94)	14 (10.8, 20.2)	9.38 (7.29, 13.15)	8.7 (6.7, 12.4)
	Apex Thoracic (Skin)	1.97 (1.53, 2.76)	7.7 (5.9, 11)	2.88 (2.24, 4.04)	7.1 (5.5, 10.1)	14.14 (10.99, 19.84)	12.4 (9.5, 17.8)
	Apex Thoracic (Vest)	1.99 (1.54, 2.79)	6.8 (5.2, 9.6)	3.11 (2.42, 4.37)	7.2 (5.6, 10.3)	8.53 (6.63, 11.96)	7.6 (5.9, 10.8)

m·s^{-1}, metres per second; TE, typical error; CI, confidence interval; CV, coefficient of variation; BT, Blue Trident; steps·min^{-1}, steps per minute; $vGRF_{peak}$, peak vertical ground reaction force; kN, kilonewtons; K_{vert}, vertical stiffness; kN·m^{-1}, kilonewtons per metre.

Table 4-5. Intra-day reliability statistics for gait characteristics determined from the thoracic spine at each running velocity.

		3-4 $m \cdot s^{-1}$		5-6 $m \cdot s^{-1}$		7-8 $m \cdot s^{-1}$	
	Site	TE (95% CI)	CV% (95% CI)	TE (95% CI)	CV% (95% CI)	TE (95% CI)	CV% (95% CI)
Contact time (s)							
	BT Thoracic	0.022 (0.017, 0.031)	10.2 (7.9, 14.7)	0.011 (0.008, 0.015)	5.1 (3.9, 7.2)	0.007 (0.005, 0.010)	5.4 (4.2, 7.6)
	Apex Thoracic (Skin)	0.006 (0.005, 0.009)	2.6 (2.0, 3.7)	0.005 (0.004, 0.007)	2.7 (2.1, 3.8)	0.006 (0.004, 0.008)	4.2 (3.2, 5.9)
	Apex Thoracic (Vest)	0.007 (0.005, 0.010)	3.3 (2.6, 4.7)	0.007 (0.005, 0.010)	3.8 (2.9, 5.4)	0.003 (0.002, 0.004)	1.9 (1.5, 2.7)
Step time (s)							
	BT Thoracic	0.025 (0.019, 0.035)	7.0 (5.4, 10)	0.012 (0.009, 0.017)	3.5 (2.7, 4.9)	0.022 (0.017, 0.031)	8.4 (6.4, 11.9)
	Apex Thoracic (Skin)	0.005 (0.004, 0.007)	1.4 (1.1, 1.9)	0.007 (0.005, 0.010)	2.1 (1.7, 3.0)	0.006 (0.004, 0.008)	2.0 (1.6, 2.9)
	Apex Thoracic (Vest)	0.003 (0.002, 0.004)	0.7 (0.5, 0.9)	0.006 (0.004, 0.008)	1.7 (1.3, 2.4)	0.007 (0.005, 0.010)	2.8 (2.2, 3.9)
Flight time (s)							
	BT Thoracic	0.006 (0.004, 0.008)	5.3 (4.1, 7.4)	0.006 (0.005, 0.009)	8.2 (6.3, 11.6)	0.007 (0.005, 0.010)	5.4 (4.2, 7.6)
	Apex Thoracic (Skin)	0.006 (0.005, 0.009)	4.5 (3.5, 6.4)	0.003 (0.002, 0.004)	2.2 (1.7, 3.0)	0.006 (0.005, 0.009)	4.8 (3.7, 6.8)
	Apex Thoracic (Vest)	0.005 (0.004, 0.007)	3.6 (2.8, 5.1)	0.006 (0.005, 0.009)	4.4 (3.4, 6.2)	0.002 (0.002, 0.004)	1.8 (1.4, 2.5)
Step frequency (steps$\cdot$min^{-1})							
	BT Thoracic	11.32 (8.88, 15.88)	7.0 (5.4, 10)	6.30 (4.89, 8.83)	3.6 (2.8, 5.1)	17.55 (13.64, 24.62)	8 (6.2, 11.4)
	Apex Thoracic (Skin)	2.19 (1.70, 3.08)	1.4 (1.1, 1.9)	3.80 (2.96, 5.33)	2.1 (1.7, 3.0)	4.13 (3.21, 5.79)	1.9 (1.5, 2.7)
	Apex Thoracic (Vest)	1.07 (0.83, 1.50)	0.7 (0.5, 0.9)	3.01 (2.34, 4.22)	1.7 (1.3, 2.4)	6.41 (4.98, 8.99)	2.8 (2.2, 3.9)
Step length (m)							
	BT Thoracic	0.10 (0.08, 0.14)	8.4 (6.5, 12)	0.06 (0.04, 0.08)	3.1 (2.4, 4.4)	0.24 (0.18, 0.33)	12.7 (9.8, 18.3)
	Apex Thoracic (Skin)	0.03 (0.02, 0.04)	2.1 (1.6, 2.9)	0.03 (0.03, 0.05)	1.9 (1.5, 2.7)	0.05 (0.04, 0.06)	2.4 (1.8, 3.3)
	Apex Thoracic (Vest)	0.03 (0.02, 0.04)	2.1 (1.6, 30)	0.03 (0.03, 0.05)	2.1 (1.6, 2.9)	0.05 (0.04, 0.08)	2.8 (2.2, 4.0)

Table 3-5. (continued).

	Site	3-4 m·s^{-1}		5-6 m·s^{-1}		7-8 m·s^{-1}	
		TE (95% CI)	CV% (95% CI)	TE (95% CI)	CV% (95% CI)	TE (95% CI)	CV% (95% CI)
$vGRF_{peak}$ (kN)							
	BT Thoracic	0.05 (0.04, 0.06)	3.0 (2.3, 4.2)	0.06 (0.05, 0.09)	3.8 (2.9, 5.4)	0.03 (0.02, 0.04)	1.4 (1.1, 1.9)
	Apex Thoracic (Skin)	0.04 (0.03, 0.05)	1.9 (1.5, 2.7)	0.05 (0.04, 0.07)	2.7 (2.1, 3.9)	0.03 (0.02, 0.04)	1.2 (0.9, 1.6)
	Apex Thoracic (Vest)	0.03 (0.02, 0.04)	1.5 (1.2, 2.1)	0.06 (0.04, 0.08)	3.0 (2.4, 4.3)	0.04 (0.03, 0.06)	1.7 (1.3, 2.3)
K_{vert} (kN·m^{-1})							
	BT Thoracic	2.87 (2.23, 4.02)	12.7 (9.8, 18.3)	3.98 (3.09, 5.58)	15.0 (11.5, 21.6)	6.95 (5.40, 9.75)	7.0 (5.4, 9.9)
	Apex Thoracic (Skin)	1.59 (1.24, 2.24)	6.1 (4.7, 8.6)	3.36 (2.61, 4.71)	8.0 (6.2, 11.4)	6.40 (4.97, 8.98)	6.3 (4.8, 8.9)
	Apex Thoracic (Vest)	1.17 (0.91, 1.64)	4.1 (3.2, 5.8)	3.33 (2.59, 4.67)	8.7 (6.7, 12.4)	5.40 (4.20, 7.58)	4.5 (3.5, 6.4)

m·s^{-1}, metres per second; TE, typical error; CI, confidence interval; CV, coefficient of variation; BT, Blue Trident; steps·min^{-1}, steps per minute; $vGRF_{peak}$, peak vertical ground reaction force; kN, kilonewtons; K_{vert}, vertical stiffness; kN·m^{-1}, kilonewtons per metre.

4.6 Discussion

This study assessed the validity and reliability of thoracic-mounted IMUs, including those contained in commonly worn GNSS units, for deriving selected running gait characteristics, including $vGRF_{peak}$ and K_{vert}. The thoracic spine, irrespective of device used (Blue Trident or Apex), had a nearly perfect F1 score (≥0.95; see

Table 4-2) for the detection of IC and provided valid results for step time, step frequency, step length and K_{vert} (see Table 4-3, Figure 4.5 and Figure 4.6). In addition, excellent inter-day reliability was observed for all gait characteristics, including $K_{vert,}$ determined from Apex thoracic sites (see Table 4-4). These results support those from meta-analysis indicating IMU placement site is not the limiting factor to validity and reliability of gait characteristics [167]. Therefore, practitioners can confidently use thoracic-mounted IMUs contained within GNSS units worn in a vest, and the algorithm described in this work, to analyse running gait in the field. This could provide opportunities for assessing changes in running gait that may manifest with fatigue or as useful data during return-to-running programs following lower limb injury or concussion [176].

Although thoracic spine IMUs have been used to quantify running gait characteristics, their ability to provide valid detection of IC events relative to a criterion has not been established [21, 22]. The median F1 score for the thoracic spine (Blue Trident and Apex sites) was 0.97 (see Table 1) which compares favorably to 0.94 reported previously for the tibia [128]. This demonstrates the utility of thoracic-mounted IMUs to detect IC relative to a criterion site [18, 19]. Lower precision was observed at 7-8 $m \cdot s^{-1}$ than 3-4 and 5-6 $m \cdot s^{-1}$ which is reflective of the thoracic spine recording more false positives compared to the tibia and lumbar spine sites. This is potentially due to the values derived from the thoracic site being impacted by increased forward lean and trunk bounce (causing extraneous movement of the Blue Trident and Apex devices) which are higher in sprinting than slower speed running [110]. However, F1 values were still >0.90 at the thoracic spine irrespective of device used (Blue Trident or Apex), which confirms the suitability of the thoracic site for the detection of IC even during sprinting.

In contrast to step time, contact time and flight time from the Apex devices attached to the thoracic spine had a larger MD compared to those calculated from the tibia (see Table 2 and Figure 3) and this may be due to the challenge of detecting TO accurately using trunk accelerometer data alone [18]. The algorithm used in the current study detected toe-off from negative peaks in the anteroposterior accelerometer waveform [17], while other work has used a combination of gyroscope and accelerometer data, which may improve detection accuracy [18]. Although mean differences were larger for contact time than step time, the mean difference from the criterion for the Apex devices attached directly to the skin (MD ± SD = -0.028 ± 0.018 s) and housed in the vest (MD ± SD = -0.029 ± 0.016 s) showed an underestimation of contact time that is consistent with research comparing the lumbar spine and a force plate at 3-4 $m{\cdot}s^{-1}$ (MD = -0.029 s) [17]. This suggests that using an algorithm originally developed to derive contact time from the lumbar spine is also valid at the thoracic spine. Furthermore, the agreement with tibia- and lumbar spine-derived values for contact time was best at the fastest speed (7-8 $m{\cdot}s^{-1}$) for both Blue Trident and Apex sensors, and this is in line with the findings reported from foot-mounted accelerometers at speeds ranging between 4.3 and 8.0 $m{\cdot}s^{-1}$ [97].

The test-retest error in spatiotemporal variables derived from thoracic spine sensors has not been previously quantified. Irrespective of running velocity, this study showed between-day CV values of ≤8.9% for contact time, step time, flight time, step frequency and step length from Blue Trident and Apex thoracic sites (see Table 4-4), and this is consistent with work that concluded these same variables as reliable from foot-mounted IMUs [81, 97]. A finding of note from the reliability analysis was that the Apex devices (skin and vest) had a lower CV (≤6.2%) for all spatiotemporal variables and were more reliable than the Blue Trident sensor (see Table 3). This confirms that practitioners can derive reproducible values of spatiotemporal variables from thoracic IMUs, such as those embedded within Apex GNSS units. However, as per the method of the current study, practitioners should still ensure that the same devices are used by the same athletes and that vests are fitted appropriately to ensure accuracy and consistency in data collection.

Stiffness refers to the relationship between a given force and an object's or body's capacity to resist deformation [69]. In running, K_{vert} is used to describe the motion of the body's centre of mass during ground contact where fatigue has been shown to result in reductions in K_{vert} [67]. It has been suggested that K_{vert} can be quantified during running from a thoracic-mounted IMU (contained in a GNSS unit), however this work used only a single subject case study and, critically, the underlying computational approach for detecting gait events was not provided [21]. Based on the algorithmic approach used here, at least 86.7% of K_{vert} values from the thoracic spine (Blue Trident and Apex devices) fell within the LoA across all speeds, while those determined from the Apex sites (skin and vest) had an accuracy of 100% at 7-8 $m{\cdot}s^{-1}$ (see Table 4-3 and Figure 4.5). Although an underestimation of K_{vert} was observed at 7-8 $m{\cdot}s^{-1}$ compared to the tibia (see Table 4-3 and Figure 4.5), our results show that thoracic IMUs can provide a valid representation of K_{vert}, particularly during sprinting. In addition, K_{vert} from the Apex devices (skin and vest; CV ≤8.7%) showed better between-day reliability than has been previously reported (CV = 9.5%; see Table 4-4) [22]. This adds further support to the value of the algorithmic approach outlined in this study for the determination of K_{vert} from thoracic IMUs contained within GNSS units for both research and applied purposes [11, 166].

Validity results for $vGRF_{peak}$ were similar to those for K_{vert} which is likely due to these variables using the same inputs in the spring-mass model calculations [14]. In the current study, the between-day CV% for $vGRF_{peak}$ from the thoracic site (Blue Trident and Apex devices) was ≤3.7% across all speeds, which is approximately five-fold lower than reported previously [149]. The reason for this is not completely clear and although it may be related to the approach taken for event detection, the method used in previous work was not clearly described [149]. Our results suggest that deriving $vGRF_{peak}$ from thoracic-mounted IMUs may be useful for practitioners monitoring running gait where this metric may be used as a surrogate measure of lower-limb loading during training and injury rehabilitation [166].

A potential limitation of this study is that most subjects shared a very similar anthropometric profile which, coupled with the use of tightly regulated velocities (3-4, 5-6 and 7-8 $m \cdot s^{-1}$), resulted in the data being clustered around a narrow range of values. Future work should consider recruiting subjects with varying anthropometric profiles and using self-selected running speeds. Finally, this study did not examine gait characteristics derived from left and right sides, as the focus of this work was on the thoracic placement site itself. Given the potential practical applications for assessing asymmetry during return to play post-injury, future investigations may apply the method described here to calculate spatiotemporal variables, $vGRF_{peak}$ or K_{vert} for left and right limbs.

In conclusion, thoracic spine IMUs contained within commonly worn vest-mounted GNSS units are suitable for field-based running gait analysis. This provides opportunities to quantify distance and speed metrics alongside gait characteristics from a single device. This reduces the need for practitioners to use additional sensors at other sites and allows a more detailed analysis of athlete external load.

4.7 Practical Applications

Valid and reliable gait data can be derived from IMUs, particularly accelerometers, embedded within commonly worn GNSS devices. This reduces the need for additional sensors and allows practitioners to obtain speed and distance data in conjunction with discrete gait characteristics, such as $vGRF_{peak}$ and K_{vert}. These values may be useful in assessing fatigue-related changes and during lower-limb injury rehabilitation or monitoring return of normal gait post-concussion. The values shown here may be useful as thresholds in practical applications (e.g., injury prevention, gait re-training, fatigue monitoring) to determine whether any changes seen (signal) exceed the inherent technological and biological error (noise) associated with measuring these variables using thoracic-mounted IMUs.

5 Chapter 5: Study Three – Thoracic-worn Accelerometers Detect Fatigue-Related Changes in Vertical Stiffness During Sprinting

Publication statement:

This chapter is in the publication form of the following paper accepted by *The Journal of Strength and Conditioning Research*.

Horsley, B.J., et al., *Thoracic-worn Accelerometers Detect Fatigue-Related Changes in Vertical Stiffness During Sprinting*. The Journal of Strength and Conditioning Research, 2023. **38**(2): p. 283-289.

5.1 Linking Paragraph

The thoracic spine site is suitable to derive spatiotemporal gait characteristics, $vGRF_{peak}$ and K_{vert} from accelerometer technology in the field, and this confirms the suggestion from Study 1 that attachment location is not the limiting factor to validity and reliability. The results from Study 2 may be attractive for practitioners working in sport as they can utilise accelerometers contained within commonly worn GNSS units to quantify running gait characteristics alongside distance and speed metrics all from the single device. A potentially advantageous use of thoracic-mounted accelerometers is monitoring changes in running characteristics due to fatigue. Therefore, Chapter 5 investigates the fatigue-related changes in gait characteristics derived from thoracic-mounted accelerometers following a repeated sprinting task.

5.2 Abstract

Thoracic-mounted accelerometers are valid and reliable for analysing gait characteristics and may provide the opportunity to assess running-related neuromuscular fatigue (NMF) during training and competition without the need for additional tests, such as a countermovement jump (CMJ). However, their sensitivity for detecting fatigue-related changes in gait across different speeds is unclear. We therefore assessed the changes in accelerometer-derived gait characteristics, including vertical stiffness (K_{vert}), following a repeated sprint protocol (RSP). Sixteen recreationally active subjects performed single and repeated CMJs on a force plate and 40 m run-throughs overground at 3-4, 5-6 and 7-8 $m \cdot s^{-1}$ pre-post a 12 x 40 m RSP. Gait characteristics (contact time, step frequency, step length, K_{vert} etc.) were derived from an accelerometer contained within a global navigation satellite system unit on the thoracic spine using a validated algorithm. Changes in running gait and CMJ performance were assessed using a linear mixed-effects model (95% confidence interval [95% CI]; effect size [ES]). Significance was set at $p<0.05$. A significant reduction in K_{vert} occurred at 7-8 $m \cdot s^{-1}$ following the RSP (-8.51 $kN \cdot m^{-1}$ [-13.9, -3.11]; $p = 0.007$; ES [95% CI] = -0.39 [-0.62, -0.15]) which coincided with a decreased jump height (-0.03 m [-0.04, -0.01]; $p = 0.002$; ES [95% CI] = -0.87 [-1.41, -0.30]). However, all other gait characteristics were not significantly different irrespective of speed. Thoracic-worn accelerometers can detect changes in K_{vert} at 7-8 $m \cdot s^{-1}$ which may be useful for monitoring NMF during sprinting. However, a RSP does not result in altered gait mechanics in subsequent running at lower speeds.

5.3 Introduction

Team-sport athletes perform a variety of high-intensity movements, such as sprinting, directional changes and rapid accelerations and decelerations [177]. The frequent execution of these tasks is associated with neuromuscular fatigue (NMF) which impairs physical performance and is therefore important to monitor [51, 178]. Electrical or magnetic stimulation provides a direct measure of central and peripheral NMF [45], but this approach is impractical in team-sport [51]. Single and repeated countermovement jump (CMJ) tests may be used as an alternative to monitor fatigue status where a variety of jump-derived measures, such as flight time:contraction time (FT:CT) or vertical stiffness (K_{vert}), can be used to quantify the fatigue response following training or a match [179, 180]. However, although specific metrics from a CMJ have been shown to reflect NMF from team-sport activity and that movement strategy is affected when players compete in the presence of NMF, a dedicated testing session is required to complete a CMJ, resulting in more time commitments for busy athletes [179]. Ideally, assessment of running-related NMF would occur during training or match performance. Furthermore, CMJ tests do not provide insight into the specific changes in gait that explain the demonstrated alterations to fatigue-induced changes in movement strategy [11, 38].

Microtechnology sensors, notably accelerometers, offer a solution to quantify running activity that may be used to monitor NMF [11, 21, 161]. Accelerometers are high sample rate (≥100 Hz) sensors that measure gravitational acceleration in three axes (anteroposterior, vertical and mediolateral) and are typically contained within global navigation satellite system (GNSS) units worn on the thoracic spine by team-sport athletes. As such, accelerometers provide a time efficient alternative to assess fatigue status as all athletes can be monitored simultaneously. This potentially reduces the need for additional tests (e.g., CMJ) and provides opportunities to monitor discrete changes in movement (i.e., running) strategy that manifest from NMF during performance, such as in training or a match [11, 12, 161].

PlayerLoad™, which is a proprietary metric calculated from the summation of instantaneous rate of change from the individual accelerometer vectors, is an example of a variable that has been used to assess changes in movement strategy as a result of NMF [11, 12, 161]. A reduction in the contribution of the vertical accelerometer vector to the total PlayerLoad™ value in the presence of NMF has been observed during simulated and real team-sport match play [11, 12]. However, quantifying changes in individual accelerometer vectors does not explain the precise changes in movement strategy due to NMF. As NMF impairs running mechanics [67, 181], it is reasonable to suggest that modifications in gait characteristics may be responsible for the fatigue-induced changes to PlayerLoad™.

A proposed explanation for the reduced contribution of the vertical accelerometer vector to total PlayerLoad™ with NMF is reductions in vertical stiffness (K_{vert}). In running, K_{vert} represents the motion of the body's centre of mass during ground contact relative to the vertical ground reaction force ($vGRF_{peak}$) [13]. With NMF, there is an impaired ability to resist collapse of the lower body during ground contact resulting in a greater displacement of the centre of mass, longer contact time and shorter flight time that subsequently reduces running economy [15]. It may therefore be useful to monitor K_{vert} by using its mechanical inputs of contact time, flight time and body mass, all of which can be estimated from thoracic-mounted accelerometers contained within GNSS units [14].

Earlier investigations showed that valid representations of K_{vert} can be obtained from GNSS-embedded accelerometers compared to an instrumented treadmill [21]. Although this suggests it is possible to analyse running gait from thoracic-mounted sensors, this work used a single subject case study design and was performed on a treadmill, therefore the practical applications to field-based sports are likely limited. To extend this work, we provided a detailed method to determine initial contact (IC) and toe-off (TO) events from accelerometer waveforms obtained from the thoracic spine to calculate a variety of running gait characteristics, including K_{vert}, at varying speeds [182]. Our preceding work to this current study showed that valid and reliable values of K_{vert}, contact time, flight time and $vGRF_{peak}$ can be obtained from GNSS-embedded accelerometers during overground running at 3-4, 5-6 and 7-8 $m \cdot s^{-1}$. These results provide an opportunity for practitioners to analyse running gait in the field from sensors already worn by athletes [182]. However, the ability to classify an athlete's fatigue status as a function of their running gait from thoracic-mounted accelerometers (as they are worn in sport) is not clear. Therefore, investigating their sensitivity for quantifying changes due to NMF at a variety of running speeds is warranted.

This study therefore aimed to investigate the acute changes in running gait characteristics, derived from accelerometers worn on the thoracic spine, following a commonly used intervention aimed at inducing NMF [67]. A secondary aim was to determine whether changes in running gait due to NMF coincided with a decrement in CMJ-derived metrics related to NMF.

5.4 Methods

5.4.1 Experimental Approach to the Problem

This study used a pre-post intervention design to investigate how NMF impacts running gait characteristics derived from thoracic-mounted accelerometers. A 12 x 40 m repeated sprint protocol was used as the intervention to induce NMF, and running gait characteristics were assessed via separate run-throughs at jog (3-4 $m \cdot s^{-1}$), stride (5-6 $m \cdot s^{-1}$) and sprint (7-8 $m \cdot s^{-1}$) speeds. In addition, changes in single and repeated CMJ parameters were also assessed pre-post the 12 x 40 m protocol. Testing was conducted over 10.9 ± 6.4 days, where subjects were required to attend one familiarisation and another session dedicated to the pre-post fatigue intervention.

5.4.2 Subjects

An a priori power analysis was conducted in G*Power (version 3.1.9.6) to estimate the sample size required for observing a Cohen's *d* effect size of 0.4 [183]. Based on a power of 80% and an alpha level of 0.05, 10 men (age: 27.2 ± 4.4 years; height: 181.1 ± 7.4 cm; mass: 79.0 ± 8.5 kg) and 6 women (age: 28.2 ± 2.5 years; height: 165.9 ± 4.7 cm; mass: 67.7 ± 10.9 kg) who were free from injury and familiar with high-intensity activity were recruited for this study. Most subjects (11) were recreational runners who performed at least one training run per week, while 5 subjects were amateur team-sport athletes and were therefore training and competing 2-4 days per week. Subjects provided written informed consent based on their understanding of the study design, risks and potential benefits. This study was approved by the Australian Catholic University Human Research Ethics Committee (2020-21H).

5.4.3 Procedures

5.4.3.1 Familiarisation

Familiarisation occurred in the following order: single CMJ, repeated CMJ, 40 m run-throughs at each speed (3-4, 5-6 and 7-8 $m \cdot s^{-1}$) and repeated sprint protocol. Jump testing was performed on a force plate sampling at 1000 Hz (FDLite, ForceDecks, Vald Performance, Brisbane, Australia) which was calibrated according to manufacturer recommendations prior to testing. For the single CMJ, subjects were instructed to maintain their hands on their hips and jump as high as possible [54]. Similar procedures were followed for the repeated CMJ to determine K_{vert}, the only difference being subjects performed two consecutive jumps for maximum height while minimising ground contact time between jumps [184]. The repeated CMJ was used to determine whether changes in K_{vert} during running were also mirrored in jumping. ForceDecks software provides a measure of K_{vert} (referred to as passive stiffness) which represents the ratio between $vGRF_{peak}$ and centre of mass displacement (COM_{dis}) at landing from the first jump [184]. After the CMJ tests, subjects were familiarised with 40 m run-throughs performed at 3-4, 5-6 and 7-8 $m \cdot s^{-1}$ which required subjects to accelerate for 20 m and maintain the target velocity for the subsequent 20-40 m split. Velocity was monitored via electronic timing gates (Swift DUO™, Swift Performance, Brisbane, Australia) positioned at 20 and 40 m. This run-through procedure was used in our preceding work demonstrating the validity and reliability of thoracic-derived gait parameters, and was adopted here to assess the fatigue response at a range of speeds [182]. Finally, subjects were introduced to the repeated sprint protocol which was used as the fatigue intervention. The protocol required subjects to perform 12 x 40 m maximal repeated sprints in an alternating direction and interspersed with 30 s of passive recovery (see Figure 5.1), and this has been shown to induce fatigue-related changes in running gait characteristics, including K_{vert} [67]. Familiarisation only required subjects to perform 6 x 40 m repeated sprints, where each sprint commenced from a stationary position with the subject's toe on the start line.

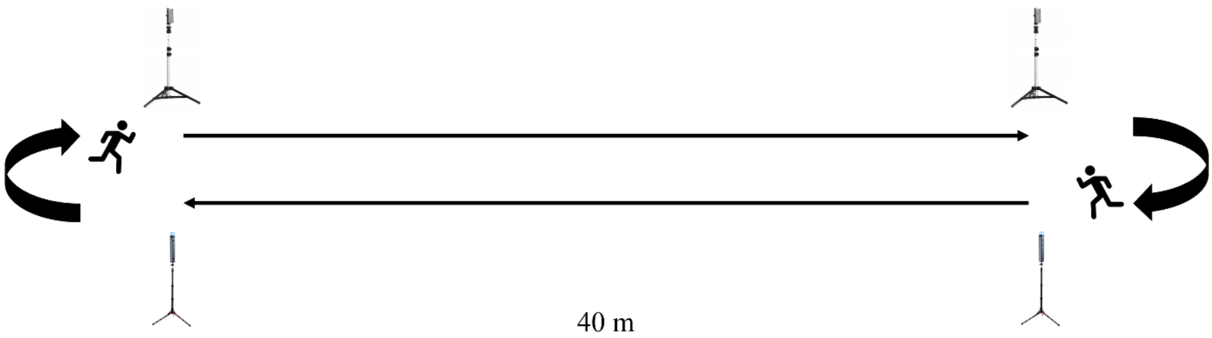

Figure 5.1. Diagram of the repeated sprint protocol used as the fatigue intervention. Participants performed 12 x 40 m repeated sprints in an alternating direction with 30 s passive recovery between each sprint.

5.4.3.2 Fatigue Intervention

The pre-post fatigue intervention was completed on an outdoor artificial grass surface. During testing, subjects wore a GNSS device (Apex, STATSports®, Newry, Northern Ireland; 84 x 43 x 20 mm; 72 g) that contains a triaxial accelerometer (ADXL375; 100 Hz; ±200 g), gyroscope (100 Hz; ±200 g) and magnetometer (10 Hz; ±16 G). The Apex unit was housed in a tightly fitted vest between the scapulae, where the positive direction of the *x* accelerometer vector pointed to the right, *y* superiorly and *z* posteriorly. Data from the accelerometer were recorded onboard the device during testing and downloaded for post-processing.

A 10-minute standardised warm-up consisting of various running patterns over 20 m and dynamic stretches was completed to ensure subjects were physically prepared for maximal running [54]. Subjects then performed one trial of a single and repeated CMJ on a force plate to obtain baseline measures of FT:CT, jump height and passive stiffness. Pre-fatigue run-throughs at 3-4, 5-6 and 7-8 $m \cdot s^{-1}$ over 40 m were then performed in a counterbalanced order. An extra timing gate was positioned 5 m behind the start line and was used to synchronise the accelerometer data from the Apex device with the timing system. This was achieved by subjects swinging their arm through the sync gate and having a researcher simultaneously tap their thoracic-mounted GNSS unit which allowed for an identifiable spike in the accelerometer signal that was used to extract data pertaining to the 20-40 m section. Subjects then walked around the sync gate to the start line, accelerated for the first 20 m and held the required running speed between 20 and 40 m. Two successful trials were performed at each speed (3-4, 5-6 and 7-8 $m \cdot s^{-1}$).

The subsequent fatigue intervention required subjects to perform 12 x 40 m repeated sprints following the procedures described earlier (see Figure 5.1) [67]. Strong verbal encouragement was provided to subjects to motivate them to run as fast as possible for each sprint. Immediately after the completion of the repeated sprint protocol, subjects provided a rating of perceived exertion (RPE) using Borg's CR-10 scale [185] and a rating between 0 to 10 of how fatigued they felt using a rating of fatigue scale [186]. Subjects were given, on average (mean ± standard deviation [SD]), 108 ± 14 s rest, which represented the time to reconfigure the timing gates, before performing post-intervention testing of single and repeated CMJs and 40 m run-throughs at each speed in the same counterbalanced order as pre-fatigue.

5.4.3.3 Data Processing

Raw triaxial accelerometer data were downloaded as a CSV file from STATSports® Apex Unified Raw Data Parser software (version 4.6.0.184). A custom MATLAB script (version 9.12.0.1956245, R2022a, MathWorks, Inc., Natick, MA, USA) was used to realign the Apex's accelerometer axes to match the orientation recognised by the gait event detection algorithm and extract data from the 20 to 40 m section of running [17]. This was done by trimming the accelerometer files using the sync events (spikes) and the 20 and 40 m split times to remove all data points occurring either side of the constant velocity section. Data were filtered using an Attitude and Heading Reference System (AHRS) algorithm which applies a cut-off frequency of ~50 Hz when exported from the Unified Raw Data Parser software [172].

5.4.3.4 Gait Events

Trimmed accelerometer files were put through a MATLAB algorithm to identify IC and TO gait events [17]. The computational method for determining these events from accelerometer waveforms obtained from the thoracic spine has been described thoroughly in our preceding work where it was shown that the thoracic spine can detect IC compared to a criterion with an F1 score ≥0.95 [182]. Readers can refer to our validity and reliability paper [182] and elsewhere [17] for a complete description of the algorithmic approach used here.

5.4.3.5 Running Gait Characteristics

Contact time, step time, flight time, step frequency and step length were determined from IC and TO events as previously described [182]. A spring-mass model equation was then used to estimate K_{vert} from the ratio of $vGRF_{peak}$ and COM_{dis} using contact time, flight time and subject body mass as input variables [14].

5.4.3.6 Statistical Analyses

Summary statistics for sprint times, RPE, rating of fatigue and running gait characteristics are reported as mean ± SD. The interaction between fixed effects of trial condition (pre-post 12 x 40 m sprints) and velocity (3-4, 5-6 and 7-8 $m \cdot s^{-1}$) on dependent variables (contact time, step time, flight time, step frequency, step length, $vGRF_{peak}$, COM_{dis}, K_{vert}, FT:CT, jump height and passive stiffness) were assessed using a linear mixed-effects model (*lme4* package) in R statistical software (version R-4.0.4, RStudio, PBC, Boston, MA, USA). Subject ID was used as a random effect. Trial condition (pre-post 12 x 40 m sprints) was the only fixed effect applied to CMJ data (i.e., FT:CT, jump height and passive stiffness). Where a significant difference occurred ($p < 0.05$), Tukey's post-hoc test was used for pairwise comparisons (i.e., pre-post 12 x 40 m sprints) of gait and jump parameters. In addition, Cohen's effect sizes (ES; 95% confidence interval [95% CI]) were calculated where effects of <0.2, 0.2, 0.6 and > 1.2 were considered trivial, small, moderate and large, respectively [187].

5.5 Results

Mean sprint time for the 12 x 40 m repeated sprint protocol was 6.80 ± 0.18 s where the first sprint was the fastest (6.40 ± 0.64 s) and the ninth repetition the slowest (7.00 ± 0.81

s). Subject RPE and rating of fatigue scores were 8.9 ± 1.2 and 8.0 ± 1.6, respectively, following the sprints.

Table 5-1 shows the mean ± SD of gait characteristics in pre-fatigued and fatigued conditions at each running velocity, while Table 5-2 contains the results from the linear mixed effects models. Fatigue resulted in a statistically significant reduction in K_{vert} at 7-8 $m \cdot s^{-1}$ (-8.51 $kN \cdot m^{-1}$ [-13.9, -3.11]; $p = 0.007$), showing a small effect (ES [95% CI] = -0.39 [-0.62, -0.15]) (see Table 5-2 and Figure 5.2). However, the interaction between condition (pre and post) and velocity did not explain the changes observed in any other gait characteristics (see Table 5-1).

The mean ± SD values for FT:CT, jump height and passive stiffness in the pre-fatigued condition were 0.68 ± 0.15, 0.28 ± 0.07 m and 8.78 ± 5.23 $kN \cdot m^{-1}$, respectively. In the fatigued condition, FT:CT, jump height and passive stiffness were 0.65 ± 0.13, 0.25 ± 0.04 m and 8.54 ± 5.94 $kN \cdot m^{-1}$. The pre-post change in FT:CT (-0.03 [-0.06, 0.00]; $p = 0.109$) and passive stiffness was not significant (-0.24 $kN \cdot m^{-1}$ [-1.89, 1.41]; $p = 0.803$) (see Table 5-2 and Figure 5.3). However, there was a significant moderate decrease in jump height from the single CMJ (-0.03 m [-0.04, -0.01]; $p = 0.002$; ES [95% CI] = -0.87 [-1.41, -0.30]) following the repeated sprint protocol (see Table 5-2 and Figure 5.3), and this coincided with the significant reduction in K_{vert} observed in running at 7-8 $m \cdot s^{-1}$.

Table 5-1. Mean ± SD values for gait characteristics pre-post the 12 x 40 m repeated sprint protocol.

	3-4 $m \cdot s^{-1}$		5-6 $m \cdot s^{-1}$		7-8 $m \cdot s^{-1}$	
Variable	Pre	Post	Pre	Post	Pre	Post
Contact time (s)	0.229 ± 0.019	0.224 ± 0.015	0.194 ± 0.011	0.193 ± 0.010	0.134 ± 0.010	0.142 ± 0.010
Step time (s)	0.365 ± 0.019	0.359 ± 0.020	0.318 ± 0.022	0.314 ± 0.024	0.265 ± 0.023	0.277 ± 0.020
Flight time (s)	0.136 ± 0.018	0.135 ± 0.016	0.126 ± 0.019	0.122 ± 0.019	0.130 ± 0.013	0.135 ± 0.010
Step frequency (steps·min^{-1})	164.91 ± 9.14	167.75 ± 9.04	190.00 ± 14.12	192.60 ± 15.35	230.21 ± 18.10	224.82 ± 12.35
Step length (m)	1.31 ± 0.07	1.35 ± 0.08	1.76 ± 0.14	1.74 ± 0.17	1.99 ± 0.21	2.07 ± 0.17
$vGRF_{peak}$ (kN)	1.84 ± 0.25	1.85 ± 0.26	1.90 ± 0.31	1.88 ± 0.29	2.40 ± 0.21	2.39 ± 0.25
COM_{dis} (m)	0.07 ± 0.01	0.06 ± 0.01	0.05 ± 0.01	0.05 ± 0.00	0.02 ± 0.00	0.03 ± 0.00
K_{vert} ($kN \cdot m^{-1}$)	28.88 ± 5.09	30.57 ± 4.84	41.77 ± 8.19	41.38 ± 5.76	110.11 ± 14.43	97.36 ± 16.15

$m \cdot s^{-1}$, metres per second; steps·min^{-1}, steps per minute; $vGRF_{peak}$, peak vertical ground reaction force; kN, kilonewtons; COM_{dis}, centre of mass displacement; K_{vert}, vertical stiffness; kN·m, kilonewtons per metre.

Table 5-2. Effects of trial condition and running velocity on gait and jump parameters.

Model	Fixed effects	Coefficient	df	*t* Value	*p*-value	Effect size (d) (95% CI)
Contact time (s)	Post Jog - Pre Jog	-0.006 (-0.012, 0.001)	71.4	-1.6	0.120	-0.19 (-0.42, 0.05)
Contact time (s)	Post Stride - Pre Stride	-0.001 (-0.008, 0.005)	71.4	-0.4	0.700	-0.05 (-0.28, 0.19)
Contact time (s)	Post Sprint - Pre Sprint	0.006 (-0.002, 0.014)	71.4	1.2	0.220	0.15 (-0.09, 0.38)
Step time (s)	Post Jog - Pre Jog	-0.006 (-0.013, 0.001)	71.4	-1.5	0.150	-0.17 (-0.41, 0.06)
Step time (s)	Post Stride - Pre Stride	-0.004 (-0.011, 0.003)	71.4	-0.9	0.350	-0.11 (-0.34, 0.12)
Step time (s)	Post Sprint - Pre Sprint	0.006 (-0.003, 0.016)	71.4	1.1	0.260	0.14 (-0.1, 0.37)
Flight time (s)	Post Jog - Pre Jog	-0.001 (-0.008, 0.007)	71.4	-0.1	0.890	-0.02 (-0.25, 0.22)
Flight time (s)	Post Stride - Pre Stride	-0.004 (-0.012, 0.003)	71.4	-1.1	0.290	-0.13 (-0.36, 0.11)
Flight time (s)	Post Sprint - Pre Sprint	0.002 (-0.007, 0.012)	71.4	0.4	0.697	0.05 (-0.19, 0.28)
Step frequency (steps·min^{-1})	Post Jog - Pre Jog	2.85 (-1.6, 7.30)	71.4	1.1	0.266	0.13 (-0.1, 0.37)
Step frequency (steps·min^{-1})	Post Stride - Pre Stride	2.6 (-1.85, 7.05)	71.4	1.0	0.310	0.12 (-0.11, 0.35)
Step frequency (steps·min^{-1})	Post Sprint - Pre Sprint	-0.87 (-6.81, 5.06)	71.4	-0.3	0.797	-0.03 (-0.26, 0.2)
Step length (m)	Post Jog - Pre Jog	0.04 (-0.01, 0.10)	71.4	1.3	0.189	0.16 (-0.08, 0.39)
Step length (m)	Post Stride - Pre Stride	-0.02 (-0.08, 0.04)	71.4	-0.7	0.511	-0.08 (-0.31, 0.15)
Step length (m)	Post Sprint - Pre Sprint	0.03 (-0.04, 0.11)	71.4	0.7	0.456	0.09 (-0.14, 0.32)
$vGRF_{peak}$ (kN)	Post Jog - Pre Jog	0.02 (-0.04, 0.07)	71.4	0.5	0.626	0.06 (-0.17, 0.29)
$vGRF_{peak}$ (kN)	Post Stride - Pre Stride	-0.02 (-0.08, 0.03)	71.4	-0.8	0.432	-0.09 (-0.33, 0.14)
$vGRF_{peak}$ (kN)	Post Sprint - Pre Sprint	-0.03 (-0.1, 0.05)	71.4	-0.7	0.514	-0.08 (-0.31, 0.16)
COM_{dis} (m)	Post Jog - Pre Jog	-0.003 (-0.007, 0.000)	71.4	-1.6	0.108	-0.19 (-0.43, 0.04)
COM_{dis} (m)	Post Stride - Pre Stride	-0.001 (-0.004, 0.003)	71.4	-0.4	0.721	-0.04 (-0.27, 0.19)
COM_{dis} (m)	Post Sprint - Pre Sprint	0.002 (-0.003, 0.007)	71.4	0.8	0.433	0.09 (-0.14, 0.33)
K_{vert} (kN·m^{-1})	Post Jog - Pre Jog	1.68 (-2.36, 5.73)	71.3	0.7	0.468	0.09 (-0.15, 0.32)
K_{vert} (kN·m^{-1})	Post Stride - Pre Stride	-0.39 (-4.43, 3.66)	71.3	-0.2	0.867	-0.02 (-0.25, 0.21)
K_{vert} (kN·m^{-1})	Post Sprint - Pre Sprint	-8.51 (-13.9, -3.11)	71.3	-2.8	0.007	-0.33 (-0.56, -0.09)
FT:CT	Post - Pre	-0.03 (-0.06, 0.00)	17.1	-1.7	0.109	-0.41 (-0.9, 0.09)
Jump Height (m)	Post - Pre	-0.03 (-0.04, -0.01)	17.1	-3.6	0.002	-0.87 (-1.41, -0.3)
Passive Stiffness (kN·m^{-1})	Post - Pre	-0.24 (-1.89, 1.41)	17.1	-0.3	0.803	-0.06 (-0.54, 0.41)

Jog, stride and sprint speeds defined as 3-4, 5-6 and 7-8 m·s^{-1}, respectively. CI, confidence interval; steps·min^{-1}, steps per minute; $vGRF_{peak}$, peak vertical ground reaction force; kN, kilonewtons; COM_{dis}, centre of mass displacement; K_{vert}, vertical stiffness; kN·m^{-1}, kilonewtons per metre; m·s^{-1}, metres per second.

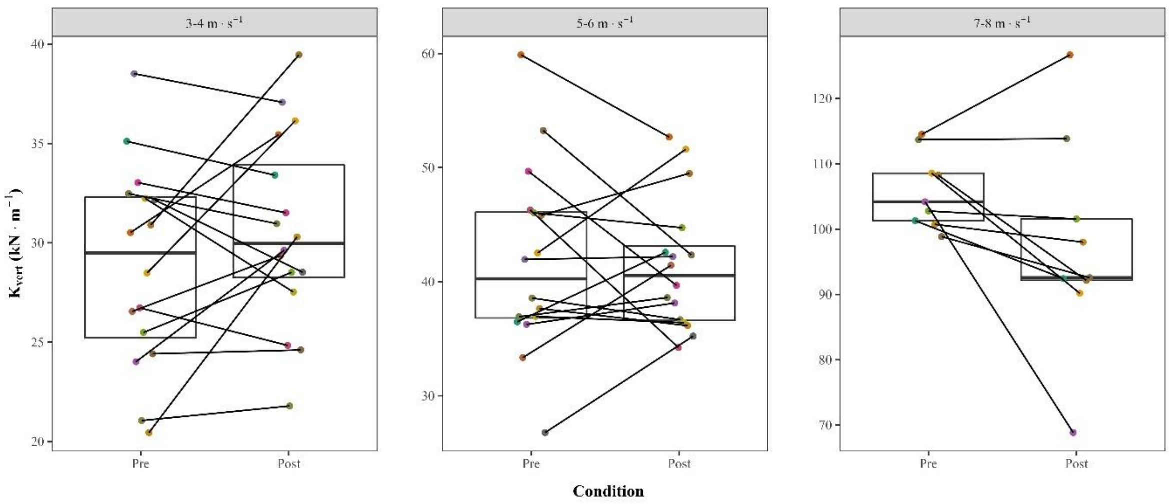

Figure 5.2. Change in K_{vert} between pre-fatigue and post-fatigue conditions at each running velocity. Individual values are plotted as points with lines connecting those belonging to the same subject. The spread of the data is represented by the boxplot where the solid black line is the median K_{vert} (kN·m^{-1}) and the box is the inter-quartile range. m·s^{-1}, metres per second; K_{vert}, vertical stiffness; kN·m^{-1}, kilonewtons per metre.

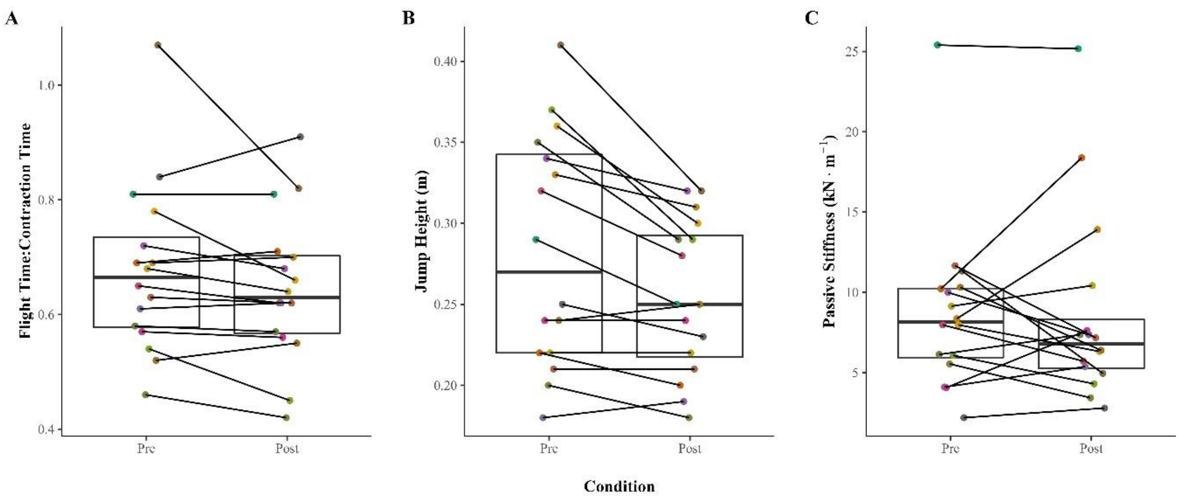

Figure 5.3. Change in FT:CT **(A)**, jump height **(B)** and passive stiffness **(C)** between pre-fatigue and post-fatigue conditions for the single and repeated countermovement jump tests. Individual values are plotted as points with lines connecting those belonging to the same subject. The spread of the data is represented by the boxplot where the solid black line is the median and the box is the inter-quartile range. kN·m^{-1}, kilonewtons per metre.

5.6 Discussion

This study aimed to quantify the fatigue-related changes in running gait characteristics derived from thoracic-mounted accelerometers and whether these corresponded to a decline in CMJ performance following an intervention consisting of 12 x 40 m repeated sprints. The major finding from this work was that during sprinting following the fatigue intervention there was a significant reduction in K_{vert} which coincided with a significant decrement in single CMJ height, and this change in K_{vert} is consistent with previous work [67, 73]. Our results support the utility of using thoracic-mounted accelerometers, such as those embedded within GNSS units, to quantify changes in running gait following high-intensity activity which provides practitioners with a useful tool that can be used in the field.

The significant reduction seen in K_{vert} during sprinting at 7-8 $m \cdot s^{-1}$ is a similar finding to previous work that used an identical fatigue protocol, however the magnitude of reduction was much less [67]. In the current study, K_{vert} was reduced in sprinting following the 12 x 40 m protocol by ~8% compared to ~16% previously [67]. The exact mechanism responsible for the smaller reduction is unclear, however it may be related to the ~20 $kN \cdot m^{-1}$ underestimation of K_{vert} measured via thoracic GNSS-embedded accelerometers [182]. Although K_{vert} was reduced at 7-8 $m \cdot s^{-1}$, there was no significant reduction at 3-4 and 5-6 $m \cdot s^{-1}$. An inspection of changes at an individual subject level suggests a more varied response at these speeds than during sprinting, with 56% and 50% of subjects increasing their K_{vert} for jog (3-4 $m \cdot s^{-1}$) and stride (5-6 $m \cdot s^{-1}$) speeds, respectively. As K_{vert}, is the ratio of $vGRF_{peak}$ and COM_{dis}, the slower speeds may have provided subjects the opportunity to manipulate their running gait mechanics, such as contact time and flight time, to maintain K_{vert} in the presence of NMF [188, 189]. However, the requirement to sprint maximally may place constraints on the ability to manipulate the components of $vGRF_{peak}$ and COM_{dis} (and subsequently K_{vert}) which has resulted in the significant reduction in K_{vert} during sprinting seen here [67, 189]. This highlights the potential for measuring changes in K_{vert} during sprinting that occurs within field sport match play and training as a means of monitoring NMF.

Fatigue induced by repeated sprint protocols, including the 12 x 40 m used in this study, has been shown to result in changes in spatiotemporal gait characteristics, such as increased contact time and decreased step frequency at high running speeds [67, 73, 190]. However, contrary to this, we observed no significant differences in spatiotemporal variables, including contact time and step frequency, during sprinting (7-8 $m \cdot s^{-1}$) despite subjects being "very fatigued" based on their rating of fatigue [186]. Although the majority (60-70%) of subjects in this study exhibited increased contact time and decreased step frequency as seen previously [67, 73, 190], the non-significant mean change for these variables at 7-8 $m \cdot s^{-1}$ suggests a variation in the individual response due to fatigue. This variation may be due to differences in training status (including 7-8 $m \cdot s^{-1}$ representing a different percentage of absolute maximum velocity for different subjects), within the subject group where other work has showed greater mechanical changes in novice runners compared to those more experienced [191, 192]. However, the lack of significant change for spatiotemporal gait characteristics at 3-4 and 5-6 $m \cdot s^{-1}$ is not surprising given NMF from repeated sprints has been shown to not result in modifications to running gait at submaximal velocities [193]. In the present study, subjects were able to maintain their contact time, flight time and step frequency, suggesting the 12 x 40 m protocol used here is likely not a large enough stimulus to elicit significant changes in spatiotemporal gait characteristics at low speed [193]. This could be because subjects have sufficiently developed underlying physical capacities, such as lower body strength, to tolerate the fatigue intervention without modification to their running gait at submaximal speeds [49, 193]. However, it is quite possible that many team-sports that require a combination of repeated sprint performance and relatively high volumes of sub-maximal running could induce higher levels of NMF than seen in the current study [11, 38, 49, 194], which in turn are discernable at slower running speeds.

Monitoring NMF via CMJ tests is common in high performance settings where fatigue from repeat sprint exercise can manifest in reduced CMJ height [58]. However, NMF does not always result in reductions in jump height [195] and it has been demonstrated that subjects can adopt a different movement strategy to maintain jump height [179]. In the current study, we observed a significant decrease in jump height (p = 0.002) following the 12 x 40 m repeated sprints which is in agreement with other findings showing a reduction with sprint exercise [58]. The reduction in jump height may be due to an impaired ability to utilise the stretch-shortening cycle following sprint fatigue [51]. However, there was a non-significant moderate reduction in FT:CT (ES [95% CI] = -0.41 [-0.90, 0.09]). In most cases (~69% of subjects), there was a reduced FT:CT following the 12 x 40 m sprints, suggesting a change in movement strategy because of NMF. However, this was ineffective in assisting subjects to maintain jump height, which is in contrast to previous work where jump height has been maintained as a function of a change in FT:CT [179]. The reason for this is unclear, although it may also be attributable to training status [191, 192].

This study used a repeated CMJ protocol to assess whether changes in K_{vert} during running were mirrored in jumping following NMF [184]. We found no significant difference (p = 0.803) in passive stiffness between pre-post conditions, which is contrary to findings in previous work following NMF [180]. One possible explanation for this is that changes in stiffness (i.e., K_{vert}) assessed during running may be more sensitive to fatigue induced via repeated sprinting than when assessed via jumping [196]. Similarly, the repeated CMJ test used here may have inherent limitations that reduce its sensitivity for assessing passive stiffness. In this protocol, passive stiffness is calculated as $vGRF_{peak}$ divided by COM_{dis} at landing from the first jump, where the height of the first jump is a factor in the landing force that must be controlled by the subject. Observation of our data showed that jump height was also reduced in the first of the repeated jumps in the post-fatigue condition (which also occurred in the single CMJ as discussed above). This resulted in a reduced $vGRF_{peak}$ and COM_{dis}, consequently allowing subjects to maintain their passive stiffness upon landing and in transition to the second jump. Therefore, a single drop jump from a standardised height (e.g., 30 cm) may be a more appropriate protocol for the assessment of K_{vert} in jumping [197].

A potential limitation of this study is the majority of our subjects shared a similar anthropometric profile which may have resulted in a narrow range of values for $vGRF_{peak}$ and K_{vert}, given body mass is an input variable [14]. Due to statistical power of our sample size (n = 16), we were also unable to analyse our data to account for differences in the post-intervention fatigue response between male and female subjects that may have been evident with a larger sample size. In addition, the use of tightly regulated speed bands could have limited the ability to detect modifications in movement strategy (as represented by a range of running gait metrics) that may have been evident in self-paced running. It is possible that the constraints of the task provided limited opportunity for subjects to select alternative running strategies, even in the presence of underlying NMF [189].

In conclusion, this work demonstrates thoracic-mounted accelerometers contained in GNSS units can detect fatigue-related changes in K_{vert} during sprinting. This provides opportunities for gaining detailed insight into athlete movement strategy which may provide useful data for monitoring running specific fatigue in sport. However, a 12 x 40 m repeated sprint protocol may not be substantial enough to evoke changes in running gait at low speed. Therefore, further work is warranted to investigate the alterations to accelerometer-derived measures of running gait following a greater stimulus, such as a team-sport match.

5.7 Practical Applications

This work confirms the ability to detect fatigue-related modifications in K_{vert} during sprinting from a thoracic-mounted sensor. This provides practitioners with the opportunity to utilise accelerometer technology contained in GNSS units to monitor running specific NMF in field-based sports. This may be particularly useful as more gross external load metrics, such as distance and speed, may not be sensitive measures of fatigue-induced changes [11, 38]. An athletes' NMF status can be assessed during training and competition rather than requiring an additional assessment task. It may be possible to isolate a 20 m section of sprinting at ~7-8 $m \cdot s^{-1}$ and apply the approach demonstrated here to assess NMF. This data may also provide additional insight into changes in movement strategy that manifest from NMF, post-concussion or in rehabilitation from lower limb musculoskeletal injury which could be useful for informing training strategies aimed at assessing recovery or restoring normal running gait [176].

6 Chapter 6: Study Four – The Within- and Post-Match Changes in Accelerometer-Derived Gait Characteristics from a Team-Sport Match Simulation Protocol

This chapter is comprised of the final experimental study that is currently being completed. Data collection for this study was delayed due to the COVID-19 pandemic which has subsequently impacted timelines and the completion of this work by submission of this thesis. However, the progress of the final experimental study is presented in this chapter and formatted for submission to The Journal of Strength and Conditioning Research in the future.

6.1 Linking Paragraph

Performing a 12 x 40 m repeated sprint protocol results in a reduction in K_{vert} during sprinting, as measured by thoracic-mounted accelerometers. This highlights the utility of using accelerometers contained in GNSS units to detect fatigue-induced modifications to running gait at high velocity. However, it appears that 12 x 40 m sprints may not be a sufficient stimulus to result in significant alterations to other running gait characteristics, such as contact time, step frequency or $vGRF_{peak}$, including at low speed. It is possible a larger stimulus, such as one more representative of team-sport match play, may lead to changes in spatiotemporal gait characteristics (e.g., contact time, step frequency, step length etc.) that occur alongside K_{vert}. Therefore, the final study of this program of research explores the fatigue-related changes in thoracic-derived gait characteristics throughout a 90-minute team-sport match simulation and at 24, 48 and 72 hours post-match. However, the completion of this study was delayed due to the impact of the COVID-19 pandemic. Therefore, this chapter details the progress of the work at the time of submission of this thesis.

6.2 Introduction

Team-sports involve high volumes of running interspersed with rapid accelerations and decelerations, changes of direction and repeated efforts [177]. These movements are associated with fatigue which can occur within and following team-sport activity [49, 198, 199]. There are a variety of ways in which fatigue can manifest, including reductions in voluntary muscle activation [49, 50], increased perception of fatigue [200], decrements in performance measures (e.g., countermovement jump [CMJ]) [179] and modifications to activity profile (e.g., reductions in high-intensity running) [31, 37]. Variables such as distance and speed can be monitored live within training and matches using global navigation satellite system (GNSS) units worn by team-sport athletes. While GNSS-derived metrics provide a global representation of running activity, they cannot explain underlying changes in running strategy (e.g., gait metrics) that may precede, or manifest independently of, any change in distance or speed. Therefore, to examine the fatigue response in running at a more discrete level, different monitoring methods are required.

The GNSS units commonly worn by athletes also contain high sample rate (100 Hz) triaxial accelerometers [201]. In sport, accelerometers have been used to derive proprietary metrics (e.g., PlayerLoad™) which are sensitive to detecting changes in movement strategy with fatigue, as measured by reductions in the contribution of the vertical vector to total PlayerLoad™ [11, 12]. Although modifications to the accumulation of PlayerLoad™ provides some insight into changes in movement strategy, these are likely to be underpinned by alterations in gait (e.g., contact time, flight time, step length, vertical stiffness [K_{vert}] etc.). Such variables have been shown to be impacted by fatigue [67, 202, 203] and they can be accurately and reliably obtained from accelerometers contained in GNSS units [182]. This may allow practitioners to access more granular information on running-induced fatigue than distance and speed or proprietary metrics.

Accelerometers contained in GNSS units are sensitive to detecting fatigue-related changes in running gait as demonstrated by reductions in K_{vert} following 12 x 40 m repeated sprints [204]. However, fatigue-driven modifications to running gait have yet to be assessed during or following team-sport matches. Assessing running fatigue within and post-match may allow expediated interventions, such as recovery strategies or training load modifications, and reduce the requirement of using additional assessment tasks (e.g., CMJ).

Although competitive team-sport matches are the ideal environment to assess fatigue-related changes in running gait, they lack experimental control (e.g., between-match variability in activity profiles) which make them problematic [205, 206]. However, match simulations, such as the soccer-specific aerobic fitness test ($SAFT^{90}$), serve as an alternative to replicate the activity profile of competition [207]. The $SAFT^{90}$ contains 6 x 15 min segments simulating the intermittent and multi-directional movements of team-sport and inducing similar physiological responses to competitive matches [207], and has been used extensively as a fatiguing intervention [208-212].

Therefore, the primary aim of this study was to assess the within- and post-simulation changes in a variety of running gait characteristics derived from GNSS-embedded accelerometers worn on the thoracic spine and determine whether fatigue-related changes in gait coincide with changes in a range of jump variables. As physical capacity has been demonstrated to mediate the deleterious effects of fatigue from matches [49, 50, 199], an additional aim was to determine whether fatigue-related changes in gait were impacted by lower body strength and power or intermittent endurance capacity.

6.3 Methods

6.3.1 Experimental Approach to the Problem

This study investigated the within- and post-match changes in running gait characteristics measured from GNSS-embedded accelerometers and jump parameters during and following a 90-minute team-sport match simulation protocol [209]. A pre-post intervention design was used that required subjects to attend six testing sessions in total, including one familiarisation, one profiling session to measure physical capacity (lower body strength and power and intermittent endurance capacity), one session comprising the 90-minute match simulation and three follow-up visits to measure the fatigue response in running gait characteristics and jump parameters up to 72 hours post-match (see Figure 6.1).

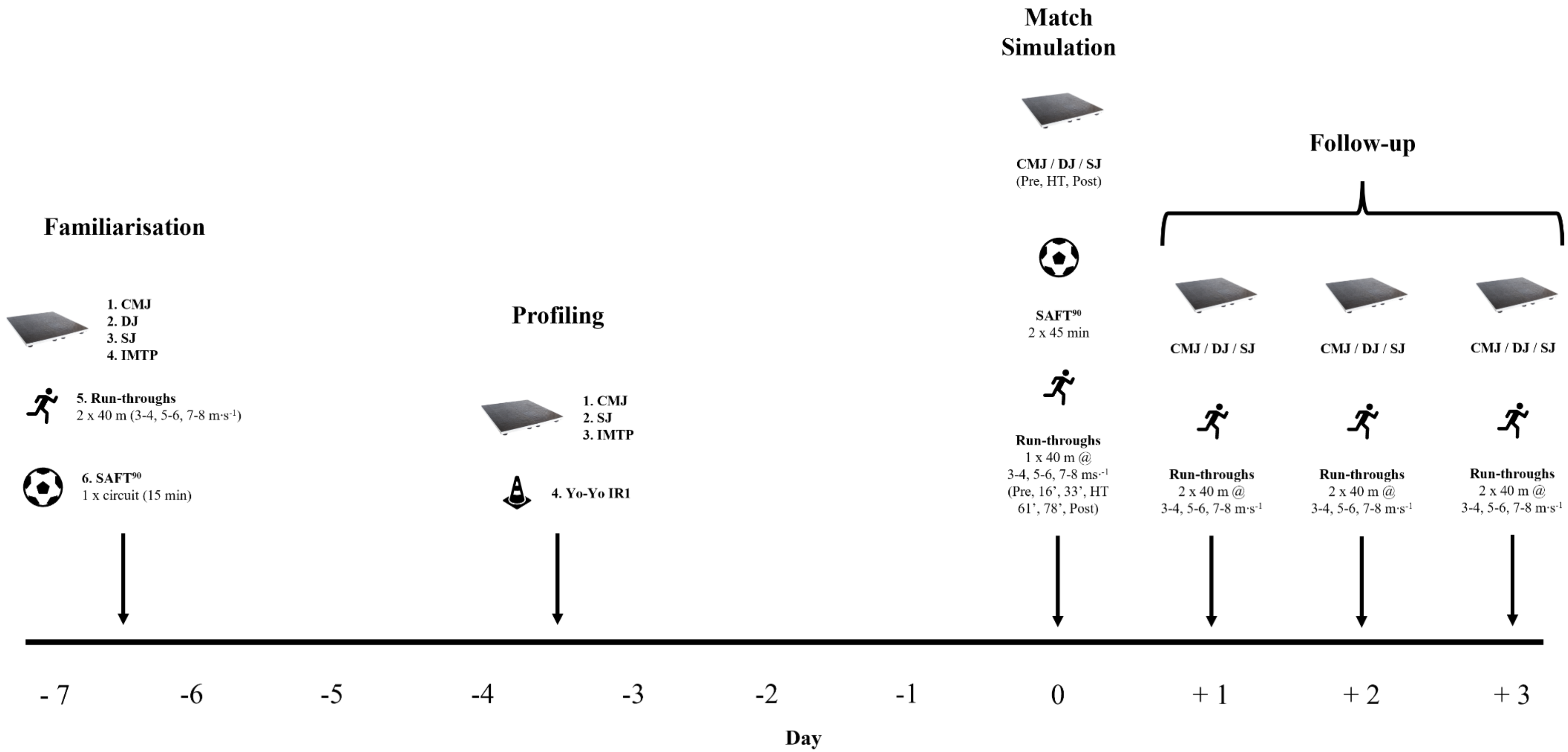

Figure 6.1. Timeline of research study. Match simulation and follow-up testing were performed on consecutive days. CMJ, countermovement jump; DJ, drop jump; SJ, squat jump; $m \cdot s^{-1}$, metres per second; SAFT^{90}, soccer-specific aerobic fitness test; Yo-Yo IR1, Yo-Yo Intermittent Recovery Level 1; HT, halftime.

6.3.2 Subjects

Three men (age: 25.3 ± 4.2 years; height: 173.2 ± 10.3 m; mass: 75.6 ± 10.7 kg) and five women (age: 24.2 ± 5.6 years; height: 164.6 ± 5.2 cm; mass: 66.3 ± 12.2 kg) familiar with high-intensity exercise and injury-free were recruited for this study. Six subjects were amateur team-sport athletes training and competing 2-4 days per week, while two subjects were recreationally active individuals accustomed to running (at least one training run per week). Subjects received written and verbal communication of the study design, risks and potential benefits and provided written informed consent prior to commencing in the study. The Australian Catholic University Human Research Ethics Committee (2022-2769H) approved this study.

6.3.3 Procedures

6.3.3.1 Familiarisation

Familiarisation occurred in the following order: CMJ, drop jump (DJ), squat jump (SJ), isometric mid-thigh pull (IMTP), 40 m run-throughs at 3-4, 5-6 and 7-8 $m{\cdot}s^{-1}$ and the SAFT[90]. Jump and IMTP tests were performed on a force plate sampling at 1000 Hz (FDLite, ForceDecks, Vald Performance, Brisbane, Australia) which was calibrated pre-testing in line with manufacturer guidelines. For the CMJ, subjects stood on the force plate and jumped as high as possible while maintaining their hands on their hips [54]. A 30 cm box was used to standardise the drop height for the DJ test [213]. Subjects stood stationary on top of the box with their hands on their hips, and following the command “drop”, stepped off the box and jumped as high as possible while minimising contact with the force plate [213]. The DJ was used in this study to assess whether changes in K_{vert} in running were also mirrored in jumping and was preferred over the repeated CMJ test due to the lack of standardisation in landing height in that test [204]. A SJ was used to assess concentric-only jump performance where subjects maintained their hands on their hips, held a self-selected squat depth for 3 s and then jumped straight up as high as possible [214]. The IMTP was used to measure maximal isometric strength of the lower body where subjects stood on the force plate while holding an immovable bar fixed to mid-thigh height [215]. A goniometer was used to ensure the hip and knee angles for each subject met the recommended guidelines of ~140-150° and 125-145°, respectively [215]. Subjects wore wrist straps to assist grip strength and strong verbal communication was given to encourage subjects to push their feet as hard and as fast as possible into the force plate for 5 s while maintaining the predetermined posture [215].

Following familiarisation of strength and power testing procedures, subjects were accustomed to running at 3-4, 5-6 and 7-8 $m \cdot s^{-1}$ over 40 m. Each run-through required subjects to accelerate for 20 m and maintain the target running speed between the 20 and 40 m marks, and this was the procedure used in the preceding two studies to the current work [182, 204]. Electronic timing gates (Swift DUO™, Swift Performance, Brisbane, Australia) were positioned at 20 and 40 m to monitor running velocity, and these are reliable for measuring sprint times over 40 m (coefficient of variation [CV] ≤1.3%) [170]. To ensure a constant velocity, subjects were instructed to achieve the required speed before the 20 m gate (~17-18 m) and maintain it until they had completely passed through the 40 m gate. To be deemed familiarised, subjects successfully completed two consecutive run-throughs at each speed. Finally, subjects were familiarised with the $SAFT^{90}$ match simulation protocol which involves 6 x 15-minute (2 x 45-minute halves) standardised running circuits performed with the aid of an audio track over a 20 m course (see Figure 6.2) [209]. Each circuit requires subjects to perform a variety of movements aimed at replicating team-sport activity, including side-stepping, cutting, accelerations and decelerations and forwards and backwards running performed at different speeds (see Figure 6.2). For the purposes of familiarisation, subjects only completed 1 x 15-minute circuit.

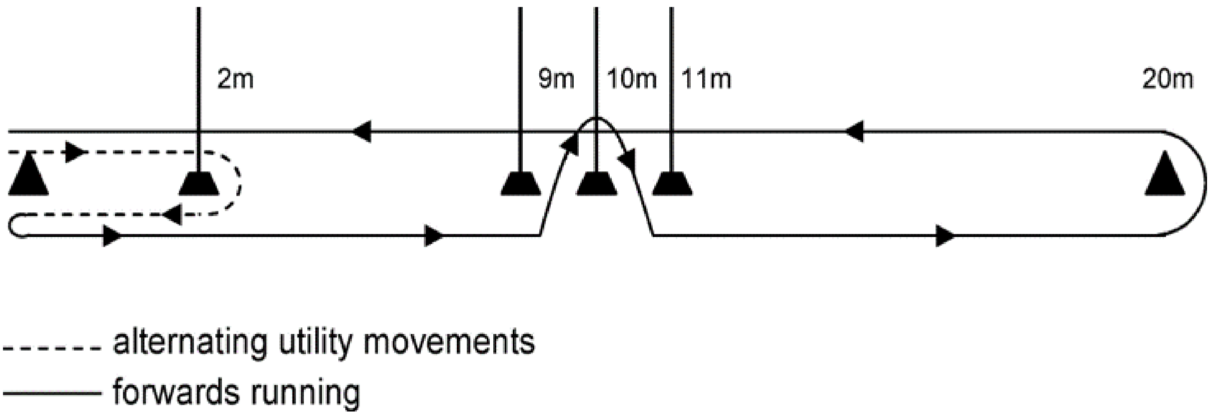

Figure 6.2. Soccer-specific aerobic fitness test (SAFT[90]). Alternating movements include accelerations, side-stepping and backwards running.

6.3.3.2 Physical Capacity Profiling

Subjects returned 6.6 ± 9.2 days following familiarisation to have their lower body strength, power and intermittent endurance capacity tested in the following order: CMJ, SJ, IMTP and Yo-Yo Intermittent Recovery Level 1 (Yo-Yo IR1; see Figure 6.1). Subjects performed two trials for each jump test (separated by ~15 seconds) and a single maximal trial for the IMTP using the same procedures outlined above. ForceDecks software (version 2.0.8245) was used to derive jump parameters (e.g., peak power relative to body mass [$W \cdot kg^{-1}$], CMJ height [m], SJ height [m] etc.) and maximal strength relative to body mass ($N \cdot kg^{-1}$) from the IMTP. The Yo-Yo IR1 required subjects to run out and back over a 20 m distance at gradually increasing speeds, interspersed with 10 s active recovery [216]. Subjects performed the test until failure to reach the finish line in time on two occasions [216], where accumulated distance (m) was used to profile intermittent endurance capacity.

6.3.3.3 Match Simulation

The SAFT^{90} match simulation was completed on an artificial grass surface 5.6 ± 2.3 days post assessment of physical capacity (see Figure 6.1). During the SAFT^{90}, subjects wore one GNSS unit (Apex, STATSports®, Newry, Northern Ireland; 10 Hz, 84 x 43 x 20 mm; 72 g) with an embedded triaxial accelerometer (ADXL375; 100 Hz; ±200 g). The Apex unit was worn between the scapulae, housed in a tightly fitted custom vest, and recorded data throughout the entire duration of the SAFT^{90} (plus additional 40 m run-throughs).

A 10-minute standardised warm-up was completed by all subjects that included various running patterns (forwards, side-stepping and carioca drill) over 20 m, dynamic stretches (e.g., high knee skips, heel flicks, hurdle walk etc.) and one build-up run at ~70, 80 and 90% of perceived maximal running speed. Following, baseline measures of CMJ, DJ, SJ (two trials separated by ~15 s) and 1 x 40 m run-through performed in a counterbalanced order at each speed (3-4, 5-6 and 7-8 $m \cdot s^{-1}$) were obtained. For each 40 m run-through, subjects performed a synchronisation procedure which is outlined in detail in Studies 2 (Chapter 4: Section 4.4.3.2) and 3 (Chapter 5: Section 5.4.3.2). The purpose of this was to synchronise the accelerometer data with the recording of the timing gates to extract data from the 20-40 m section of running for every run-through.

After baseline testing, subjects commenced the SAFT^{90} match simulation which consisted of 3 x 15-minute circuits per half interspersed with a 15-minute halftime interval [209]. Three additional run-throughs (one at each speed [3-4, 5-6 and 7-8 $m \cdot s^{-1}$]) in the same counterbalanced order were performed immediately after each circuit. Two lanes were set up so the timing gates were positioned next to the SAFT^{90}, course where after the completion of each circuit, subjects were directed straight to the synchronisation gate to perform the run-throughs. Subjects then walked straight back to the start of the SAFT^{90} course and commenced the next circuit with minimal delay. The three circuits and additional sets of run-throughs resulted in the first and second halves taking 58.10 ± 4.48 min and 58.22 ± 2.33 min to complete, respectively. At halftime and post-match, subjects also repeated the respective jump tests (CMJ, DJ and SJ) and provided a rating of perceived exertion (RPE) using Borg's CR-10 scale [185] and a rating of fatigue [186].

6.3.3.4 Follow-up Testing

Follow-up visits were scheduled at the same venue for three consecutive days post-match (+24, 48 and 72 hours; see Figure 6.1). Testing sessions were performed at a similar time of day as the SAFT^{90} where subjects performed a CMJ, DJ, SJ and 2 x 40 m run-throughs at 3-4, 5-6 and 7-8 m·s^{-1} in the same counterbalanced order. The follow-up visits were used to investigate the time-course of recovery of gait characteristics and performance in the respective jump tests.

6.3.3.5 Data Processing

STATSports® Sonra software (version 4.1.31) was used to download and export GNSS-derived data, while the same procedures as Study 3 (Section 5.4.3.3) were used to download and process the raw triaxial accelerometer data from the Apex units to identify initial contact (IC) and toe-off (TO) from a gait event detection algorithm.

6.3.3.6 Outcome Measures from the SAFT^{90}

Total distance and total high-speed running distance (>5.5 m·s^{-1}) were derived to describe the activity profile from the SAFT^{90} match simulation. To assess the fatigue response in running gait, contact time, step time, flight time, step frequency and step length were determined from identified IC and TO events, as per previous work [182]. A spring-mass model equation was then used to estimate K_{vert} from the ratio of $vGRF_{peak}$ and COM_{dis} using contact time, flight time and subject body mass as input variables [14]. Performance in the respective jump tests (CMJ, DJ and SJ) with fatigue was determined by recording CMJ height, FT:CT, passive stiffness (i.e., K_{vert} derived from the DJ in ForceDecks software; $kN \cdot m^{-1}$) and SJ height.

6.3.4 Statistical Analyses

Due to this study being ongoing and only eight participants to date completing the protocol, no statistical analysis has been conducted due to the lower than required sample size. As a result, only descriptive statistics (mean ± SD) are reported below to describe the fatigue response in running gait characteristics and jump parameters.

6.4 Results

On average, subjects ran a total distance of 12740.9 ± 583.8 m throughout the entire $SAFT^{90}$ protocol, including the six additional sets of 40 m run-throughs. Total distance travelled in the first half was 5844.9 ± 251.4 m, while the second half was 5781.6 ± 255.3. Total high-speed running distance traveled in the $SAFT^{90}$ was 341.9 ± 95.9 m, while the first and second halves were 154.4 ± 45.5 m and 133.4 ± 44.4, respectively.

Mean halftime RPE responses were 7.0 ± 1.5, while post-match was 9.5 ± 1.2. Perceptual rating of fatigue scores were 7.0 ± 1.3 at halftime and 9.8 ± 0.9 post-match, respectively.

Table 6-1 outlines the mean ± SD in changes in running gait characteristics throughout the $SAFT^{90}$ protocol and in the days post-match. Variables $vGRF_{peak}$ and K_{vert} are visualised in

Figure 6.3 and Figure 6.4, respectively, to highlight the fatigue response at both individual subject and group levels.

Descriptive statistics (mean ± SD) for jump parameters from the SAFT^{90} match simulation are detailed in Table 6-1.

Table 6-1. Mean ± SD values for gait characteristics measured from thoracic-worn accelerometers from Pre to $Post_{72}$.

Variable	Pre	First $Half_1$	First $Half_2$	Halftime	Second $Half_1$	Second $Half_2$	Post	$Post_{24}$	$Post_{48}$	$Post_{72}$
3-4 $m \cdot s^{-1}$										
Contact time (s)	0.225 ± 0.018	0.224 ± 0.014	0.229 ± 0.019	0.229 ± 0.01	0.225 ± 0.011	0.230 ± 0.015	0.232 ± 0.017	0.239 ± 0.019	0.233 ± 0.015	0.240 ± 0.02
Step time (s)	0.354 ± 0.03	0.351 ± 0.027	0.351 ± 0.026	0.349 ± 0.022	0.347 ± 0.023	0.347 ± 0.025	0.346 ± 0.022	0.355 ± 0.027	0.353 ± 0.024	0.358 ± 0.022
Flight time (s)	0.130 ± 0.013	0.126 ± 0.02	0.120 ± 0.016	0.120 ± 0.016	0.120 ± 0.018	0.116 ± 0.02	0.113 ± 0.016	0.115 ± 0.015	0.121 ± 0.016	0.118 ± 0.02
Step frequency ($steps \cdot min^{-1}$)	170.70 ± 14.96	171.95 ± 13.29	172.01 ± 13.21	172.96 ± 10.73	173.88 ± 11.53	174.09 ± 12.81	174.56 ± 11.28	170.45 ± 13.91	170.98 ± 11.48	168.23 ± 10.64
Step length (m)	1.27 ± 0.07	1.25 ± 0.07	1.23 ± 0.05	1.26 ± 0.08	1.32 ± 0.07	1.27 ± 0.11	1.28 ± 0.11	1.26 ± 0.12	1.25 ± 0.09	1.24 ± 0.07
COM_{dis} (m)	0.062 ± 0.010	0.062 ± 0.008	0.065 ± 0.011	0.064 ± 0.005	0.062 ± 0.006	0.065 ± 0.009	0.067 ± 0.010	0.070 ± 0.011	0.067 ± 0.009	0.071 ± 0.011
5-6 $m \cdot s^{-1}$										
Contact time (s)	0.197 ± 0.026	0.199 ± 0.025	0.198 ± 0.022	0.203 ± 0.022	0.196 ± 0.021	0.199 ± 0.017	0.193 ± 0.025	0.198 ± 0.023	0.191 ± 0.027	0.189 ± 0.022
Step time (s)	0.303 ± 0.024	0.297 ± 0.027	0.302 ± 0.021	0.302 ± 0.021	0.298 ± 0.019	0.300 ± 0.018	0.292 ± 0.021	0.297 ± 0.029	0.291 ± 0.039	0.290 ± 0.024
Flight time (s)	0.105 ± 0.017	0.099 ± 0.018	0.104 ± 0.014	0.099 ± 0.012	0.102 ± 0.014	0.100 ± 0.016	0.101 ± 0.016	0.100 ± 0.012	0.100 ± 0.017	0.100 ± 0.016
Step frequency ($steps \cdot min^{-1}$)	200.00 ± 14.80	204.22 ± 19.30	203.7 ± 11.98	200.34 ± 14.50	202.91 ± 13.34	202.01 ± 11.78	207.32 ± 14.46	205.34 ± 19.69	210.35 ± 27.53	209.09 ± 16.5
Step length (m)	1.68 ± 0.18	1.65 ± 0.15	1.66 ± 0.15	1.62 ± 0.10	1.63 ± 0.12	1.61 ± 0.13	1.65 ± 0.14	1.62 ± 0.14	1.59 ± 0.14	1.58 ± 0.13
COM_{dis} (m)	0.048 ± 0.013	0.049 ± 0.012	0.049 ± 0.011	0.051 ± 0.011	0.047 ± 0.010	0.049 ± 0.008	0.046 ± 0.012	0.049 ± 0.011	0.046 ± 0.013	0.045 ± 0.010
Max										
Contact time (s)	0.136 ± 0.011	0.138 ± 0.010	0.136 ± 0.013	0.139 ± 0.013	0.141 ± 0.011	0.140 ± 0.015	0.139 ± 0.012	0.134 ± 0.012	0.136 ± 0.011	0.135 ± 0.013
Step time (s)	0.261 ± 0.020	0.271 ± 0.024	0.257 ± 0.022	0.271 ± 0.028	0.267 ± 0.020	0.271 ± 0.025	0.264 ± 0.019	0.257 ± 0.021	0.260 ± 0.023	0.259 ± 0.024
Flight time (s)	0.125 ± 0.010	0.131 ± 0.015	0.122 ± 0.011	0.131 ± 0.015	0.127 ± 0.011	0.130 ± 0.014	0.126 ± 0.008	0.122 ± 0.008	0.123 ± 0.011	0.125 ± 0.012
Step frequency ($steps \cdot min^{-1}$)	233.16 ± 16.75	225.88 ± 18.69	238.16 ± 18.70	226.03 ± 22.48	227.94 ± 16.58	227.60 ± 18.26	232.40 ± 16.59	236.38 ± 18.73	234.35 ± 20.31	235.21 ± 21.4
Step length (m)	1.74 ± 0.16	1.72 ± 0.17	1.71 ± 0.22	1.76 ± 0.20	1.75 ± 0.16	1.74 ± 0.19	1.69 ± 0.13	1.70 ± 0.18	1.69 ± 0.21	1.67 ± 0.17
COM_{dis} (m)	0.023 ± 0.004	0.024 ± 0.003	0.023 ± 0.004	0.024 ± 0.005	0.024 ± 0.004	0.024 ± 0.005	0.024 ± 0.004	0.022 ± 0.004	0.023 ± 0.004	0.023 ± 0.004

$m \cdot s^{-1}$, metres per second; $steps \cdot min^{-1}$, steps per minute; $vGRF_{peak}$, peak vertical ground reaction force; kN, kilonewtons; COM_{dis}, centre of mass displacement; K_{vert}, vertical stiffness; $kN \cdot m^{-1}$, kilonewtons per metre.

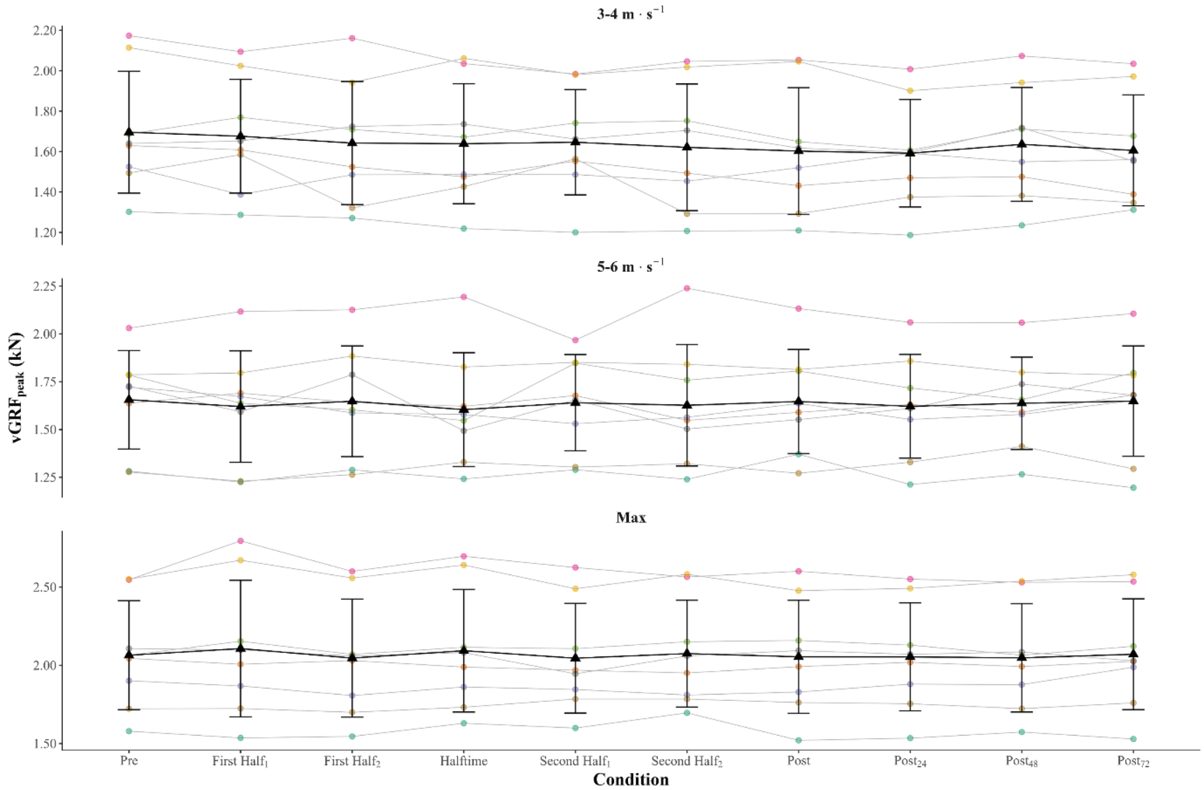

Figure 6.3. Response in $vGRF_{peak}$ from pre to three days post-match simulation at each running velocity. Black lines are group mean ± SD, while faint lines are individual subject data. $m{\cdot}s^{-1}$, metres per second; $vGRF_{peak}$, peak vertical ground reaction force; kN, kilonewtons.

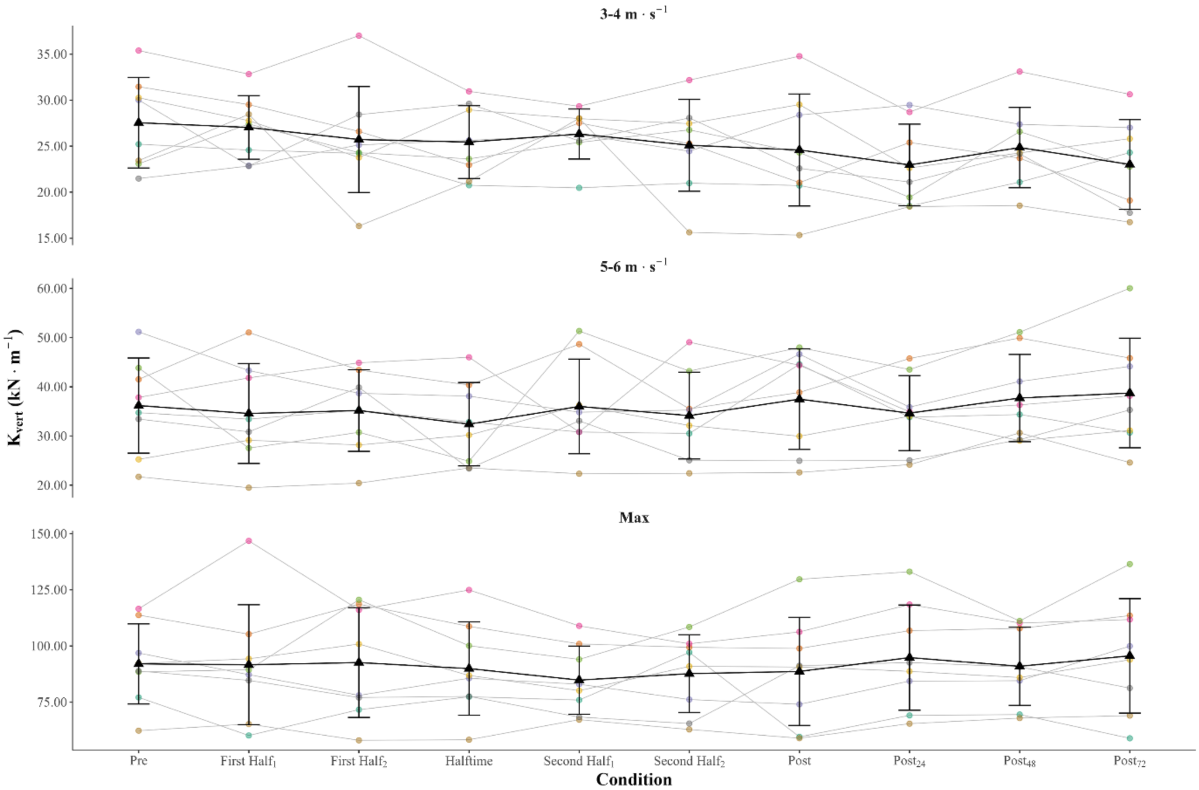

Figure 6.4. Response in K_{vert} from pre to three days post-match simulation at each running velocity. Black lines are group mean ± SD, while faint lines are individual subject data. $m \cdot s^{-1}$, metres per second; K_{vert}, vertical stiffness; $kN \cdot m^{-1}$, kilonewtons per metre.

Table 6-2. Mean ± SD values for jump parameters from Pre to $Post_{72}$.

Variable	Pre	Halftime	Post	$Post_{24}$	$Post_{48}$	$Post_{72}$
CMJ Height (m)	0.26 ± 0.07	0.26 ± 0.07	0.27 ± 0.06	0.26 ± 0.06	0.27 ± 0.05	0.28 ± 0.07
FT:CT	0.59 ± 0.11	0.59 ± 0.11	0.61 ± 0.09	0.60 ± 0.16	0.59 ± 0.09	0.62 ± 0.1
Passive Stiffness ($kN \cdot m^{-1}$)	9.36 ± 5.17	9.12 ± 5.36	8.47 ± 3.86	10.44 ± 6.17	9.84 ± 6.39	7.78 ± 3.92
SJ Height (m)	0.25 ± 0.06	0.24 ± 0.06	0.25 ± 0.06	0.25 ± 0.06	0.26 ± 0.05	0.26 ± 0.05

7 Chapter 7: Discussion and Conclusions

This research program was designed to investigate the validity and reliability of thoracic-worn Inertial Measurement Units (IMUs) for the analysis of a variety of running gait characteristics in the field. The thoracic spine site was the focus of this thesis as IMUs are typically worn at this location, contained within global navigation satellite system (GNSS) units worn by team-sport athletes. In many sports, these devices are worn in tightly fitted purpose designed vests but are sometimes in pouches sewn into the playing tops of athletes. Therefore, the thoracic spine site may be advantageous for practitioners as they could analyse running gait from inertial data and measure distance and speed from GNSS data, all from the same device. To our knowledge, four studies have investigated the use of the thoracic spine site for measuring a variety of spatiotemporal variables and vertical stiffness (K_{vert}). But, prior to this thesis, it had been difficult to ascertain the validity and reliability of this placement site due to a variety of factors. One study used a single subject case study design which provided limited data but some early proof of concept. In general, there has been a lack of adequate description of how initial contact (IC) and toe-off (TO) events have been determined from the peaks in accelerometer waveforms (e.g., no description on the timing for peak detection). In addition, no study has calculated the validity of sensors worn at the level of the thoracic spine to detect IC or TO compared to a criterion (e.g., force plate or tibia-worn sensor), and this is important to establish as the accurate identification of these events underlie the calculation of spatiotemporal gait characteristics. Some studies using thoracic-mounted IMUs have assessed the validity and reliability of contact time, flight time, peak vertical ground reaction force ($vGRF_{peak}$) and K_{vert} metrics, but these have only been presented in low-velocity running (e.g., 3 $m \cdot s^{-1}$) or as single statistics (e.g., bias, coefficient of variation [CV] etc.) across running encompassing a range of speeds (e.g., 2.8-7.5 $m \cdot s^{-1}$). The validity and reliability of these metrics have therefore not been presented at high speed (e.g., $\geq$7 $m \cdot s^{-1}$) in isolation, nor have different velocities thoroughly been explored to determine their impact on measures of spatiotemporal gait variables and K_{vert} from the thoracic spine site. The validity and reliability of other commonly analysed metrics of running gait, such as step frequency and step length, obtained from sensors worn on the thoracic spine is also unknown.

Therefore, this thesis aimed to expand on previous work by firstly conducting a systematic review and meta-analysis to assess the impact of IMU placement site on running gait validity and reliability (Study 1). Following, the validity and reliability of thoracic-worn IMUs to derive a variety of selected gait characteristics was evaluated across multiple running speeds (Study 2). The foundation for calculating gait characteristics from data obtained from IMUs worn at the level of the thoracic spine was based on an event detection algorithm previously validated for the lumbar spine. However, the underlying assumptions for informing the detection of IC and TO events were modified from the original algorithm to capture these events at differing speeds in the current work. Specifically, this involved adjusting the minimum and maximum time intervals in which eligible IC and TO events could be identified from the accelerometer data. These modifications to the algorithm were informed by prior work demonstrating the time between consecutive IC events is decreased and TO occurs sooner within a step cycle when speed increases. This algorithm was chosen because of its robustness in accommodating a variety of running styles due to it not relying on absolute threshold values (e.g., in g units) for accelerometer peak detection which are common in many other algorithms. Instead, different gait styles can be analysed as it offers contingencies for when accelerometer peaks are higher or lower in magnitude and when they occur earlier or later than expected, as well as in situations where multiple peaks are present in the data. It also provides a step-by-step account of the computation for determining IC and TO events in greater detail than that described in other work using thoracic-worn IMUs, where only a basic description of how the accelerometer waveform was analysed is outlined (e.g., ground contacts determined from vector magnitude traces). Having a thorough step-by-step description provides transparency to IC and TO detection and avoids the black box approach where explanation for how gait measures are obtained is not clearly outlined. This allows researchers to replicate the approach for gait event detection in future studies, while practitioners can be confident in the derived outcome measures (e.g., contact time, step length etc.) knowing they are based on sound underlying principles.

The ability to analyse running gait characteristics from sensors commonly worn by athletes has potential practical applications for athlete monitoring. It is possible to quantify fatigue from accelerometers worn on the thoracic spine (contained in GNSS units) as measured by reductions in the contribution of the vertical vector to total PlayerLoad™ (a proprietary metric based on resultant acceleration). Although changes in the composite accelerometer vectors indicate a fatigue-driven modification to movement (running) strategy, it does not explain the precise mechanisms responsible. It may be that fatigue-induced changes in gait may be the underlying cause, and these data may be useful in providing a detailed analysis of the fatigue response in running during training or matches. Assessing athlete fatigue as a function of changes in running gait could aid practitioner decision making on adjustments to training load, while the development of systems that enable the live monitoring of gait may allow expeditious interventions within a training session or match. Therefore, the final two studies of this thesis examined whether IMUs worn at the level of the thoracic spine can detect fatigue-related changes in running gait characteristics following an acute intervention (Study 3) and within and following performance of a simulated team-sport match (Study 4).

7.1.1 Study 1

Many IMU attachment locations, such as the foot (often located on the dorsal aspect), distal and mid tibia, sacrum and lumbar spine, have been used for assessing running gait. However, it has not been well understood whether this variation in attachment location impacts the validity and reliability of gait measures. Eligible studies which calculated the validity and reliability of IMUs in running were included in a systematic review from which quality of research was assessed using a modified version of the Downs and Black checklist due to its use in other similar review papers pertaining to sports science. Meta-analysis from Study 1 (Chapter 3) showed no statistically significant differences between contact time, flight time, step frequency and step length measured from IMUs attached to the foot, tibia and lumbar spine compared to values from motion capture, high-speed camera, force plate and photocell systems, which are all accepted criterions for gait analysis. However, only nine of the 39 articles in the systematic review were included in the meta-analysis due to inconsistent reporting of mean ± SD values from the individual papers and studies not assessing validity at a similar speed. Consequently, the small sample size of eligible studies resulted in wide confidence intervals for the summary effects (represented by the width of the polygon in the forest plot) for some variables, such as flight time and lumbar spine-derived step frequency. It is therefore important to acknowledge that this may have influenced the non-significant findings of the meta-analysis, and had more studies been eligible for inclusion, different summary effects may have been observed. Regardless, the findings from Study 1 suggests placement site itself is not the primary limiting factor to the measurement of running gait from IMUs, but validity and reliability may be more dependent on the method used for determination of IC and TO events. This may include the way data is extracted, processed and analysed, such as considerations relating to the sensors used (accelerometer, gyroscope or combination of sensors), pre-processing approaches (e.g., resampling and filtering), whether single or multiple data channels (i.e., vertical, anteroposterior, mediolateral or resultant) are used for event detection, or pattern recognition techniques using machine learning. It is commonly acknowledged that attaching IMUs higher up the kinetic chain leads to greater signal attenuation, and this has been suggested to be a potential limitation for analysing gait characteristics from IMUs worn on the thoracic spine. However, the results from the meta-analysis demonstrate that valid measures of running gait can be obtained from IMUs worn on the lumbar spine despite them being further away from the foot-ground interface than those worn on the foot and tibia. Although the thoracic spine level is even further from the site of foot-ground contact, the results from Study 1 suggest it is possible to derive valid and reliable gait characteristics from this attachment location. This may be aided by the gait event detection algorithm outlined earlier not being reliant on absolute threshold values for peak detection which, in turn, may reduce any potential limitation due to signal attenuation.

7.1.2 Study 2

As described in the opening paragraph of this chapter, gait characteristics, such as contact time and step frequency, are dependent on the accurate identification of IC and TO. Imprecision in the detection of these events will lead to misrepresentations of any subsequent calculated values. Therefore, it was important to determine the accuracy of the thoracic spine site to identify IC compared to a criterion and whether this translates into accurate and reliable derivations of selected running gait characteristics. A nuance of the gait event detection algorithm used in the current work is it detects IC first and then assigns TO to every previously identified IC event, as per the assumptions in the timing of these events described earlier. As a result, an IC event cannot be recorded without an accompanying TO. Given the number of these two events will be the same, only the proportion of IC events accurately detected from the thoracic spine were quantified. Inertial sensors were attached to the distal tibia and lumbar spine as criterions in Study 2 as these sites, per the results from Study 1, are valid for deriving running gait characteristics. The first major finding from Study 2 (Chapter 4) was that thoracic-worn IMUs, including those contained in GNSS units, can correctly identify IC (i.e., compared to IC detected at criterion sites) and they have a low false positive rate (i.e., it does not record an IC event when one has not been detected at criterion sites), as reflected by a nearly perfect F1 score (≥0.95). This level of accuracy was evident across a range of running speeds, including sprinting (7-8 $m \cdot s^{-1}$), and demonstrates thoracic-worn IMUs are valid for determining IC events. As outlined above, the focus of this study was to quantify the proportion of IC events detected by the thoracic spine compared to the tibia and lumbar spine sites (criterions). Study 2 did not apply any timing threshold from which an IC event from the thoracic spine could be correctly classified like previous work has done with other sites (e.g., distal tibia). It was clear from pilot work that a time delay exists where the peaks constituting IC occur in the accelerometer data between criterion sites (tibia and lumbar spine) and the thoracic spine. Assuming this time delay remains consistent for subsequent IC events, the derived outcome measures should not be impacted. However, it may be worthwhile quantifying the exact difference in timing (milliseconds) from which an IC event is detected by the thoracic spine compared to criterion assessments (e.g., force plate, tibia-mounted IMU etc.), therefore future work may consider this.

The other key findings from Study 2 were valid and reliable measures of contact time step time, flight time, step frequency, step length $vGRF_{peak}$ and K_{vert} were obtained from the thoracic spine site. Step time, step frequency and step length showed the highest level of agreement with the tibia site (≥87.5% of difference values falling within the limits of agreement) and were the most reproducible (CV ≤2.8% across all speeds). Step time, step frequency and step length rely only on IC for calculation (i.e., they do not require TO) which is easier to detect as peaks in the accelerometer signal representing IC are typically larger in magnitude than the peaks adjacent to them. The validity and reliability of step time, step frequency and step length are likely reflective of the thoracic spine site possessing high precision and recall for detecting IC events, as per the nearly perfect F1 score. Whilst the accuracy of the thoracic spine site to identify TO was not analysed in isolation (like it was for IC) due to reasons described earlier, it is possible that variation in the timing of TO detection may have had a small influence on some of the other metrics. For example, TO is identified from peaks in the anteroposterior accelerometer signal which can vary in size and number within the window for TO detection. This makes it more difficult for the algorithm to discern which peaks constitute the correct TO, so any variation in the timing through which TO was determined (e.g., first eligible peak versus second eligible peak) may have contributed to the slightly lower agreement (compared to step-related metrics) between the thoracic spine and criterion sites for contact time and flight time. Despite this, all K_{vert} (from which contact time and flight time underpin) values from the GNSS devices fell within the limits of agreement at 7-8 ms^{-1} when assessed against the tibia site. Considering this result alongside CV values of ~7% across all running speeds, Study 2 demonstrates that K_{vert} can be validly and reliably calculated from GNSS devices worn on the thoracic spine which is promising for detecting fatigue-related changes.

Another finding of note from the reliability analysis was the GNSS units outperformed (CV ≤6.2%) the thoracic-mounted Blue Trident IMUs for all spatiotemporal variables, and this may be explained by the differences in data processing post-testing between the respective devices. For example, data from the GNSS units were downloaded using specialised software provided by STATSports® which is not usually available to customers. When exporting data from this software, an IMU filter is applied in the background using a Madgwick Attitude and Heading Reference System (AHRS) algorithm which filters the data at a higher cut-off frequency (~50 Hz) and aligns the accelerometer axes to a true vertical and horizontal coordinate system. As a result, the accelerometer waveform appears smoother compared to that obtained from the Blue Trident IMU from which data was only downsampled and filtered at 20 Hz (see Section 4.4.3.3 for description). It is possible that this difference in data processing technique lead to an improved reproducibility of the gait event detection algorithm to identify IC and TO with data obtained from the GNSS devices. Although a CV of ~6% for some metrics may still be considered high by some researchers, it is important to consider this value in the context of any change (signal) observed. Should practitioners observe changes that exceed the CV (noise), the values derived from thoracic-mounted IMUs still lend themselves to being practically useful as the CV alone is less relevant than the signal relative to the noise.

The findings from Study 2 demonstrate that thoracic-worn IMUs are a viable option for analysing running gait in the field, including spatiotemporal variables (e.g., step time and step length), $vGRF_{peak}$ and K_{vert}. Given the results from Study 2 apply to IMUs contained in GNSS units, this provides the opportunity for both researchers and practitioners to quantify a variety of gait metrics from devices that are already being worn by team-sport athletes. This could be useful in quantifying changes that occur in running gait with fatigue without the requirement of using additional sensors at other sites, such as the foot or tibia.

7.1.3 Study 3

Fatigue has been shown to result in altered running gait mechanics, such as (but not limited to) longer contact times, shorter step lengths and reductions in K_{vert}. Studies demonstrating such changes in running gait have utilised lab-based measuring systems (e.g., motion capture, force plate etc.) or IMUs attached at sites other than the thoracic spine. Using the algorithmic approach from Study 2, it may be feasible to quantify fatigue-driven changes in gait from IMUs contained within GNSS units worn at the level of the thoracic spine. Study

3 (Chapter 5) assessed this pre-post an intervention consisting of 12 x 40 m repeated sprints where running gait was assessed using the same 40 m run-throughs and speeds as described in the published chapters for Studies 2 (Chapter 4) and 3 (Chapter 5). Although not described in Chapter 5, the total number of trials performed at a given speed post the 12 x 40 m intervention ranged from 2-4, with the maximum being 3 at 7-8 ms^{-1} (3 participants). Significant reductions in K_{vert} (-8.51 $kN{\cdot}m^{-1}$ [-13.9, -3.11]; $p = 0.007$) were evident in sprinting following the fatiguing protocol which is a consistent finding of previous work. Although reductions in K_{vert} may be explained by running at slower speeds, it is unlikely that this was a factor in the results of this study due to velocity being tightly regulated within a 1 $m{\cdot}s^{-1}$ window at each of the three sets speeds (3-4, 5-6 and 7-8 $m{\cdot}s^{-1}$) in both the pre and post fatigue protocols. This suggests that any changes seen in K_{vert} have occurred as a function of fatigue induced by the repeated sprint protocol rather than due to participants running more slowly. The reduction in K_{vert} observed in Study 3 presents opportunities for practitioners to quantify this metric from sensors already being worn in sport to monitor fatigue-related changes in running. The use of gait metrics, such as $K_{vert,}$ provides more granular information on running activity and the fatigue response than typical locomotor metrics. For example, commonly measured variables, such as distance and speed, may be maintained in the presence of fatigue and can be influenced by other match contextual factors, such as team and opposition tactics, playing position or scoreline. However, K_{vert} might be useful to provide insight into the discrete movement strategy changes during fatigue, including those that may precede, or manifest independently, from any potential change in distance and speed. Although commonly used countermovement jump (CMJ) tests also detect changes in movement strategy with fatigue, the potential to do this in running provides a more specific assessment as changes in gait characteristics could be monitored during normal training activities or within matches. In turn, this opens opportunities for

invisible monitoring and reduces the requirement of additional testing procedures (e.g., CMJ test).

7.1.4 Study 4

While Study 3 demonstrates that thoracic-worn IMUs are capable of detecting fatigue-related changes in running gait, as measured by reductions in K_{vert} during sprinting, a 12 x 40 m repeated sprint protocol only equates to a total running distance of 480 m. This is substantially less than the total distances covered in some field-based team-sports, such as soccer and Australian football, where players travel >10 km in a match interspersed with periods of high-intensity running. Therefore, a key focus of Study 4 was to assess the fatigue response in running from thoracic-mounted IMUs using a team-sport match simulation, specifically the $SAFT^{90}$. This protocol requires the performance of accelerations and decelerations, changes of direction and forwards and backwards running at a variety of speeds over a 20 m course. The $SAFT^{90}$ has been shown to produce similar internal physiological responses to match play and replicates the running volumes (~10 km) observed in competition. It has also been used extensively as a fatiguing protocol to determine the impact on risk factors associated with injury (e.g., hamstring peak torque and lower-limb joint angles and moments) and a variety of neuromuscular (e.g., voluntary muscle activation) and performance (e.g., CMJ, sprint times and isokinetic tests) responses. However, this thesis presents no statistical inferences for Study 4 due to the completion of this work being ongoing following the delays in data collection for Studies 2 and 3 caused by the COVID-19 pandemic. It would also be inappropriate to conduct any statical analysis with a sample size of only eight participants, which is approximately half the sample size required for this study to be complete. Data collection for Study 4 will continue following the submission of this thesis.

7.1.5 Personal Reflections

Not unexpectedly, the completion of this body of work was presented with numerous challenges. Although the respective studies were performed with strong scientific rigour and have several applied outcomes, it is still an opportunity to reflect on the challenges experienced and consider what may have been done differently. Due to the design of the experimental studies (Studies 2-4), one major hurdle was finding a suitable venue that could accommodate the space required to complete the various running protocols (i.e., 40 m run-throughs, 40 m repeated sprint protocol and the SAFT[90]). In addition, it was decided that an artificial turf venue would be most suitable to ensure consistency of surface between testing sessions. However, this limited the potential venue options, and we were forced to use two different locations for testing, one for strength and power testing and another ~20-30 minutes' drive away for the running assessment. Consequently, this added a layer of logistical complexity for participants as they were required to travel to multiple sites over the course of the study duration. Although COVID-19 delays contributed the most to Study 4's incompletion (to date), it is very likely that the requirement to attend two different testing sites on multiple occasions was partly responsible for the challenges with recruiting participants for this final study. Had we foreseen the uptake for participation in Study 4 being an issue prior to recruitment commencing, steps would have been taken to revise the design of the study which may have included using a different surface (e.g., natural grass) so other venues that were closer to our main testing site could be used to reduce the travel burden on participants. However, Study 4 will continue, and the aforementioned challenges will be overcome to ensure this important work gets completed. Study 4 has the potential to be another crucial step towards the ability to analyse running gait characteristics within real matches from thoracic-mounted IMUs, and it is imperative that this work is seen through so this is an option for practitioners in the future.

7.1.6 Key Outcomes

This body of work presents several key outcomes that can be used to inform the analysis of running gait in team-sports. These include:

- Validity and reliability of running gait measures from IMUs is not conditional solely on placement site. Instead, determination of running gait variables is more dependent on the method by which inertial data is extracted, processed and analysed.
- Thoracic-mounted IMUs, including those contained in GNSS units, are capable of detecting IC with a nearly perfect level of precision and recall during running at a variety of speeds.
- Thoracic-mounted IMUs, including those contained in GNSS units, can be used to calculate valid and reliable measures of contact time, step time, flight time, step frequency, step length, $vGRF_{peak}$ and K_{vert} across a variety of running speeds.
- The IMUs contained in GNSS units can detect fatigue-related changes in running gait as measured by reductions in K_{vert} during sprinting (7-8 $m{\cdot}s^{-1}$) following 12 x 40 m repeated sprints.

7.2 Limitations

7.2.1 Subject Anthropometry

As outlined in their respective chapters, Studies 2 (Section 4.6) and 3 (Section 5.6) used participants that had a similar body mass. It is unclear whether the results presented in this thesis would be the same if the participants were more varied in their anthropometry. Although signal attenuation was not a major issue for detecting IC and TO from the thoracic spine level in the current work, it is possible that participant anthropometry, such as being taller or heavier, may change the appearance of the accelerometer waveform which, in turn, could affect event detection. For example, larger amounts of body tissue may lead to a more attenuated accelerometer signal which could result in less precision to detect TO events. Conversely, event detection may be improved in those who are shorter in stature as the thoracic level is closer to the foot-ground interface than those who are taller. Future work may consider recruiting participants with a more varied anthropometric profile to better understand the impact of body mass and height on the accuracy of event detection.

7.2.2 Requirement of Steady State Period

The experimental studies outlined in this thesis utilised a 20 m section of constant speed straight-line running to analyse gait. However, not all running in sport training and competition is performed in a linear fashion and often involves accelerations, decelerations, changes of direction and curvilinear running. Whether it is possible to derive valid and reliable gait characteristics from non-linear relatively constant paced running is unclear from the current work and this may be worthy of further investigation. However, although practitioners are currently limited to analysing sections of constant speed running (albeit relatively short, i.e., 20 m) to calculate metrics of interest (e.g., K_{vert}) from thoracic-mounted IMUs, team-sport activity profiles demonstrate numerous periods of ~20 m straight-line running which are suitable for the analysis of running gait. (see Section 7.3.1 for an explanation on how this may be achieved).

7.2.3 Running Surface

Another potential limitation of the current work is the type of surface used for the investigations. All experimental studies were completed on an artificial grass pitch to ensure consistency in the surface across multiple testing sessions. Although artificial grass surfaces are used in some team-sports, many others are played on natural grass only (e.g., Australian football) or on hard surfaces, such as a sprung floor (e.g., basketball). It is therefore unclear whether the results presented in this thesis directly translate to running on different surfaces. It is possible that the gravitational acceleration values would be dampened on natural grass and heightened on harder surfaces compared to artificial grass, which has the potential to impact the accuracy of event (IC and TO) detection. However, as the algorithm used in the current project is not reliant on threshold values (e.g., in g units) for accelerometer peak detection, it is hypothesised that the results for artificial grass would also be observed had testing been conducted on different surfaces.

7.2.4 Footwear

All participants wore their usual athletic shoes during experimental testing, and this may be a limitation as field-based athletes wear cleats during training and matches. Studs or cleats on the soles of sports shoes protrude into the ground when running on natural and artificial grass surfaces, but it is unclear from this work what the impact would be on the accelerometer waveform.

7.2.5 Fastest Velocity Band

The current work analysed running gait at three different velocities which were 3-4, 5-6 and 7-8 $m \cdot s^{-1}$. The two slower speeds were selected based on previous work, while 7-8 $m \cdot s^{-1}$ was chosen as pilot testing revealed this was an attainable speed for many amateur team-sport athletes and recreational runners. Although an average velocity of 7-8 $m \cdot s^{-1}$ over 20 m was a challenging speed for some participants to achieve, it likely does not represent the maximal running velocity for many high-performance athletes. Therefore, whether the results observed at 7-8 $m \cdot s^{-1}$ in Study 2 would translate to faster speeds (e.g., >8 $m \cdot s^{-1}$) is unclear. It is possible that the accuracy of detecting IC events from the thoracic spine site would decrease at faster speeds. As Study 2 showed, the F1 scores declined from running at 3-4 $m \cdot s^{-1}$ (0.99) to 7-8 $m \cdot s^{-1}$ (0.95) when using GNSS-embedded IMUs. However, it should be acknowledged that the thoracic spine site still possessed a high level of precision and recall in detecting IC at 7-8 $m \cdot s^{-1}$, and this is potentially promising for accurately identifying these events at faster speeds. As Study 3 demonstrated, there appears to be greater sensitivity for detection of fatigue-induced changes at high speed. Therefore, greater differences due to fatigue may be evident at speeds faster than the 8 $m \cdot s^{-1}$ used in this study.

7.2.6 Left-Right Values

As the thoracic spine placement itself was the focus of this thesis, the current work did not explore values for left and right sides independently. Many studies using IMUs for gait analysis, such as those included in the systematic review in Study 1, have reported values that are based on the average of both left and right sides, and this thesis followed the same approach. Although this has been a common way to present spatiotemporal gait data and K_{vert} from IMUs, particularly from those worn on the trunk, it is a limitation of the research in this area. Having the ability to derive left and right sides independently from a single sensor, such as one worn on the thoracic spine, would increase the practical usefulness of IMUs for analysing running gait in the field. This could be achieved by leveraging the mediolateral accelerometer data – as has occurred in previous work, including that from which the algorithm used in this thesis was based – to distinguish left and right foot-ground contacts by examining the direction (positive or negative) of the peaks. The gait characteristics analysed throughout this thesis could then be calculated for independent sides which may be useful during return from lower limb injury where values from injured versus non-injured limbs may be compared to progress an athlete through rehabilitation. There is also a potential role for assessing changes in symmetry on a regular basis as a means of early identification of maladaptation to training and competition. Section 7.4.2 expands on how this may be possible in future work.

7.2.7 Lack of Fatigue-Related Changes in Gait

The results from Study 3 showed only K_{vert} resulted in a statistically significant change from pre to post 12 x 40 m sprints, and this was despite the mean ± SD values of other variables (e.g., contact time) following a response that is typically seen in fatigue (i.e., longer durations). It should be acknowledged that the lack of fatigue-induced changes to gait as measured by thoracic-mounted IMUs does not preclude the existence of neuromuscular fatigue (NMF) that may have been detectable with laboratory-based techniques. For example, central and/or peripheral fatigue may have been detected post the fatigue interventions with the use of twitch interpolation from magnetic or electrical stimulation. Although electrical or magnetic stimulation provides a direct measure of NMF, the premise of this work was to provide a more practical field-based alternative to assess fatigue, specifically using technology that already exists in team-sport.

7.2.8 GNSS Device Placement

Tightly fitted vests are typically worn during team-sport training and matches to house GNSS devices. However, in some cases, these devices are housed in small pouches that are sewn directly into the back of the playing tops worn by athletes, as is common in Australian football. Tightly fitted vests were used in this thesis, and it was ensured that they were fitted correctly to each individual to minimise any extraneous movement that might have impacted gait event detection. Therefore, it cannot be guaranteed that the validity and reliability results observed in Study 2 translate to situations where GNSS devices are not secured in vests but are instead fitted in playing tops. As IC is determined from peaks in inertial data, it is possible that extraneous peaks caused by poorly fitted clothing may reduce the ability of the algorithm to discern which ones constitute a TO event, and this may result in miscalculations of variables like contact time and flight time. However, it is likely the peaks constituting IC events would still be larger than anything occurring because of a loose fit, meaning step time, step frequency and step length variables should still be measured accurately.

7.2.9 Participant Demographics

Out of the 16 participants who participated in Studies 2 and 3, only six were female. Other work has shown males and females manipulate their running strategy differently when fatigued, so it is possible this was also the case in the current work. However, analysing males and females independently was not possible due to only 16 participants being recruited in total and the uneven numbers between sexes. As such, it is unclear from this work whether the magnitude of change in contact time, step frequency, K_{vert} etc. differs between sexes.

7.2.10 Match Simulation

Although the $SAFT^{90}$ has been validated from both a physiological demand and activity profile perspective, it remains a shuttle run test that does not contain other technical skill actions common in team-sport. As such, the $SAFT^{90}$ does not mimic team-sport matches exactly, so it is unclear whether the fatigue response in running gait would be different if it were assessed from competitive games. This provides an avenue for further exploration of the changes in running gait during and following competitive (instead of simulated) match play (see Section 7.4.2).

7.3 Practical Applications

7.3.1 Invisible Monitoring and Match Analysis

This thesis demonstrates practitioners can analyse running gait features from IMU sensors housed within GNSS units that are already being worn by team-sport athletes. This provides opportunities for invisible monitoring where gait characteristics can be measured across a large squad of athletes simultaneously during normal training or match activities. Rather than using timing gates (as used in the current work), practitioners may leverage the GNSS data as a practically applicable solution to extract 20-30 m periods of constant velocity running. This could be from standardised straight-line runs over ~20-40 m in training (e.g. during a warm-up) – like the ones used in the experimental studies of this thesis – where the gait event detection algorithm outlined here could then be applied to the corresponding accelerometer data to monitor running fatigue. Such data could be used to assess the need for recovery interventions and modifying ensuing post-match training loads. This type of approach may also extend to training or match analysis where data may be used to plan subsequent rotation strategies across a match to manage athlete fatigue. As mentioned in Section 7.2.2, although competitive match play presents a more chaotic environment to analyse running gait than the experimental conditions of this thesis, there are numerous situations in matches where athletes run at a constant velocity over ~20 m (e.g., running to and from interchange bench in Australian football or running to position between game stoppages), and these periods can be extracted from the raw GNSS file (easily obtainable from GNSS software providers) and then the corresponding accelerometer data can be analysed as per the approach demonstrated in this thesis.

7.3.2 Injury Rehabilitation

Data on running gait characteristics may also be practically useful during injury rehabilitation. Practitioners may use values of $vGRF_{peak}$, for example, from GNSS-embedded accelerometers as a surrogate measure for lower limb loading during return-to-running programs. These data may be beneficial for progressing an athlete through rehabilitation, such as from anterior cruciate ligament reconstruction, by comparing pre- versus post-injury values (including asymmetry) without the need for additional sensors or lab-based testing. Lastly, it has been highlighted throughout this thesis that using thoracic-worn IMUs to analyse running gait can provide a detailed understanding of the discrete movement patterns that underpin changes in athlete movement (running) strategy. This could be beneficial for assessing changes in running mechanics post-concussion where an understanding of an athlete's usual gait pattern may provide a useful baseline for ensuring the restoration of normal gait mechanics following concussion.

7.4 Future Research Directions

7.4.1 Running on Different Surfaces

As testing in the current work was performed solely on artificial grass, future work should examine the differences in the derived values during running on natural grass and other artificial surfaces (e.g., sprung wooden floor). As noted in Section 7.2.3, some sports (e.g., Australian football) are only played on natural grass and others on hard surfaces (e.g., basketball), and this work would inform subsequent studies assessing the fatigue-related changes in running gait within competitive matches.

7.4.2 Running Gait Fatigue During Competition

Following the work presented in this thesis, a potential progression from Study 4 would be to assess changes in running gait during competitive (instead of simulated) team-sport match play. Team-sports, such as Australian football and soccer, permit players to wear GNSS devices during competition but not boot- or tibia-mounted sensors. Future work may identify sections of running from positional data from GNSS, as described in Section 7.3.1, to analyse changes in running gait during competitive match play. This could be applied to existing and future data sets to provide further insight into the fatigue-related changes in running gait that may be heightened due to the higher intensity of competition.

7.4.3 Analysis of Asymmetry

Analysis of left-right asymmetry is another avenue for further research which has the potential to extend the practical usefulness of applying the gait event detection algorithm described in this work to thoracic spine accelerometer data. Having the ability to discriminate left and right sides from thoracic-mounted IMUs would provide even greater detail when examining an athlete's gait pattern, and this may be possible by integrating mediolateral accelerometer data to distinguish the side in which a gait event occurs. Future work establishing the validity and reliability of such an approach to quantify left and right values for the gait characteristics presented throughout this thesis would therefore be worthwhile. This information could be valuable for injury rehabilitation specialists by informing strategies aimed at returning an athlete to running activity following lower limb injury or as useful data for gait retraining.

7.4.4 Acceleration and Deceleration Strategies

Finally, Studies 3 and 4 focused on identifying changes in movement strategy that occur in constant speed running, but many team-sports also comprise a high frequency of accelerations and decelerations. Other work has shown athletes display changes in their movement strategy when accelerating and decelerating with fatigue, and this may also be measurable from thoracic-mounted IMUs. It is possible that changes in acceleration and deceleration strategy could be greater than that of constant speed running. However, it is unclear whether the algorithmic approach outlined here for quantifying IC and TO would be suitable due to the increased forward tilt of the trunk in early acceleration and the dramatic changes in velocity that occur when accelerating and decelerating. However, future work could incorporate other sensors that are contained in GNSS units, such as gyroscopes, to build on the current algorithm and develop a method for quantifying gait characteristics during these phases of running.

8 Chapter 8: Extended Methodology

8.1 Deriving Gait Characteristics

Section 8.1 describes the methodology for deriving gait characteristics from inertial measurement units (IMUs), including those worn the thoracic spine, in greater detail than that outlined in the published work. The steps described in this section formed the basis for analysing running gait in experimental studies 2, 3 and 4.

8.1.1 Configuration of IMUs

During data collection for Study 2 (Chapter 4), participants were equipped with two global navigation satellite system (GNSS) devices (Apex, STATSports®, Newry, Northern Ireland; 84 x 43 x 20 mm; 72 grams) which contained a triaxial accelerometer (ADXL375; 100 Hz; ±200 g), gyroscope (100 Hz; ±2000 deg·s^{-1}) and magnetometer (10 Hz; ±16 G). One Apex device was secured to the skin using Hypafix retention tape (Hypafix®, BSN medical, Hamburg, Germany; see Figure 8.1) and another housed in a tightly fitted custom vest designed by STATSports® directly over the top. Participants also wore four IMUs (Blue Trident, IMeasureU, Auckland, New Zealand; 42 x 27 x 11 mm; 9.5 grams). Each IMU was attached to participants as depicted in Figure 8.1 where manufacturer designed straps contained the tibia IMUs and the same Hypafix tape secured those on the lumbar spine and thoracic spine. In Studies 3 (Chapter 5) and 4 (Chapter 6), participants only wore one GNSS device in a vest.

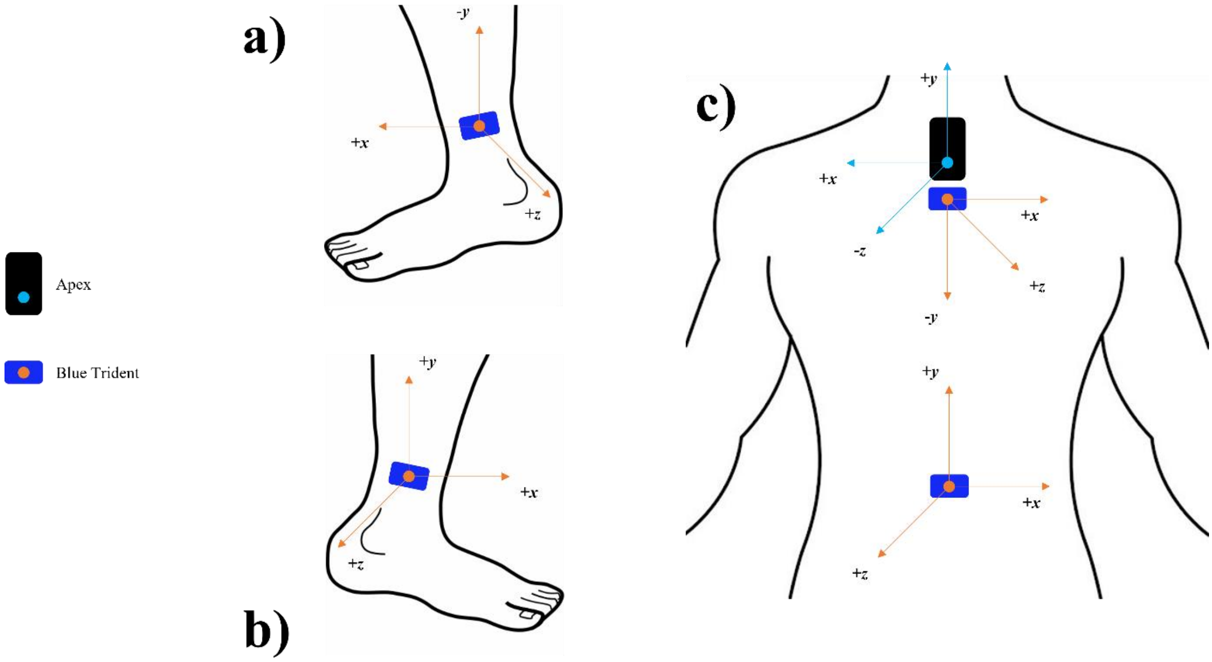

Figure 8.1. Orientation of accelerometer vectors for right tibia **(a),** left tibia **(b)** and lumbar and thoracic spine **(c)**. One Apex unit was secured direct to the skin, while another was worn over the top in a tightly fitted vest. The positive and negative directions of the *y* axis were different for each tibia **(a and b)** due to the way the Blue Trident sensors were attached on the medial aspect of the lower leg. The *x* axes of the Apex accelerometers were realigned during data processing so positive pointed right **(c)**. For the Blue Trident sensors, *y* and *z* axes of the right tibia **(a)** were flipped so positive was to the superior and right, respectively, and the *z* axes of the lumbar and thoracic spine were rotated so positive pointed anteriorly **(c)**. This was done to match the vector systems recognised by the algorithm described by the original authors [17].

Each Apex device was turned on manually before attachment, whereas the Blue Trident IMUs were configured within Nexus software (version 2.12.0, VICON, Oxford, UK) once they were secured to the participant. Each Blue Trident IMU was connected to Nexus via Bluetooth®, represented by the green play button next to each IMU (see Figure 8.2), and then the high-g capture rate was selected to collect accelerometer data at 1600 Hz and ±200 g. This is shown as the *Output Preset* in Figure 8.3. Live data streaming in Nexus was not of interest during testing, therefore the lowest stream rate (30 Hz) was selected (see Figure 8.3).

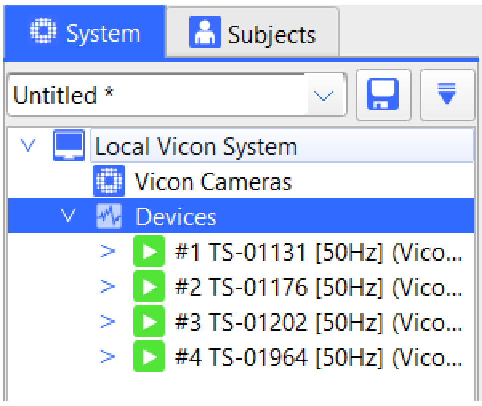

Figure 8.2. Bluetooth® connection of Blue Trident IMUs with Nexus.

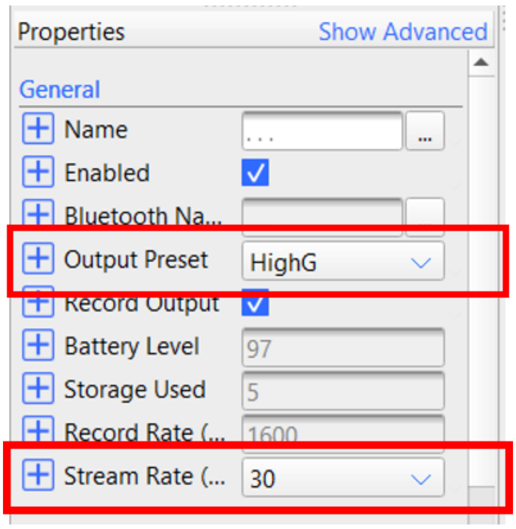

Figure 8.3. High-g capture rate and 30 Hz stream rate selected in Nexus.

8.1.2 Running Protocol

Participants completed 40 m run-throughs at 3-4, 5-6 and 7-8 m·s^{-1} where electronic timing gates (Swift DUO™, Swift Performance, Brisbane, Australia) were positioned at -5 m from the start line, 20 and 40 m (see Figure 8.4). Each run-through began with participants standing behind the gate positioned 5 m behind the start line which was used to synchronise the accelerometer data with the timing system (see Section 8.1.3 for description and Figure 8.4). Following, participants walked around the sync gate to the start line (0 m) and then commenced the run-through by accelerating to the target velocity prior to reaching the 20 m gate and then maintaining the required speed between 20 and 40 m (see Figure 8.4). Participants were instructed to avoid slowing down until they had fully passed the 40 m gate. A walk back recovery was provided to participants before attempting the next run-through where two trials were completed at each speed (3-4, 5-6 and 7-8 m·s^{-1}) in a counterbalanced order. Trials were repeated if they fell outside of the desired velocity range by more than 0.1 m·s^{-1}.

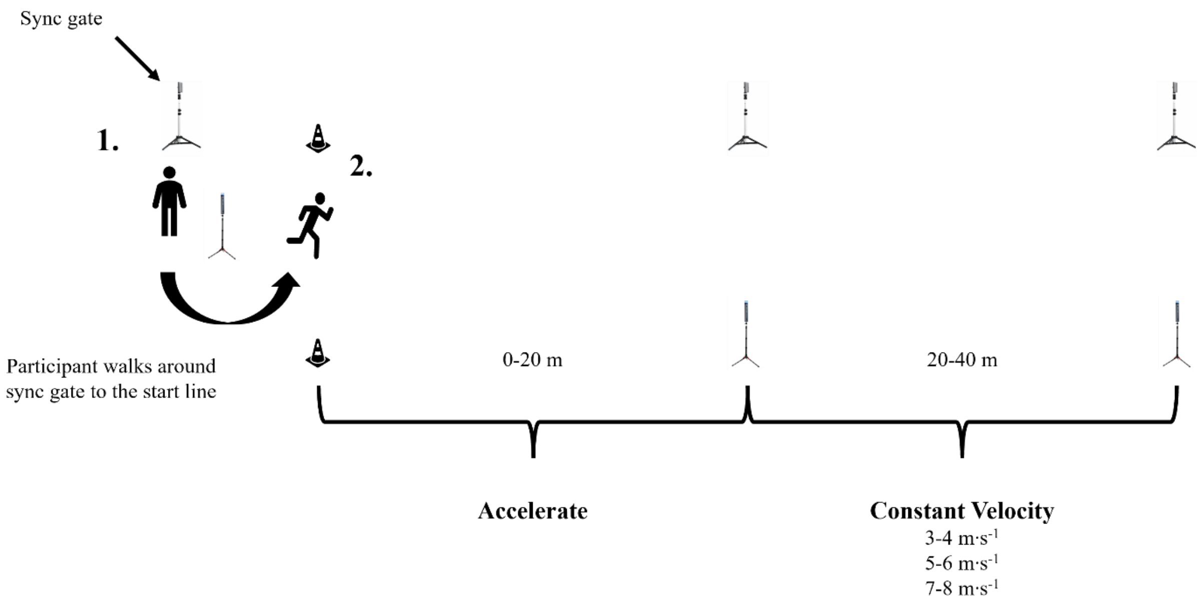

Figure 8.4. Schematic representation of the 40 m run-throughs.

8.1.3 Data Recording

Apex accelerometer data were recorded continuously onboard the device throughout the entire testing session, whereas Blue Trident data were collected for each individual trial by manually starting and stopping the recording in Nexus before and after each participant completed their 40 m run-through. Once recording in Nexus started, participants were instructed to perform a synchronisation event that constituted stomping their right leg and swinging their arm through another timing gate positioned 5 m behind the start line. This elicited a spike in the vertical accelerometer signal of the right tibia Blue Trident IMU that coincided with the start of the recording of the timing gate system (see Figure 8.5). As participants stomped their right leg, a researcher simultaneously tapped the thoracic-mounted Apex devices to evoke another identifiable event for synchronisation with the Blue Trident IMUs and timing system. In Studies 3 (Chapter 5) and 4 (Chapter 6) where only a single Apex device was worn, participants were not required to stomp their right leg. Once testing was complete, raw triaxial accelerometer data were downloaded and exported as a CSV file from STATSports® Apex Unified Raw Data Parser software and Nexus, respectively.

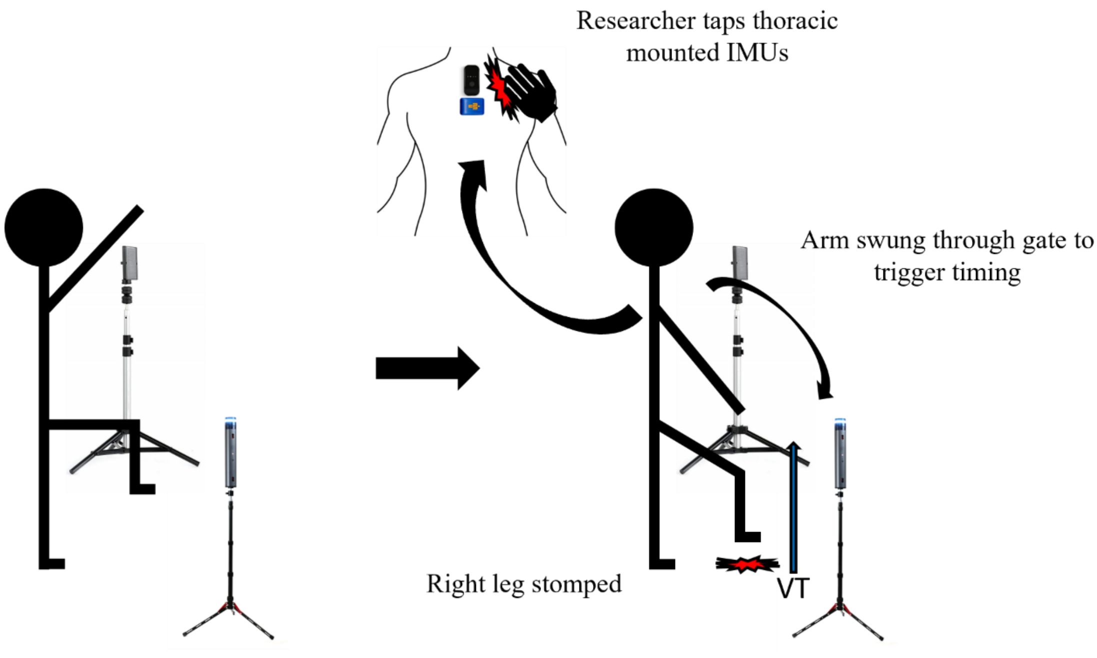

Figure 8.5. Illustration of synchronisation event at the start of each trial.

8.1.3.1 *Parser Software*

Through the support of STATSports®, Apex Unified Raw Data Parser software (version 4.6.0.184) was obtained to download and export raw data recorded from the Apex devices. Data were downloaded at 100 Hz (see Figure 8.6), where each file contained all trials completed by the respective participant. Apex data were aligned with true vertical and horizontal coordinate systems which was computed by an internal Kalman filter and filtered at ~50 Hz using an Attitude and Heading Reference System (AHRS) algorithm [172] (see Figure 8.6).

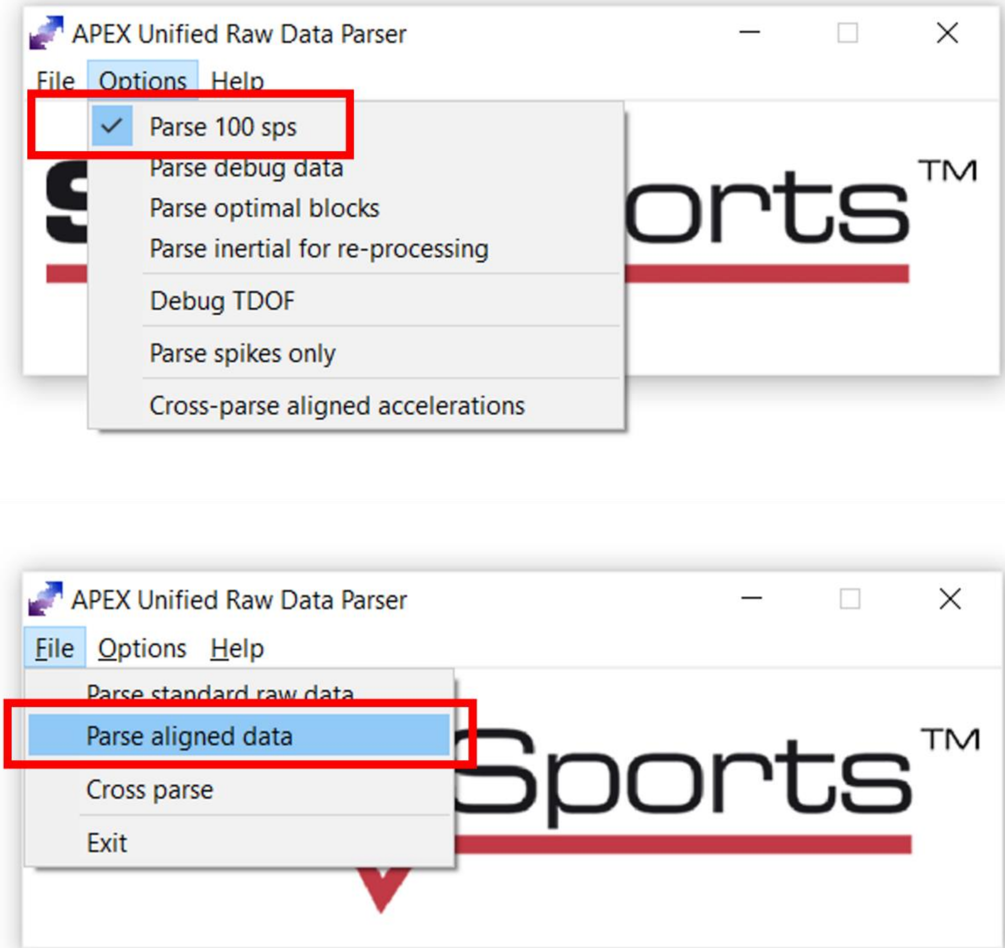

Figure 8.6. Apex data was aligned and parsed at 100 Hz.

8.1.4 Data Synchronisation

A custom MATLAB script (version 9.12.0.1956245, R2022a, MathWorks, Inc., Natick, MA, USA) was used to trim the accelerometer files with reference to the synchronisation events detailed in Section 8.1.3. The MATLAB code in Figure 8.7 was used to find the maximum vertical acceleration value (*val*) and the associated row number (*idx*) from the right tibia Blue Trident IMU data between a predefined subsection of the data representing the initial moments of the trial recording (i.e., from the start of recording in Nexus to briefly following execution of the synchronisation procedure).

```
69      %% Identify peak to sync with start of timing system.
70      % Get peak (at right ankle).
71 -    [val, idx] = max(ra.Ay(1:16519));
72
73      % Trim data up to peak - first frame (0 s).
74 -    ra(1:idx-1, :) = [];
75 -    la(1:idx-1, :) = [];
76 -    ls(1:idx-1, :) = [];
77 -    ts(1:idx-1, :) = [];
78
```

Figure 8.7. MATLAB code used to synchronise Blue Trident IMU data with the timing gate system. Synchronisation stomp was obtained by finding the row number (*idx*) corresponding to the maximum vertical acceleration value (*val*) within a subsection of the data (line 71). All data leading up to the synchronisation stomp was then deleted from each IMU file (lines 74-77).

A similar procedure was used for the Apex data, where a single trial was extracted from the entire data capture (noting the Apex accelerometer recorded continuously; see Figure 8.8) before finding the maximum vertical acceleration value (*val*) and the associated row number (*idx*), as per the method for the Blue Trident IMU data.

```
31    %% Extract individual trials using plot.
32    trial = acceldata(52741:54709, :); % Enter row numbers either side of trial data.
33
34    figure
35    stackedplot(trial);
36
37    %% Identify peak to sync with start of timing system.
38    [val, idx] = max(trial.Ay(1:400)); % Find maximum in vertical accleration data.
39
40
41    % Trim data up to peak - first frame (0 s).
42    trial(1:idx-1, :) = [];
43
```

Figure 8.8. MATLAB code used to synchronise the Apex accelerometer data with the timing gate system. Individual trials were extracted from the entire data capture (line 32) before the synchronisation tap of the Apex device was obtained by finding the row number (*idx*) corresponding to the maximum vertical acceleration value (*val*) within a subsection of the data (line 38). All data leading up to the synchronisation tap was then deleted (lines 42).

All data points up until the row number that represented the synchronisation event (*idx*) were then deleted (see Figure 8.7 and Figure 8.8). For example, if the maximum vertical acceleration value occurred in row number 11535, rows 1 to 11534 were removed from the data. The first row in the trimmed data was then set as frame number one as this was when the timing gate system started recording. Figure 8.9 shows the right tibia Blue Trident vertical accelerometer data following removal of all data up until the participant stomping their right leg.

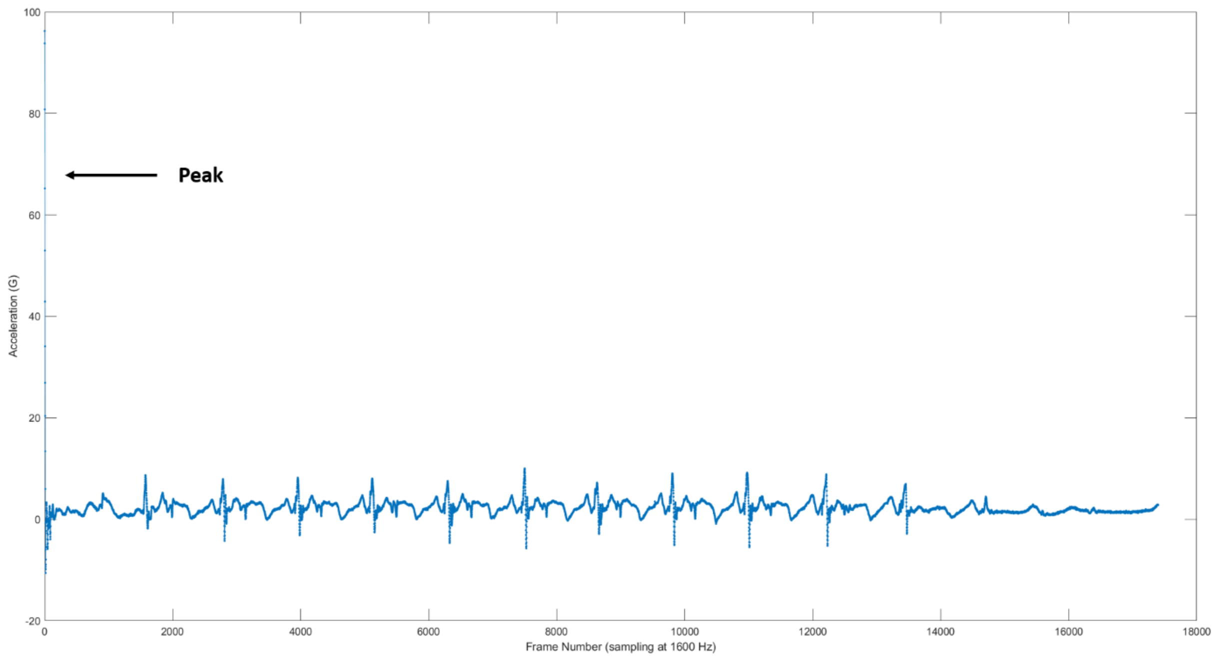

Figure 8.9. Vertical accelerometer data from the right tibia. Peak occurring at frame number 1 represents the participant stomping their right leg and simultaneously triggering the first timing gate (-5 m) by swinging their right arm through the beam. All accelerometer data up until that point was removed.

8.1.5 Data Extraction

Data used for analysis was extracted between 20 and 40 m marks of each trial (constant velocity zone; see Figure 8.4). Once participants triggered the first timing gate (-5 m) by swinging their right arm through the beam (see Figure 8.5), the time (s) it took them to pass through the 20 and 40 m gates were used as reference for trimming the remaining accelerometer data. The example MATLAB code shown in Figure 8.10 converted time in seconds for 20 and 40 m splits to a frame number by multiplying by the sample rate of the device (1600 Hz for the Blue Trident IMUs and 100 Hz for the Apex units). All rows (frames) from the start of the trial to crossing 20 m, and from crossing 40 m to the end of the trial were then trimmed from the data (see Figure 8.10).

```
100     %% Trim data either side of 20 and 40 m.
101     % Time taken (s) to 20 m.
102     gate20 = 10.366; % Manual input.
103
104     % Time taken (s) to 40 m.
105     gate40 = 15.373; % Manual input.
106
107     % Frames (rows) to trim.
108     gate20_frames = round(gate20 * 1600); % 1 s = SAMPLE frames.
109     gate40_frames = round(gate40 * 1600);
110
111     % Trim data between 20 and 40 m.
112     ra_trim = ra_full(gate20_frames:gate40_frames, :);
113     la_trim = la_full(gate20_frames:gate40_frames, :);
114     ls_trim = ls_full(gate20_frames:gate40_frames, :);
115     ts_trim = ts_full(gate20_frames:gate40_frames, :);
116
```

Figure 8.10. MATLAB code used to extract data between the 20-40 m section of constant velocity running. Lines 102 and 105 represent the split times for the 40 m run-throughs. These were converted to a frame number (lines 108-109) which were used as references points for deleting all data points occurring outside of the 20-40 m section.

In the example in Figure 8.10, where a participant took 10.4 s from triggering the synchronisation gate to breaking the beam at 20 m (10.4 x 1600 = 16640 frames) and 15.4 s to cross 40 m (15.4 x 1600 = 24640 frames), only accelerometer data occurring between rows 16640 and 24640 were extracted and used for analysis. The result of this process is visualised in Figure 8.11 for the Blue Trident data and Figure 8.12 for the Apex data.

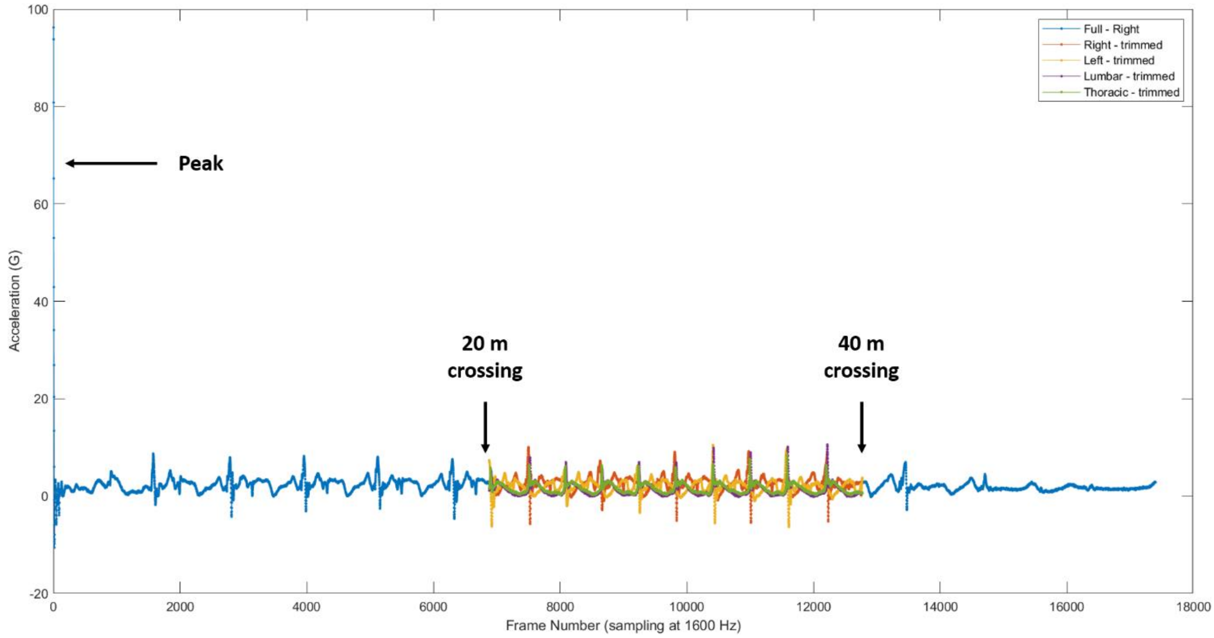

Figure 8.11. Vertical accelerometer data from Blue Trident IMUs. Blue line (right tibia) shows entire trial. Orange (right tibia), yellow (left tibia), purple (lumbar spine) and green (thoracic spine) lines show the extracted sections for each site.

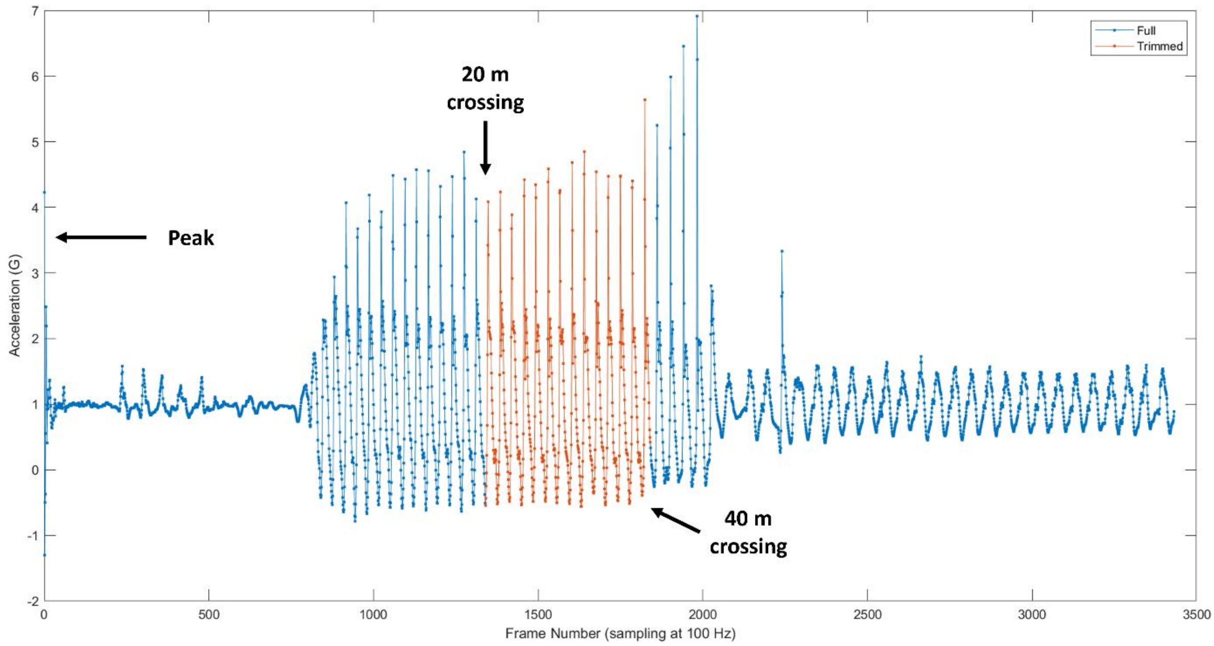

Figure 8.12. Vertical accelerometer data for one Apex unit from the thoracic spine, where the entire trial (blue line) is overlayed with the trimmed section (orange line) used for analysis.

8.1.6 Combining Tibia Data

Once the accelerometer files were trimmed so only the 20-40 m section remained, left and right tibia data were combined into a single file. This allowed the tibia to be treated as a single site, identical to the lumbar spine and thoracic spine sites. Figure 8.13 shows the vertical (*y*) accelerometer waveform for the left and right tibia prior to merging the two files.

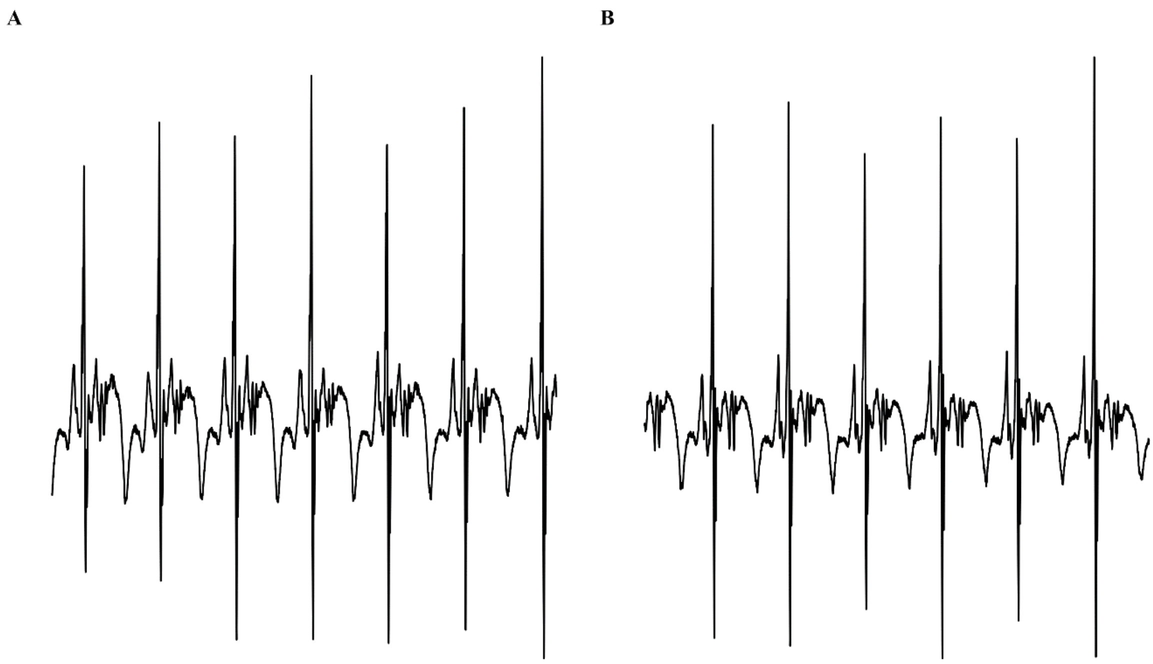

Figure 8.13. Vertical (*y*) accelerometer waveform for left **(A)** and right **(B)** tibia. Data is from trimmed 20-40 m section at a running speed of 3-4 $m \cdot s^{-1}$.

Individual values between left and right sides were compared so only the highest values of the left versus right data remained to form the merged tibia file, and this was repeated for each accelerometer axis (*x, y* and *z*). For example, if the vertical acceleration value for the left tibia was 22.8 g and the right was 1.5 g, the value for the left was retained in the merged file. This approach was used so the magnitude of the peaks representing gait events were maintained in the accelerometer waveform. This was particularly important for the vertical (*y*) accelerometer waveform as this was the predominant axis used for detecting IC and TO from the tibia [17].

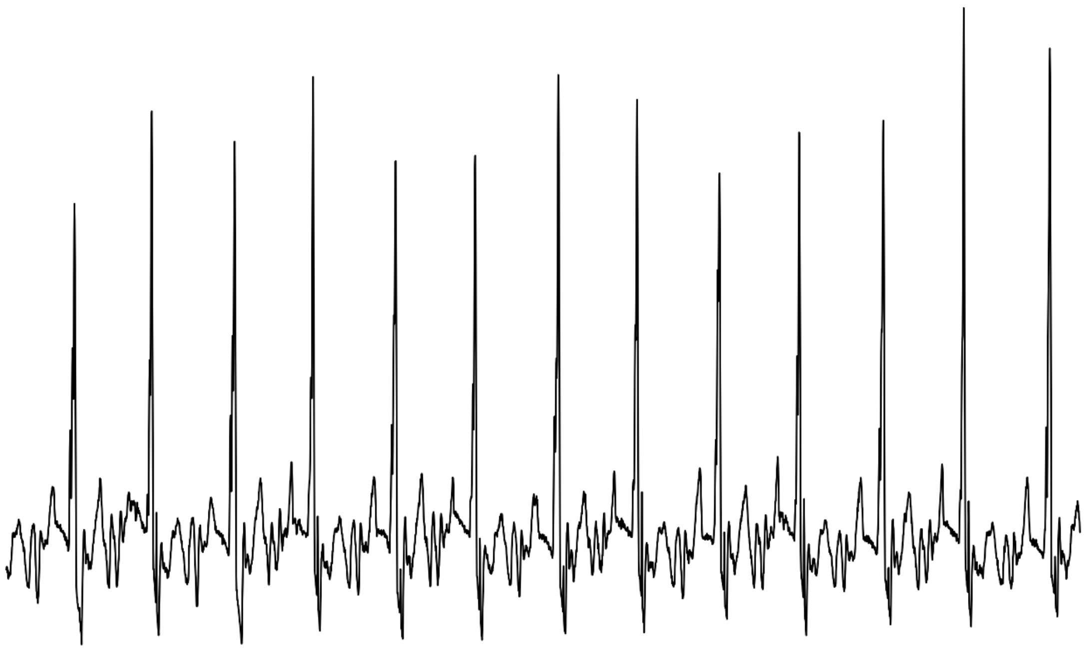

Figure 8.14. Result of the vertical (*y*) accelerometer waveform following the merging of left and right tibia data. Maintaining the maximum values between left versus right sides ensures the magnitude of the peaks are not attenuated.

8.1.7 Vector Realignment and Downsampling

Some accelerometer vectors were realigned from that shown in Figure 8.1 to match the vector systems recognised by the gait event detection algorithm [17]. Realignment was achieved by multiplying each data point by -1. The *y* (vertical) and *z* (mediolateral) axes of the right tibia Blue Trident data were corrected so positive was pointing superiorly and to the right, respectively. The *z* axis (anteroposterior) of the lumbar spine and thoracic spine Blue Trident data were rotated so positive pointed anteriorly, while the *x* (mediolateral) axis of the Apex data was realigned so positive pointed right.

Once the accelerometer vectors were realigned, the Blue Trident data were downsampled from 1600 to 100 Hz to match the sample rate of data collected from the Apex units. This was achieved by first creating a custom moving average function (*MovingAverage4IMU*; see Figure 8.15) in MATLAB which was designed to average consecutive rows of 16 data points within each accelerometer signal (*x*, *y* and *z*) along the length of the file. A code snippet of this custom function is detailed in Figure 8.15.

```
1
2  function [MASignal] = MovingAverage4IMU(sig, startt, endd)
3
4  len1 = length(sig);
5  avgSignal = [];
6
7  for i = 1:len1 / 16
8
9          % Make average.
10         sig1 = sum(sig(startt:endd)) / length(sig(startt:endd));
11
12         % Save average value.
13         avgSignal = [avgSignal sig1];
14
15         % Shift the position.
16         startt = endd + 1;
17         endd = endd + 16;
18 end
19
20 MASignal = avgSignal;
21
22 end
```

Figure 8.15. MATLAB code used to downsample the Blue Trident IMU data from 1600 to 100 Hz. Consecutive rows of 16 data points were averaged along the length of the respective IMU files (lines 7-18).

The *MovingAverage4IMU* function was then applied to *x*, *y* and *z* axes within each Blue Trident data file, as outlined in the code in Figure 8.16. Essentially, each accelerometer axis was downsampled individually and then joined back together to create a new data frame containing all three axes that were later processed through the gait event detection algorithm (see Figure 8.16).

```
31    tib = table2array(tib);
32    lumbar = table2array(lumbar);
33    thoracic = table2array(thoracic);
34
35    tib_Az = MovingAverage4IMU(tib(:, 2), 1, 16)';
36    tib_Ax = MovingAverage4IMU(tib(:, 3), 1, 16)';
37    tib_Ay = MovingAverage4IMU(tib(:, 4), 1, 16)';
38    tib_frame = (1:length(tib_Az))';
39    tib = [tib_frame, tib_Az, tib_Ax, tib_Ay];
40
41    lumbar_Ax = MovingAverage4IMU(lumbar(:, 2), 1, 16)';
42    lumbar_Az = MovingAverage4IMU(lumbar(:, 3), 1, 16)';
43    lumbar_Ay = MovingAverage4IMU(lumbar(:, 4), 1, 16)';
44    lumbar_frame = (1:length(lumbar_Az))';
45    lumbar = [lumbar_frame, lumbar_Az, lumbar_Ax, lumbar_Ay];
46
47    thoracic_Ax = MovingAverage4IMU(thoracic(:, 2), 1, 16)';
48    thoracic_Az = MovingAverage4IMU(thoracic(:, 3), 1, 16)';
49    thoracic_Ay = MovingAverage4IMU(thoracic(:, 4), 1, 16)';
50    thoracic_frame = (1:length(thoracic_Az))';
51    thoracic = [thoracic_frame, thoracic_Az, thoracic_Ax, thoracic_Ay];
```

Figure 8.16. MATLAB code used to apply a custom downsampling function to each individual accelerometer axis (*x*, *y* and *z*) for the Blue Trident data. Lines 35-37 show an example of this for the tibia site. Once individual accelerometer axes were downsampled, they were joined back together in a new data frame (line 39).

8.1.8 Data Filtering

A fourth order zero-lag Butterworth filter with a cut-off of 20 Hz was applied to data collected from the Blue Trident IMUs. This cut-off was based on prior recommendations and an inspection of the data that showed the peaks in the accelerometer signals were not too heavily attenuated [110]. No additional filter to that described in Section 8.1.3.1 was applied to the Apex accelerometer data.

8.1.9 Algorithm

Trimmed, realigned and filtered accelerometer data were processed through two previously validated gait event detection algorithms in MATLAB [17]. One algorithm was applied to tibial accelerometer data, while another was used for detecting gait events from the lumbar spine and thoracic spine [17]. Both algorithms identified initial contact (IC) and toe-off

(TO) events within the patterns (peaks) of the accelerometer signals, where a peak constitutes a data point that is greater (or lesser if peak is negative) than its two neighbouring values.

The original authors of the algorithm based event detection on the assumption that consecutive IC events on the ipsilateral limb could not occur earlier than 0.50 s apart [17]. This was due to the fact that only one IMU was used on the lower limb in the original paper [17]. Given tibial accelerometer data were merged to create a single file, this assumption was modified to 0.20 s to detect consecutive left and right IC events during trials completed at 3-4 and 5-6 $m \cdot s^{-1}$. For trials at 7-8 $m \cdot s^{-1}$, the minimum time between consecutive IC events was set to 0.18 s. In both circumstances, these modified assumptions were informed by previously reported thresholds [167], as outlined in Study 1 (Chapter 3), and were also applied to the lumbar spine and thoracic spine data.

The window for detecting a TO event was also modified from the original authors' MATLAB code. This resulted in a TO occurring no later than 80% of the time between the prior and next (consecutive) IC during running at 3-4 and 5-6 $m \cdot s^{-1}$ which is just prior to 50% of the entire gait cycle (IC on contralateral limbs; see Figure 8.17) [173]. This window was further adjusted for 7-8 $m \cdot s^{-1}$ where a TO could not occur earlier than 0.10 s after the prior IC and no later than 55% of the time between the prior and next IC (~25-30% of gait cycle; see Figure 8.17) [173].

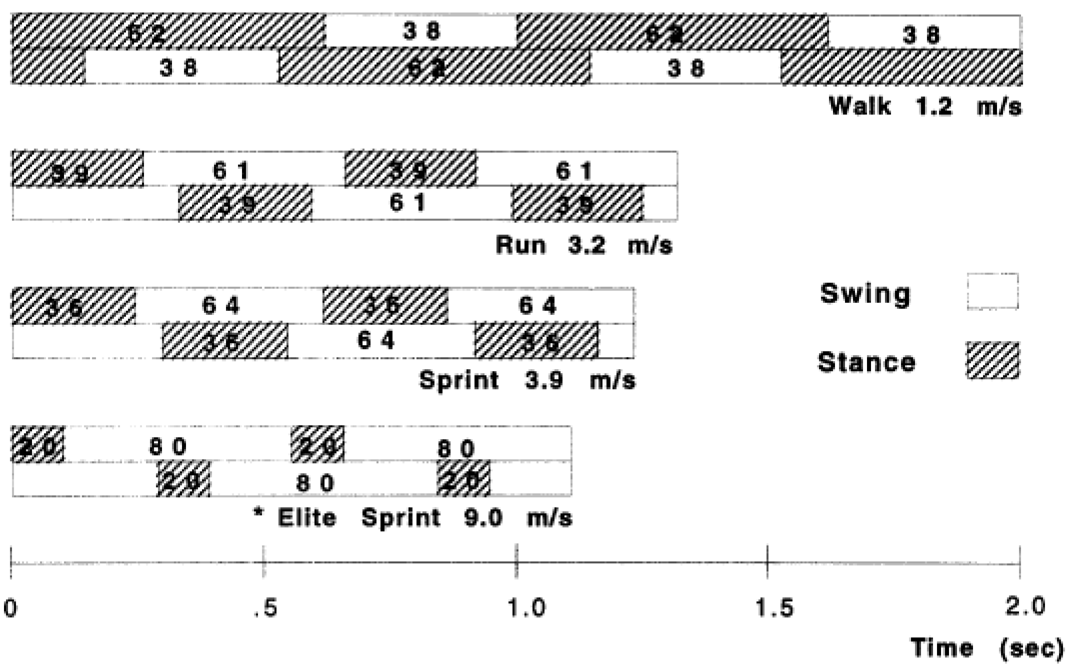

Figure 8.17. Variation in gait cycle with speed of movement. The start of each bar represents initial contact (IC). Figure from Novacheck et al. [173].

8.1.9.1 Tibia

Figure 8.18 details the sequence of steps in which IC and TO events were detected from tibial accelerometer data.

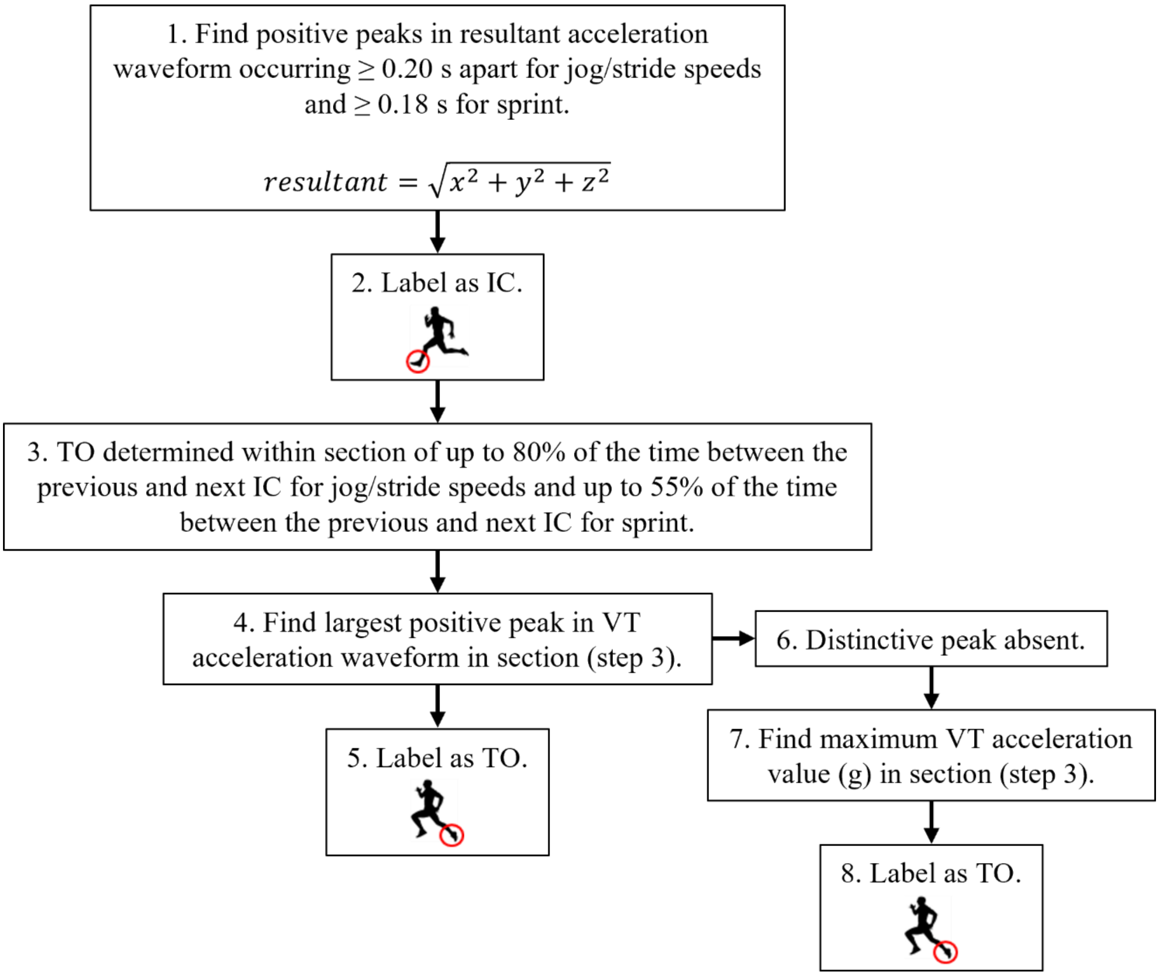

Figure 8.18. Flowchart illustrating how gait events (IC and TO) are determined from tibial accelerometer data [17]. Jog, stride and sprint speeds defined as 3-4, 5-6 and 7-8 $m \cdot s^{-1}$, respectively. IC, initial contact; TO, toe-off; VT, vertical; g, gravitational acceleration; $m \cdot s^{-1}$, metres per second.

As noted in Figure 8.18, where a distinctive peak (defined in Section 8.1.9) was not observed in the accelerometer signal, the maximum value within the subsection of the data was used to label TO. This additional criterion ensured no potential TO events were missed. Figure 8.19 shows the output obtained from the algorithm in MATLAB, where detected IC events are labelled with pink vertical lines and TO events with light blue vertical lines.

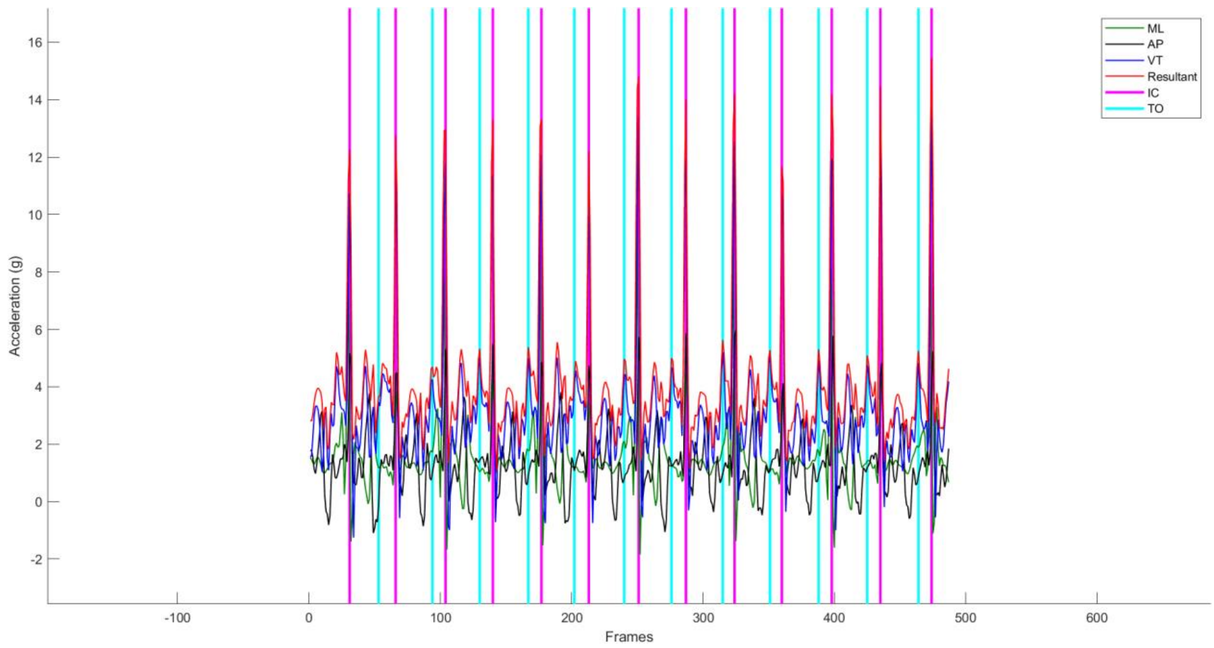

Figure 8.19. Example output from MATLAB showing detected IC and TO events from tibial accelerometer data during running at a speed of 3-4 m·s^{-1}. ML, mediolateral; AP, anteroposterior; VT, vertical; IC, initial contact, TO, toe-off.

8.1.9.2 Lumbar and Thoracic Spine

Figure 8.20 describes how gait events were determined from the lumbar spine and thoracic spine.

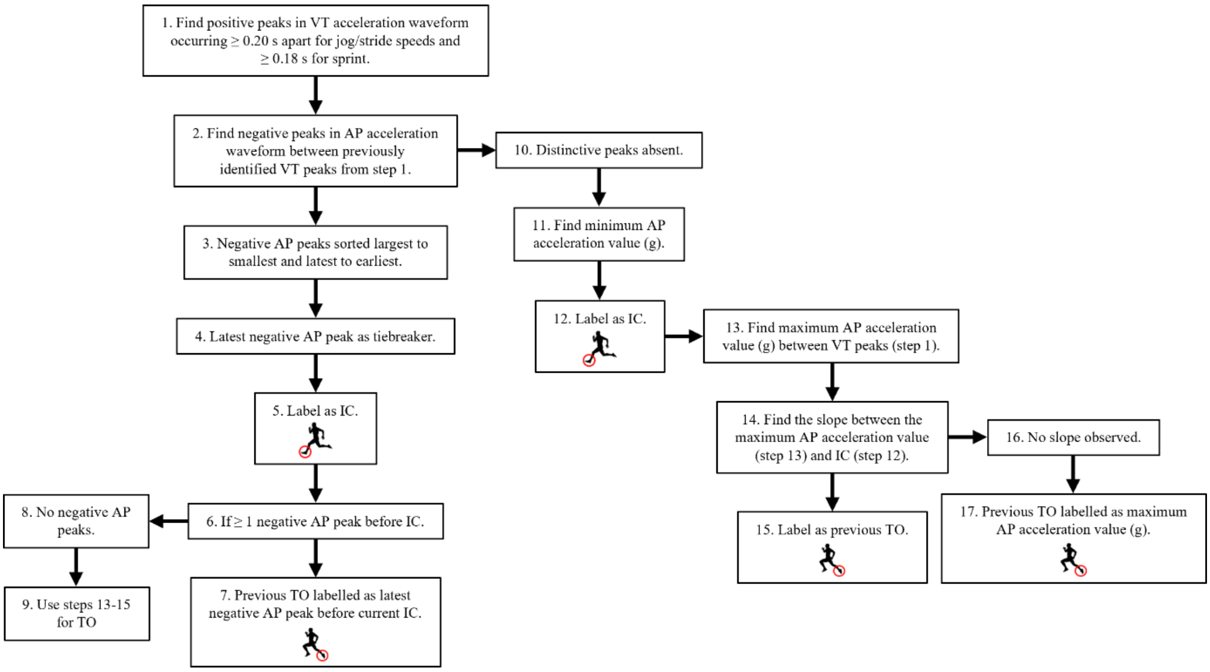

Figure 8.20. Flowchart illustrating how gait events (IC and TO) are determined from accelerometer data obtained from the lumbar and thoracic spine [17]. Jog, stride and sprint speeds defined as 3-4, 5-6 and 7-8 m·s^{-1}, respectively. VT, vertical; AP, anteroposterior; IC, initial contact; TO, toe-off; m·s^{-1}, metres per second.

The lumbar spine algorithm (which was also applied to the thoracic spine) utilised vertical and anteroposterior accelerometer signals to search for positive and negative peaks, as defined in Section 8.1.9. Like the tibia, where distinctive peaks were not observed in the data, the maximum acceleration value (g) within the specified section was used to label gait events. Figure 8.21 shows the output obtained from MATLAB for Apex accelerometer data collected from the thoracic spine.

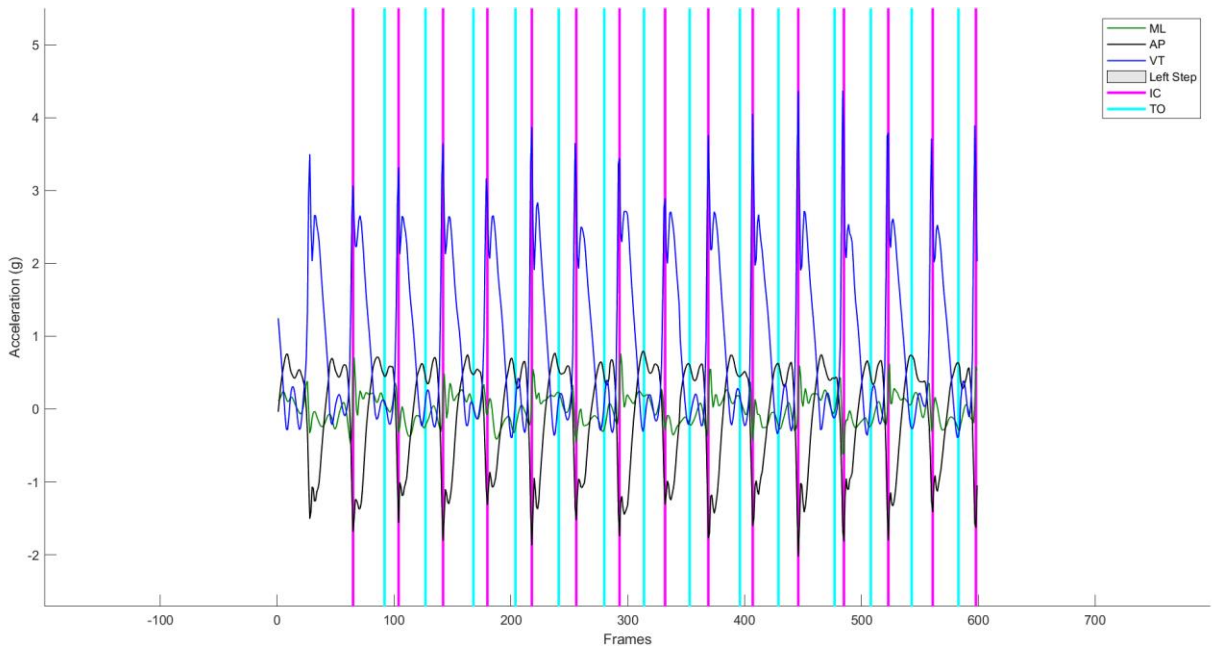

Figure 8.21. Example output from MATLAB showing detected IC and TO events. Data is from an Apex device attached to the thoracic spine at a running speed of 3-4 $m \cdot s^{-1}$. Note that left-sided steps were not assessed here. ML, mediolateral; AP, anteroposterior; VT, vertical; IC, initial contact, TO, toe-off.

Gait events from both algorithms were determined using a sliding window approach [17]. Window sizes were set to 1 s and a change in the next window start time to 0.01 s which allowed for smaller sections of data to be processed one by one. Potential gait events were determined for each window to create a final list of unique ICs and TOs which then underwent a final evaluation. Consecutive IC events were analysed to determine if they occurred too close to each other according to step one in Figure 8.18 and Figure 8.20. Where two consecutive IC events were too close together, but within acceptable ranges of the previously established IC and the next potential IC, the one with the largest magnitude in the accelerometer signal (resultant for tibia and anteroposterior for lumbar spine and thoracic spine) were chosen over the other [17]. All TO events that occurred before or at the same time as their corresponding IC were removed. Where two TO events were labelled between consecutive ICs, or TO events occurred too close together but were within acceptable ranges of the finalised ICs, the TO with the largest magnitude in the accelerometer signal (vertical for tibia and anteroposterior for lumbar and thoracic spine) were preferred [17].

Detected IC and TO events were saved in individual arrays where the values represent the frame number in which the event occurred. An example of this is shown in Figure 8.22 for data obtained from an Apex unit on the thoracic spine at 3-4 m·s^{-1}. These values were then used to calculate several gait characteristics by dividing the frame number by the sample rate of the data (100 Hz).

IC_gps
15x1 double

	1
1	65
2	104
3	142
4	180
5	218
6	256
7	293
8	332
9	369
10	407
11	446
12	485
13	523
14	561
15	598
16	

TO_gps
14x1 double

	1
1	92
2	127
3	168
4	204
5	241
6	280
7	314
8	353
9	396
10	429
11	477
12	508
13	543
14	583
15	

Figure 8.22. Finalised IC and TO gait events identified by the gait event detection algorithm from an Apex accelerometer mounted on the thoracic spine. IC, initial contact; TO, toe-off.

8.1.10 Gait Calculations

With IC and TO events known, gait characteristics, including spring-mass variables, were calculated for each site. Contact time was calculated as the time (s) from IC to TO of the same limb, while step time was determined from the time (s) between consecutive IC events (i.e., right-left). With contact time and step time known, flight time was calculated from equation 1, as previously described [81].

$$Flight\ time\ (s) = Step\ time\ (s) - Contact\ time\ (s) \qquad [1]$$

As average running velocity was determined from each trial, step length was calculated as

$$Step\ length\ (m) = velocity\ (m \cdot min^{-1})\ /\ step\ frequency\ (steps \cdot min^{-1}) \qquad [2]$$

where

$$step\ frequency\ (steps \cdot min^{-1}) = 60\ /\ step\ time\ (s) \qquad [3]$$

Contact time and flight time were then input into a spring-mass equation [14], along with participant body mass, to determine vertical stiffness (K_{vert}; equation 4), defined as the ratio of peak vertical ground reaction force ($vGRF_{peak}$; equation 5) and centre of mass displacement (COM_{dis}; equation 6) and calculated as

$$\hat{k}_{vert} = vGRF_{peak}/COM_{dis} \qquad [4]$$

with

$$vGRF_{peak} = mg\ \pi/2\ (t_f/t_c + 1) \qquad [5]$$

$vGRF_{peak}$ being the maximal ground reaction force during contact in kilonewtons (kN), *m* is the participant's body mass in kilograms (kg), *g* is gravitational acceleration and t_c and t_f are contact time and flight time in s, respectively. The vertical displacement of the centre of mass during ground contact is represented by COM_{dis} (equation 6) and is calculated as

$$COM_{dis} = vGRF_{peak} t_c^2/m\pi^2 + g t_c^2/8 \qquad [6]$$

8.2 Repeated Countermovement Jump Test

Section 8.2 details the repeated countermovement jump (CMJ) test that was used in Study 3 (Chapter 5) to assess K_{vert} in jumping.

8.2.1 Setup and Protocol

Jump testing formed part of the experimental protocol for Study 3 (Chapter 5) to assess the fatigue response following repeated sprints. This included a repeated CMJ on a force plate (FDLite, ForceDecks, Vald Performance, Brisbane, Australia) sampling at 1000 Hz to measure stiffness between consecutive jumps [184]. Before testing, the force plate was calibrated according to manufacturer recommendations. Participants then stood still on the force plate with hands on their hips and were instructed to perform two jumps as high as possible while minimising contact with the force plate between each [184]. Two trials were completed with 10-15 s rest between each. Participants repeated trials if they either landed off the force plate or too close to the edge. ForceDecks software (version 2.0.7594) was used to collect data which provides a measure of K_{vert}, referred to as passive stiffness, that represents the ratio between $vGRF_{peak}$ and COM_{dis} at landing from the first jump. An example output in ForceDecks software of a repeated CMJ test is depicted in Figure 8.23.

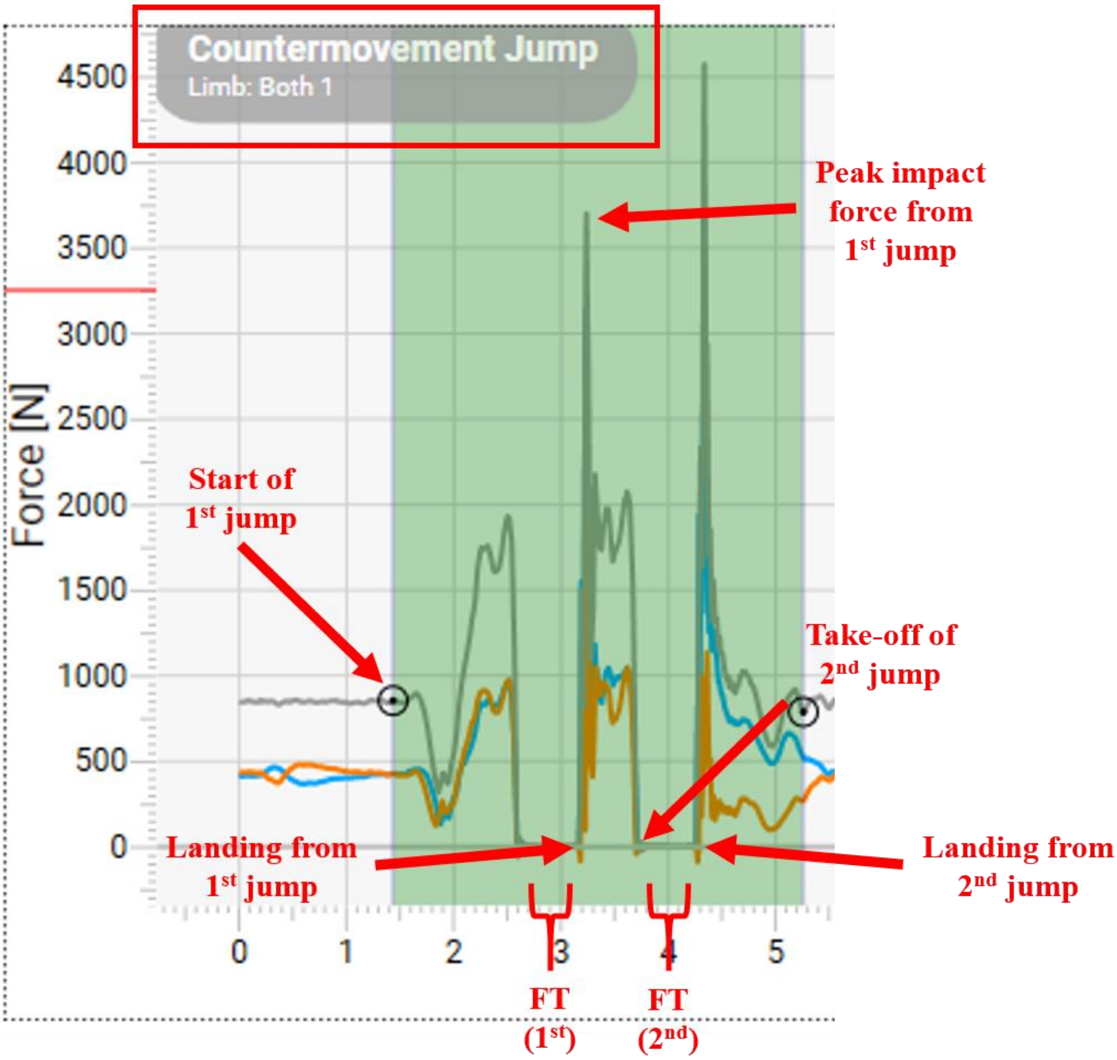

Figure 8.23. ForceDecks software showing the raw data from a repeated CMJ trial. Test types were auto-detected from the software which tagged each trial as a single CMJ (red box). Vertical force is represented by the grey line, while blue and orange lines represent left and right force, respectively. CMJ, countermovement; FT, flight time.

8.2.2 Manual Tagging

The repeated CMJ is not listed as a test type within the ForceDecks software, therefore, trials were auto-detected as a single CMJ (see Figure 8.23). Before force plate data was exported, the trial ranges were cleared from the raw data and a new trial range was assigned to relabel each trial as a drop jump (see Figure 8.24). This allowed the software to automatically calculate passive stiffness at landing following the first jump. The start of the trial range was set from flight time of the first jump (when force was zero) to the end of landing from the second jump (when vertical force returned to baseline; see Figure 8.24).

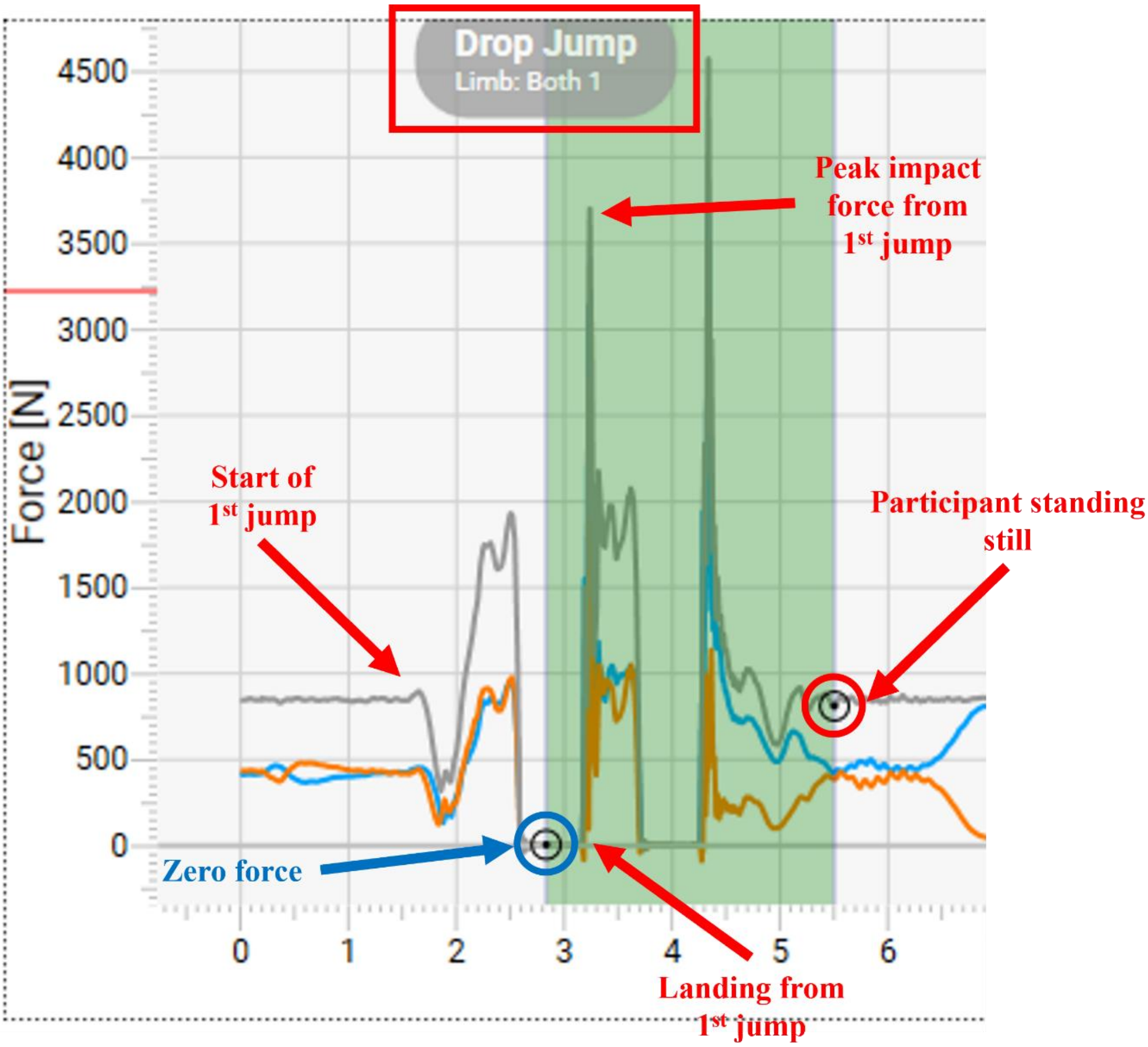

Figure 8.24. Trials relabelled as drop jumps. The trial range occurred between the participant being in the air from the first jump (force at zero; blue arrow) and the participant completing their landing from the second jump. Passive stiffness was calculated during the landing phase after the first jump. Vertical force is represented by the grey line, while blue and orange lines represent left and right force, respectively.

8.2.3 Passive Stiffness

Once each trial was relabeled as a drop jump, passive stiffness was derived from the ForceDecks software which represented the peak impact force at landing (from the first jump) divided by COM_{dis} from contact at landing (from the first jump) to its minimum (see Figure 8.25) [184]. Passive stiffness was expressed in $N{\cdot}m^{-1}$ (Newtons per metre) which was converted to $kN{\cdot}m^{-1}$ (kilonewtons per metre) by dividing N by 1000 for comparison to values obtained during the running component of the experimental protocol.

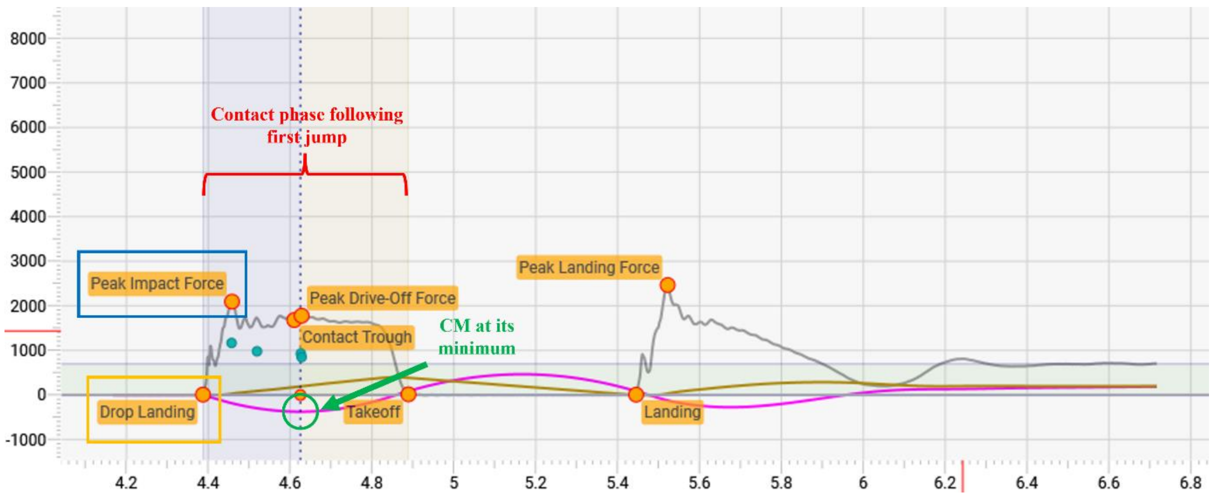

Figure 8.25. Passive stiffness was determined by the peak impact force (blue box) at landing from the first jump divided by displacement of the CM during the contact phase of landing from the first jump. The height of the CM is represented by the pink line, where the point at which the CM reaches its minimum is highlighted by the green circle. Vertical force is represented by the grey line, while the gold line is impulse. As the test was tagged as a drop jump, drop landing (yellow box) illustrates landing from the first jump in the repeated CMJ. CM, centre of mass; CMJ, countermovement jump.

8.3 Soccer-Specific Aerobic Fitness Test

Section 8.3 describes the soccer-specific aerobic fitness test (SAFT^{90}) that was used in Study 4 (Chapter 6) to assess the fatigue-related changes in running gait from a protocol that simulates the activity profile of team-sport.

8.3.1 Setup and Protocol

The SAFT^{90} is a 90-minute standardised protocol that has been designed to simulate the physiological responses and intermittent and multidirectional activity profile of team-sport match play, specifically soccer [207]. Athletes who complete the SAFT^{90} cover a distance of 10.7 km, of which 1.5 km (14%) is performed at between 15.0-25.0 km·h^{-1} [207]. There are 1350 changes of direction over the 90 minutes, while this protocol has also been shown to elicit an average heart rate of 162 ± 2 beats per minute and an oxygen consumption of 38.9 ± 4.1 millilitres per kilogram per minute [207]. The SAFT^{90} has been used extensively in other work to assess a variety of factors related to fatigue and injury [208-212, 217].

The SAFT^{90} involved participants completing a 20 m course (see Figure 8.26) for 2 x 45-minute halves, where each half was divided into 3 x 15-minute standardised running circuits [209]. Each circuit was performed with the aid of an audio track to prompt participants which movements to perform at a given time. These movements included walking, jogging, striding and sprinting, forwards and backwards running, accelerations and decelerations, side-stepping and changes of direction. Following the completion of 3 x 15-minute circuits, a 15-minute halftime interval was provided to participants.

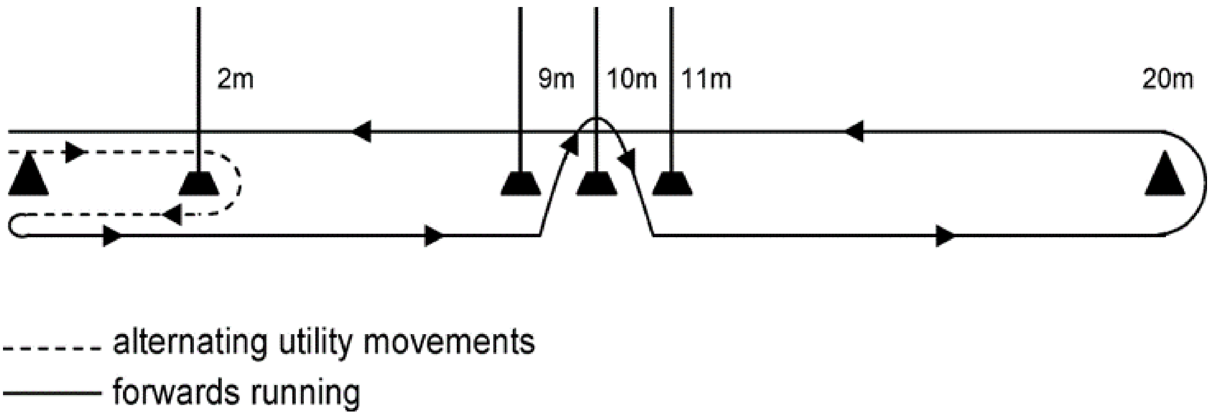

Figure 8.26. Soccer-specific aerobic fitness test (SAFT^{90}). Alternating movements include accelerations, side-stepping and backwards running.

8.3.2 Match Perceptual and Fatigue Response

To assess the impact of fatigue on running gait characteristics and jump variables, 40 m run-throughs and three different jump tests (CMJ, drop jump [DJ] and squat jump [SJ]) on a force plate were performed at specific intervals before, during and after the SAFT^{90} match simulation. Table 8-1 details the sequence of testing, including obtaining an RPE and rating of fatigue from participants at halftime and the conclusion of the match simulation.

Table 8-1. Timing of testing procedures during the SAFT^{90} match simulation.

Minute	Test	Minute	Test
Pre	CMJ, DJ, SJ, 1 x run-through at 3-4, 5-6 and 7-8 m·s^{-1}	45-60’	SAFT^{90} circuit
0-15’	SAFT^{90} circuit	61’	1 x run-through at 3-4, 5-6 and 7-8 m·s^{-1}
16’	1 x run-through at 3-4, 5-6 and 7-8 m·s^{-1}	62-77’	SAFT^{90} circuit
17-32’	SAFT^{90} circuit	78’	1 x run-through at 3-4, 5-6 and 7-8 m·s^{-1}
33’	1 x run-through at 3-4, 5-6 and 7-8 m·s^{-1}	79-90^{+4}’	SAFT^{90} circuit
34-45^{+4}’	SAFT^{90} circuit	Post	CMJ, DJ, SJ, 1 x run-through at 3-4, 5-6 and 7-8 m·s^{-1}, RPE, RoF
HT	CMJ, DJ, SJ, 1 x run-through at 3-4, 5-6 and 7-8 m·s^{-1}, RPE, RoF		

CMJ, countermovement jump; rCMJ, repeated countermovement jump; SJ, squat jump; SAFT^{90}, soccer-specific aerobic fitness test; HT, halftime; RPE, rating of perceived exertion; RoF, rating of fatigue.

Jump testing (CMJ, DJ and SJ) followed the same procedures as outlined in Section 6.3.3 of Study 4 (Chapter 6), while 40 m run-throughs were completed as per the description in Section 8.1.2 of this current chapter. As shown in Figure 8.27, two lanes were set up where the SAFT^{90} course was in one and the timing gates for the 40 m run-throughs in the other. Once participants completed each 15-minute circuit of the SAFT^{90} (lane 2; see Figure 8.27), they immediately proceeded to the first gate in lane 1 and performed the synchronisation procedure, as per Section 8.1.3, before completing the 40 m run-through at the required speed (3-4, 5-6 and 7-8 m·s^{-1}). Once all three run-throughs were completed, participants walked back to the start of the SAFT^{90} course and commenced the next 15-minute circuit with minimal delay. At the time of submitting this thesis, three circuits of the SAFT^{90} and additional sets of run-throughs equated to the first and second halves taking 58.10 ± 4.48 min and 58.22 ± 2.33 min to complete, respectively.

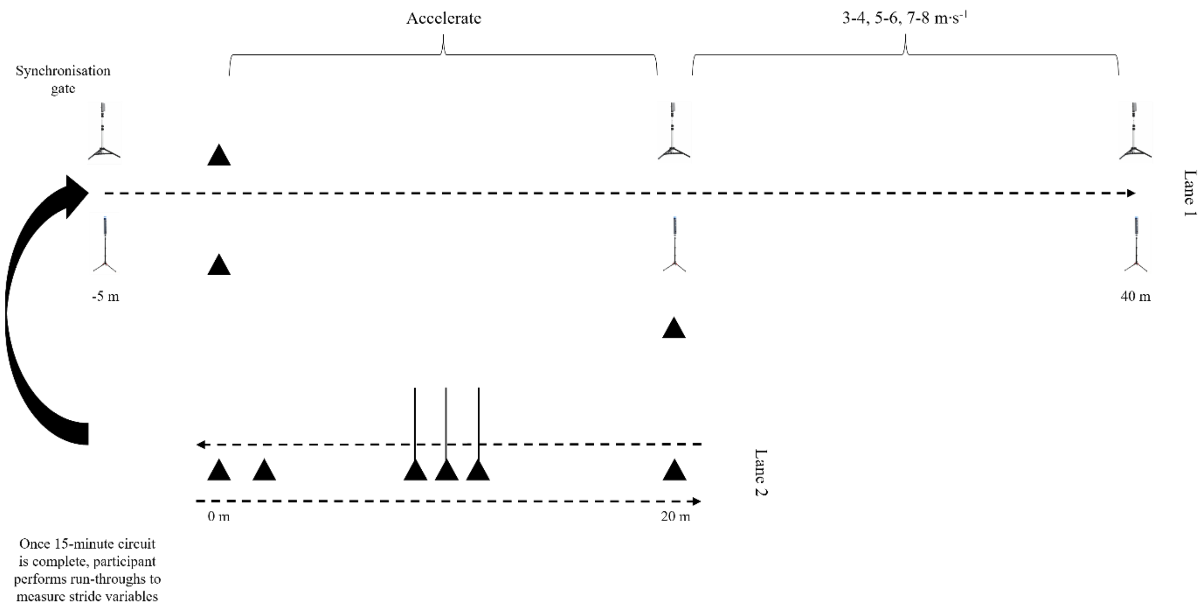

Figure 8.27. Setup of the timing gates (lane 1) and SAFT^{90} course (lane 2). Agility poles were positioned at 2, 8, 10 and 12 m in the SAFT^{90} course which were used for a variety of multidirectional movements. Following each 15-minute circuit, participants completed 1 x 40 m run-through at 3-4, 5-6 and 7-8 m·s^{-1}. This involved performing a synchronisation procedure at the gate positioned -5 m behind the start line, accelerating from 0 to 20 m, then maintaining the target running speed between 20 and 40 m.

9 Chapter 9: References

1. Halson, S.L., *Monitoring training load to understand fatigue in athletes.* Sports Medicine, 2014. **44**(2): p. 139-147.

2. Crang, Z.L., et al., *The validity and reliability of wearable microtechnology for intermittent team sports: a systematic review.* Sports Medicine, 2021. **51**: p. 549-565.

3. Spangler, R., et al., *Inertial sensors are a valid tool to detect and consistently quanitfy jumping.* International Journal of Sports Medicine, 2018. **39**(10): p. 802-808.

4. Chambers, R.M., et al., *Automatic detection of one-on-one tackles and ruck events using microtechnology in rugby union.* Journal of Science and Medicine in Sport, 2019. **22**(7): p. 827-832.

5. Balloch, A.S., et al., *Assessment of a novel algorithm to determine change-of-direction angles while running using inertial sensors.* The Journal of Strength and Conditioning Research, 2020. **34**(1): p. 134-144.

6. Glassbrook, D.J., et al., *Measurement of lower-limb asymmetry in professional rugby league: a technical note describing the use of inertial measurement units.* PeerJ, 2020. **8**: p. e9366.

7. Gómez-Carmona, C.D., et al., *Accelerometry as a method for external workload monitoring in invasion team sports. a systematic review.* PLoS ONE, 2020. **15**(8): p. e0236643.

8. Murray, N.B., et al., *Automatic detection of pitching and throwing events in baseball with inertial measurement sensors.* International Journal of Sports Physiology and Performance, 2017. **12**(4): p. 533-537.

9. Jowitt, H.K., et al., *Auto detecting deliveries in elite cricket fast bowlers using microsensors and machine learning.* Journal of Sports Sciences, 2020. **38**(7): p. 767-772.

10. Boyd, L.J., K. Ball, and R.J. Aughey, *Quantifying external load in Australian football matches and training using accelerometers.* International Journal of Sports Physiology and Performance, 2013. **8**(1): p. 44-51.

11. Cormack, S.J., et al., *Influence of neuromuscular fatigue on accelerometer load in elite Australian football players.* International Journal of Sports Physiology and Performance, 2013. **8**(4): p. 373-378.

12. Rowell, A.E., et al., *A standardized small sided game can be used to monitor neuromuscular fatigue in professional A-League football players.* Frontiers in Physiology, 2018. **9**.

13. Brughelli, M. and J. Cronin, *Influence of running velocity on vertical, leg and joint stiffness.* Sports Medicine, 2008. **38**(8): p. 647-657.

14. Morin, J.-B., et al., *A simple method for measuring stiffness during running.* Journal of Applied Biomechanics, 2005. **21**(2): p. 167-180.

15. McMahon, T.A., G. Valiant, and E.C. Frederick, *Groucho running.* Journal of Applied Physiology, 1987. **62**(6): p. 2326-2337.

16. Dugan, S.A. and K.P. Bhat, *Biomechanics and analysis of running gait.* Physical Medicine and Rehabilitation Clinics of North America, 2005. **16**(3): p. 603-621.

17. Benson, L.C., et al., *Automated accelerometer-based gait event detection during multiple running conditions.* Sensors, 2019. **19**(7): p. 1483.

18. Yang, Y., et al., *Inertial sensor estimation of initial and terminal contact during in-field running.* Sensors, 2022. **22**(13): p. 4812.

19. Aubol, K.G. and C.E. Milner, *Foot contact identification using a single triaxial accelerometer during running.* Journal of Biomechanics, 2020. **105**: p. 109768.

20. Glassbrook, D.J., et al., *Foot accelerations are larger than tibia accelerations during sprinting when measured with inertial measurement units.* Journal of Sports Sciences, 2019: p. 1-8.

21. Buchheit, M., A. Gray, and J.B. Morin, *Assessing stride variables and vertical stiffness with GPS-embedded accelerometers: preliminary insights for the monitoring of neuromuscular fatigue on the field.* Journal of Sports Science and Medicine, 2015. **14**: p. 698-701.

22. Eggers, T.M., et al., *Measuring vertical stiffness in sport with accelerometers: exercise caution!* The Journal of Strength and Conditioning Research, 2018. **32**(7): p. 1919-1922.

23. Selye, H., *Stress and the General Adaptation Syndrome.* British Medical Journal, 1950. **1**(4667): p. 1383-1392.

24. Issurin, V.B., *New horizons for the methodology and physiology of training periodization.* Sports Medicine, 2010. **40**(3): p. 189-206.

25. Chiu, L.Z. and J.L. Barnes, *The fitness-fatigue model revisited: implications for planning short-and long-term training.* Strength & Conditioning Journal, 2003. **25**(6): p. 42-51.

26. Banister, E., *Modeling elite athletic performance.* Physiological testing of elite athletes, 1991. **403**: p. 424.

27. Impellizzeri, F.M., et al., *Use of RPE-based training load in soccer.* Medicine & Science in Sports & Exercise, 2004. **36**(6): p. 1042-1047.

28. Coutts, A.J., et al., *Heart rate and blood lactate correlates of perceived exertion during small-sided soccer games.* Journal of Science and Medicine in Sport, 2009. **12**(1): p. 79-84.

29. Johnston, R.J., et al., *Movement profiles, match events, and performance in Australian football.* The Journal of Strength and Conditioning Research, 2016. **30**(8): p. 2129-2137.

30. Cummins, C., et al., *Global positioning systems (GPS) and microtechnology sensors in team sports: a systematic review.* Sports Medicine, 2013. **43**(10): p. 1025-1042.

31. Aughey, R.J., *Australian football player work rate: evidence of fatigue and pacing?* International Journal of Sports Physiology and Performance, 2010. **5**(3): p. 394-405.

32. Coutts, A.J., et al., *Match running performance in elite Australian Rules Football.* Journal of Science and Medicine in Sport, 2010. **13**(5): p. 543-548.

33. Aughey, R.J., *Applications of GPS technologies to field sports.* International Journal of Sports Physiology and Performance, 2011. **6**(3): p. 295-310.

34. Carling, C., *Interpreting physical performance in professional soccer match-play: should we be more pragmatic in our approach?* Sports Medicine, 2013. **43**(8): p. 655-633.

35. Thomas, G., et al., *Computer vision for sports: Current applications and research topics.* Computer Vision and Image Understanding, 2017. **159**: p. 3-18.

36. Luteberget, L.S., M. Spencer, and M. Gilgien, *Validity of the Catapult ClearSky T6 local positioning system for team sports specific drills, in indoor conditions.* Frontiers in Physiology, 2018. **9**.

37. Bradley, P.S. and T.D. Noakes, *Match running performance fluctuations in elite soccer: indicative of fatigue, pacing or situational influences?* Journal of Sports Sciences, 2013. **31**(15): p. 1627-1638.

38. Mooney, M.G., et al., *Impact of neuromuscular fatigue on match exercise intensity and performance in elite Australian football.* The Journal of Strength and Conditioning Research, 2013. **27**(1): p. 166-173.

39. Enoka, R.M. and J. Duchateau, *Translating fatigue to human performance.* Medicine & Science in Sports & Exercise, 2016. **48**(11): p. 2228-2238.

40. Meeusen, R., et al., *Prevention, diagnosis and treatment of the overtraining syndrome.* European Journal of Sport Science, 2006. **6**(1): p. 1-14.

41. Kuipers, H. and H. Keizer, *Overtraining in elite athletes: review and directions for the future.* Sports Medicine, 1988. **6**: p. 79-92.

42. Kreher, J.B. and J.B. Schwartz, *Overtraining syndrome: a practical guide.* Sports Health, 2012. **4**(2): p. 128-138.

43. Weakley, J., S.L. Halson, and I. Mujika, *Overtraining syndrome symptoms and diagnosis in athletes: Where is the research? A systematic review.* International Journal of Sports Physiology and Performance, 2022. **17**(5): p. 675-681.

44. Kremenic, I.J., et al., *Central fatigue after cycling evaluated using peripheral magnetic stimulation.* Medicine & Science in Sports & Exercise, 2009. **41**(7): p. 1461-1466.

45. Schillings, M.L., et al., *Relative contributions of central and peripheral factors to fatigue during a maximal sustained effort.* European Journal of Applied Physiology, 2003. **90**(5-6): p. 562-568.

46. Gibson, A.S.C. and T. Noakes, *Evidence for complex system integration and dynamic neural regulation of skeletal muscle recruitment during exercise in humans.* British Journal of Sports Medicine, 2004. **38**(6): p. 797-806.

47. Rampinini, E., et al., *Match-related fatigue in soccer players.* Medicine & Science in Sports & Exercise, 2011. **43**(11): p. 2161-2170.

48. Pointon, M., et al., *Cold water immersion recovery following intermittent-sprint exercise in the heat.* European Journal of Applied Physiology, 2012. **112**: p. 2483-2494.

49. Tofari, P.J., J.G. Kemp, and S.J. Cormack, *Self-paced team-sport match simulation results in reductions in voluntary activation and modifications to biological, perceptual, and performance measures at halftime and for up to 96 hours postmatch.* The Journal of Strength and Conditioning Research, 2018. **32**(12): p. 3552-3563.

50. Tofari, P.J., J.G. Kemp, and S.J. Cormack, *Measuring the response to simulated fixture congestion in soccer.* Science and Medicine in Football, 2020. **4**(4): p. 293-304.

51. Fowles, J.R., *Technical issues in quantifying low-frequency fatigue in athletes.* International Journal of Sports Physiology and Performance, 2006. **1**(2): p. 169-171.

52. Nicol, C., J. Avela, and P.V. Komi, *The stretch-shortening cycle: a model to study naturally occurring neuromuscular fatigue.* Sports Medicine, 2006. **36**: p. 977-999.

53. Strojnik, V. and P.V. Komi, *Fatigue after submaximal intensive stretch-shortening cycle exercise.* Medicine & Science in Sports & Exercise, 2000. **32**(7): p. 1314-1319.

54. Cormack, S.J., et al., *Reliability of measures obtained during single and repeated countermovement jumps.* International Journal of Sports Physiology and Performance, 2008. **3**(2): p. 131-144.

55. Gathercole, R., et al., *Alternative countermovement-jump analysis to quantify acute neuromuscular fatigue.* International Journal of Sports Physiology and Performance, 2015. **10**(1): p. 84-92.

56. Gathercole, R.J., T. Stellingwerff, and B.C. Sporer, *Effect of acute fatigue and training adaptation on countermovement jump performance in elite snowboard cross athletes.* The Journal of Strength and Conditioning Research, 2015. **29**(1): p. 37-46.

57. Kennedy, R. and D. Drake, *The effect of acute fatigue on countermovement jump performance in rugby union players during preseason.* Journal of Sports Medicine and Physical Fitness, 2017. **57**(10): p. 1261-1266.

58. Jiménez-Reyes, P., et al., *Jump height loss as an indicator of fatigue during sprint training.* Journal of Sports Sciences, 2019. **37**(9): p. 1029-1037.

59. Cavagna, G.A., *Elastic bounce of the body.* Journal of Applied Physiology, 1970. **29**(3): p. 279-282.

60. Kozey, S.L., et al., *Accelerometer output and MET values of common physical activities.* Medicine & Science in Sports & Exercise, 2010. **42**(9): p. 1776-1784.

61. Chambers, R., et al., *The use of wearable microsensors to quantify sport-specific movements.* Sports Medicine, 2015. **45**: p. 1065-1081.

62. Gastin, P.B., et al., *Tackle and impact detection in elite Australian football using wearable microsensor technology.* Journal of Sports Sciences, 2014. **32**(10): p. 947-953.

63. McNamara, D.J., et al., *The validity of microsensors to automatically detect bowling events and counts in cricket fast bowlers.* International Journal of Sports Physiology and Performance, 2015. **10**(1): p. 71-75.

64. Beato, M. and B. Drust, *Acceleration intensity is an important contributor to the external and internal training load demands of repeated sprint exercises in soccer players.* Research in Sports Medicine, 2021. **29**(1): p. 67-76.

65. Boyd, L.J., K. Ball, and R.J. Aughey, *The reliability of MinimaxX accelerometers for measuring physical activity in Australian football.* International Journal of Sports Physiology and Performance, 2011. **6**(3): p. 311-321.

66. Beato, M., et al., *Monitoring fatigue during intermittent exercise with accelerometer-derived metrics.* Frontiers in Physiology, 2019. **10**.

67. Girard, O., J.-P. Micallef, and G.P. Millet, *Changes in spring-mass model characteristics during repeated running sprints.* European Journal of Applied Physiology, 2011. **111**(1): p. 125-134.

68. Hanley, B. and A.K. Mohan, *Changes in gait during constant pace treadmill running.* The Journal of Strength and Conditioning Research, 2014. **28**(5): p. 1219-1225.

69. McMahon, T.A. and G.C. Cheng, *The mechanics of running: how does stiffness couple with speed?* Journal of Biomechanics, 1990. **23**: p. 65-78.

70. Bret, C., et al., *Leg strength and stiffness as ability factors in 100 m sprint running.* Journal of Sports Medicine and Physical Fitness, 2002. **42**(3): p. 274-281.

71. Farley, C.T. and O. Gonzalez, *Leg stiffness and stride frequency in human running.* Journal of Biomechanics, 1996. **29**(2): p. 181-186.

72. Cavagna, G., N. Heglund, and P. Willems, *Effect of an increase in gravity on the power output and the rebound of the body in human running.* Journal of Experimental Biology, 2005. **208**(12): p. 2333-2346.

73. Morin, J.B., et al., *Spring-mass model characteristics during sprint running: correlation with performance and fatigue-induced changes.* International Journal of Sports Medicine, 2006. **27**(2): p. 158-165.

74. Serpell, B.G., et al., *A review of models of vertical, leg, and knee stiffness in adults for running, jumping or hopping tasks.* Journal of Sports Sciences, 2012. **30**(13): p. 1347-1363.

75. Morin, J.-B., et al., *Effects of altered stride frequency and contact time on leg-spring behavior in human running.* Journal of Biomechanics, 2007. **40**(15): p. 3341-3348.

76. Brown, A.M., R.A. Zifchock, and H.J. Hillstrom, *The effects of limb dominance and fatigue on running biomechanics.* Gait & Posture, 2014. **39**(3): p. 915-919.

77. Benson, L.C., et al., *The use of wearable devices for walking and running gait analysis outside of the lab: A systematic review.* Gait & Posture, 2018. **63**: p. 124-138.

78. Camomilla, V., et al., *Trends supporting the in-field use of wearable inertial sensors for sport performance evaluation: a systematic review.* Sensors, 2018. **18**(3): p. 873.

79. Lee, J.B., R.B. Mellifont, and B.J. Burkett, *The use of a single inertial sensor to identify stride, step, and stance durations of running gait.* Journal of Science and Medicine in Sport, 2010. **13**(2): p. 270-273.

80. Sinclair, J., et al., *Determination of gait events using an externally mounted shank accelerometer.* Journal of Applied Biomechanics, 2013. **29**(1): p. 118-122.

81. García-Pinillos, F., et al., *Absolute reliability and concurrent validity of the Stryd system for the assessment of running stride kinematics at different velocities.* The Journal of Strength and Conditioning Research, 2021. **35**(1): p. 78-84.

82. Patoz, A., et al., *A single sacral-mounted inertial measurement unit to estimate peak vertical ground reaction force, contact time, and flight time in running.* Sensors, 2022. **22**(3): p. 784.

83. Falbriard, M., et al., *Accurate estimation of running temporal parameters using foot-worn inertial sensors.* Frontiers in Physiology, 2018. **9**.

84. Bergamini, E., et al., *Estimation of temporal parameters during sprint running using a trunk-mounted inertial measurement unit.* Journal of Biomechanics, 2012. **45**(6): p. 1123-1126.

85. García-Pinillos, F., et al., *Agreement between the spatiotemporal gait parameters from two different wearable devices and high-speed video analysis.* PLoS ONE, 2019. **14**(9).

86. Kenneally-Dabrowski, C.J., B.G. Serpell, and W. Spratford, *Are accelerometers a valid tool for measuring overground sprinting symmetry?* International Journal of Sports Science & Coaching, 2018. **13**(2): p. 270-277.

87. Vanrenterghem, J., et al., *Training load monitoring in team sports: a novel framework separating physiological and biomechanical load-adaptation pathways.* Sports Medicine, 2017. **47**(11): p. 2135-2142.

88. Spencer, M., et al., *Time–motion analysis of elite field hockey, with special reference to repeated-sprint activity.* Journal of Sports Sciences, 2004. **22**(9): p. 843-850.

89. Buchheit, M., et al., *Integrating different tracking systems in football: multiple camera semi-automatic system, local position measurement and GPS technologies.* Journal of Sports Sciences, 2014. **32**(20): p. 1844-1857.

90. Stevens, T.G., et al., *Measuring acceleration and deceleration in soccer-specific movements using a local position measurement (LPM) system.* International Journal of Sports Physiology and Performance, 2014. **9**(3): p. 446-456.

91. Duffield, R., et al., *Accuracy and reliability of GPS devices for measurement of movement patterns in confined spaces for court-based sports.* Journal of Science and Medicine in Sport, 2010. **13**(5): p. 523-525.

92. Jennings, D., et al., *The validity and reliability of GPS units for measuring distance in team sport specific running patterns.* International Journal of Sports Physiology and Performance, 2010. **5**(3): p. 328-341.

93. Varley, M.C., I.H. Fairweather, and R.J. Aughey, *Validity and reliability of GPS for measuring instantaneous velocity during acceleration, deceleration, and constant motion.* Journal of Sports Sciences, 2012. **30**(2): p. 121-127.

94. Gabbett, T., D. Jenkins, and B. Abernethy, *Physical collisions and injury during professional rugby league skills training.* Journal of Science and Medicine in Sport, 2010. **13**(6): p. 578-583.

95. Gastin, P.B., et al., *Quantification of tackling demands in professional Australian football using integrated wearable athlete tracking technology.* Journal of Science and Medicine in Sport, 2013. **16**(6): p. 589-593.

96. Warman, G.E., et al., *Using microtechnology to quantify torso angle during match-play in field hockey.* The Journal of Strength and Conditioning Research, 2019. **33**(10): p. 2648-2654.

97. Ammann, R., W. Taube, and T. Wyss, *Accuracy of PARTwear inertial sensor and Optojump optical measurement system for measuring ground contact time during*

running. The Journal of Strength and Conditioning Research, 2016. **30**(7): p. 2057-2063.

98. Gabbett, T.J., *Quantifying the physical demands of collision sports: does microsensor technology measure what it claims to measure?* The Journal of Strength and Conditioning Research, 2013. **27**(8): p. 2319-2322.

99. Bouten, C.V., et al., *Assessment of energy expenditure for physical activity using a triaxial accelerometer.* Medicine & Science in Sports & Exercise, 1994. **26**(12): p. 1516-1523.

100. Bouten, C.V., et al., *A triaxial accelerometer and portable data processing unit for the assessment of daily physical activity.* IEEE Transactions on Biomedical Engineering, 1997. **44**(3): p. 136-147.

101. Swartz, A.M., et al., *Estimation of energy expenditure using CSA accelerometers at hip and wrist sites.* Medicine & Science in Sports & Exercise, 2000. **32**(9): p. 450-456.

102. Troiano, R.P., et al., *Physical activity in the United States measured by accelerometer.* Medicine & Science in Sports & Exercise, 2008. **40**(1): p. 181-188.

103. Skotte, J., et al., *Detection of physical activity types using triaxial accelerometers.* Journal of Physical Activity & Health, 2014. **11**(1): p. 76-84.

104. Barrett, S., A. Midgley, and R. Lovell, *PlayerLoad™: reliability, convergent validity, and influence of unit position during treadmill running.* International Journal of Sports Physiology and Performance, 2014. **9**(6): p. 945-952.

105. McGrath, D., et al., *Gyroscope-based assessment of temporal gait parameters during treadmill walking and running.* Sports Engineering, 2012. **15**(4): p. 207-213.

106. Wundersitz, D.W.T., et al., *Validity of an upper-body-mounted accelerometer to measure peak vertical and resultant force during running and change-of-direction tasks.* Sports Biomechanics, 2013. **12**(4): p. 403-412.

107. Nedergaard, N.J., et al., *The feasibility of predicting ground reaction forces during running from a trunk accelerometry driven mass-spring-damper model.* PeerJ, 2018. **6**: p. e6105.

108. Raper, D.P., et al., *Use of a tibial accelerometer to measure ground reaction force in running: a reliability and validity comparison with force plates.* Journal of Science and Medicine in Sport, 2018. **21**(1): p. 84-88.

109. Nedergaard, N.J., et al., *The relationship between whole-body external loading and body-worn accelerometry during team-sport movements.* International Journal of Sports Physiology and Performance, 2017. **12**(1): p. 18-26.

110. Edwards, S., et al., *Caution using data from triaxial accelerometers housed in player tracking units during running.* Journal of Sports Sciences, 2019. **37**(7): p. 810-818.

111. Lafortune, M.A., M.J. Lake, and E.M. Hennig, *Differential shock transmission response of the human body to impact severity and lower limb posture.* Journal of Biomechanics, 1996. **29**(12): p. 1531-1537.

112. Derrick, T.R., J. Hamill, and G.E. Caldwell, *Energy absorption of impacts during running at various stride lengths.* Medicine & Science in Sports & Exercise, 1998. **30**(1): p. 128-135.

113. Lucas-Cuevas, A.G., et al., *The location of the tibial accelerometer does influence impact acceleration parameters during running.* Journal of Sports Sciences, 2017. **35**(17): p. 1734-1738.

114. Moher, D., et al., *Preferred reporting items for systematic reviews and meta-analyses: the PRISMA statement.* Annals of Internal Medicine, 2009. **151**(4): p. 264-269.

115. Downs, S.H. and N. Black, *The feasibility of creating a checklist for the assessment of the methodological quality both of randomised and non-randomised studies of health care interventions.* Journal of Epidemiology & Community Health, 1998. **52**(6): p. 377-384.

116. Glassbrook, D.J., et al., *The demands of professional rugby league match-play: a meta-analysis.* Sports Medicine, 2019. **5**: p. 1-20.

117. Zrenner, M., et al., *Comparison of different algorithms for calculating velocity and stride length in running using inertial measurement units.* Sensors, 2018. **18**(12): p. 4194.

118. Cavanagh, P.R. and M.A. Lafortune, *Ground reaction forces in distance running.* Journal of Biomechanics, 1980. **13**(5): p. 397-406.

119. Chew, D.-K., et al., *Estimating running spatial and temporal parameters using an inertial sensor.* Sports Engineering, 2018. **21**(2): p. 115-122.

120. Watari, R., et al., *Validation of a torso-mounted accelerometer for measures of vertical oscillation and ground contact time during treadmill running.* Journal of Applied Biomechanics, 2016. **32**(3): p. 306-10.

121. Dorschky, E., et al., *Estimation of gait kinematics and kinetics from inertial sensor data using optimal control of musculoskeletal models.* Journal of Biomechanics, 2019. **95**: p. 109278.

122. Ngoh, K.J., et al., *Estimation of vertical ground reaction force during running using neural network model and uniaxial accelerometer.* Journal of Biomechanics, 2018. **76**: p. 269-273.

123. Gurchiek, R.D., et al., *The use of a single inertial sensor to estimate 3-dimensional ground reaction force during accelerative running tasks.* Journal of Biomechanics, 2017. **61**: p. 263-268.

124. Mitschke, C., T. Heß, and T.L. Milani, *Which method detects foot strike in rearfoot and forefoot runners accurately when using an inertial measurement unit?* Applied Sciences, 2017. **7**(9): p. 959.

125. Mitschke, C., F. Zaumseil, and T.L. Milani, *The influence of inertial sensor sampling frequency on the accuracy of measurement parameters in rearfoot running.* Computer Methods in Biomechanics and Biomedical Engineering, 2017. **20**(14): p. 1502-1511.

126. Pairot de Fontenay, B., et al., *Validating commercial wearable sensors for running gait parameters estimation.* IEEE Sensors Journal, 2020. **20**(14): p. 7783-7791.

127. Pogson, M., et al., *A neural network method to predict task- and step-specific ground reaction force magnitudes from trunk accelerations during running activities.* Medical Engineering and Physics, 2020. **78**: p. 82-89.

128. Tan, H.X., et al., *Time series classification using a modified LSTM approach from accelerometer-based data: a comparative study for gait cycle detection.* Gait & Posture, 2019. **74**: p. 128-134.

129. Winter, S.C., et al., *Validation of a single inertial sensor for measuring running kinematics overground during a prolonged run.* Journal of Fitness Research, 2016. **5**(1): p. 14-23.

130. Neugebauer, J.M., K.H. Collins, and D.A. Hawkins, *Ground reaction force estimates from ActiGraph GT3X+ hip accelerations.* PLoS ONE, 2014. **9**(6): p. e99023.

131. Hall, J.P., et al., *The biomechanical differences between barefoot and shod distance running: a systematic review and preliminary meta-analysis.* Sports Medicine, 2013. **43**(12): p. 1335-1353.

132. Gindre, C., et al., *Reliability and validity of the Myotest for measuring running stride kinematics.* Journal of Sports Sciences, 2016. **34**(7): p. 664-670.

133. Mo, S. and D.H. Chow, *Accuracy of three methods in gait event detection during overground running.* Gait & Posture, 2018. **59**: p. 93-98.

134. Fadillioglu, C., et al., *Automated gait event detection for a variety of locomotion tasks using a novel gyroscope-based algorithm.* Gait & Posture, 2020. **81**: p. 102-108.

135. Machulik, C., et al., *Validation of an inertial measurement unit based magnetic timing gate system during running and sprinting.* German Journal of Sports Medicine, 2020. **71**(3): p. 69-75.

136. Simon, S.R., *Quantification of human motion: gait analysis—benefits and limitations to its application to clinical problems.* Journal of Biomechanics, 2004. **37**(12): p. 1869-1880.

137. Lienhard, K., D. Schneider, and N.A. Maffiuletti, *Validity of the Optogait photoelectric system for the assessment of spatiotemporal gait parameters.* Medical Engineering & Physics, 2013. **35**(4): p. 500-504.

138. Muro-de-la-Herran, A., B. Garcia-Zapirain, and A. Mendez-Zorrilla, *Gait analysis methods: an overview of wearable and non-wearable systems, highlighting clinical applications.* Sensors, 2014. **14**(2): p. 3362-3394.

139. Schwarzer, G., *meta: an R package for meta-analysis.* R News, 2007. **7**(3): p. 40-45.

140. Borenstein, M. and J.P. Higgins, *Meta-analysis and subgroups.* Prevention Science, 2013. **14**(2): p. 134-143.

141. Higgins, J.P., et al., *Measuring inconsistency in meta-analyses.* British Medical Journal, 2003. **327**(7414): p. 557-560.

142. Viechtbauer, W. and M.W.L. Cheung, *Outlier and influence diagnostics for meta-analysis.* Research Synthesis Methods, 2010. **1**(2): p. 112-125.

143. Quintana, D.S., *From pre-registration to publication: a non-technical primer for conducting a meta-analysis to synthesize correlational data.* Frontiers in Physiology, 2015. **6**.

144. Schwarzer, G., J.R. Carpenter, and G. Rücker, *Meta-Analysis with R*. 1 ed. Use R! 2015: Springer International Publishing Switzerland.

145. Lewis, S. and M. Clarke, *Forest plots: trying to see the wood and the trees.* British Medical Journal, 2001. **322**(7300): p. 1479-1480.

146. Gouttebarge, V., et al., *Reproducibility and validity of the Myotest for measuring step frequency and ground contact time in recreational runners.* Journal of Human Kinetics, 2015. **45**: p. 19-26.

147. Norris, M., I.C. Kenny, and R. Anderson, *Comparison of accelerometry stride time calculation methods.* Journal of Biomechanics, 2016. **49**(13): p. 3031-3034.

148. Brahms, C., et al., *Stride length determination during overground running using a single foot-mounted inertial measurement unit.* Journal of Biomechanics, 2018. **71**: p. 302-305.

149. Buchheit, M., et al., *Neuromuscular responses to conditioned soccer sessions assessed via GPS-embedded accelerometers: insights into tactical periodization.* International Journal of Sports Physiology and Performance, 2018. **13**: p. 577-583.

150. Wouda, F.J., et al., *Estimation of vertical ground reaction forces and sagittal knee kinematics during running using three inertial sensors.* Frontiers in Physiology, 2018. **9**: p. 218.

151. Powers, D.M., *Evaluation: from precision, recall and F-measure to ROC, informedness, markedness and correlation.* Journal of Machine Learning Technologies, 2011. **2**(1): p. 37-63.

152. Hreljac, A. and R.N. Marshall, *Algorithms to determine event timing during normal walking using kinematic data.* Journal of Biomechanics, 2000. **33**(6): p. 783-786.

153. Zeni Jr., J., J. Richards, and J. Higginson, *Two simple methods for determining gait events during treadmill and overground walking using kinematic data.* Gait & Posture, 2008. **27**(4): p. 710-714.

154. Borenstein, M., et al., *A basic introduction to fixed-effect and random-effects models for meta-analysis.* Research Synthesis Methods, 2010. **1**(2): p. 97-111.

155. Keller, T.S., et al., *Relationship between vertical ground reaction force and speed during walking, slow jogging, and running.* Clinical Biomechanics, 1996. **11**(5): p. 253-259.

156. Hunter, J.P., R.N. Marshall, and P.J. McNair, *Relationships between ground reaction force impulse and kinematics of sprint-running acceleration.* Journal of Applied Biomechanics, 2005. **21**(1): p. 31-43.

157. Verheul, J., et al., *Measuring biomechanical loads in team sports – from lab to field.* Science and Medicine in Football, 2020. **4**(3): p. 246-252.

158. Ruddy, J.D., et al., *Modeling the risk of team sport injuries: a narrative review of different statistical approaches.* Frontiers in Physiology, 2019. **10**.

159. Hopkins, W.G., *Measures of reliability in sports medicine and science.* Sports Medicine, 2000. **30**(1): p. 1-15.

160. Thorborg, K., et al., *Clinical assessment of hip strength using a hand-held dynamometer is reliable.* Scandinavian Journal of Medicine & Science in Sports, 2010. **20**(3): p. 493-501.

161. Garrett, J., et al., *A novel method of assessment for monitoring neuromuscular fatigue in Australian rules football players.* International Journal of Sports Physiology and Performance, 2018. **14**(5): p. 598-605.

162. Walker, E.J., et al., *Inertial sensors to estimate the energy expenditure of team-sport athletes.* Journal of Science and Medicine in Sport, 2016. **19**(2): p. 177-181.

163. Wundersitz, D.W., et al., *Validity of a trunk-mounted accelerometer to assess peak accelerations during walking, jogging and running.* European Journal of Sport Science, 2015. **15**(5): p. 382-390.

164. Greenland, S., M.A. Mansournia, and D.G. Altman, *Sparse data bias: a problem hiding in plain sight.* British Medical Journal, 2016. **352**: p. i1981.

165. Lin, L., *Bias caused by sampling error in meta-analysis with small sample sizes.* PLoS ONE, 2018. **13**(9): p. e0204056.

166. Crowell, H.P. and I.S. Davis, *Gait retraining to reduce lower extremity loading in runners.* Clinical Biomechanics, 2011. **26**(1): p. 78-83.

167. Horsley, B.J., et al., *Does site matter? Impact of Inertial Measurement Unit placement on the validity and reliability of stride variables during running: a systematic review and meta-analysis.* Sports Medicine, 2021. **51**: p. 1449-1489.

168. McLean, B.D., et al., *The fit matters: influence of accelerometer fitting and training drill demands on load measures in rugby league players.* International Journal of Sports Physiology and Performance, 2018. **13**(8): p. 1083-1089.

169. Borg, D.N., et al., *Calculating sample size for reliability studies.* PM&R, 2022. **14**(8): p. 1018-1025.

170. Kolsky, D.C., et al., *Reliability of a 40 m sprint in recreationally and moderately trained male and female groups.* Journal of Science and Medicine in Sport, 2010. **12**: p. e65.

171. Buttfield, A. and K. Ball, *The practical application of a method of analysing the variability of within-step accelerations collected via athlete tracking devices.* Journal of Sports Sciences, 2020. **38**(3): p. 343-350.

172. Madgwick, S.O., et al., *An extended complementary filter for full-body MARG orientation estimation.* IEEE/ASME Transactions on Mechatronics, 2020. **25**(4): p. 2054-2064.

173. Novacheck, T.F., *The biomechanics of running.* Gait & Posture, 1998. **7**(1): p. 77-95.

174. Bland, J.M. and D.G. Altman, *Measuring agreement in method comparison studies.* Statistical Methods in Medical Research, 1999. **8**(2): p. 135-160.

175. Arachchige, C.N., L.A. Prendergast, and R.G. Staudte, *Robust analogs to the coefficient of variation.* Journal of Applied Statistics, 2022. **49**(2): p. 268-290.

176. DuBose, D.F., et al., *Lower extremity stiffness changes following concussion in collegiate football players.* Medicine & Science in Sports & Exercise, 2017. **49**(1): p. 167-172.

177. Taylor, J.B., et al., *Activity demands during multi-directional team sports: a systematic review.* Sports Medicine, 2017. **47**(12): p. 2533-2551.

178. Edwards, R., *Biochemical basis of fatigue in exercise performance*. 1983, Champaign, IL: Human Kinetics.

179. Cormack, S.J., R.U. Newton, and M.R. McGuigan, *Neuromuscular and endocrine responses of elite players to an Australian rules football match.* International Journal of Sports Physiology and Performance, 2008. **3**(3): p. 359-374.

180. Boozari, S., et al., *Effect of gastrocnemius kinesio taping on countermovement jump performance and vertical stiffness following muscle fatigue.* Journal of Sport Rehabilitation, 2018. **27**(4): p. 306-311.

181. Girard, O., et al., *Mechanical alterations during interval-training treadmill runs in high-level male team-sport players.* Journal of Science and Medicine in Sport, 2017. **20**(1): p. 87-91.

182. Horsley, B.J., et al., *Validity and reliability of thoracic-mounted inertial measurement units to derive gait characteristics during running.* The Journal of Strength and Conditioning Research, 2023. **38**(2): p. 274-282.

183. Faul, F., et al., *G* Power 3: a flexible statistical power analysis program for the social, behavioral, and biomedical sciences.* Behavior Research Methods, 2007. **39**(2): p. 175-191.

184. Serpell, B.G., et al., *Vertical stiffness and muscle strain in professional Australian football.* Journal of Sports Sciences, 2014. **32**(20): p. 1924-1930.

185. Borg, G., *Borg's perceived exertion and pain scales*. 1998, Champaign, IL: Human Kinetics.

186. Micklewright, D., et al., *Development and validity of the rating-of-fatigue scale.* Sports Medicine, 2017. **47**(11): p. 2375-2393.

187. Hopkins, W., et al., *Progressive statistics for studies in sports medicine and exercise science.* Medicine & Science in Sports & Exercise, 2009. **41**(1): p. 3-13.

188. Moore, I.S., et al., *Humans optimize ground contact time and leg stiffness to minimize the metabolic cost of running.* Frontiers in Sports and Active Living, 2019. **1**.

189. Bartlett, R., J. Wheat, and M. Robins, *Is movement variability important for sports biomechanists?* Sports Biomechanics, 2007. **6**(2): p. 224-243.

190. Edouard, P., et al., *Sprint acceleration mechanics in fatigue conditions: compensatory role of gluteal muscles in horizontal force production and potential protection of hamstring muscles.* Frontiers in Physiology, 2018. **9**: p. 1706.

191. Sweeting, A.J., et al., *When is a sprint a sprint? A review of the analysis of team-sport athlete activity profile.* Frontiers in Physiology, 2017. **8**.

192. Maas, E., et al., *Novice runners show greater changes in kinematics with fatigue compared with competitive runners.* Sports Biomechanics, 2018. **17**(3): p. 350-360.

193. Morin, J.-B., et al., *High-intensity sprint fatigue does not alter constant-submaximal velocity running mechanics and spring-mass behavior.* European Journal of Applied Physiology, 2012. **112**(4): p. 1419-1428.

194. Rowell, A.E., et al., *Identification of sensitive measures of recovery after external load from football match play.* International Journal of Sports Physiology and Performance, 2017. **12**(7): p. 969-976.

195. Rodacki, A.L.F., N.E. Fowler, and S.J. Bennett, *Vertical jump coordination: fatigue effects.* Medicine & Science in Sports & Exercise, 2002. **34**(1): p. 105-116.

196. Maloney, S.J. and I.M. Fletcher, *Lower limb stiffness testing in athletic performance: a critical review.* Sports Biomechanics, 2021. **20**(1): p. 109-130.

197. Fitzpatrick, J.F., et al., *The reliability of potential fatigue-monitoring measures in elite youth soccer players.* The Journal of Strength and Conditioning Research, 2021. **35**(12): p. 3448-3452.

198. Mohr, M., P. Krustrup, and J. Bangsbo, *Fatigue in soccer: a brief review.* Journal of Sports Sciences, 2005. **23**(6): p. 593-599.

199. Johnston, R.D., et al., *Influence of physical qualities on post-match fatigue in rugby league players.* Journal of Science and Medicine in Sport, 2015. **18**(2): p. 209-213.

200. McLean, B.D., et al., *Neuromuscular, endocrine, and perceptual fatigue responses during different length between-match microcycles in professional rugby league players.* International Journal of Sports Physiology and Performance, 2010. **5**(3): p. 367-383.

201. Boyd, L., et al., *Practical application of accelerometers in Australian football.* Journal of Science and Medicine in Sport, 2010. **13**(1): p. e14-e15.

202. García-Pinillos, F., et al., *Does fatigue alter step characteristics and stiffness during running?* Gait & Posture, 2020: p. 259-263.

203. Riazati, S., et al., *Fatigue induced changes in muscle strength and gait following two different intensity, energy expenditure matched runs.* Frontiers in Bioengineering and Biotechnology, 2020. **8**: p. 360.

204. Horsley, B.J., et al., *Thoracic-worn accelerometers detect fatigue-related changes in vertical stiffness during sprinting.* The Journal of Strength and Conditioning Research, 2023. **38**(2): p. 283-289.

205. Kempton, T., A.C. Sirotic, and A.J. Coutts, *Between match variation in professional rugby league competition.* Journal of Science and Medicine in Sport, 2014. **17**(4): p. 404-407.

206. Kempton, T., et al., *Match-to-match variation in physical activity and technical skill measures in professional Australian Football.* Journal of Science and Medicine in Sport, 2015. **18**(1): p. 109-113.

207. Lovell, R., B. Knapper, and K. Small. *Physiological responses to SAFT90: a new soccer-specific match simulation*. in *Verona-Ghirada Team Sport Conference*. 2008. Treviso, Italy.

208. Small, K., et al., *The effects of multidirectional soccer-specific fatigue on markers of hamstring injury risk.* Journal of Science and Medicine in Sport, 2008. **13**(1): p. 120-125.

209. Lovell, R., et al., *Effects of different half-time strategies on second half soccer-specific speed, power and dynamic strength.* Scandinavian Journal of Medicine & Science in Sports, 2013. **23**(1): p. 105-113.

210. De Ste Croix, M., et al., *ACL injury risk in elite female youth soccer: changes in neuromuscular control of the knee following soccer-specific fatigue.* Scandinavian Journal of Medicine & Science in Sports, 2014. **25**(5): p. e531-e538.

211. Marshall, P.W., et al., *Hamstring muscle fatigue and central motor output during a simulated soccer match.* PloS One, 2014. **9**(7): p. e102753.

212. Barrett, S., et al., *Within-match PlayerLoad patterns during a simulated soccer match: potential implications for unit positioning and fatigue management.* International Journal of Sports Physiology and Performance, 2016. **11**(1): p. 135-140.

213. McMahon, J.J., et al., *A proposed method for evaluating drop jump performance with one force platform.* Biomechanics, 2021. **1**(2): p. 178-189.

214. Gathercole, R.J., et al., *Comparison of the capacity of different jump and sprint field tests to detect neuromuscular fatigue.* The Journal of Strength and Conditioning Research, 2015. **29**(9): p. 2522-2531.

215. Comfort, P., et al., *Effect of knee and trunk angle on kinetic variables during the isometric midthigh pull: test–retest reliability.* International Journal of Sports Physiology and Performance, 2015. **10**(1): p. 58-63.

216. Bangsbo, J., *YO-YO tests*. 1st ed. 1996, Copenhagen, Denmark: August Krogh Institute.

217. Raja Azidin, R.F., et al., *Effects of treadmill versus overground soccer match simulations on biomechanical markers of anterior cruciate ligament injury risk in side cutting.* Journal of Sports Sciences, 2015. **33**(13): p. 1332-1341.

Appendix I: Research Portfolio

Publications

1. Horsley, B.J., et al., *Does site matter? Impact of Inertial Measurement Unit placement on the validity and reliability of stride variables during running: a systematic review and meta-analysis.* Sports Medicine, 2021. **51**: p. 1449-1489.

Contribution statement: BH, PT, JD and SC contributed to the development of the review and implementation of the search strategy. BH carried out the meta-analysis with assistance from NM. BH, PT, NM and SC collectively interpreted the results of the systematic review and meta-analysis, while BH drafted the manuscript. All authors contributed to editing and revising the manuscript and approved the final version prior to submission.

Approximate percentage contributions – B. J. Horsley 55%; P. J. Tofari 12.5%; S. L. Halson 5%; J. G. Kemp 2.5%; J. Dickson 2.5%; N. Maniar 10%; S. J. Cormack 12.5%.

I acknowledge that my contribution to the above publication is 55%:

Benjamin Horsley Date 07/07/2023

As principal supervisor, I certify that the above contributions are true and correct:

Stuart Cormack Date 07/07/2023

Co-author signatures:

Paul Tofari Date 07/07/2023

Shona Halson Date 07/07/2023

Justin Kemp Date 07/07/2023

Jessica Dickson Date 07/07/2023

Nirav Maniar Date 07/07/2023

2. Horsley, B.J., et al., *Validity and reliability of thoracic-mounted Inertial Measurement Units to derive gait characteristics during running.* The Journal of Strength and Conditioning Research, 2023. **38**(2): p. 274-282.

Contribution statement: BH, PT and SC were responsible for the design of the study. Data collection was carried out by BH, while BH, DC and MC were involved in data processing. BH, SC and RJ performed the statistical analysis. The manuscript was written by BH with editing contributions from all authors.

Approximate percentage contributions – B. J. Horsley 55%; P. J. Tofari 15%; S. L. Halson 2.5%; J. G. Kemp 1%; D. Chalkley 4%; M. H. Cole 2.5%; R. D. Johnston 5%; S. J. Cormack 15%.

I acknowledge that my contribution to the above publication is 55%:

Benjamin Horsley Date 07/07/2023

As principal supervisor, I certify that the above contributions are true and correct:

Stuart Cormack Date 07/07/2023

Co-author signatures:

Paul Tofari Date 07/07/2023

Shona Halson Date 07/07/2023

Justin Kemp Date 07/07/2023

Daniel Chalkley Date 07/07/2023

Michael Cole Date 07/07/2023

Rich Johnston Date 07/07/2023

3. Horsley, B.J., et al., *Thoracic-worn accelerometers detect fatigue-related changes in vertical stiffness during sprinting.* The Journal of Strength and Conditioning Research, 2023. **38**(2): p. 283-289.

Contribution statement: BH, PT and SC were responsible for the design of the study. Data collection and post-processing was carried out by BH. Statistical analysis was performed by BH and SC with assistance from RJ. The manuscript was written by BH with editing contributions from all authors.

Approximate percentage contributions – B. J. Horsley 66.5%; P. J. Tofari 12.5%; S. L. Halson 2.5%; J. G. Kemp 1%; R. D. Johnston 5%; S. J. Cormack 12.5%.

I acknowledge that my contribution to the above publication is 66.5%:

Benjamin Horsley Date 07/07/2023

As principal supervisor, I certify that the above contributions are true and correct:

Stuart Cormack Date 07/07/2023

Co-author signatures:

Paul Tofari Date 07/07/2023

Shona Halson Date 07/07/2023

Justin Kemp Date 07/07/2023

Rich Johnston Date 07/07/2023

4. Horsley, B.J., et al., *The within- and post-match changes in accelerometer-derived stride variables from a team-sport match simulation protocol.*

Contribution statement: BH, PT and SC were responsible for the design of the study. Collection and post-processing of data was carried out by BH. Statistical analysis was performed by BH and SC with assistance from RJ. The manuscript was written by BH with editing contributions from all authors.

Approximate percentage contributions – B. J. Horsley 72.5%; P. J. Tofari 10%; S. L. Halson 2.5%; R. D. Johnston 5%; S. J. Cormack 10%.

I acknowledge that my contribution to the above pending publication is 72.5%:

Benjamin Horsley Date 07/07/2023

As principal supervisor, I certify that the above contributions are true and correct:

Stuart Cormack Date 07/07/2023

Co-author signatures:

Paul Tofari Date 07/07/2023

Shona Halson Date 07/07/2023

Rich Johnston Date 07/07/2023

Appendix II: Published Paper Forming the Basis of Chapter 3

Reference:

Horsley, B.J., et al., *Does site matter? Impact of Inertial Measurement Unit placement on the validity and reliability of stride variables during running: a systematic review and meta-analysis.* Sports Medicine, 2021. **51**: p. 1449-1489.

Please view the published version online at:

https://link.springer.com/article/10.1007/s40279-021-01443-8

Appendix III: Published Paper Forming the Basis of Chapter 4

Reference:

Horsley, B.J., et al., *Validity and reliability of thoracic-mounted Inertial Measurement Units to derive gait characteristics during running.* The Journal of Strength and Conditioning Research, 2023. **38**(2): p. 274-282.

Please view the published version online at:

https://journals.lww.com/nsca-jscr/abstract/2024/02000/validity_and_reliability_of_thoracic_mounted.8.aspx

Appendix IV: Published Paper Forming the Basis of Chapter 5

Reference:

Horsley, B.J., et al., *Thoracic-worn accelerometers detect fatigue-related changes in vertical stiffness during sprinting.* The Journal of Strength and Conditioning Research, 2023. **38**(2): p. 283-289.

Please view the published version online at:

https://journals.lww.com/nsca-jscr/abstract/2024/02000/thoracic_worn_accelerometers_detect.9.aspx

Appendix V: Ethics Approvals, Letters to Participants and Consent Forms

Study 2: Letter to Participants and Consent Form

ACU Human Ethics Committee Approval Number: 2020-11H

ACU
AUSTRALIAN CATHOLIC UNIVERSITY

PARTICIPANT INFORMATION LETTER

PROJECT TITLE:	The validity and reliability of thoracic-mounted inertial measurement units to derive stride variables during overground running
PRINCIPAL INVESTIGATOR:	Associate Professor Stuart Cormack
STUDENT RESEARCHER:	Mr Benjamin Horsley
STUDENT'S DEGREE:	Doctor of Philosophy

Dear Participant,

You are invited to participate in the research project described below.

What is the research project about?
The research project aims to determine the validity and reliability of inertial measurement units (IMUs) mounted on the upper back to derive stride variables, including contact time, flight time, vertical ground reaction force and vertical stiffness, during overground running at different speeds.

Who is undertaking the research project?
This project is being conducted by Mr Benjamin Horsley (B.Ex.Sci, B.App.Sci (Honours)) and will form the basis for the degree of Doctor of Philosophy at Australian Catholic University under the supervision of Associate Professor Stuart Cormack (PhD, M.App.Sci, B.App.Sci), who has a strong background in exercise and sports performance.

Are there any risks associated with participating in this study?
Like all exercise testing requiring maximal exertion, there exists the risk of injury. However, as you, the participant, regularly compete in sport and are familiar with high-intensity exercise, you will be less susceptible to injury.

What will I be asked to do?
You will be required to attend three testing sessions in total over a 10-14-day period, including one familiarisation session and two experimental sessions. Familiarisation will provide you with the opportunity to become accustomed to the testing procedures to be used in subsequent visits. During familiarisation, you will perform a series of run-throughs over 40 m at different speeds. Each run-through will require you to accelerate over 20 m and hold a constant running speed for a further 20 m. The speeds at which you will run are 3-4, 5-6 and 7-8 metres per second, which will be the equivalent of running the 20-40 m split in 5.0-6.7, 3.3-4.0 and 2.5-2.9 seconds for each of the three speed zones, respectively. Electronic timing gates will be used to monitor your running speed to ensure you are achieving the target speed zones. Following familiarisation, you

will return up to a week later to perform your first set of experimental trials (using the procedures outlined above) and then repeat those same trials again 3-7 days later. During the experimental trials, you will be equipped with two global positioning system (GPS) devices. One GPS device will be attached directly to your skin (approximately level with the second thoracic vertebrae) using sports strapping tape, whereas the other will be housed in a tightly fitted vest that you will wear directly over the top of the GPS device mounted to the skin. You will also wear four IMUs secured at both ankles, lower back and upper back below the GPS devices. Sports strapping tape will be used to secure the IMUs to the skin on the lower and upper back, while purpose-built straps will secure the ankle IMUs. You will perform a minimum of two trials at each speed zone (3-4, 5-6 and 7-8 metres per second) on each day of testing, with a three-minutes rest between each trial. Should your running velocity fall outside of the target zone, trials will be repeated.

How much time will the research project take?
The familiarisation and experimental sessions will take approximately 60 minutes to complete. This equates to approximately three hours in total for the research project.

What are the benefits of the research project?
Participation in this project will provide you with some detailed information on your stride characteristics at different running speeds. In the long-term, it is hoped that the results of this study will provide practitioners with a method for accurately and reliably capturing data relating to an athlete's running gait from a sensor location, i.e. upper back, that is often used in team-sport.

Can I withdraw from the study?
Participation in this study is completely voluntary. You are not under any obligation to participate. If you agree to participate, you can withdraw from the study at any time without adverse consequences. If you are a student of Australian Catholic University, participation or withdrawal from this research project will not affect your academic progress. Any data collected prior to your withdrawal will be kept securely on file by the researchers and will not be used for data analysis or future reporting.

Will anyone else know the results of the research project?
Your personal information and any data collected during this study will be kept confidential. The only people who will have access to this information are the researchers (Associate Professor Stuart Cormack, Dr Paul Tofari and Mr Benjamin Horsley). Data will be aggregated to be used in sports science publications and presentations. No individual will be identifiable.

Will I be able to find out the results of the research project?
Once you have completed your participation in the research project, the researchers will provide you with a summary of your individual results from the testing sessions.

Who do I contact if I have questions about the research project?
If you have any questions or queries about the research project, please do not hesitate to contact Associate Professor Stuart Cormack via Stuart.Cormack@acu.edu.au or on 0418 323 915.

What if I have a complaint or any concerns?
The study has been reviewed by the Human Research Ethics Committee at Australian Catholic University (review number 2020-11H). If you have any complaints or concerns about the conduct of the research project, you may write to the Manager of the Human Research Ethics and Integrity Committee care of the Office of the Deputy Vice Chancellor (Research).

Manager, Ethics and Integrity
c/o Office of the Deputy Vice Chancellor (Research)
Australian Catholic University
North Sydney Campus
PO Box 968
NORTH SYDNEY, NSW 2059
Ph.: 02 9739 2519
Fax: 02 9739 2870
Email: resethics.manager@acu.edu.au

Any complaint or concern will be treated in confidence and fully investigated. You will be informed of the outcome.

I want to participate! How do I sign up?
A consent form is included below this information letter. Please read the consent form and fill out your details to confirm your voluntary participation. Your personal records will be kept securely on REDCap's system.

Yours sincerely,

Associate Professor Stuart Cormack, Dr Paul Tofari and Mr Benjamin Horsley

CONSENT FORM

Copy for Participant to Keep

TITLE OF PROJECT:	THE VALIDITY AND RELIABILITY OF THORACIC-MOUNTED INERTIAL MEASUREMENT UNITS TO DERIVE STRIDE VARIABLES DURING OVERGROUND RUNNING
APPLICATION ID:	2020-11H
PRINCIPAL INVESTIGATOR:	Associate Professor Stuart Cormack
CO-SUPERVISOR:	Dr Paul Tofari
STUDENT RESEARCHER:	Benjamin Horsley

I, ... (the participant), have read (or, where appropriate, have had read to me) and understood the information provided in the Letter to Participants. Any questions I have asked has been answered to my satisfaction. I agree to participate in this research project, understanding my participation could require up to three hours of contact time. I am aware and agree to participate in three days of testing requiring me to perform a series of runs over 40 m at 3-4, 5-6 and 7-8 $m \cdot s^{-1}$ while wearing four inertial measurement units and two global positioning system devices. I realise that I can withdraw my consent at any time without adverse consequences. I understand that any data collected prior to my withdrawal will be kept securely on file by the researchers and will not be used for data analysis or future reporting. I agree that research data collected for the study may be published or may be provided to other researchers in a form that does not identify me in any way. If applicable, as a student at Australian Catholic University, my participation or withdrawal from this research project will not negatively affect my academic progress.

NAME OF PARTICIPANT:

SIGNATURE: DATE:

SIGNATURE OF PRINCIPAL INVESTIGATOR:

DATE:

SIGNATURE OF STUDENT RESEARCHER:

DATE:

Study 3: Letter to Participants and Consent Form

ACU Human Ethics Committee Approval Number: 2020-21H

PARTICIPANT INFORMATION LETTER

PROJECT TITLE:	The effect of neuromuscular fatigue on changes in stride variables derived from inertial measurement units following a repeated sprint protocol
PRINCIPAL INVESTIGATOR:	Associate Professor Stuart Cormack
STUDENT RESEARCHER:	Mr Benjamin Horsley
STUDENT'S DEGREE:	Doctor of Philosophy

Dear Participant,

You are invited to participate in the research project described below.

What is the research project about?
The objective of the research project is to determine the effect that a repeated sprint protocol aimed at inducing fatigue has on changes in stride variables, including contact time, flight time, vertical ground reaction force and vertical stiffness, derived from inertial measurement units (IMUs) attached to the ankles, lower and upper back.

Who is undertaking the research project?
This project is being conducted by Mr Benjamin Horsley (B.Ex.Sci, B.App.Sci (Honours)) and will form the basis for the degree of Doctor of Philosophy at Australian Catholic University under the supervision of Associate Professor Stuart Cormack (PhD, M.App.Sci, B.App.Sci), who has a strong background in exercise and sports performance.

Are there any risks associated with participating in this study?
Like all exercise testing requiring maximal exertion, there exists the risk of injury. However, as you, the participant, regularly compete in sport and are familiar with high-intensity exercise, you will be less susceptible to injury.

What will I be asked to do?
You will be required to attend four testing days in total, including two familiarisation sessions and two experimental sessions over approximately a 7-day period. Familiarisation will provide you with the opportunity to become accustomed to the testing procedures used in subsequent visits. On day one of familiarisation, you will perform a single and repeated countermovement jump (CMJ), squat jump and isometric mid-thigh pull (IMTP) test. The following day (day two), you will be familiarised with a 40 m sprint test, the repeated sprint protocol to be used as the fatigue intervention and a series of run-throughs over 40 m at three different speeds (3-4, 5-6 and 7-8 metres per second). As an introduction to the repeated sprint protocol, you will perform 6 x 40 m maximal sprints interspersed with 30 seconds passive recovery. For each run-through,

you will accelerate for 20 m and then hold a constant running speed for a further 20 m, where electronic timing gates will be used to monitor your speed. Each target speed will be the equivalent of running the 20-40 m split in 5.0-6.7, 3.3-4.0 and 2.5-2.9 seconds, respectively. Approximately 48 hours after familiarisation, we will test your single and repeated CMJ, squat jump and IMTP to profile your lower body strength and power, as well as have you perform a 40 m sprint test to determine your maximal running velocity. Once pre-testing is complete, you will return approximately three days later to undergo experimental testing. During this session, you will be equipped with two global positioning system (GPS) devices. One GPS device will be attached directly to your skin (approximately level with the second thoracic vertebrae) using sports strapping tape, whereas the other will be housed in a tightly fitted vest that you will wear directly over the top of the GPS device mounted to the skin. You will also wear four IMUs secured at both ankles, lower back and upper back below the GPS devices. Sports strapping tape will be used to secure the IMUs to your skin on the lower and upper back, while purpose-built straps will secure the ankle IMUs. Once you have been fitted with your devices, you will perform single and repeated CMJ tests on a force plate to obtain markers of fatigue status. Immediately following, you will perform a minimum of 2 x 40 m run-throughs at each target speed (3-4, 5-6 and 7-8 metres per second), with a three-minutes rest between each trial. Trials will be repeated should your running velocity fall outside of the target zone. The repeated sprint protocol, consisting of 12 x 40 m sprints interspersed with 30 seconds recovery, will be performed following your first set of run-throughs. Once you have completed the repeated sprint protocol, you will provide us with a numerical rating of your perceived exertion during the repeated sprint protocol and how fatigued you feel following the 12 x 40 m sprints using a 0-10 scale in both instances. You will then perform post-testing of the single and repeated CMJ and a minimum of another 2 x 40 m run-throughs at each of the three speeds.

How much time will the research project take?
Familiarisation and measurement of physical capacity will take approximately two hours in total to complete (one hour each). Performance of the fatigue intervention (repeated sprint protocol) and pre- and post-testing will take approximately one hour to complete. This equates to approximately four hours in total for the research project.

What are the benefits of the research project?
As a participant in this study, you will have the opportunity to be involved in complimentary, professional and scientific testing that will provide insight into your physical capacity. In the long-term, it is hoped that the results of this study will provide an understanding of how an athlete's stride changes when they are fatigued. An improved understanding of the fatigue-induced modifications to an athlete's stride may help to inform practitioners in developing enhanced athlete management strategies aimed at minimising running performance decrements due to accumulated fatigue.

Can I withdraw from the study?
Participation in this study is completely voluntary. You are not under any obligation to participate. If you agree to participate, you can withdraw from the study at any time without adverse consequences. If you are a student at Australian Catholic University, participation or withdrawal from this research project will not affect your academic progress. Any data collected

prior to your withdrawal will be kept securely on file by the researchers and will not be used for data analysis or future reporting.

Will anyone else know the results of the research project?
Your personal information and any data collected during this study will be kept confidential. The only people who will have access to this information are the researchers (Associate Professor Stuart Cormack, Dr Paul Tofari and Mr Benjamin Horsley). Data will be aggregated to be used in sports science publications and presentations. No individual will be identifiable.

Will I be able to find out the results of the research project?
Once you have completed your participation in the research project, the researchers will provide you with a summary of your individual results from the testing sessions.

Who do I contact if I have questions about the research project?
If you have any questions or queries about the research project, please do not hesitate to contact Associate Professor Stuart Cormack via Stuart.Cormack@acu.edu.au or on 0418 323 915.

What if I have a complaint or any concerns?
The study has been reviewed by the Human Research Ethics Committee at Australian Catholic University (review number 2020-21H). If you have any complaints or concerns about the conduct of the research project, you may write to the Manager of the Human Research Ethics and Integrity Committee care of the Office of the Deputy Vice Chancellor (Research).

Manager, Ethics and Integrity
c/o Office of the Deputy Vice Chancellor (Research)
Australian Catholic University
North Sydney Campus
PO Box 968
NORTH SYDNEY, NSW 2059
Ph.: 02 9739 2519
Fax: 02 9739 2870
Email: resethics.manager@acu.edu.au

Any complaint or concern will be treated in confidence and fully investigated. You will be informed of the outcome.

I want to participate! How do I sign up?

A consent form is included below this information letter. Please read the consent form and fill out your details to confirm your voluntary participation. Your personal records will be kept securely on REDCap's system.

Yours sincerely,

Associate Professor Stuart Cormack, Dr Paul Tofari and Mr Benjamin Horsley

CONSENT FORM

Copy for Participant to Keep

TITLE OF PROJECT:	THE EFFECT OF NEUROMUSCULAR FATIGUE ON CHANGES IN STRIDE VARIABLES DERIVED FROM INERTIAL MEASUREMENT UNITS FOLLOWING A REPEATED SPRINT PROTOCOL
PRINCIPAL INVESTIGATOR:	Associate Professor Stuart Cormack
CO-SUPERVISOR:	Dr Paul Tofari
STUDENT RESEARCHER:	Benjamin Horsley

I, ... (the participant), have read (or, where appropriate, have had read to me) and understood the information provided in the Letter to Participants. Any questions I have asked has been answered to my satisfaction. I agree to participate in this research project, understanding my participation requires me to attend four testing days totalling approximately four hours. I am aware and agree to participate in testing requiring me to perform single and repeated countermovement jump tests, squat jump, isometric mid-thigh pull, 40 m sprint test and a series of run-throughs completed over 40 m at 3-4, 5-6 and 7-8 $m \cdot s^{-1}$ either side of a 12 x 40 m repeated sprint protocol, realising that I can withdraw my consent at any time without adverse consequences. It has been explained to me that I will also be required to wear four inertial measurement units and two global positioning system devices during testing. I understand that any data collected prior to my withdrawal will be kept securely on file by the researchers and will not be used for data analysis or future reporting. I agree that research data collected for the study may be published or may be provided to other researchers in a form that does not identify me in any way. If applicable, as a student at Australian Catholic University, my participation or withdrawal from this research project will not negatively affect my academic progress.

NAME OF PARTICIPANT:

SIGNATURE: DATE:

SIGNATURE OF PRINCIPAL INVESTIGATOR:

DATE:

SIGNATURE OF STUDENT RESEARCHER:

DATE:

Study 4: Letter to Participants and Consent Form

ACU Human Ethics Committee Approval Number: 2022-2769H

PARTICIPANT INFORMATION LETTER

PROJECT TITLE:	The within- and post-match changes in accelerometer-derived stride variables from a team-sport match simulation protocol
PRINCIPAL INVESTIGATOR:	Associate Professor Stuart Cormack
STUDENT RESEARCHER:	Mr Benjamin Horsley
STUDENT'S DEGREE:	Doctor of Philosophy

Dear Participant,

You are invited to participate in the research project described below.

What is the research project about?

The objective of the research project is to determine the changes in running stride variables during and following a 90-minute team-sport match simulation protocol. Wearable sensors will be attached to the ankles, lower back and upper back where the most effective placement site for determining changes in stride variables will form part of the analysis. This project is also investigating whether lower body strength, power or aerobic fitness influences the fatigue-related modifications to stride variables.

Am I eligible to participate in the research project?

To participate in this study, you are to be 18-40 years of age, injury free and regularly participate in high-intensity exercise or play sport. As this study includes a team-sport match simulation, familiarity with high-intensity exercise is important to successfully complete the protocol. Participation also requires attending six testing sessions over approximately 10-14 days, including four sessions on consecutive days, so schedule flexibility is required to complete these sessions in a timely manner.

Who is undertaking the research project?

This project is being conducted by Mr Benjamin Horsley (B.Ex.Sci, B.App.Sci (Honours)) and will form the basis for the degree of Doctor of Philosophy at Australian Catholic University. Benjamin has successfully completed other research studies using wearable technology to profile fatigue in sport and will be under the supervision of Associate Professor Stuart Cormack (PhD, M.App.Sci, B.App.Sci) who has a strong background in exercise and sports performance. Dr Paul Tofari will be a co-supervisor to this research project who also has extensive research experience in exercise and sports performance.

Are there any risks associated with participating in this study?

Like all exercise testing requiring maximal exertion, there exists the risk of injury. However, as you, the participant, regularly participate in high-intensity exercise or play sport, you will be less susceptible to injury.

What will I be asked to do?

You will be required to attend six testing days in total, including one familiarisation, one profiling session, one match simulation (fatigue intervention) session and three follow-up visits over approximately 10 to 14 days (see Figure 1).

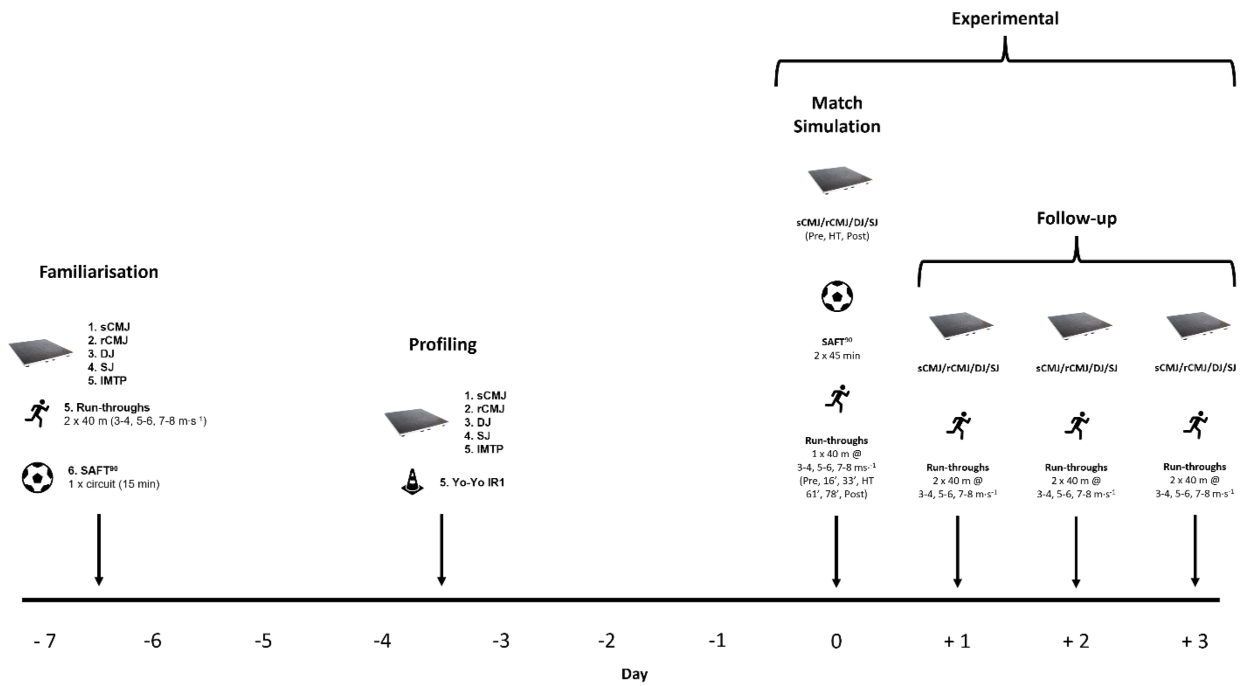

Figure 1. Research study design.

Familiarisation will accustom you to all testing procedures where you will perform a single and repeated countermovement jump (CMJ), drop jump (DJ) from a 30 cm box, squat jump (SJ) and isometric mid-thigh pull (IMTP) on a force plate, 40 m run-throughs at jog, stride and sprint running speeds and the soccer-specific aerobic fitness test (SAFT^{90}; see Figure 1). Each 40 m run-through will involve accelerating for 20 m and then maintaining a speed between 3-4, 5-6 and 7-8 metres per second for the remaining 20 m, where electronic timing gates will monitor how fast you run. The target speed will be the equivalent of running the 20-40 m section in 5.0-6.7, 3.3-4.0 and 2.5-2.9 seconds, respectively. As an introduction to the SAFT^{90}, you will perform 1 x 15-minute circuit which will require you to perform a variety of movements representative of team-sport, including side-stepping, cutting, accelerations and decelerations and forwards and backwards running at different speeds, over a 20 m course (see Figure 2). An audio track will guide you through the circuit and prompt you of which movements to perform.

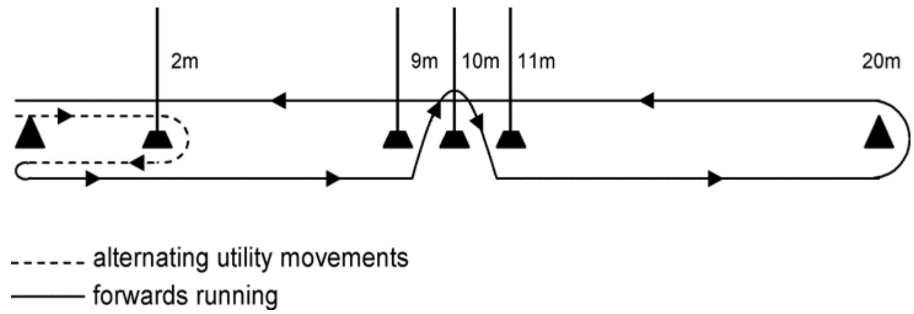

Figure 2. SAFT^{90} match simulation course.

Approximately three days after familiarisation, we will measure your strength, power and aerobic fitness (see Figure 1). The Yo-Yo Intermittent Recovery Level 1 (Yo-Yo IR1) test will determine your aerobic fitness which will require you to run back and forth over 20 m at gradually increasing speeds, interspersed with 10 seconds of active recovery, until exhaustion.

Once profiling is complete, you will return approximately three days later to perform the fatigue intervention which will comprise 2 x 45-minute periods of the SAFT^{90} match simulation (see Figure 1). During this session, you will be equipped with up to six sensors, where one will be attached to each ankle in purpose-built straps, one to the skin on the lower back using a suitable medical tape and three on the upper back – two taped direct to the skin and one housed securely in a tightly fitted sports vest. After a thorough warm-up, baseline jump testing (single and repeated CMJ, DJ and SJ) and 3 x 40 m run-throughs (one at each speed) will be performed and used as a reference to monitor the fatigue response throughout the match simulation and over the days following. You will then commence the SAFT^{90} (see Figure 2) where each 45-minute half will comprise 3 x 15-minute circuits with additional 40 m run-throughs at approximately 16 and 33 minutes. A 15-minute halftime interval will follow the completion of the first half, where you will redo the jump testing and 40 m run-throughs, as well as provide a rating of your perceived exertion and fatigue using a 0-10 scale. These tests will be performed a final time immediately post-match.

You will return the next three consecutive days to undergo follow-up testing which will measure the time-course of recovery of stride variables and jump performance following the match simulation (see Figure 1). Here, you will perform the respective jump tests (single and repeated CMJ, DJ and SJ) and 2 x 40 m run-throughs at jog, stride and sprint running speeds, with these sessions scheduled for a similar time of day as the match simulation.

How much time will the research project take?

The familiarisation and profiling sessions will be conducted at ACU's Melbourne campus and will take up to one and a half hours to complete each. The remaining four sessions will be performed off-site on an artificial turf soccer pitch in Brunswick West which provides adequate space to perform the running component of the testing. Approximately two and a half hours will be dedicated to completion of the fatigue intervention which will include the SAFT^{90} match simulation (plus 15-minute halftime interval) and time for equipping you with the accelerometers and a thorough warm-up. The final three follow-up sessions will take approximately 45 minutes each. This equates to approximately eight hours in total for the research project.

What are the benefits of the research project?
As a participant in this study, you will have the opportunity to be involved in complimentary, professional and scientific testing that will provide insight into your physical capacity, including your strength, power and aerobic capacity. In the long-term, it is hoped that the results of this study will provide an understanding of how an athlete's stride pattern changes when they are fatigued from a match. An improved understanding of the fatigue-induced modifications to an athlete's stride may help inform athlete management strategies aimed at minimising running performance decrements due to accumulated fatigue. Upon full completion in this study, you will receive a $50 gift voucher as a thank you for your valued participation.

Can I withdraw from the study?
Participation in this study is completely voluntary. You are not under any obligation to participate. If you agree to participate, you can withdraw from the study at any time without adverse consequences. If you are a student at Australian Catholic University, participation or withdrawal from this research project will not affect your academic progress. Any data collected prior to your withdrawal will be kept securely on file for a minimum of five years, which is in accordance with university and legal guidelines, and will not be used for data analysis or future reporting.

Will anyone else know the results of the research project?
Your personal information and any data collected during this study will be kept confidential. The only people who will have access to this information are the researchers (Associate Professor Stuart Cormack, Dr Paul Tofari and Mr Benjamin Horsley). Data will be aggregated and used in sports science publications and presentations. No individual will be identifiable.

Will I be able to find out the results of the research project?
Once you have completed your participation in the research project, the researchers will provide you with a summary of your individual results from the testing sessions.

Who do I contact if I have questions about the research project?
If you have any questions or queries about the research project, please do not hesitate to contact Associate Professor Stuart Cormack via Stuart.Cormack@acu.edu.au or on 0418 323 915.

What if I have a complaint or any concerns?
The study has been reviewed by the Human Research Ethics Committee at Australian Catholic University (review number 2022-2769H). If you have any complaints or concerns about the conduct of the research project, you may write to the Manager of the Human Research Ethics and Integrity Committee care of the Office of the Deputy Vice Chancellor (Research).

Manager, Ethics and Integrity
c/o Office of the Deputy Vice Chancellor (Research)
Australian Catholic University
North Sydney Campus
PO Box 968
NORTH SYDNEY, NSW 2059
Ph.: 02 9739 2519
Fax: 02 9739 2870
Email: resethics.manager@acu.edu.au

Any complaint or concern will be treated in confidence and fully investigated. You will be informed of the outcome.

I want to participate! How do I sign up?

A consent form is included below this information letter. Please read the consent form and fill out your details to confirm your voluntary participation. Your personal records will be kept on the REDCap platform which is a secure web-based research data management system.

Yours sincerely,

Associate Professor Stuart Cormack, Dr Paul Tofari and Mr Benjamin Horsley

CONSENT FORM

Copy for Participant to Keep

TITLE OF PROJECT:	THE WITHIN- AND POST-MATCH CHANGES IN ACCELEROMETER-DERIVED STRIDE VARIABLES FROM A TEAM-SPORT MATCH SIMULATION PROTOCOL
PRINCIPAL INVESTIGATOR:	Associate Professor Stuart Cormack
CO-SUPERVISOR:	Dr Paul Tofari
STUDENT RESEARCHER:	Benjamin Horsley

I, ... (the participant), have read (or, where appropriate, have had read to me) and understood the information provided in the Letter to Participants. Any questions I have asked has been answered to my satisfaction. I agree to participate in this research project, understanding my participation requires me to attend six testing days totalling approximately eight hours. I am aware and agree to participate in testing requiring me to perform single and repeated countermovement jumps, drop jump, squat jump, isometric mid-thigh pull, Yo-Yo Intermittent Recovery Level 1 test, 40 m run-throughs at 3-4, 5-6 and 7-8 $m \cdot s^{-1}$ and a 90-minute team-sport match simulation protocol, realising that I can withdraw my consent at any time without adverse consequences. It has been explained to me that I will also be required to wear up to six accelerometers during testing, some of which will be attached directly to my skin. I understand that any data collected prior to my withdrawal will be kept securely on file for the minimum period of five years, as per university and legal policies, and will not be used for data analysis or future reporting. I agree that research data collected for the study may be published or may be provided to other researchers in a form that does not identify me in any way. If applicable, as a student at Australian Catholic University, my participation or withdrawal from this research project will not negatively affect my academic progress.

NAME OF PARTICIPANT:

SIGNATURE: DATE:

SIGNATURE OF PRINCIPAL INVESTIGATOR:

DATE:

SIGNATURE OF STUDENT RESEARCHER:

DATE: